1977

X-ray Crystallographic And Preparative Studies On Carbene Complexes Of Platinum(ii)

Robert Francis Stepaniak

NOTICE

The quality of this microfiche is heavily dependent upon the quality of the original thesis submitted for microfilming. Every effort has been made to ensure the highest quality of reproduction possible.

If pages are missing, contact the university which granted the degree.

Some pages may have indistinct print especially if the original pages were typed with a poor typewriter ribbon or if the university sent us a poor photocopy.

Previously copyrighted materials (journal articles, published tests, etc.) are not filmed.

Reproduction in full or in part of this film is governed by the Canadian Copyright Act, R.S.C. 1970, c. C-30. Please read the authorization forms which accompany this thesis.

THIS DISSERTATION
HAS BEEN MICROFILMED
EXACTLY AS RECEIVED

AVIS

La qualité de cette microfiche dépend grandement de la qualité de la thèse soumise au microfilmage. Nous avons tout fait pour assurer une qualité supérieure de reproduction.

S'il manque des pages, veuillez communiquer avec l'université qui a conféré le grade.

La qualité d'impression de certaines pages peut laisser à désirer, surtout si les pages originales ont été dactylographiées à l'aide d'un ruban usé ou si l'université nous a fait parvenir une photocopie de mauvaise qualité.

Les documents qui font déjà l'objet d'un droit d'auteur (articles de revue, examens publiés, etc.) ne sont pas microfilmés.

La reproduction, même partielle, de ce microfilm est soumise à la Loi canadienne sur le droit d'auteur, SRC 1970, c. C-30. Veuillez prendre connaissance des formules d'autorisation qui accompagnent cette thèse.

LA THÈSE A ÉTÉ
MICROFILMÉE TELLE QUE
NOUS L'AVONS REÇUE

X-RAY CRYSTALLOGRAPHIC AND PREPARATIVE STUDIES ON CARBENE COMPLEXES OF PLATINUM(II)

by

Robert Francis Stepaniak
Department of Chemistry

Submitted in partial fulfillment of
the requirements for the degree of
Doctor of Philosophy

Faculty of Graduate Studies
The University of Western Ontario
London, Ontario
February, 1977

to my parents

and

to Karen

ABSTRACT

The structures of five square planar, cationic carbene complexes of Pt(II) have been determined from single crystal X-ray diffraction studies. The following compounds have been examined.

Trans-methyl(methyl-N,N-dimethylaminocarbene)bis-(dimethylphenylphosphine)platinum(II) hexafluorophosphate, $[Pt\{CH_3C{=}{-}N(CH_3)_2\}CH_3\{P(CH_3)_2C_6H_5\}_2]PF_6$. Full matrix least-squares refinement on F, of 162 variables using 1865 significant ($I>3\sigma(I)$) intensity data obtained by diffractometric techniques gave agreement factors $R_1 = 0.041$ and $R_2 = 0.062$. The planar carbene ligand lies perpendicular to the square plane of the metal, and the Pt-C(sp^2) distance is 2.079(13) Å. The C(sp^2)-N bond is 1.266(15) Å long. A Pt-C(methyl) bond length of 2.147(11) Å is observed.

Trans-methyl(2-oxacyclopentilidene)bis(dimethyl-phenylphosphine)platinum(II) hexafluorophosphate, $[Pt(CH_2C{=}{-}OCH_2CH_2)CH_3\{P(CH_3)_2C_6H_5\}_2]PF_6$. Least-squares refinement of 160 variables based on 1763 data converged at $R_1 = 0.044$ and $R_2 = 0.048$. The carbene ligand is present in the form of a five membered ring with C(sp^2)-O of 1.26(2) Å. The Pt-C(sp^2) distance is 2.00(2) Å and the C(methyl) atom lies 2.08(2) Å from .

Trans-chloro(3-hydroxypropyl-N,N-dimethylamino-carbene)bis(dimethylphenylphosphine)platinum(II) hexafluoro-phosphate, $[Pt\{HO(CH_2)_3C{=}{-}N(CH_3)_2\}Cl\{P(CH_3)_2C_6H_5\}_2]PF_6$.

Refinement of 187 variables using 3421 observations gave $R_1 = 0.047$ and $R_2 = 0.054$. The Pt-C(sp^2) bond length is 1.978(12) Å and the C(sp^2)-N distance is 1.293(16) Å. The Pt-Cl bond is 2.356(4) Å long.

Trans-p-tolylisocyanide(methyl-N,N-dimethylaminocarbene)-bis(dimethylphenylphosphine)platinum(II) hexafluorophosphate, $[Pt\{CH_3C{=}{-}N(CH_3)_2\}(C{\equiv}N\text{-}p\text{-}C_6H_4CH_3)\{P(CH_3)_2C_6H_5\}_2](PF_6)_2$. 185 variables were refined employing 4025 observations converging at $R_1 = 0.042$ and $R_2 = 0.048$. The carbene ligand is disordered such that two possible orientations occur, one related to the other by approximate 180° rotation about the Pt-C(sp^2) bond. A disorder model was successfully refined in the form of two rigid groups superimposed on one another so that the methyl C atoms occupy the same electron density peaks. Refinement of a disorder multiplicity parameter gave a value of 0.68(2). The mean Pt-C(sp^2) bond length is 2.08(1) Å and the Pt-C(isocyanide) bond is 1.958(13) Å long. The carbene ligand lies at an angle of 72.5° to the square plane and the isocyanide ligand is approximately linear.

Trans-methyl-N,N-dimethylaminocarbene(dimethylamino-p-tolylaminocarbene)bis(dimethylphenylphosphine)platinum(II) hexafluorophosphate, $[Pt\{CH_3C{=}{-}N(CH_3)_2\}\{C(N(CH_3)_2)NH\text{-}p\text{-}C_6H_4CH_3\}\{P(CH_3)_2C_6H_5\}_2](PF_6)_2$. Refinement of 216 variables based on 5336 observations gave $R_1 = 0.054$ and $R_2 = 0.064$. The methyl-N,N-dimethylaminocarbene ligand is disordered as above. The final value for the multiplicity parameter

is 0.585(18). The mean Pt-C(sp^2) distance is 2.09(4) Å while the Pt-C(sp^2) bond length to the ordered carbene ligand is 2.058(10) Å. The C(sp^2)-N distances are 1.337(11) Å and 1.306(12) Å to the N atoms of the p-tolylamino and dimethylamino substituents respectively.

Disorder of the PF_6 anions was observed in all but one of the structures.

The structural results are discussed in terms of bonding about the C(sp^2) atom. The metal-ligand bond lengths are examined for the effects of trans influence. The relative orientations of the phosphine ligands are compared and a method for calculating phosphine cone angles from X-ray crystallographic data is proposed. The cone angles are defined as a function of rotation of the phosphine ligand about the M-P bond.

Some new complexes of the type trans-$[PtLX\{P(CH_3)_2C_6H_5\}_2]^{n+}(PF_6^-)_n$ have been prepared, where L is a secondary carbene, tertiary carbene or formimidoyl ligand, X is Cl^-, isocyanide, or tertiary carbene and n = 1 or 2. Infrared, ^1H NMR, analytical and physical data for these complexes are presented and discussed. X-ray structural determinations have been performed on two of the dicationic compounds.

ACKNOWLEDGEMENTS

The author is very grateful to Dr. N.C. Payne under whose direction this research was carried out. His helpfulness, encouragement and patience are deeply appreciated.

The author expresses his gratitude to the members of the X-ray t'd group both past and present. Dr. D.B. Crump, Dr. B.W. Davies and R.G. Ball are thanked for providing valuable advice and assistance when it was needed and for suggesting suitable diversion when it was required.

Dr. M.H. Chisholm, Dr. L.E. Manzer and Dr. K. Yasufuku are thanked for furnishing samples and for helpful discussions. The author is thankful to Dr. D.F. Christian and Dr. H.C. Clark for valuable discussions and assistance. M.J. Dymarski and C.R.C. Milne are thanked for valuable discussions. Thanks are also due to other members of the chemistry department for helpful advice.

The National Research Council of Canada is thanked for the award of a Bursary (1972-3) and a Scholarship (1975-6).

TABLE OF CONTENTS

LIST OF PHOTOGRAPHIC PLATES

LIST OF TABLES

LIST OF FIGURES

NOMENCLATURE

The following abbreviations for common organic substituents have been used throughout this work:

Abbreviation	Name	Formula
Me	methyl	$-CH_3$
Et	ethyl	$-CH_2CH_3$
Pr	propyl	$-CH_2CH_2CH_3$
Bu	butyl	$-(CH_2)_3CH_3$
Ph	phenyl	$-C_6H_5$
Cy	cyclohexyl	$-C_6H_{11}$

CHAPTER 1

INTRODUCTION

Coordination compounds of transition metals play important catalytic roles in homogeneous, heterogeneous and enzymatic processes. The ability of transition metals to provide vacant coordination sites, to activate molecules so that they undergo reactions not normally observed for the uncoordinated compounds, and to stabilize entities which do not usually exist in a 'free' state, is to a large extent responsible for this catalytic activity (1, 2). Molecules such as H_2, O_2, N_2, CO, olefins and acetylenes are activated on coordination to metal complexes, whereas species such as H^-, alkyl and aryl groups, cyclobutadienes, cyclopentadienyls, carbenes and carbynes are stabilized. It is, therefore, not surprising that a great deal of research in organometallic chemistry during the past several decades has been devoted to the preparation and study of transition metal compounds of small molecules, and of complexes where reactive organic intermediates have been trapped by coordination to a metal atom (3).

For the past twelve years, one area of organometallic chemistry has generated much enthusiasm and has seen a remarkable growth rate. The preparation of transition metal carbene complexes was first reported in 1964 (4). These compounds were prepared by the reaction sequence shown.

$$W(CO)_6 + LiPh \xrightarrow{Et_2O} (OC)_5WCOPh^-Li^+ \xrightarrow{Me_4NCl}$$

$$[Me_4N]^+[(CO)_5WCOPh]^- \xrightarrow{H^+} (CO)_5W{=}C(OH)(Ph) \xrightarrow{CH_2N_2} (CO)_5W{=}C(OMe)(Ph)$$

not isolated

To date nine review articles on transition metal carbene complexes have appeared in print (5-13). In this thesis are described some studies on square planar cationic carbene complexes of divalent platinum.

1.1 The Carbene Ligand

Organic carbenes such as CH_2 are highly reactive species which usually have short lifetimes. They undergo a variety of reactions including additions to aromatic systems, olefins, acetylenes, nitriles and insertions into C-H bonds (14).

In transition metal complexes, the divalent carbon species are trapped as ligands (Fig. 1.1). These compounds have approximately sp^2 hybridization at the C atom and neither C-X nor C-Y is a formal multiple bond. Stabilization of the electron deficient $C(sp^2)$ atom can come from X, Y or M, depending on the nature of each in a given compound. Coordinated carbene ligands can conveniently be divided into three major classes. Methylene is by definition the only primary carbene; both X and Y are hydrogen atoms (Fig. 1.1). If only one of X or Y is a hydrogen atom, then a secondary carbene is present, whereas if neither X nor Y are hydrogen, then the carbene is tertiary. X and/or Y can be H, alkyl, aryl, oxy-, amino-, thio-, or seleno-substituents, but the majority of complexes have the nucleophilic oxy-, amino-, or thio-groups.

Examples of all three classes of carbene complexes are known. Only recently has a complex containing a primary carbene ligand been prepared (15). The X-ray crystallographic structure determination of this compound, $Ta(CH_2)MeCp_2$, has been completed (16). Secondary carbene complexes can be divided into two groups 2a and 2b.

Figure 1.1

Types of Carbene Ligands

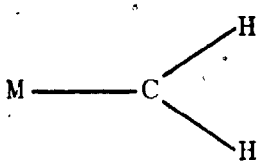

1°, Primary

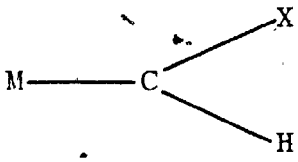

2a

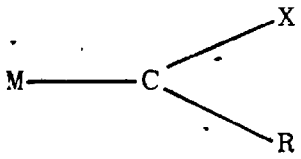

2b

2°, Secondary

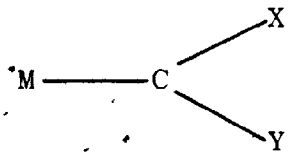

3a

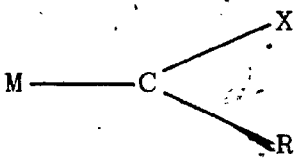

3b

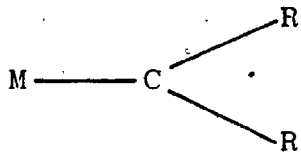

3c

3°, Tertiary

X, Y = oxy-, amino-, thio-, seleno-

R = alkyl, aryl

(Fig. 1.1), where 2a contains a nucleophilic substituent X or Y, and 2b has an alkyl or aryl substituent, R. Complexes containing ligands 2a are quite common (17-20) and structural studies have been reported (20, 21). A complex of group 2b has been isolated (22). Tertiary carbene ligands can be classified in a similar manner into three groups. Ligands of group 3a have strongly nucleophilic substituents X and Y, and for those of 3b, one of X or Y has been replaced by an alkyl or aryl entity. These two groups encompass approximately 80% of all carbene complexes, and they are the most thoroughly studied (8-10). The first carbene complexes reported by Fischer are in category 3b (5-7). Finally, if both X and Y are alkyl or aryl substituents, the carbene ligands belong to group 3c. Some complexes of this classification are known (23-29) and crystallographic structural data are available for several compounds (29-33). Complexes containing vinylidene ligands are included in group 3c (25-29, 32).

Carbene complexes of a large number of the transition metals have been isolated (8). All compounds are either cationic or neutral; no anionic carbene complexes have yet been prepared. The carbene ligands are generally unidentate, but complexes containing bidentate carbene ligands have been isolated. X-ray crystallographic studies have been performed on several of these (33-37). The crystal structure of a complex containing a tridentate carbene ligand and several of compounds where the carbene is a

bridging group between two metal atoms have been reported as well (29, 30, 39, 40). Complexes containing up to four carbene ligands have been isolated (41, 42) and the X-ray crystal structure of one such compound has been completed (42).

1.2 Bonding Trends in Transition Metal Carbene Complexes

The sp^2 hybridized C(carbene) atom of the coordinated ligand is electron deficient. The electronic structure is:

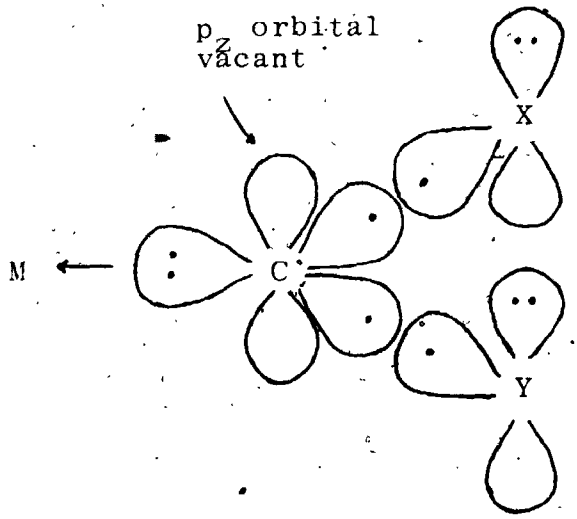

M, C, X, and Y are all co-planar. Stabilization of C (carbene) can come from filled p orbitals on X and Y in the form of pπ-pπ interactions, or from filled metal d orbitals through dπ-pπ bonding. In all cases electron donation is directed towards the vacant p_z orbital of the carbene C atom.

The determination of the extent of stabilization of C(carbene) from the metal atom and from the electron rich substituents has been the impetus for the accumulation of a large amount of spectroscopic and structural data. The neutral tertiary carbene complexes of Cr, Mo, and W have been studied most extensively, and a brief discussion

of some of the results obtained serves as a good introduction both to bonding trends in carbene systems and to some of the experimental techniques employed. Infrared (43) and X-ray photo-electron spectra (44) of pentacarbonyl (alkoxycarbene)Cr(0) complexes show that considerable metal-C(carbene) π bonding occurs. ^{13}C NMR chemical shift data (45) as well as MO calculations (46) on these same alkoxycarbene systems show the strongly electrophilic nature of C(carbene). A series of X-ray crystal structures has been performed on carbonyl carbene Cr(O) complexes (31, 47-54). All structures show considerable double bond character between C(carbene) and the nucelophilic substituents. The bond order has been estimated to be approximately 1.7 (10). The Cr-C(carbene) bond lengths show a large range (2.00 to 2.16 Å). The longest distances correspond to complexes with aminocarbene ligands, whereas shorter distances are observed for oxy- and thiocarbene compounds. Dipole moment experiments and infrared spectral data on carbonyl carbene complexes of Cr(O) show that the C(carbene) atom is stabilized by nucleophilic substituents in the order amino > thio > seleno > oxy (7). In general, spectroscopic and structural data indicate that the amount of metal-ligand $d\pi$-$p\pi$ bonding is dependent on the nucleophilicity of the substituents X and Y, and that carbenes are better σ donors and poorer π acceptors than the CO ligand (5-10).

The research on zerovalent Cr, W, and Mo carbene

systems is the subject of three review articles (5-7). Structure, bonding and reactivity of transition metal carbene complexes has been reviewed by Cotton and Lukehart (10) and by Lappert and co-workers (8, 9).

In view of the discussions on the mode of bonding, there is some question as to whether these ligands are true carbenes, and does the 'carbene' nomenclature apply. It has been suggested that the names carbenoid (10), stabilized carbonium ion (9), or for aminocarbenes, metallated amidinium ions (34) better describe the ligands. But, because of its convenience, the 'carbene' terminology remains in common use.

1.3 Carbene Complexes of Platinum(II)

i. Preparation

The first carbene compounds of Pt(II) were the Chugaev salts (35) reported in 1915. It was not until recently (34, 56, 57) that these were recognized as carbene complexes.

A large number of complexes prepared by various synthetic routes has now been isolated. These complexes are square planar and most commonly contain tertiary carbenes of the types 3a and 3b, but secondary carbene complexes have also been obtained. The modes of preparation of these compounds can conveniently be divided into five categories. Examples of the fundamental reactions are listed (8-10).

I. Reaction of nucleophilic reagents with isocyanides.

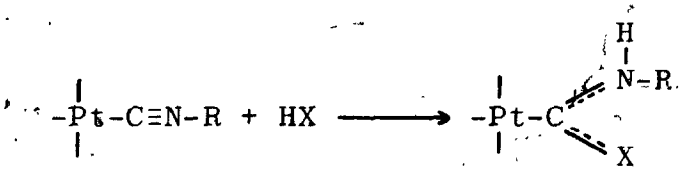

X = OR, SR, NR'R"

R = alkyl, aryl

R',R" = H, alkyl, aryl

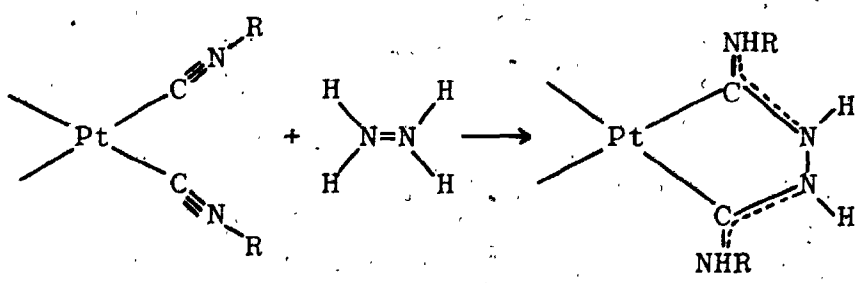

R = alkyl, aryl

II. Carbenes from acetylenic intermediates.

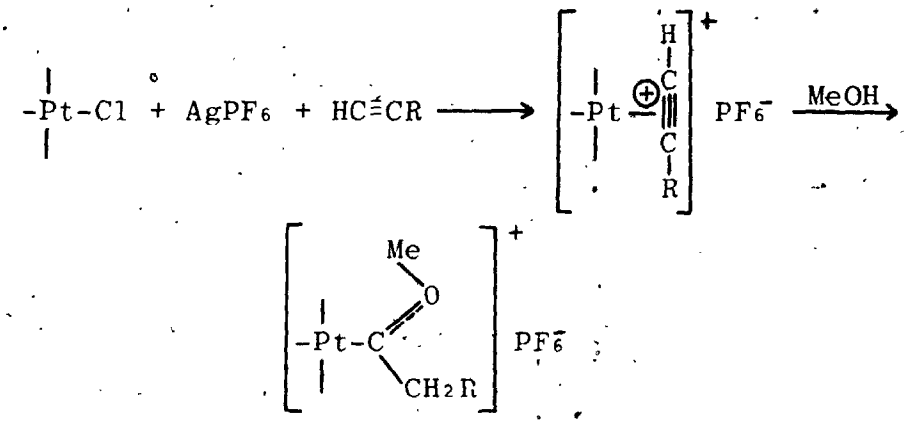

R = H, alkyl, aryl

III. Carbenes from electron rich precursors.

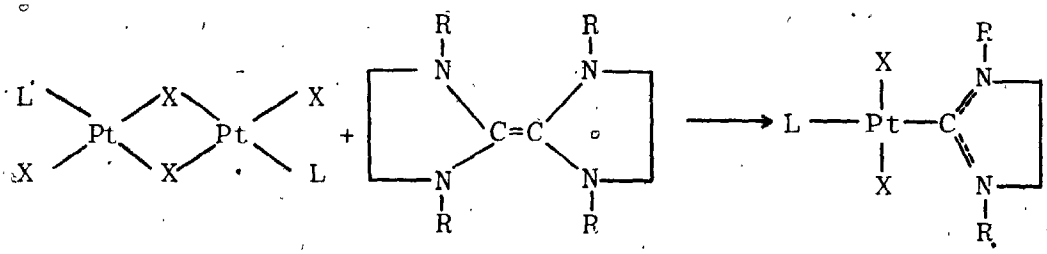

L = phosphine

X = halogen

R = H, alkyl, aryl

IV. Protonation or methylation of double bonds (58-61).

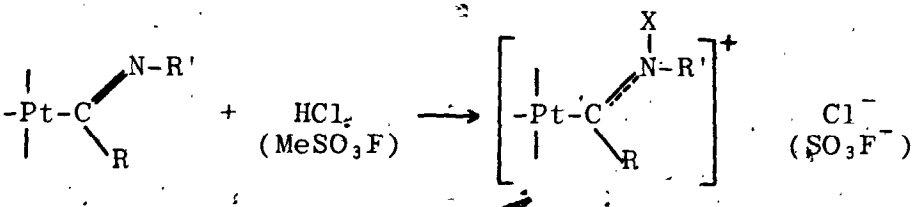

X = H, Me

R = H, alkyl, aryl

R' = alkyl, aryl

V. Carbene complexes from carbene precursors.

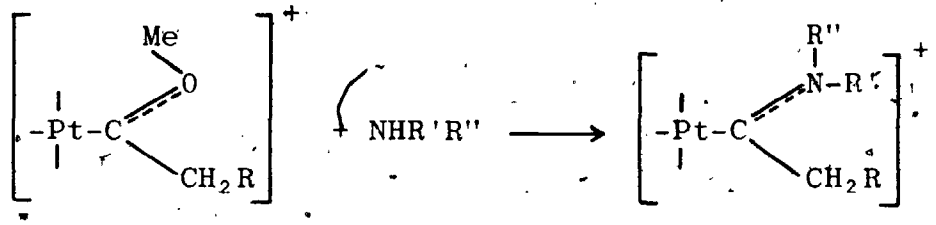

R, R', R" = H, alkyl, aryl

Reactions I, II, IV and V are utilized as preparative routes in this work, but carbene complexes prepared by reactions II and V are most important with respect to the X-ray crystallographic experiments to be discussed.

ii. Interest in Platinum(II) Carbene Complexes

Square planar Pt(II) carbene complexes allow the investigation of the bonding of these ligands to a divalent metal atom. Neutral, monocationic and dicationic compounds can be prepared and studied and the Pt(II) species are often precursors to octahedral Pt(IV) carbene complexes.

Chisholm and Clark first isolated carbene complexes from reactions of type II in 1970 (62, 63). A large number of these carbene compounds have been examined spectroscopically. ^{1}H NMR, ^{13}C NMR and IR (62-65) data have been discussed. The results are in keeping with those expected for an electrophilic C(carbene) atom, and tend to indicate that oxy-substituents stabilize this atom to a greater extent than amino groups. The reactivities of complexes containing these ligands confirm this observation in that oxycarbenes are more reactive than the amino ones, (64). ^{1}H NMR data indicate that alkoxycarbene

ligands are better σ donors and poorer π acceptors than coordinated acetylenes (65).

Because of the four coordinate and planar nature of the Pt(II) compounds, they are ideally suited for trans influence studies.

a. Trans Influence

The trans influence of a ligand in a transition metal complex has been defined as the extent to which a ligand weakens the bond trans to itself in the equilibrium state of that complex (66). Obviously, this can often determine the reactivity of a given complex.

A variety of spectroscopic techniques have been utilized in the investigation of the trans influence phenomenon including NMR, IR, NQR, and ESCA. X-ray crystallography is also an important tool for trans influence studies (67). A systematic examination of the crystallographic trans influence of various 'carbon donor' ligands has recently been undertaken. The changes in Pt-Cl bond lengths in neutral square-planar complexes of divalent Pt are monitored as the ligands trans to Cl^- are varied (68).

Thus, the X-ray crystal structure determinations of carbene complexes of Pt(II) can provide not only bonding information, but also valuable data on the trans influence of the ligands present.

b. X-ray Crystal Structure Determinations

When this research was undertaken, the X-ray crystallographic investigations of three square planar carbene complexes of Pt(II) had been reported (69, 70). Since that time, more complete documentation of two of these structures has been published (71), and two new studies have been completed (34, 72) in addition to the experiments performed in our laboratories.

This project was undertaken to examine the bonding of different carbene ligands in cationic square-planar complexes of Pt(II), and to determine how the trans influence of this ligand affects the metal-ligand bond at the opposite coordination site in the solid state. A further question of importance is to what extent is the bonding of the carbene ligand affected by ligands of varying trans influence?

The solid state structures of five carbene complexes have been determined. All are of the form

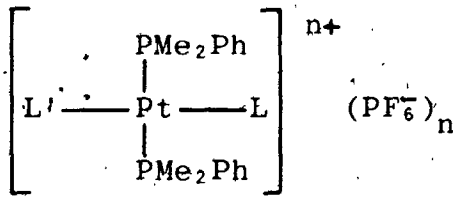

where L is a tertiary alkoxy- or alkylaminocarbene of type 3b (Fig. 1.1) and L' is a methyl, chloro, isocyanide or carbene ligand. Mutually trans phosphine ligands are present in all complexes so that L and L' have similar environments allowing intimate comparison of bonding and trans influence trends.

1.4 Structure Determination by X-ray Crystallographic Methods

The techniques employed in performing the X-ray experiment, from the time suitable crystals are selected to the time final atomic positional parameters are obtained are quite complicated, yet relatively standard from experiment to experiment in a given laboratory. To avoid repetition, this portion of a structure determination will be described in detail in Chapter 2 and will be summarized in the other sections of this work.

The general techniques and procedures involved in obtaining a good set of intensity data have been well described in several texts (73-75). In the past few years there have been major advances in the sophistication of X-ray equipment; so much so that virtually all steps in the procurement of an intensity data set have been automated. Levels of automation tend to vary from laboratory to laboratory. Because of this, the experimental techniques involved in obtaining a data set can vary considerably. Thus, it is felt by this author that a somewhat detailed description of the techniques used to collect the intensity data is warranted. Furthermore, a good knowledge of the experimental procedure followed and the care taken in implementing this procedure tends to instill in the reader an added level of confidence in the data, and thus, in the results of the experiment.

CHAPTER 2

THE CRYSTAL AND MOLECULAR STRUCTURE OF TRANS-METHYL(METHYL-N,N-DIMETHYLAMINOCARBENE)BIS(DIMETHYLPHENYLPHOSPHINE)PLATINUM(II) HEXAFLUOROPHOSPHATE

Trans-$[Pt\{CH_3C{=}{=}N(CH_3)_2\}CH_3\{P(CH_3)_2C_6H_5\}_2]PF_6$

2.1 Introduction

Chisholm and Clark have prepared a series of square planar cationic Pt(II) aminocarbene complexes by the reaction of simple primary and secondary amines such as $NHMe_2$ with the corresponding methoxycarbene species (64). In these complexes, the carbene ligand occupies a coordination site trans to a methyl ligand. Spectroscopic data indicate that both the methyl and carbene ligands exert a strong trans influence (67). There is also considerable interest in the bonding of the carbene ligand.

The X-ray crystal structure determination of the title complex was undertaken to examine the geometry of the carbene ligand and its mode of bonding to the metal atom, and to examine the extent to which each of the metal-carbon bonds is affected by the trans influence of the ligand opposite.

2.2 The X-ray Experiment

i. Photographic Examination

A sample of the complex was kindly supplied by Chisholm. Colourless blocks with prismatic faces were obtained by recrystallization from a dichloromethane/ether mixture. A single crystal with well developed faces was chosen and showed sharp extinctions under polarized light. The crystal was mounted on a glass fibre affixed to a goniometer head, such that a direction along which extinction occurred was approximately parallel to the length of the fibre. The goniometer head was then transferred to a Weissenberg camera. The crystal was first centered optically so that it was in line with the collimator, and the center of gravity remained coincident with the camera rotation axis as the crystal was rotated.

Oscillation photographs were recorded to align the crystal. Mirror symmetry indicating the presence of a mirror plane perpendicular to the axis of rotation was observed on these photographs. This observation rules out the presence of a triclinic lattice.

A series of Weissenberg photographs was then recorded, each over a sixteen hour period. No additional mirror symmetry was observed on these photographs. The conclusion to be drawn from this is that the compound crystallizes in a monoclinic space group, and that the rotation axis is the symmetry axis b. Zero, first and second level photographs were taken. These were projections of the $h0\ell$,

h1ℓ, and h2ℓ classes of reflections.

The goniometer head was then transferred to a precession camera. Since the b and b* axes are coincident in the monoclinic system, and since the rotation axis for Weissenberg photography was fortuitously b, there was little problem in aligning a reciprocal lattice axis with the precession camera rotation axis. A series of alignment photographs were taken to find the zones corresponding to the a*b* and b*c* nets. A series of precession photographs was then taken at the two zones, giving projections of the classes of reflections 0kℓ, 1kℓ, 2kℓ, and hk0, hk1, hk2. These photographs showed the presence of a mirror plane perpendicular to b*, thus confirming the lattice to be monoclinic. Measurement of the precession photographs provided data for a calculation of the unit cell parameters. These values agreed well with those obtained from the measurement of the Weissenberg photographs. The final unit cell parameters obtained from the photographic study are as follows:

a = 8.48 Å	α = 90.0°
b = 10.94 Å	β = 94.0°
c = 28.48 Å	γ = 90.0°
$a^* = 0.1182\ Å^{-1}$	α^* = 90.0°
$b^* = 0.09141\ Å^{-1}$	β^* = 86.0°
$c^* = 0.03519\ Å^{-1}$	γ^* = 90.0°

The Weissenberg and precession photographs were examined

carefully for systematic extinctions. Observed were: h0ℓ for ℓ odd, and 0k0 for k odd. These absences are only consistent with the space group $P2_1/c$, C_{2h}^5, No. 14 (76). The density of the crystals was measured by the flotation method (73) in a mixture of carbontetrachloride and 1,2dibromoethane. The value determined was 1.77(1) g cm^{-3}. The calculated density for four formula units in the unit cell is 1.76 g cm^{-3}. With this cell mass, no symmetry constraints are imposed upon the ions.

ii. Automated Data Collection

a. The Data Crystal

A thick prismatic crystal with sharp extinctions, well developed faces, and of similar morphology to that used for the photographic study was selected for the collection of intensity data.

The data crystal was mounted in a random orientation on a glass fibre which had been affixed to a brass pin with molten shellac. The brass pin was locked into place on a Nonius eucentric goniometer head. This mounting procedure was adopted to prevent crystal movement and to minimize the possibility of multiple diffraction (77).

Measurement of the crystal on a microscope fitted with a filar eyepiece showed the dimensions to be 0.39mm x 0.23mm x 0.17mm. In an optical goniometric study of the crystal, faces of the forms {001}, {110}, {011} and the individual faces (0$\bar{1}$0), (012) and (100) were identified. A diagram of the

crystal is shown in Fig. 2.1, and a summary of the crystal data is presented in Table 2.1.

b. Crystal Alignment and Centering

Since the advent of the modern automatic diffractometer about a decade ago, the degree of automation has increased markedly to the point where a large portion of the crystal alignment and centering operation, as well as all intensity data collection, can be performed under computer control. The extent of automation tends to vary somewhat from laboratory to laboratory.

The quality of the data obtained in this way is highly dependent on how well the crystal has been aligned and centered. This is probably the single most important step in the X-ray experiment.

A detailed description of the apparatus and of the crystal alignment and centering procedure employed, is therefore presented.

The goniometer head with the data crystal was transferred to the spindle axis of a Picker four circle computer controlled diffractometer. A photograph of the goniostat and a schematic diagram showing the four axes of rotation, 2θ, ω, χ, and ϕ are presented in Plate 1 and Fig. 2.2 respectively. The 2θ and ω circles are coaxial. With such an arrangement the crystal can be rotated to any orientation desired.

The X-ray source was a Dunlee fine focus X-ray tube, with

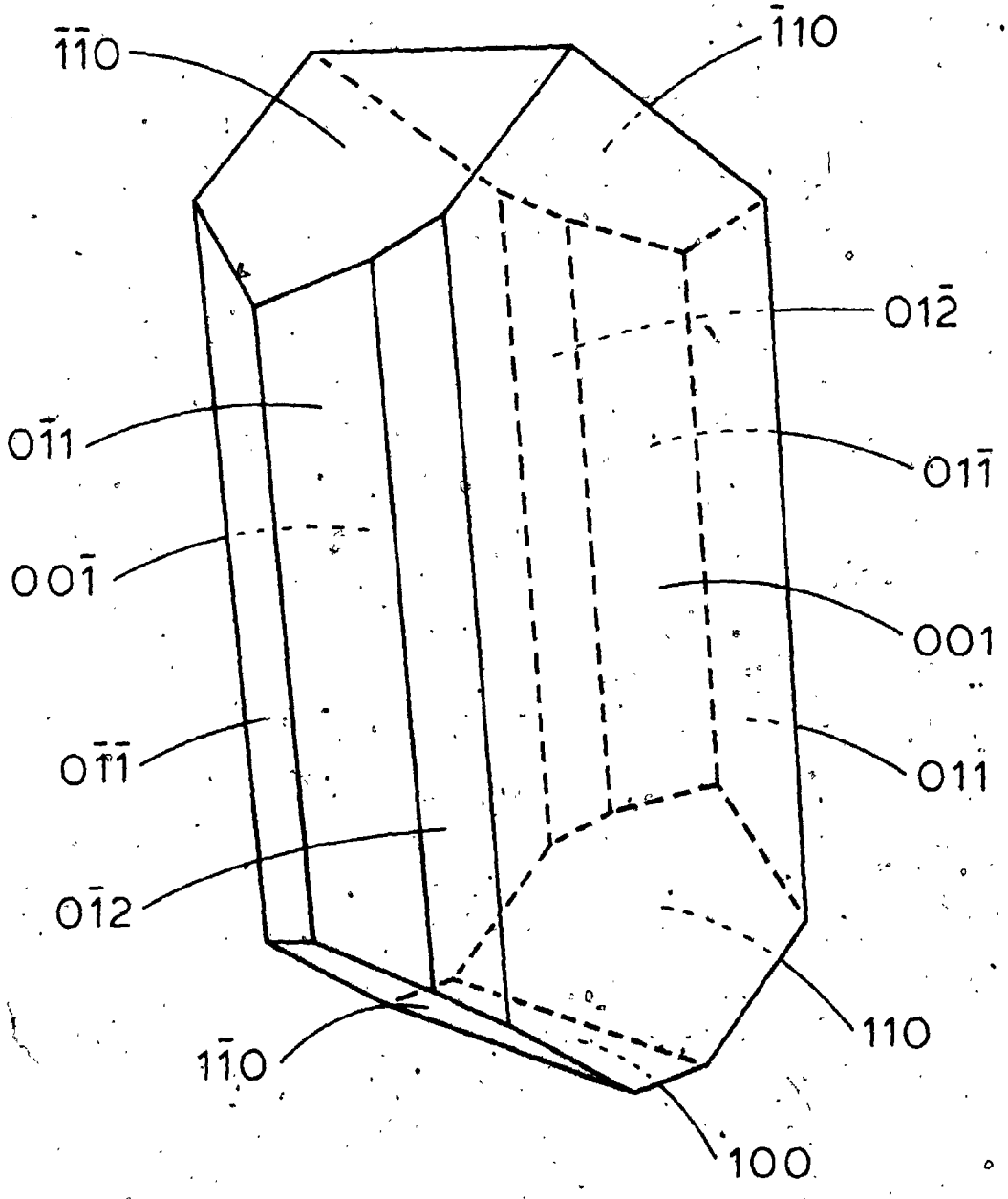

Fig. 2.1

A Drawing of the Data Crystal

Faces with dotted edges are hidden from view.

TABLE 2.1

Crystal Data for Trans-$[Pt(MeC{=}NMe_2)Me(PMe_2Ph)_2]PF_6$

$C_{21}H_{34}F_6NP_3Pt$	f.w. = 704.5
Analysis found (calculated)	C, 35.99 (35.90); H, 5.04 (4.88); N, 1.88 (1.99)
Crystal description	colourless blocks with prismatic faces
Systematic absences	$h0\ell$, $\ell \neq 2n$; $0k0$, $k \neq 2n$
Laue symmetry	2/m
Crystal system	monoclinic
Space group	$P2_1/c$, C_{2h}^5
Equivalent positions (4)	$\pm(x, y, z)$, $\pm(x, \frac{1}{2} + y, \frac{1}{2} - z)$
Cell constants	a = 8.515(2) Å, α = 90.0° b = 10.934(2) Å, β = 93.93(1)° c = 28.549(7) Å, γ = 90.0°
Cell volume	2652 Å^3
Wavelength used for cell determination	1.54056 Å
Temperature at which cell was determined	19°C
Method of density determination	flotation ($C_2H_4Br_2/CCl_4$)
Density (observed) (calculated)	1.77(1)g cm^{-3} 1.76g cm^{-3}
Z	4
Symmetry constraints	none

PHOTOGRAPHIC PLATE 1

The Picker FACS-1 Four Circle Diffractometer

Employed in this Study

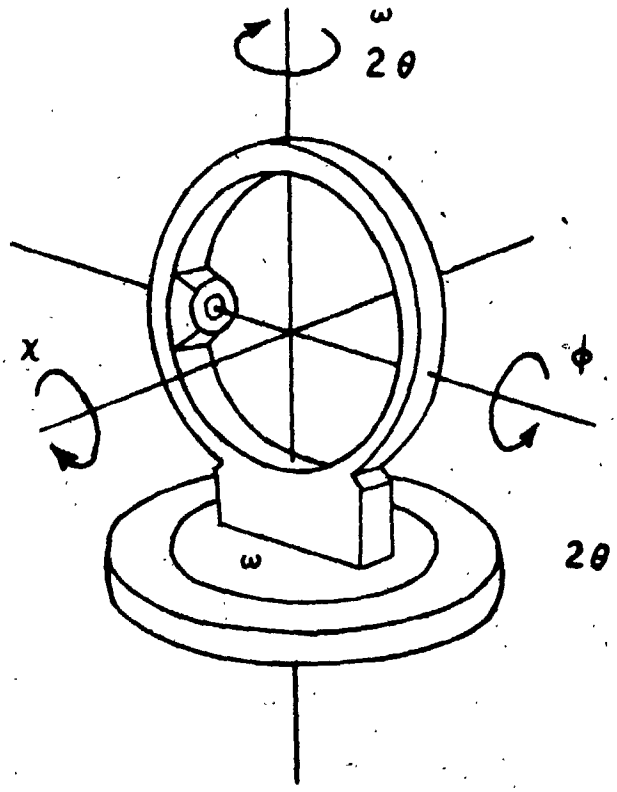

Fig. 2.2 Schematic Representation of the Goniostat

copper anode. Power to the X-ray source was provided by a stabilized power supply set at 40 kilovolts and 14 milliamps. The X-ray beam was directed to the crystal via a 1.0mm collimator. A pulse height discriminator, set to accept about 90% of the CuKα peak, and a nickel foil (0.018mm) filter placed between the crystal and the scintillation counter detecting device, gave approximately monochromatic CuKα radiation.

All automatic operation of the diffractometer was carried out by PDP8-L computer (78, 79). Except when drive motors are disengaged, all operations are controlled through the computer from a teletype.

By disengaging the proper drive motors on the goniostat, the crystal could be rotated manually about the spindle axis and the χ circle. The crystal was centered optically with respect to goniometer head translations and height such that the center of mass was at the point of intersection of the four rotation axes of the goniostat.

The next step was to determine the orientation of the crystal axes with respect to those of the diffractometer. At least two intense reflections had to be found. Since the crystal had been studied by optical goniometry, and the faces (001),(00$\bar{1}$) and (100) had been identified, the c* and a* axes should be readily found. With a wide open aperture, the detector was driven to the 2θ angle for the strong reflection 004. The crystal was rotated about the ϕ and χ axes to a point where the crystal faces (001) and (00$\bar{1}$) were

perpendicular to the diffraction vector. The shutter was opened. Slight adjustments were made to the χ and ϕ settings until intense radiation was detected. The angular settings were recorded. Similarly, the strong reflection 200 was found. The χ and ϕ drive motors were re-engaged; the aperture was closed to a narrow slit and accurate angular settings for 2θ, χ and ϕ were found by maximizing the intensity of the particular reflection, first on each individual rotation axis, and then the centering programs of Busing and Levy (78, 79), written for the PDP8-L computer were employed. Using the angular settings for the 2 reflections and the cell constants obtained from the photographic study, an orientation matrix was computed (79), from which approximate angular settings for other reflections could be obtained. The reflection 020 was then found quite readily at the computed angles.

2θ scans up each axis were recorded on a chart recorder, and the relative intensities of the axial reflections were compared successfully to those observed on the photographs. ω scans were recorded on the three low angle axial reflections to check the mosaicity of the crystal (80). These were performed with a wide open aperture and a take-off angle of 0.5° on the tube, a condition which yielded a narrow source. The average scan width at half height was found to be 0.079°, a satisfactory value (80).

The optical centering of the crystal was checked by centering a strong reflection at four different settings of

the goniostat. The reflection chosen for this was (104) (2θ = 16.79, χ = 27.44, ϕ = 234.78). This reflection was centered for the angular settings ($\pm 2\theta$, χ, ϕ) and ($\pm 2\theta$, 180.0 + χ, ϕ). Variations of the 2θ and ϕ angles at the four settings gave an indication of the centering with respect to the ϕ axis, while the variations in χ were used to decide if the crystal or x-ray tube had to be raised or lowered. No significant fluctuation of the setting angles at the four orientations was observed; hence, the crystal and tube positions were not changed.

In order to obtain a more accurate orientation matrix and thus more precise unit cell constants, 14 different reflections with high 2θ values ($23° < 2\theta < 65°$), and χ and ϕ settings spanning the ranges over which the data were to be collected, were centered. A narrow counter aperture and low take-off angle on the x-ray tube were used. The setting angles of these reflections were used to refine the orientation matrix and the cell parameters. The procedure was repeated until good agreement between observed and calculated setting angles was achieved. This refinement was carried out using the program PICKTT*. The unit cell parameters so obtained are presented in Table 2.1. Also obtained from the least-squares refinement was a χ zero value which allows for a systematic error in the programmed χ centering routines where χ is maximized at a value

---

* Details of computer programs are given in Appendix I.

intermediate between the $CuK\alpha_1$ and $K\alpha_2$ peaks, rather than at the $K\alpha_1$ peak. Estimated standard deviations on the refined parameters were also obtained.

The unit cell derived in this manner is a 'diffractometer cell' since the values obtained may be affected by systematic errors in the crystal alignment and centering, and by imperfections in the diffractometer itself (81).

c. Intensity Data Collection and Processing

In preparation for data collection, six intense reflections representative of the regions of reciprocal space over which the data were to be collected were chosen as standard reflections. These were carefully examined with respect to peak quality and intensity before and after data collection. Also, the intensities of these reflections were measured after every 100 reflections recorded throughout data collection. This served as a good method to monitor the electronic stability of the instrument, as well as any changes in the crystal itself. The standard reflections chosen were ($\bar{2}00$,200,020,004,241 and 441).

The aperture dimensions selected for data collection were 0.4cm x 0.4cm. The take-off angle on the source was chosen to be 1.5°. At this angle, the peak intensity of a strong reflection was about 80% of the maximum observed as a function of take-off angle. The data were collected by the $\theta - 2\theta$ scan technique. As the counter travels through the peak performing a 2θ scan of x degrees, it is

accompanied by a rotation of x/2 degrees about the ω axis. A scan rate of 1°/min was selected. The scan range was symmetric about the calculated 2θ value, being 0.5 degrees on both the high and low angle sides.

The 2θ value is calculated on the CuKα_1 peak, but the Kα radiation also has a Kα_2 component. A typical peak profile is shown in Fig. 2.3. The α_1 and α_2 peaks are separated by a dispersion angle Δ. This angle can become significant at high 2θ values so a dispersion correction dependent on the value of 2θ was applied to the scan width. With such a correction the scan would begin 0.5° below the Kα_1 peak and end 0.5° above the Kα_2 peak with an actual scan range of 0.5°+Δ°+0.5°.

Stationary counter, stationary crystal background counts of 10 seconds were taken at the start and end of each scan. Cu foil attenuators were inserted automatically when the intensity of the diffracted beam exceeded about 7000 counts/second during the scan. The thicknesses of the Cu foil were chosen to give attenuator factors of about 2.2, and these have been measured accurately.

The intensity data were collected in four shells over the 2θ range $2.5° \leq 2\theta \leq 90°$. All data in the index ranges h = 0 to 8, k = 0 to 10 and ℓ = -27 to 27 were collected.

Six days were required to obtain 3064 data. Collection was terminated at this point because the standard reflections showed a sudden decrease in intensity and peak quality. This occurred during the collection of those reflections for

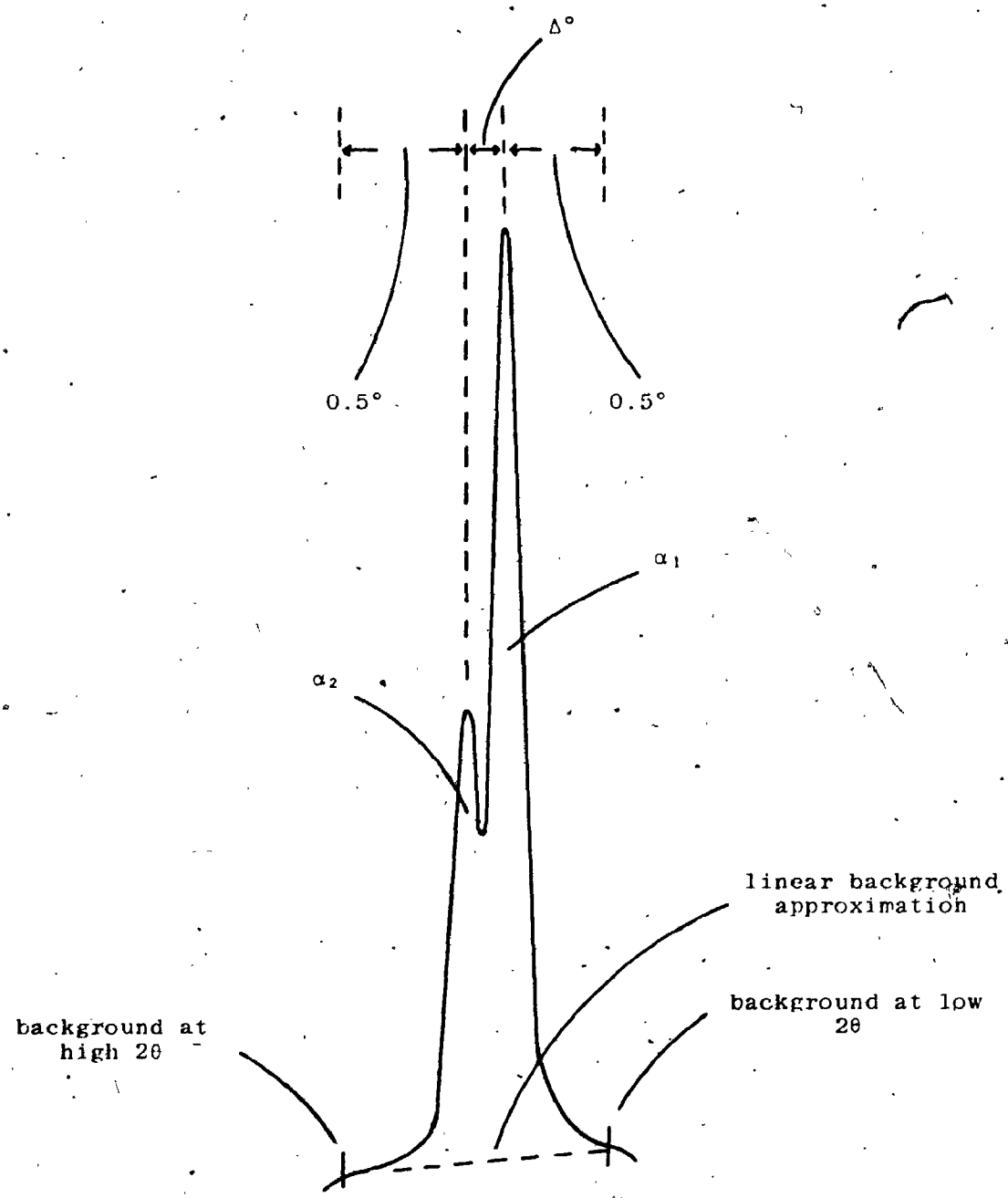

Fig. 2.3 Peak Profile of a Typical Reflection.

which $75° < 2\theta < 90°$. A careful examination of the standard reflections showed the first 2860 observations to be unaffected by the observed decomposition. Over the period that these intensities were recorded, 020 and 004 increased by 8% whereas the remaining standard reflections showed only slight fluctuations of less than 5%. The conditions for data collection are summarized in Table 2.2.

All 3064 data were processed using the program WOFACA. This procedure involved correcting the recorded intensities for background radiation, Lorentz, and polarization effects (75). The background radiation was accounted for by assuming a linear intensity relationship between the points at which stationary background counts were recorded. The Lorentz correction is related to the value of 2θ and arises because the time required for a reciprocal lattice point to pass though the sphere of reflection is not constant, but varies with its position in reciprocal space. The polarization correction, also related to 2θ, accounts for the fact that the diffracted ray is partially polarized. Reflection efficiency is dependent on the Bragg angle.

The net integrated intensity was calculated using the expression

$$I = CT - \tfrac{1}{2}(t_c/t_b)(B_1+B_2)$$

and standard deviations, $\sigma(I)$ were assigned to all data from the formula

$$\sigma(I) = [CT + 0.25(t_c/t_b)^2(B_1+B_2) + (pI)^2]^{\frac{1}{2}}$$

where I is the integrated intensity, CT is the integrated

TABLE 2.2

Experimental Conditions for Data Collection

Radiation		Cu Kα
Wavelength		1.54056 Å
Filter		Ni foil (0.018mm)
Mean ω scan width at half height (reflections)		0.079° (200, 020, 004)
Reflections centered, in 2θ range		14; 23° < 2θ < 65°
Scan range	a) low angle side of 2θ	0.5°
	b) high angle side of 2θ	0.5°
Scan rate		1.0° min^{-1}
Stationary background count time		10 sec
% available Bragg intensity obtained for a given reflection		80%
Take-off angle		1.5°
Tube KV; mA		40; 14
Collimator size		1.0mm
Crystal-counter distance		32cm
Crystal-aperture distance		30cm
Aperture dimensions		4mm x 4mm
2θ range		2.5° < 2θ < 90.0°
Shells (No.; high angle limit)		4; 40°, 60°, 75°, 90°
Index limits		$0 \leq h \leq 8$, $0 \leq k \leq 10$, $-27 \leq \ell \leq 27$
No. of data collected		3064
No. of data used		2860
p value		0.03
No. of reflections with $I > 3\sigma(I)$		1865
μ (Cu Kα)		115.5cm^{-1}
Crystal faces		{001}, {110}, {011}, $(0\bar{1}0)$, $(01\bar{2})$, (100)
Crystal dimensions		0.39mm x 0.23mm x 0.17mm
Absorption correction		gaussian
Transmission coefficients	a) minimum	0.147
	b) maximum	0.239

peak count obtained in time t_c, and B_1 and B_2 are the background counts obtained in time t_b. The value for p, the 'fudge factor' (81) was chosen to be 0.03.

All reflections with $I>3\sigma(I)$ were corrected for absorption. The absorption correction was performed using the Gaussian option of the program AGNOST (82). The absorption coefficient for Cu radiation for the complex was calculated to be $115.5cm^{-1}$. Values for μ/ρ were taken from Cromer and Liberman (83). The maximum and minimum transmission coefficients were observed to be 0.239 and 0.147 respectively, representing a variation of about 60%.

Of the 3064 data collected, only 2860 reflections were used in the actual structure solution and refinement. Of these, 1864 reflections had $F^2>3\sigma(F^2)$ and the final refinement was carried out on these observations only.

2.3 Structure Solution and Refinement

i. Structure Solution

The structure factor amplitudes are related to the observed intensities.

$$|F_o| \alpha \sqrt{I}$$

Thus, from the intensity data alone one cannot determine if F_o is positive or negative. A 'phase' must be assigned to each observation before an electron density map can be computed. To accomplish this the program FORDAP was utilized to compute a three dimensional Patterson function using the quantities F_o^2. From the Patterson maps the positions of three heavy atoms were calculated (Pt and two phosphine P atoms). These atoms account for 31% of the electrons in the unit cell and thus 31% of the scattering. These atom positions were used to 'phase' the model.

One cycle of least-squares refinement on the Pt and 2 P atoms was calculated using the program WOCLS. The parameters varied were an overall scale factor and the x, y and z coordinates of the atoms. The functions being minimized in the least-squares refinement are the agreement factors R_1 and R_2.

$$R_1 = \frac{\Sigma(||F_o|-|F_c||)}{\Sigma|F_o|} \qquad R_2 = \left(\frac{\Sigma w(|F_o|-|F_c|)^2}{\Sigma w F_o^2}\right)^{\frac{1}{2}}$$

where $|F_o|$ and $|F_c|$ are the observed and calculated structure factor amplitudes and w is the weight given by $4F_o^2/\sigma^2(F_o^2)$. The general expression for $|F_{hk\ell}|$ and the equations for the isotropic and anisotropic thermal parameters are presented

in Appendix II.

The agreement factors R_1 and R_2 were calculated to be 0.357 and 0.480 respectively after the first cycle of least-squares refinement. A series of difference Fourier syntheses (calculated using the program FORDAP) and least-squares cycles produced positional parameters for the remaining non-hydrogen atoms in the formula unit.

The scattering factors f, describe the x-ray scattering of the various atoms present in the molecule as a function of $\lambda^{-1}\sin\theta$. In all calculations the values for Pt, P, F, N, and C were those obtained by Cromer and Waber (84). H atom scattering factors were taken from Stewart, Davidson, and Simpson (85). The effects of anomalous dispersion for Pt and P atoms were included in the calculations of F_c (86). The values of $\Delta f'$ and $\Delta f''$ were those calculated by Cromer and Liberman (83).

ii. Rigid Group Refinement

For compounds which contain a large number of atoms the computing expenses involved in calculating least-squares cycles can be immense, especially if all atoms are refined with anisotropic thermal parameters. This large expense is in fact wasted if it is used to examine entities whose structures are already well known. Furthermore, the amount of available computer "core" often limits the number of parameters that can be varied in least-squares calculations. Rigid group refinement can be undertaken to reduce

both computing costs and 'core' requirements.

Least-squares refinement of a rigid group of atoms involves maintaining the internal geometry of the group, and changing only its position and orientation with respect to the unit cell origin and axes. Each rigid group has its own origin and its own orthonormal coordinate system. The positions of the atoms in the rigid group are defined in terms of this coordinate system. The group system is related to the crystallographic one by the position of the group origin in crystallographic coordinates (x_g, y_g, z_g) and by three angles ($\delta, \varepsilon, \eta$) (87) which relate the group axial directions to those of the crystallographic axes. These six parameters are varied in the least-squares calculations. The temperature factors of the group atoms can be combined as an overall group isotropic thermal parameter (where all individual group atom thermal parameters are set equal to the calculated overall value), or as individual isotropic group atom temperature factors. Overall values are refined in the early stages of a structure solution and the individual isotropic parameters in the later stages of the experiment. Rigid group constraints can be readily removed at any time during the structure solution in favour of individual atom refinement. This is often done if significant distortions from ideal geometry are expected.

In the complex examined in this chapter the phosphine phenyl rings and the six F atoms of the PF_6 anion were

refined as rigid groups. The two phenyl rings were assumed to have D_{6h} symmetry, and a C-C bond distance of 1.392 Å (88). The center of gravity of the phenyl ring was selected as the group origin. In order to give the PF_6 anion some degree of freedom, and to allow for the anomalous dispersion of the P atom, only the six F atoms were refined as a rigid group with O_h symmetry. The origin was chosen as the center of the octahedron, and each F atom was calculated to be 1.58 Å from that point. The six orientation parameters as well as an overall isotropic temperature factor were refined for each group. Individual isotropic thermal parameters were calculated for phenyl C atoms later in the experiment. Hence, the number of parameters varied for one rigid group can be seven or twelve compared with fifty-four in the case of individual atom anisotropic refinement.

When the three rigid groups were incorporated into full matrix least-squares calculations, together with the other non-hydrogen atoms, agreement factors $R_1 = 0.083$ and $R_2 = 0.141$ were obtained after two cycles of refinement. Only the Pt and two phosphine P atoms were allowed to vibrate anisotropically. Overall group thermal parameters were refined.

iii. Rigid Group Refinement and the Disorder Problem

When the positions of all non-hydrogen atoms had been determined, and refined to give a chemically reasonable geometry, a difference Fourier synthesis was calculated

over the unique region of the unit cell to make certain that all major peaks of electron density had been accounted for. Six peaks of density greater than 2.0 $e\text{Å}^{-3}$ were observed in the region of the PF_6 anion. As these form a second octahedron about the P atom, disorder of the anion is present. The occurrence of disorder of ions such as PF_6^-, SbF_6^-, ClO_4^- etc. is not an uncommon feature of solid state structures of ionic complexes paired with these ions. The highly symmetrical ions present a virtually spherical profile. Because of this they can often occur in more than one orientation in the crystal lattice.

In situations such as this where a whole group of atoms can occupy any one of several closely related orientations in the lattice, constraints often have to be applied in order to achieve a successful refinement. This is especially true if the electron density maps show that the two possible orientations overlap to some extent. To apply the desired constraints, rigid group refinement can readily be adopted if the structure of the disordered entity is well known.

To account for the disorder of the PF_6 ion, a second rigid group of six F atoms was refined. An occupancy factor for the two F6 groups was introduced such that the total multiplicity of the two rigid groups equalled 1.0. The individual atom occupany factors were constrained to equal the overall group value. The appropriate constraints to the derivatives were also applied. The normal positional

parameters were refined for each rigid group. Initially, the overall thermal parameter of only one F6 group was refined, to which that of the second was equated. On successful refinement of the disorder model this constraint was removed and overall thermal parameters were varied for both F6 rigid groups. Inclusion of the final disorder model in two cycles of least-squares refinement where 162 parameters were varied with respect to 1865 observations produced agreement factors $R_1 = 0.050$ and $R_2 = 0.077$. This calculation was performed with all non-group atoms except the P atom of the anion allowed to vibrate anisotropically. Individual group atom thermal parameters were varied for the phenyl rigid groups.

iv. Hydrogen Atom Contributions

The cation contains thirty-four H atoms. Hence, the scattering due to thirty-four electrons per cation had not yet been included in the model. This comprises a significant portion of the X-ray scattering, being roughly equivalent to the scattering of two P atoms. It was, therefore, felt that if evidence of H atoms could be observed in electron density maps, then their presence should be accounted for in the final model.

Fourier sections were calculated for each of the eight methyl groups in the cation. These electron density maps were calculated for the planes in which the methyl H atoms were expected to lie. Each Fourier section contained three

major peaks. Positional parameters were calculated to correspond best to the peak positions, utilizing the known geometry of a methyl group with a C-H distance 1.09 Å and a H-C-H angle of 109.47°. The program METHROT was used to accomplish this calculation. Contributions to F_c were obtained for all 24 methyl H atoms. The contributions of the ten phenyl H atoms to F_c were calculated utilizing the known geometry of a phenyl ring. A C-H distance of 1.049 Å was assumed. All hydrogen atoms were assigned temperature factors of 4.0 $Å^2$.

After two cycles of full matrix least-squares refinement where hydrogen parameters were included, but not refined, the C-H geometries were examined. Some substantial shifts were observed in some of the methyl C atom positions. This is not surprising since a C atom has only six electrons, and a further three electrons due to nearby H atoms had not previously been included. The H atom positional parameters were recalculated on the basis of the new C atom positions. Further refinement and examination showed negligible deviations from ideal geometry.

v. Final Refinement

The conditions for the final cycles of full matrix least-squares refinement were as follows. All non-group non-hydrogen atoms except for the P atom of the anion were refined with anisotropic thermal parameters. The phenyl ring group atoms were refined with individual isotropic

temperature factors. An overall thermal parameter was refined for each F6 group. H atom contributions were calculated as described above and incorporated in the final least-squares calculations.

For low angle reflections F_o was observed to be consistently smaller than F_c. This was considered to be a result of secondary extinction (89). An extinction coefficient was, therefore, refined in the final least-squares calculations. The final value obtained for this parameter was $3.8(4) \times 10^{-6}$. The expression for secondary extinction is given in Appendix II.

Two full matrix least-squares cycles varying 162 parameters and employing 1865 observations converged the final model generating agreement factors $R_1 = 0.041$ and $R_2 = 0.062$. A summary of the conditions and results of the final least-squares cycles is presented in Table 2.3. The final individual atom positional and thermal parameters are shown in Table 2.4. Rigid group parameters are given in Table 2.5. Refinement of the disorder multiplicity parameter for the PF_6 anion gave a value of 0.50(2).

A statistical examination of the structure factors in terms of various combinations of Miller indices, magnitudes of F_o, $\lambda^{-1}\sin\theta$, and diffractometer setting angles was calculated using the program RANGER. No abnormal trends were observed in the data, suggesting an adequate weighting scheme. The largest peak on a final difference Fourier synthesis calculated over the unique region of the unit cell

TABLE 2.3

Conditions and Results of Final Full Matrix Least-Squares Calculations

Observations	1865
Variables	162
Ratio (observations/variables)	11.5
Rigid groups	4
Disorder models (No.; entities)	1; PF_6 anion
Non-group atoms	14
a) Anisotropic	13
b) Isotropic	1
H atoms included; No. (type)	34; 24(methyl), 10(phenyl)
Extinction coefficient	$3.8(4) \times 10^{-6}$
Maximum value of (parameter shift/standard deviation)	0.185
Agreement factors R_1	0.041
R_2	0.062
Final error on an observation of unit weight	3.51
Final difference Fourier synthesis:	
a) Position of largest peak	(-0.200, 0.150, 0.380)
b) Electron density	0.76(4)
c) Associated with	disordered PF_6 anion

TABLE 2.4

Individual Atom Positional and Thermal Parameters

Atom	x	y	z	U_{11}[a]	U_{22}	U_{33}	U_{12}	U_{13}	U_{23}
Pt	-0.25377(6)[b]	0.16554(4)	0.15203(2)	459(7)	367(5)	385(5)	-39(2)	62(3)	15(2)
P(1)	-0.1603(4)	0.0439(3)	0.0946(1)	625(26)	387(19)	437(19)	19(17)	72(17)	1(15)
P(2)	-0.3607(4)	0.2741(3)	0.2105(1)	477(25)	521(21)	377(18)	-30(18)	81(15)	-8(16)
P(3)	-0.3485(4)	0.1853(3)	0.4178(1)	597(11)					
N	-0.1915(15)	0.3900(9)	0.0971(4)	860(105)	454(72)	620(74)	88(70)	259(73)	113(63)
C(1)	-0.3705(16)	0.0076(10)	0.1777(4)	837(105)	400(73)	567(78)	-121(69)	219(70)	-42(63)
C(2)	-0.1359(18)	0.3182(10)	0.1290(5)	796(128)	316(80)	600(89)	41(72)	122(83)	-95(70)
C(3)	0.0287(16)	0.3458(10)	0.1510(5)	484(105)	524(86)	722(92)	-123(65)	-13(79)	-41(63)
C(4)	-0.3492(17)	0.3707(12)	0.0732(4)	580(111)	737(92)	560(84)	145(80)	44(79)	235(72)
C(5)	-0.1093(19)	0.5007(12)	0.0804(5)	1290(143)	462(86)	971(108)	-193(88)	421(98)	248(82)
C(11)	-0.3026(14)	0.0195(10)	0.0460(4)	606(99)	523(83)	689(86)	-153(68)	-54(71)	-88(66)
C(12)	-0.1043(15)	-0.1109(11)	0.1104(4)	695(104)	493(81)	797(94)	161(75)	160(76)	37(73)
C(21)	-0.5680(16)	0.3030(12)	0.1991(5)	486(107)	779(96)	971(109)	-103(78)	231(81)	-188(84)
C(22)	-0.3446(18)	0.2009(12)	0.2685(4)	1145(132)	644(89)	483(81)	-129(87)	276(82)	-2(70)

[a] The U_{ij}'s are the thermal parameters in terms of mean-square amplitudes of vibration in $\AA^2$. Values are given as U x 10^4. The expression for the thermal ellipsoid is given in Appendix II.

[b] Numbers in parentheses given here and in other tables are estimated standard deviations in the least significant digits.

TABLE 2.5

Rigid Group Parameters

Group	x_g[a]	y_g	z_g	δ	ϵ	η	Multiplicity
Ph-1	0.1421(7)	0.1694(5)	0.0543(2)	-2.234(6)	-2.425(5)	-2.630(6)	
Ph-2	-0.2044(6)	0.5392(5)	0.2273(2)	-2.124(7)	-2.298(5)	3.006(7)	
1-F6	-0.3493(9)	0.1855(7)	0.4186(3)	3.363(10)	2.316(6)	-3.367(11)	0.50(2)
2-F6	-0.3471(10)	0.1853(7)	0.4181(3)	-1.992(10)	-2.529(8)	-2.179(8)	0.50(2)

[a] x_g, y_g, and z_g are the fractional coordinates of the group origin, and δ, ϵ, and η (radians) are the group orientation angles.

had an electron density of 0.76(4) $e\mathring{A}^{-3}$. This peak is located at (-0.200,0.150,0.380) and is associated with the PF_6 anion. This indicates that the disorder model is not an exact representation of the disorder present. The calculated model does, however, account for an overwhelming portion of the electron density.

The derived positional parameters of the group atoms are given in Table 2.6 and calculated H atom positions are shown in Table 2.7. A list of the observed and calculated structure amplitudes, obtained using the program LIST, and given as $10|F_o|$ and $10|F_c|$ (electrons), is presented in Appendix III. The program PUBLISH was used to obtain atom and group thermal and positional parameters and their standard deviations in tabular form.

TABLE 2.6

Derived Group Atom Parameters

	Atom	x	y	z	B(Å²)	
Ph-1						
	1C(1)[a]	0.0126(8)	0.1071(7)	0.0696(3)	3.8(2)	
	1C(2)	0.1618(10)	0.0871(7)	0.0915(2)	5.0(3)	
	1C(3)	0.2913(8)	0.1494(8)	0.0762(3)	6.2(3)	
	1C(4)	0.2716(9)	0.2318(8)	0.0391(3)	6.0)3)	
	1C(5)	0.1225(11)	0.2518(7)	0.0172(2)	5.8(3)	
	1C(6)	-0.0070(8)	0.1895(7)	0.0324(3)	4.4(3)	
Ph-2						
	2C(1)	-0.2757(9)	0.4252(5)	0.2214(3)	3.6(2)	
	2C(2)	-0.1597(9)	0.4436(6)	0.2576(2)	5.1(3)	
	2C(3)	-0.0885(8)	0.5577(8)	0.2635(3)	5.9(3)	
	2C(4)	-0.1332(10)	0.6533(6)	0.2332(3)	6.0(4)	
	2C(5)	-0.2491(10)	0.6348(6)	0.1970(3)	5.4(3)	
	2C(6)	-0.3204(8)	0.5208(7)	0.1911(2)	3.9(3)	
1-F6						
	1F(1)	-0.1657(9)	0.1933(12)	0.4309(5)		
	1F(2)	-0.3216(15)	0.0899(10)	0.3785(4)		
	1F(3)	-0.3606(18)	0.0774(9)	0.4549(4)	B(group) = 8.8(4)	
	1F(4)	-0.3770(15)	0.2810(9)	0.4587(4)		
	1F(5)	-0.3380(18)	0.2936(9)	0.3823(4)		
	1F(6)	-0.5329(9)	0.1777(12)	0.4063(5)		
2-F6						
	2F(1)	-0.2235(15)	0.2327(14)	0.3836(4)		
	2F(2)	-0.2082(15)	0.1369(13)	0.4529(4)		
	2F(3)	-0.3401(17)	0.3129(9)	0.4441(5)	B(group) = 9.5(4)	
	2F(4)	-0.4860(14)	0.2336(13)	0.3833(4)		
	2F(5)	-0.3537(16)	0.0576(9)	0.3921(4)		
	2F(6)	-0.4707(15)	0.1378(13)	0.4526(4)		

[a] Ring C atoms are numbered sequentially. 1C(1) is bonded to P(1).

TABLE 2.7

Derived Hydrogen Atom Positional Parameters

Atom	x	y	z
	Methyl Hydrogen Atoms		
C(1)-H1	-0.3648	-0.0671	0.1526
C(1)-H2	-0.3133	-0.0200	0.2114
C(1)-H3	-0.4937	0.0297	0.1822
C(11)-H1	-0.3432	0.1085	0.0319
C(11)-H2	-0.2189	-0.0312	0.0184
C(11)-H3	-0.4027	-0.0309	0.0575
C(12)-H1	-0.1938	-0.1512	0.1311
C(12)-H2	-0.0924	-0.1644	0.0789
C(12)-H3	0.0083	-0.1092	0.1315
C(21)-H1	-0.6303	0.2160	0.1963
C(21)-H2	-0.6100	0.3546	0.2289
C(21)-H3	-0.5878	0.3552	0.1673
C(22)-H1	-0.2242	0.2084	0.2838
C(22)-H2	-0.4243	0.2456	0.2914
C(22)-H3	-0.3765	0.1044	0.2648
C(3)-H1	0.0668	0.2720	0.1748
C(3)-H2	0.1104	0.3538	0.1234
C(3)-H3	0.0273	0.4317	0.1705
C(4)-H1	-0.4144	0.2993	0.0910
C(4)-H2	-0.4208	0.4552	0.0730
C(4)-H3	-0.3423	0.3421	0.0364
C(5)-H1	0.0064	0.5117	0.1015
C(5)-H2	-0.0828	0.4942	0.0436
C(5)-H3	-0.1763	0.5848	0.0853
	Phenyl Hydrogen Atoms[a]		
1-H(2)	0.1765	0.0252	0.1197
1-H(3)	0.4038	0.1337	0.0926
1-H(4)	0.3695	0.2778	0.0273
1-H(5)	0.1077	0.3134	-0.0109
1-H(6)	-0.1196	0.2049	0.0162
2-H(2)	-0.1263	0.3718	0.2805
2-H(3)	-0.0013	0.5720	0.2908
2-H(4)	-0.0794	0.7394	0.2375
2-H(5)	-0.2823	0.7066	0.1739
2-H(6)	-0.4073	0.5064	0.1636

[a] Ring H atoms are numbered sequentially. 1-H(2) is bonded to 1C(2), 1-H(3) is bonded to 1C(3), etc.

2.4 Description of the Structure

An ORTEP diagram showing the final structure and atom labelling scheme of the cation is shown in Fig. 2.4. In Fig. 2.5 is a view of the inner coordination sphere of the metal atom and of the carbene ligand. Fig. 2.6 gives a stereoview of the cation. The shapes and sizes of the atoms in all diagrams are determined by the final isotropic and anisotropic thermal parameters drawn at the 50% probability level.

A selection of intramolecular bond distances and angles, including standard deviations as estimated from the inverse matrix is presented in Table 2.8. These quantities were calculated using the program ORFFE. The shortest cation-anion distance is 3.18 Å between atoms C(5) and 1F(1). This distance is of the magnitude expected for the packing of discrete anionic and cationic components. The PF_6 anion occupies two equally probably orientations in the lattice. The P-F distances range from 1.56(1) to 1.60(1) Å; a slight distortion from the value of 1.58 Å observed for $NaPF_6$ (90, 91). F-P-F angles range from 88.7(6)° to 91.3(6)° where a value of 90.0° is expected, and from 178.1(6)° to 179.0(7)° where 180.0° is the ideal value. Deviations result since the P atom is not constrained to lie at the center of gravity of the F6 octahedron.

The cation has an approximately square planar geometry. The Pt atom, two phosphine P atoms, C(methyl) atom and the

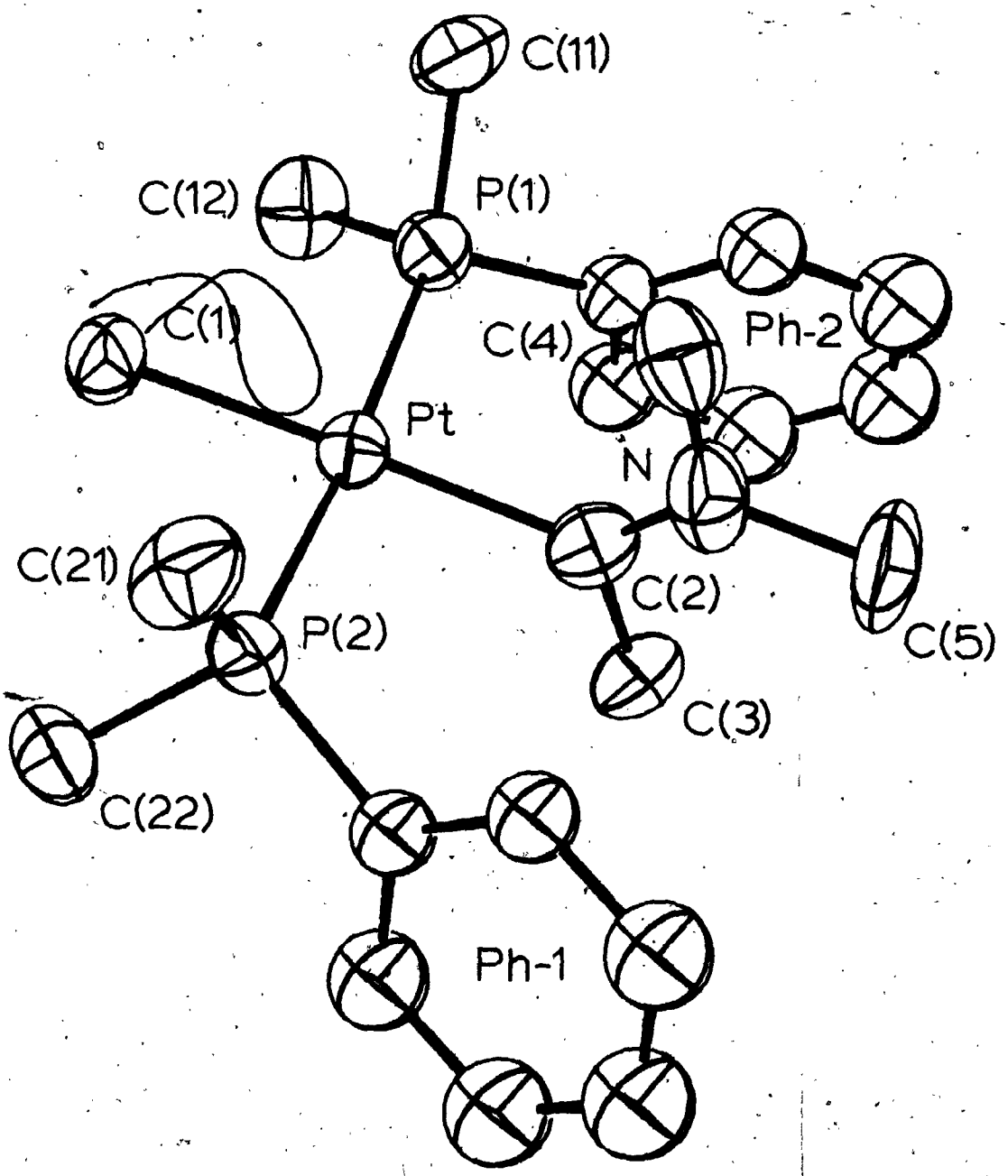

Fig. 2.4

An ORTEP View of the Cation Showing the Atom Numbering Scheme. 50% probability ellipsoids are drawn.

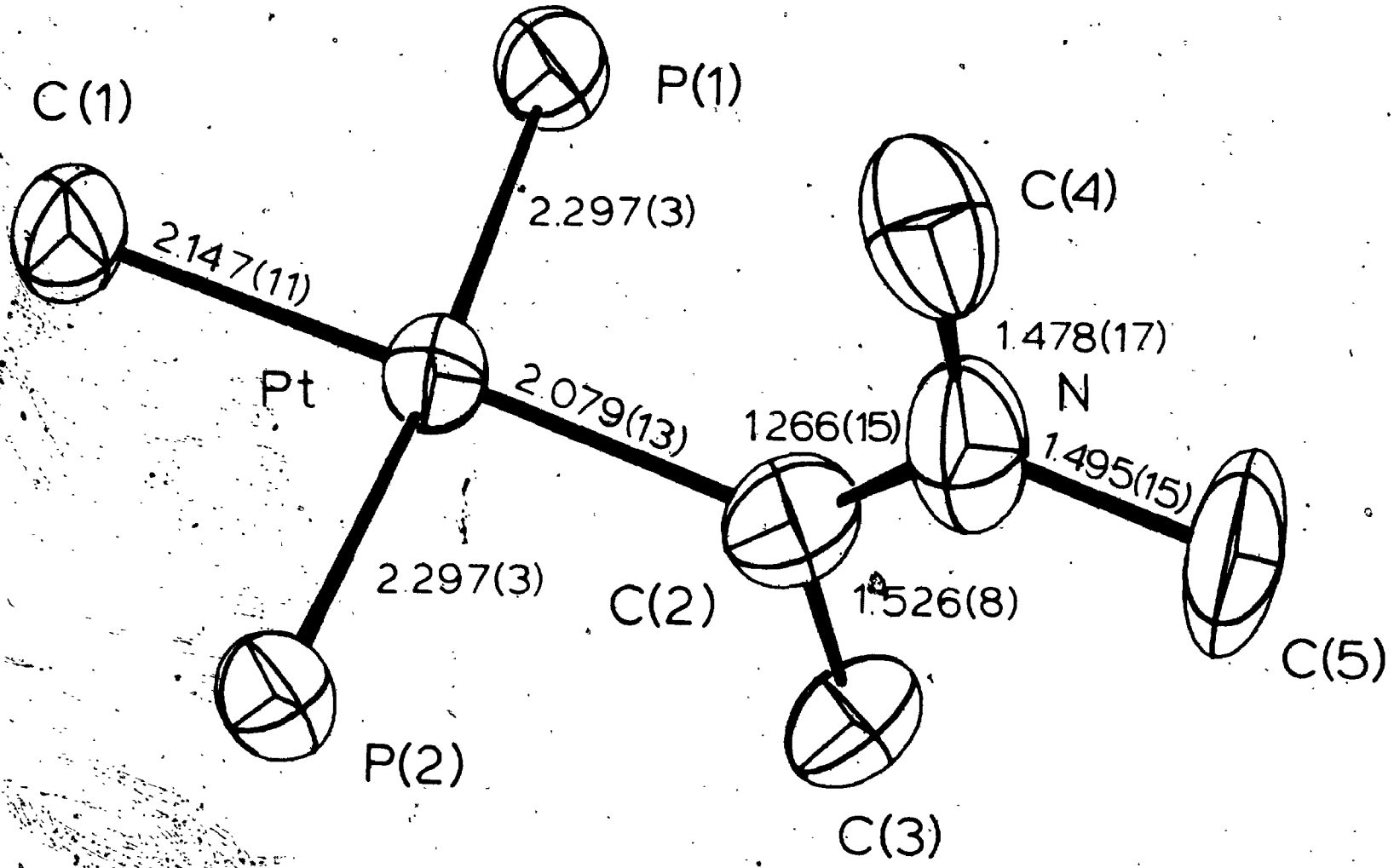

Fig. 2.5

The Carbene Ligand and the Inner Coordination Sphere of the Metal Atom

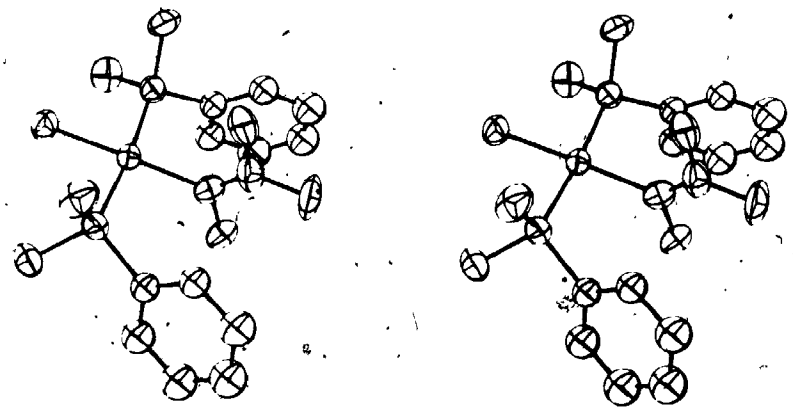

Fig. 2.6

A Stereoview of the Cation

TABLE 2.8

Selected Intramolecular Bond Distances and Angles

DISTANCES(A)		ANGLES(deg.)	
Metal Atom Inner Coordination Sphere			
Pt-P(1)	2.297(3)	P(1)-Pt-P(2)	175.3(1)
Pt-P(2)	2.290(3)	C(1)-Pt-C(2)	178.3(5)
Pt-C(1)	2.147(11)	C(1)-Pt-P(1)	88.3(3)
Pt-C(2)	2.079(13)	C(1)-Pt-P(2)	87.2(3)
		C(2)-Pt-P(1)	92.3(3)
		C(2)-Pt-P(2)	92.3(3)
Phosphine Ligands			
		Pt-P(1)-C(11)	112.9(4)
P(1)-C(11)	1.796(12)	Pt-P(1)-C(12)	117.6(4)
P(1)-C(12)	1.806(13)	Pt-P(1)-1C(1)	113.0(3)
P(1)-1C(1)	1.819(8)	Pt-P(2)-C(21)	113.2(5)
P(2)-C(21)	1.801(15)	Pt-P(2)-C(22)	115.1(4)
P(2)-C(22)	1.834(13)	Pt-P(2)-2C(1)	114.8(3)
P(2)-2C(1)	1.821(8)	C(11)-P(1)-C(12)	101.9(6)
		C(11)-P(1)-1C(1)	105.8(5)
		C(12)-P(1)-1C(1)	104.3(6)
		C(21)-P(2)-C(22)	104.5(7)
		C(21)-P(2)-2C(1)	104.1(6)
		C(22)-P(2)-2C(1)	103.9(5)
Carbene Ligand			
C(2)-N	1.266(15)	Pt-C(2)-N	124(1)
C(2)-C(3)	1.526(18)	Pt-C(2)-C(3)	118.6(9)
N-C(4)	1.478(17)	C(2)-N-C(4)	122(1)
N-C(5)	1.495(15)	C(2)-N-C(5)	125(1)
		C(4)-N-C(5)	113(1)
		N-C(2)-C(3)	117(1)

carbene C(sp^2) atom define an equatorial plane. A weighted least-squares plane given in Table 2.9 has been calculated through these atoms. The C(methyl) atom is found to lie 0.043(13) Å above this plane. Some distortion also occurs in the equatorial plane itself. The phosphine ligands are bent back away from the carbene ligand, for the P(1)-Pt-P(2) angle is 175.3(1)° while the mean C(1)-Pt-P angle is 87.8(5)°. The two Pt-P distances are equivalent, as would be expected since both phosphine ligands are in similar environments. The mean bond length is 2.294(3) Å.

The phosphine ligands are oriented similarly with respect to an approximate mirror plane through the Pt, C(methyl) and the carbene ligand, and the two phenyl rings occupy positions on the same side of the Pt atom as the carbene. The phosphorus to phenyl ring bonds lie almost in the equatorial plane of the metal atom, and the planes of the phenyl rings, Ph-1 and Ph-2, are oriented at angles of 85° and 75° with respect to the equatorial plane. The phenyl rings were constrained as rigid groups during refinement, and the internal geometry is fixed as described. Variation in the angles that the phenyl ring makes with the P-C(phenyl) bond can occur, however. The orientation is described in terms of the angles P(1)-1C(1)-1C(2), P(1)-1C(1)-1C(6), and P(1)-1C(1)-1C(4) for Ph-1, and the corresponding angles for Ph-2 as shown below. In an ideal situation these angles would be 120.0°, 120.0° and 180.0° respectively. In the final structure the angles are: 121.1(6)°, 119.2(6)°,

TABLE 2.9

Weighted Least-Squares Planes

Atom	Deviation from Plane(Å)
Atoms included: Pt, P(1), P(2), C(1), C(2)	
Equation of Plane: 6.441x - 2.436y + 15.98z = 0.391	
Pt	0.0007(5)
P(1)	-0.019(3)
P(2)	-0.018(3)
C(1)	0.043(13)
C(2)	0.019(16)
Atoms included: N, C(2), C(3), C(4), C(5)	
Equation of Plane: 3.88x - 6.067y - 20.74z = 5.126	
N	0.002(10)
C(2)	-0.008(12)
C(3)	0.006(13)
C(4)	0.004(13)
C(5)	-0.004(14)

and 172.1(4)°, for Ph-1 and 120.6(5)°, 119.2(5)° and 176.3(4)° for Ph-2. Some significant distortion occurs in that the phenyl rings are bent in towards the carbene ligand by a small amount. The two methyl C atoms on each phosphine ligand lie above and below the square plane of the Pt. Both ligands exhibit a distorted tetrahedral geometry. The six P-C distances are equivalent, having a mean value of 1.812(6) Å. Distortion of the phosphine ligands from ideal tetrahedral geometry is exemplified by the mean Pt-P-C angle of 114.4(7)° and by the mean C-P-C angle of 104.1(5)°. 109.47° is the ideal tetrahedral value.

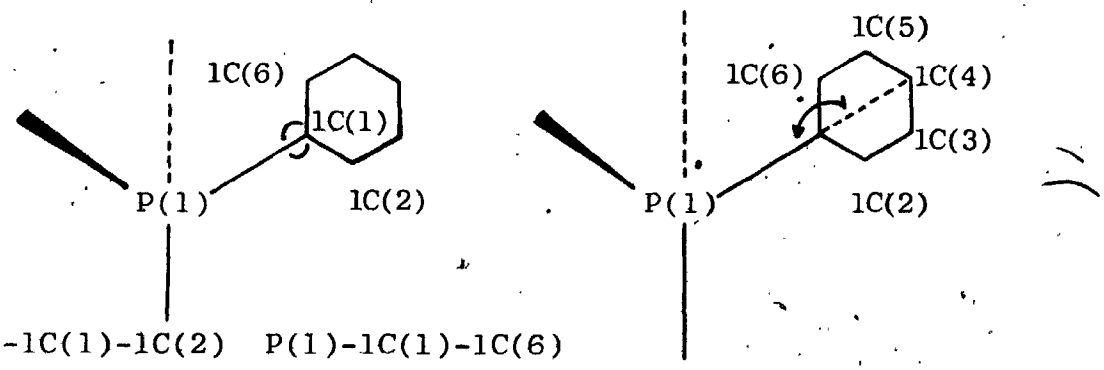

P(1)-1C(1)-1C(2) P(1)-1C(1)-1C(6)

P(1)-1C(1)-1C(4)

The carbene ligand is planar and coordinated to the metal atom via the trigonal C(sp^2) atom. A weighted least-squares plane has been calculated through the atoms of the carbene ligand as shown in Table 2.9. The C(sp^2) atom deviates most from the plane (0.008(12) Å). An angle of 87.3(4)° is observed between the plane of the carbene ligand and the equatorial plane of the metal atom. The Pt-C(sp^2) distance is 2.079(13) Å. N-C(methyl) distances of 1.478(17) Å and 1.495(15) Å are found to atoms C(4) and C(5) respectively,

and a $C(sp^2)$-C(methyl) distance of 1.526(18) A is observed. The $C(sp^2)$-N distance is 1.266(15) Å, indicative of considerable multiple bond character. Bond angles about C(2) exemplify the sp^2 character; the mean value being 120(2)°. The N atom also displays sp^2 hybridization. The angles about this atom are C(2)-N-C(4)=122(1)°, C(2)-N-C(5)=125(1)°, and C(4)-N-C(5)=113(1)°. Also, the N atom and the atoms bonded to it are coplanar as indicated by the weighted least-squares plane calculated through the carbene ligand (Table 2.9).

Trans to the carbene is the methyl ligand. The C atom is 2.147(11) Å away from the Pt atom.

2.5 Discussion

Dimethylphenylphosphine is a very interesting ligand due to its symmetry. The phenyl ring is a considerably more bulky substituent than the two methyl groups. Such a dissymmetry might be expected to be a large factor in determining the orientation of the phosphine ligand in the solid state, if steric factors are to come into play. In complexes of this type, the substituents cis to the phosphines, which in this case are the methyl and the carbene ligands, seem to exert little steric influence on the phosphines. Thus, the phenyl rings of the phosphine ligand both lie on the carbene side of the cation as is seen in Fig. 2.4. The complexes trans-[Pt(MeC=OMe)Me(PMe_2Ph)$_2$]PF_6 and trans-[Pt(MeC≡CMe)Me(PMe_2Ph)$_2$]PF_6 have been examined by X-ray crystallographic methods (92, 93). These compounds also have mutually trans phosphines occupying positions cis to a methyl ligand. The fourth coordination site in the square plane is occupied by a methylmethoxycarbene ligand in the former and by a dimethylacetylene ligand in the latter. In these complexes the carbene and acetylene ligands lie perpendicular to the square plane, but the phosphine orientations are quite different from those in the complex under study. For these compounds the phenyl substituents of the phosphine ligands lie on the methyl side of the Pt atom. This corresponds to approximately a 180° rotation about the metal phosphorus bond and is somewhat surprising since the two carbene

complexes are related to one another by the reaction:

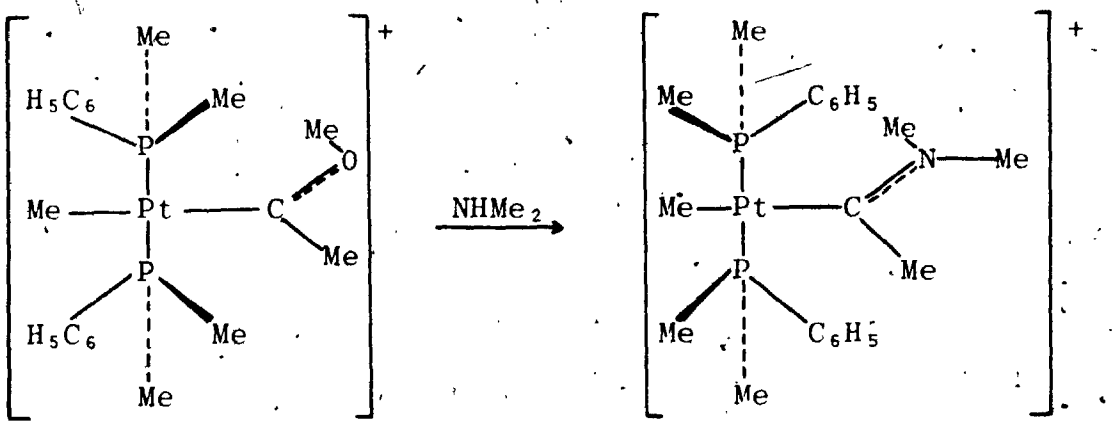

I II

Another interesting observation is that in complex I the carbene ligand is disordered in the solid state due to two possible orientations of the carbene ligand, related to each other by a 180° rotation about the Pt-C(sp^2) bond. No such disorder is observed in the solid state for complex II, under study in this chapter.

Carbenes and methyl are ligands which exert a strong trans influence (67).

The strong trans influence of the carbene ligand seems to cause a long Pt-C(methyl) bond of 2.147(11) Å. The sum of the covalent radii is 2.08 Å (94). In the complex trans-$Pt(CH_2SiMe_3)Cl(PMe_2Ph)_2$ (95) where C(sp^3) is trans to Cl^-, the Pt-C bond length is 2.079(14) Å. The bond distance in the title complex is longer by 3.8σ.

The observed Pt-C(sp^2) distance to the carbene is 2.079(11) Å and the sum of the covalent radii is 2.04 Å (94). In the structural examination of the acylimino-Pt

complex trans-Pt(MeC=NC$_6$H$_4$Cl)(PEt$_3$)$_2$ (96) where C(sp^2) is trans to I$^-$, a Pt-C(sp^2) bond length of 2.029(11) Å was observed. The distances in the two complexes differ by 2.9σ. Hence, a significant lengthening of the Pt-C (carbene) bond due to the trans influence of the methyl ligand is not observed.

The carbene ligand plane lies perpendicular to the metal equatorial plane and is in the optimum orientation for π back bonding from the Pt $5d_{xy}$ orbital into the vacant p_z orbital of C(sp^2) but no evidence of such π interaction is observed in the long Pt-C(sp^2) distance.

Within the carbene ligand, the mean N-C(methyl) distance is 1.486(9) Å. The N-C(sp^2) bond length is 1.266(15) Å. It is thus evident that considerable electron density is being contributed by the N atom to stabilize the electron deficient C(2). Further proof of this is observed in the planarity of the ligand and in the increase in the C(4)-N-C(5) angle from 109.47 in an ideal tetrahedral situation to 113(1)°.

An account of this work has been published (97).

CHAPTER 3

THE CRYSTAL AND MOLECULAR STRUCTURE OF TRANS-METHYL(2-OXACYCLOPENTILIDINE)BIS(DIMETHYLPHENYLPHOSPHINE)PLATINUM(II)HEXAFLUOROPHOSPHATE, Trans-$[Pt(\overline{CH_2C{-}{-}OCH_2CH_2})CH_3\{P(CH_3)_2C_6H_5\}_2]PF_6$

3.1. Introduction

Chisholm and Clark have studied the reactions of methanolic solutions of trans-$PtMeCl(PMe_2Ph)_2$ with terminal acetylenes in the presence of $AgPF_6$. The products obtained are square planar cationic complexes containing methoxycarbene ligands of the type shown below.

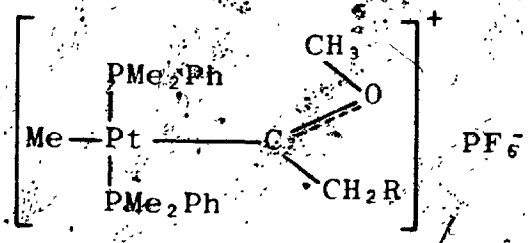

R = H, alkyl, aryl.

The specific reaction with acetylene gas gives a complex containing the methylmethoxycarbene ligand. The structure of this compound has been determined in the solid state by X-ray crystallographic methods (92), and the carbene ligand has been found to adopt a trans stereochemistry with respect to the C—O bond.

The same reaction with 1-butyne-4-ol does not give the expected analogous methoxycarbene complex. Instead, an

intramolecular cyclization reaction occurs preferrentially, and the complex shown below can be isolated. Due to its

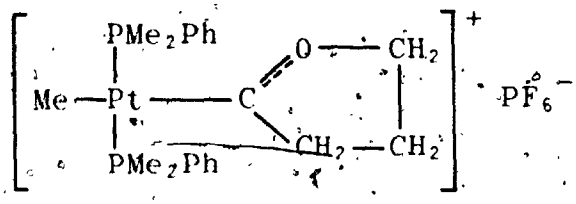

cyclic nature, the 2-oxacyclopentilidene ligand is constrained to have a cis configuration.

An examination of the solid state structure of this complex was undertaken to determine the geometry of the carbene ligand and to study its coordination to the metal atom. Oxy-substituents are not expected to stabilize the electrophilic C(carbene) as well as amino-groups due to the higher electronegativity of oxygen. Because of this, the bonding in the oxycarbene compounds may differ considerably from that in corresponding aminocarbene systems (such as that in Chapter 2). ^{13}C NMR spectra of complexes such as these show marked differences in C(carbene) chemical shifts and in ^{195}Pt coupling constants to C(carbene) and C(methyl) (98).

Also of interest in the structural study of this complex is the strong trans influence of the methyl and carbene ligands and its effect on the bond lengths in the inner coordination sphere of the metal atom.

3.2 Experimental

A sample of the complex was kindly supplied by Manzer. After several attempts, crystals considered suitable for X-ray study were obtained by slow evaporation from methylene chloride solution. The crystal data are provided in Table 3.1. Photographic analysis of the classes of reflections (0-2)kℓ, h(0-2)ℓ, and hk(0-2) showed the following systematic extinctions: hk0, h$\neq$2n; 0kℓ, $\ell\neq$2n; h0ℓ, $\ell\neq$2n. These absences are consistent only with the centric space group Pcca, D_{2h}^{8}, No. 54 (76). The structure was solved and successfully refined in this space group.

Details of the data collection procedure are summarized in Table 3.2. The intensities of 5348 reflections were recorded. Six standard reflections were monitored. Of these, the intensities of the reflections 400 and $\bar{4}00$ increased an average by 10%; 002 and 00$\bar{2}$ showed an increase in intensity of approximately 28%; 020 and 0$\bar{2}$0 showed only slight fluctuations. In each case the peak quality was closely examined, and no significant deterioration in peak structure was observed. Such increases may be a result of slight changes in mosaicity giving a decrease in extinction effects. Extinction is most pronounced for very intense reflections and the effect is such that a lower intensity than expected is observed for a given reflection, i.e. $F_o^2 < F_c^2$ (72).

No correction for the observed intensity changes of the standard reflections was applied to the data. All data

TABLE 3.1

Crystal Data for Trans-$[Pt(\overline{CH_2C{=}OCH_2CH_2})Me(PMe_2Ph)_2]PF_6$

$C_{21}H_{31}F_6OP_3Pt$	f.w. = 703.4
Analysis found (calculated)	C, 35.97 (35.94); H, 4.31 (4.41)
Crystal description	colourless tabular blocks
Systematic absences	hk0, $h \neq 2n$; h0ℓ, $\ell \neq 2n$; 0kℓ, $\ell \neq 2n$
Laue symmetry	mmm
Crystal system	orthorhombic
Space group	Pcca, D_{2h}^9
Equivalent positions (8)	$\pm(x, y, z)$, $\pm(\frac{1}{2} - x, \bar{y}, z)$, $\pm(\frac{1}{2} + x, \bar{y}, \frac{1}{2} + z)$, $\pm(\bar{x}, y, \frac{1}{2} - z)$
Cell constants	a = 15.503(7)Å α = 90.0° b = 18.81(1)Å β = 90.0° c = 17.66(1)Å γ = 90.0°
Cell volume	2652 Å^3
Wavelength used for cell determination	0.70926 Å
Temperature at which cell was determined	22°C
Method of density determination	flotation ($C_2H_4Br_2/CCl_4$)
Density (observed) (calculated)	1.81(1)g cm^{-3} 1.81g cm^{-3}
Z	8
Symmetry constraints (cation) (anion)	none 2

TABLE 3.2

Experimental Conditions for Data Collection

Radiation	Mo Kα
Wavelength	0.70926 Å
Filter	post-filtered, Nb foil (0.07mm)
Mean ω scan width at half height (reflections)	0.062° (400, 020, 002)
Reflections centered, in 2θ range	16; 15° < 2θ < 30°
Scan range a) low angle side of 2θ b) high angle side of 2θ	0.7° 0.7°
Scan rate	1.0° min^{-1}
Stationary background count time	10 sec
% available Bragg intensity obtained for a given reflection	80%
Take-off angle	1.4°
Tube KV; mA	40; 16
Collimator size	1.0mm
Crystal-counter distance	32cm
Crystal-aperture distance	30cm
Aperture dimensions	4mm x 4mm
2θ range	2.5° < 2θ ≤ 50°
Shells (No.; high angle limit)	2; 45°, 50°
Index limits	$0 \leq h \leq 18$, $0 \leq k \leq 22$, $0 \leq \ell \leq 21$
No. of data collected	5348
p value	0.03
No. of reflections with $I > 3\sigma(I)$	1763
μ (Mo Kα)	54.68cm^{-1}
Crystal faces	{100},{010},{001},{012}
Crystal dimensions	0.36mm x 0.28mm x 0.13mm
Absorption correction	analytical
Transmission coefficients a) minimum b) maximum	0.267 0.535

were processed. Only 1763 data had $I>3\sigma(I)$. The structure was solved using these intensity data.

The crystal used for intensity data collection was measured and the crystal faces were identified (Table 3.2) with the aid of optical goniometric measurements. Absorption correction tests on a representative group of reflections showed large variations in transmission coefficients, so all data with $I>2\sigma(I)$ were corrected for absorption using the analytical routines of the program AGNOST. The transmission coefficients ranged from 0.267 to 0.535. A diagram of the crystal from which intensity data were obtained is shown in Fig. 3.1.

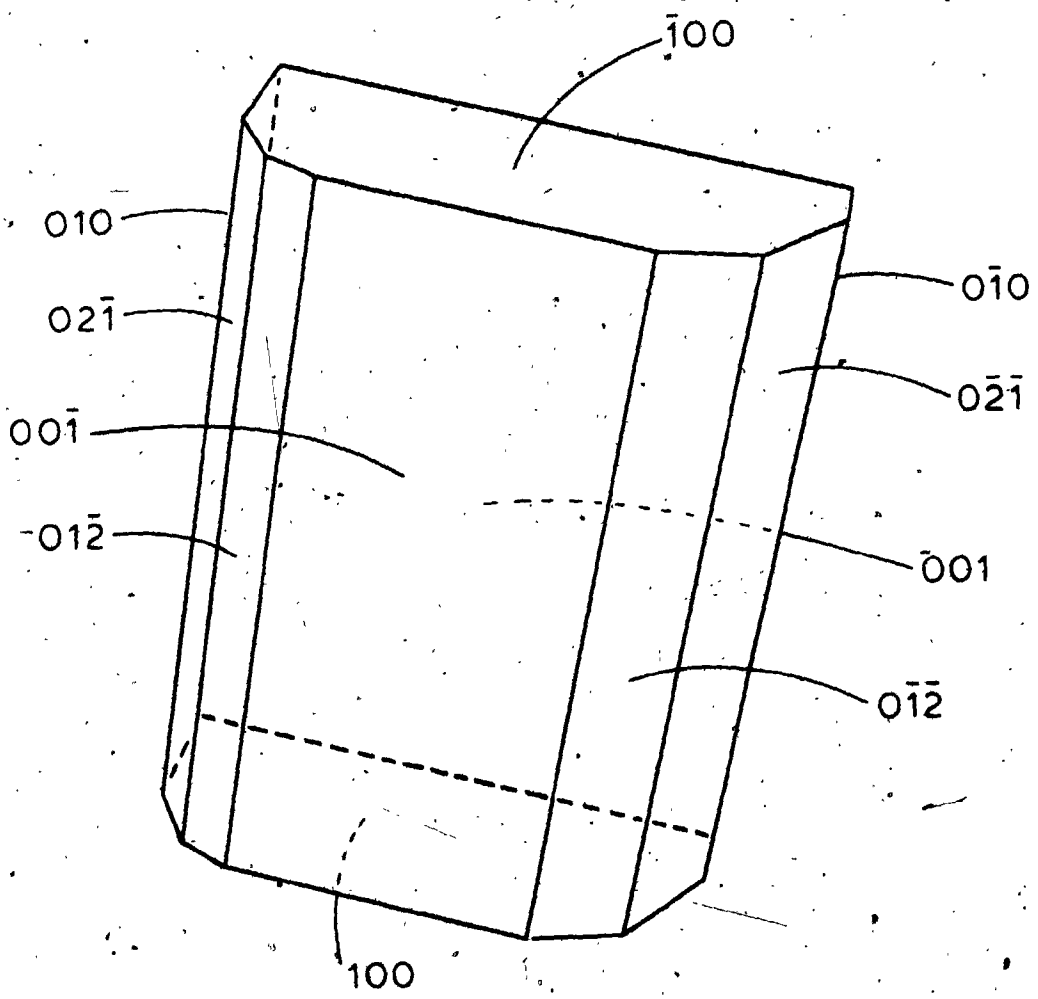

Fig. 3.1

A Drawing of the Data Crystal

Faces with dotted edges are hidden from view.

3.3 Structure Solution and Refinement

The Pt and two phosphine P atoms were located from a three dimensional Patterson synthesis. Two least-squares cycles, in which an overall scale factor and the positions of the three atoms were varied, gave agreement factors R_1 and R_2 of 0.183 and 0.268 respectively. A series of difference Fourier syntheses and least-squares calculations yielded positional parameters for the remaining twenty-nine non-hydrogen atoms.

The eight cations occupy the eight equivalent positions of site symmetry 1, whereas the anions lie on two sets of special positions, each having site symmetry 2, and four-fold multiplicity in the unit cell. The equivalent positions of the cation are given in Table 3.1, and those of the anion are:

$\frac{1}{4}, \frac{1}{2}, z$	$0, y, \frac{1}{4}$
$-\frac{1}{4}, \frac{1}{2}, \bar{z}$	$0, \bar{y}, -\frac{1}{4}$
$\frac{1}{4}, \frac{1}{2}, \frac{1}{2} + z$	$\frac{1}{2}, y, -\frac{1}{4}$
$-\frac{1}{4}, \frac{1}{2}, \frac{1}{2} - z$	$\frac{1}{2}, \bar{y}, \frac{1}{4}$

A two-fold symmetry axis of the anion must coincide with a crystallographic two-fold axis. Thus, there are two possible orientations of the PF_6 anion with respect to the crystallographic axis.

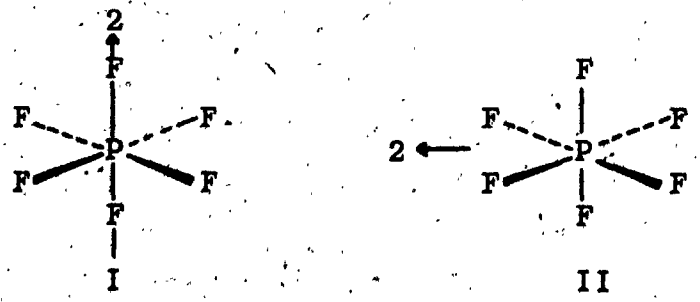

II

As was observed in the structure discussed in Chapter 2, the PF_6 anions are disordered. The disorder is such that both orientations (I and II) of the anion are present at each special position. Two disorder models were formulated, as described in Chapter 2 with two F6 rigid groups describing the disorder at each set of special positions. Two-fold symmetry is required at each special position, and the rigid group positional and orientation parameters were treated accordingly in the least-squares calculations. A multiplicity parameter was refined for each disorder model such that the net multiplicity at each special position equalled 0.5.

The rigid groups have O_h symmetry with the origin at the center of the octahedron. The distance of each F atom from the origin is 1.58 Å.

The P atoms of the anions were included as individual atoms with multiplicity 0.5, undergoing isotropic thermal motion. In the least-squares refinements, these atoms were constrained to lie on the crystallographic symmetry axis.

The phosphine phenyl rings of the cation were treated as rigid groups with D_{6h} symmetry. All non-hydrogen atoms were subjected to full matrix least-squares refinement. Non-group atoms of the cation were allowed to vibrate anisotropically. Group thermal parameters were refined for the four F6 groups and individual isotropic group atom temperature factors were varied for the phenyl ring rigid groups. Two cycles of refinement converged the model at $R_1 = 0.047$ and $R_2 = 0.054$.

The contributions to F_c of the methyl and phenyl H atoms were calculated as described in Chapter 2. Methyl C-H distances of 1.05 Å and phenyl C-H bond lengths of 1.00 Å were assumed. Positions for the methylene H atoms of the carbene ligand were obtained from the program FINDH. A C-H distance of 1.05 Å was utilized. Isotropic thermal parameters of 4.0 $Å^2$ were assigned to all H atoms.

A statistical examination of the structure factors in terms of various combinations of Miller indices, magnitudes of F_o, $\lambda^{-1}\sin\theta$, and diffractometer setting angles, showed F_o much greater than F_c for several very strong low angle reflections. The intensities were considered unreliable for the reflections (002),(020),(022), and (122); and these reflections were omitted in the final least-squares calculations.

The final model converged at $R_1 = 0.044$ and $R_2 = 0.048$. No evidence for the presence of secondary extinction was observed.

The largest peak in a final difference Fourier synthesis is located at (-0.095, 0.075, -0.225) and has an electron density of 0.73(9) $eÅ^{-3}$. This peak is associated with a disordered PF_6 anion.

The conditions and results of the final least-squares cycles are presented in Table 3.3. The final positional and thermal parameters of the non-group atoms are given in Table 3.4. Rigid group parameters are shown in Table 3.5, and the derived positional parameters of the group atoms are shown

TABLE 3.3

Conditions and Results of Final Full Matrix Least-Squares Calculations

Observations	1763
Variables	160
Ratio (observations/variables)	11.0
Rigid groups	6
Disorder models (No.; entities)	2; both PF_6 anions
Non-group atoms	15
a) Anisotropic	13
b) Isotropic	2
H atoms included; No. (type)	31; 6(methylene), 15(methyl), 10(phenyl)
Extinction coefficient	not refined
Maximum value of (parameter shift/standard deviation)	0.098
Agreement factors: R_1	0.044
R_2	0.048
Final error on an observation of unit weight	1.71 electrons
Final difference Fourier synthesis:	
a) Position of largest peak	(-0.095, 0.075, -0.225)
b) Electron density	0.73(9)e $\AA^{-3}$
c) Associated with	disordered PF_6 anion

TABLE 3.4

Individual Atom Positional and Thermal Parameters

Atom	x	y	z	U_{11}[a]	U_{22}	U_{33}	U_{12}	U_{13}	U_{23}
Pt	-0.12457(6)[b]	0.25002(6)	0.05895(3)	409(3)	453(3)	368(3)	-64(5)	-9(5)	16(11)
P(1)	-0.1838(4)	0.1377(3)	0.0590(4)	715(37)	501(31)	564(35)	-185(28)	-43(38)	83(34)
P(2)	-0.0670(3)	0.3630(3)	0.0619(3)	467(28)	503(29)	416(29)	-77(23)	-35(30)	-48(30)
P(3)	$-\frac{1}{2}$	$\frac{1}{2}$	0.3071(5)	620(19)					
P(4)	0	0.0526(4)	$-\frac{1}{4}$	689(34)					
O	-0.2098(9)	0.2841(7)	-0.0810(8)	719(97)	707(88)	696(108)	159(75)	-175(84)	96(75)
C(1)	-0.1055(16)	0.2402(14)	0.1750(11)	1287(214)	888(181)	433(102)	-527(173)	-180(141)	284(149)
C(2)	-0.1410(13)	0.2606(10)	-0.0529(12)	697(166)	221(132)	568(108)	-58(95)	196(133)	13(107)
C(3)	-0.0803(14)	0.2302(9)	-0.1128(12)	897(152)	506(154)	620(141)	-108(100)	85(130)	-134(103)
C(4)	-0.1223(26)	0.2521(20)	-0.1904(12)	2273(332)	1412(224)	485(137)	-112(292)	260(236)	-341(270)
C(5)	-0.2123(21)	0.2787(12)	-0.1657(13)	1929(308)	819(167)	380(131)	-235(180)	-391(184)	66(123)
C(11)	-0.1063(14)	0.0664(11)	0.0442(15)	772(166)	543(143)	1411(257)	-242(124)	-805(209)	224(158)
C(12)	-0.2395(17)	0.1076(14)	0.1428(14)	1067(215)	1511(242)	724(173)	-781(190)	-169(163)	99(173)
C(21)	-0.1486(11)	0.4325(11)	0.0452(14)	265(97)	705(157)	1043(205)	144(99)	-378(136)	-104(149)
C(22)	-0.0121(15)	0.3921(11)	0.1464(11)	987(181)	758(145)	415(126)	-25(134)	-151(128)	-167(113)

[a] The U_{ij}'s are the thermal parameters in terms of mean-square amplitudes of vibration in $\AA^2$. Values are given as U x 10^4. The expression for the thermal ellipsoid is given in Appendix II.

[b] Numbers in parentheses given here and in other tables are estimated standard deviations in the least significant digits.

TABLE 3.5

Rigid Group Parameters

Group	x_g[a]	y_g	z_g	δ	ε	η	Multiplicity
Ph-1	-0.3256(6)	0.1254(5)	-0.0732(6)	0.862(11)	-2.544(10)	-2.048(11)	
Ph-2	0.0701(5)	0.3740(4)	-0.0732(5)	-2.214(10)	-2.540(8)	-1.990(10)	
1-P6	-½	½	0.3076(6)	2.122(10)	3.142	-1.571	0.42(1)
2-P6	-½	½	0.2979(26)	2.107(43)	3.142	-1.571	0.08(1)
3-P6	0	0.0547(8)	-½	0.000	3.142	-0.991(13)	0.28(1)
4-P6	0	0.0520(10)	-½	0.000	3.142	-1.590(18)	0.22(1)

a. x_g, y_g, and z_g are the fractional coordinates of the group origin, and δ, ε, and η (radians) are the group orientation angles.

in Table 3.6. Calculated H atom positions are presented in Table 3.7.

A list of the observed and calculated structure amplitudes, given as $10|F_o|$ and $10|F_c|$ is presented in Appendix III.

TABLE 3.6

Derived Group Atom Parameters

	Atom	x	y	z	B(Å²)	
Ph-1						
	1C(1)[a]	-0.2617(9)	0.1271(8)	-0.0153(7)	4.3(5)	
	1C(2)	-0.3139(11)	0.1608(8)	-0.0058(7)	6.0(8)	
	1C(3)	-0.4049(7)	0.1591(8)	-0.0637(10)	7.3(6)	
	1C(4)	-0.3865(9)	0.1237(8)	-0.1310(8)	7.4(6)	
	1C(5)	-0.3072(11)	0.0900(8)	-0.1405(7)	7.2(6)	
	1C(6)	-0.2463(7)	0.0917(7)	-0.0826(9)	5.3(5)	
Ph-2						
	2C(1)	0.0111(8)	0.3729(7)	-0.0138(6)	3.0(4)	
	2C(2)	0.0019(9)	0.3417(7)	-0.0049(6)	6.0(9)	
	2C(3)	0.1510(6)	0.3429(7)	-0.0642(8)	5.5(5)	
	2C(4)	0.1292(7)	0.3752(7)	-0.1325(7)	5.6(5)	
	2C(5)	0.0484(9)	0.4064(6)	-0.1415(6)	4.7(4)	
	2C(6)	-0.0107(6)	0.4052(6)	-0.0821(8)	3.9(4)	
1-F6						
	1F(1)	-0.1632(5)	0.5440(7)	0.3075(6)		
	1F(2)	-0.3368(5)	0.4560(7)	0.3075(6)		
	1F(3)	-0.2123(6)	0.4494(3)	0.2443(6)	B(group) = 8.8(4)	
	1F(4)	-0.2877(6)	0.5506(3)	0.3707(6)		
	1F(5)	-0.2877(6)	0.5506(3)	0.2443(6)		
	1F(6)	-0.2123(6)	0.4494(3)	0.3707(6)		
2-F6						
	2F(1)	-½	½	0.2085(26)		
	2F(2)	-½	½	0.3873(26)		
	2F(3)	-0.1624(22)	0.5430(31)	0.2979(26)	B(group) = 6.8(21)	
	2F(4)	-0.3376(22)	0.4570(31)	0.2979(26)		
	2F(5)	-0.1979(37)	0.4278(18)	0.2979(26)		
	2F(6)	-0.3021(37)	0.5722(18)	0.2979(26)		
3-F6						
	3F(1)	0.0558(11)	0.0547(8)	-0.3248(7)		
	3F(2)	-0.0558(11)	0.0547(8)	-0.1752(7)		
	3F(3)	-0.0803(5)	-0.0048(8)	-0.2846(7)	B(group) = 9.5(7)	
	3F(4)	0.0803(5)	-0.0048(8)	-0.2154(7)		
	3F(5)	0.0803(5)	0.1141(8)	-0.2154(7)		
	3F(6)	-0.0803(5)	0.1141(8)	-0.2846(7)		
4-F6						
	4F(1)	-0.0020(19)	0.0520(10)	-0.3394		
	4F(2)	0.0020(19)	0.0520(10)	-0.1606		
	4F(3)	0	-0.0321(10)	-¼	B(group) = 9.1(9)	
	4F(4)	0	0.1360(10)	-¼		
	4F(5)	-0.1019	0.0520(10)	-0.2482(16)		
	4F(6)	0.1019	0.0520(10)	-0.2518(16)		

[a] Ring C atoms are numbered sequentially. 1C(1) is bonded to P(1)

2 4

OF/DE

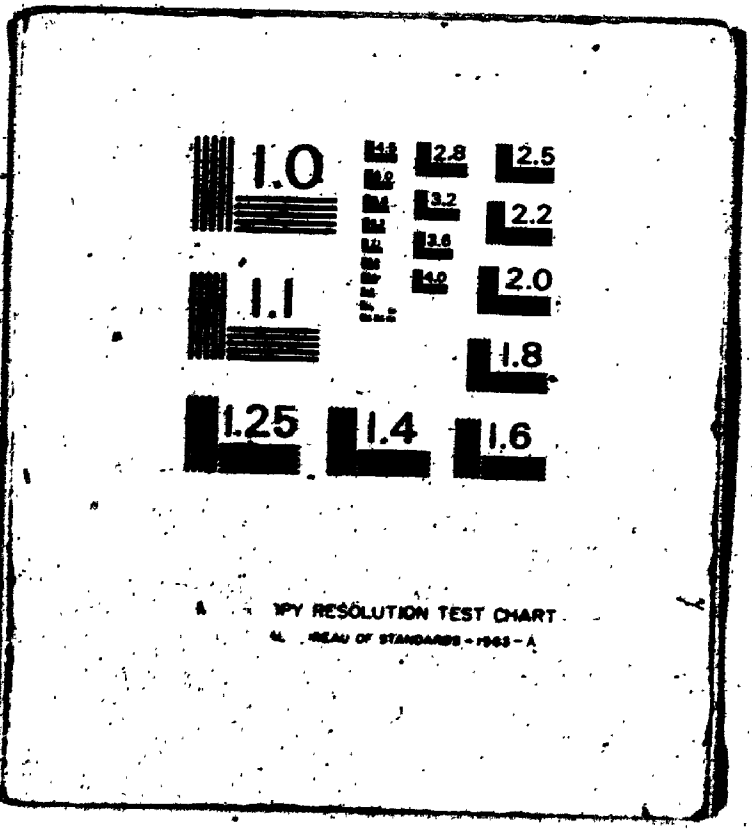
1.0
1.1
1.25
1.4
1.6
2.8
3.2
3.6
4.0
2.5
2.2
2.0
1.8
RESOLUTION TEST CHART
BUREAU OF STANDARDS - 1963 - A

TABLE 3.7

Derived Hydrogen Atom Positional Parameters

Atom	x	y	z
Methyl Hydrogen Atoms			
C(1)-H(1)	-0.1277	0.1910	0.1932
C(1)-H(2)	-0.0392	0.2453	0.1868
C(1)-H(3)	-0.1390	0.2813	0.2029
C(11)-H(1)	-0.0573	0.0707	0.0847
C(11)-H(2)	-0.1378	0.0175	0.0499
C(11)-H(3)	-0.0802	0.0710	-0.0102
C(12)-H(1)	-0.2765	0.1519	0.1641
C(12)-H(2)	-0.2814	0.0670	0.1288
C(12)-H(3)	-0.1954	0.0926	0.1833
C(21)-H(1)	-0.1870	0.4385	0.0934
C(21)-H(2)	-0.1179	0.4807	0.0323
C(21)-H(3)	-0.1879	0.4173	-0.0010
C(22)-H(1)	0.0335	0.3533	0.1623
C(22)-H(2)	0.0199	0.4402	0.1354
C(22)-H(3)	-0.0568	0.3991	0.1900
Methylene Hydrogen Atoms			
C(3)-H(1)	-0.0771	0.1747	-0.1076
C(3)-H(2)	-0.0182	0.2519	-0.1068
C(4)-H(1)	-0.1248	0.2084	-0.2267
C(4)-H(2)	-0.0855	0.2930	-0.2157
C(5)-H(1)	-0.2581	0.2410	-0.1834
C(5)-H(2)	-0.2242	0.3276	-0.1905
Phenyl Hydrogen Atoms[a]			
1H(2)	-0.3561	0.1870	0.0426
1H(3)	-0.4613	0.1837	-0.0563
1H(4)	-0.4306	0.1224	-0.1718
1H(5)	-0.2946	0.0642	-0.1884
1H(6)	-0.1894	0.0675	-0.0894
2H(2)	0.1080	0.3182	0.0443
2H(3)	0.2093	0.3203	-0.0578
2H(4)	0.1716	0.3758	-0.1751
2H(5)	0.0326	0.4292	-0.1903
2H(6)	-0.0887	0.4270	-0.0882

[a] Phenyl H atoms are numbered sequentially. 1H(2) is bonded to 1C(2), 1H(3) is bonded to 1C(3), etc.

3.4 Description of the Structure

The nearest cation-anion approach is 3.08 Å between atoms C(4) and 4F(4). This distance is consistent with that normally observed for the packing of discrete anionic and cationic components. Fig. 3.2 is an ORTEP diagram of the cation, showing the atom labelling scheme. The inner coordination sphere of the metal atom and the carbene ligand are depicted in Fig. 3.3. A stereoview of the cation is presented in Fig. 3.4. Selected intramolecular bond distances and angles together with their standard deviations are given in Table 3.8.

The PF_6 anion occupies two sets of special positions with 2 site symmetry. There are two orientations of the six F atoms at each site due to disorder of the anion. The final refined multiplicity parameters for the disordered groups were 0.42(1) and 0.28(1). The more abundant orientation of the anion at each site is that in which no F atoms lie on the symmetry axis (II). This orientation occurs 84% of the time for the F atoms related to P(3) and 56% of the time for those about P(4).

Since the P atoms were not constrained to lie at the center of gravity of the F6 octahedra, some distortion of the octahedral geometry of the anions is possible. The mean P-F distance is 1.58(1) Å, where 1.58 Å is expected (90, 91). The mean F-P-F angle for <u>trans</u> F atoms is 177(1)° and that for <u>cis</u> F atoms is 89.9(4)°. Similar deviations from ideality were observed in Chapter 2.

the least-squares plane although the carbene ligand (Table 3.9). C(4) is the only atom in the carbene ligand not bonded to C(2) or O, and is the only one that deviates significantly (3.3σ) from the least-squares plane. This is also the atom which shows the greatest thermal motion as observed from the large thermal elipsoids in Figs. 3.2-3.4.

The C(methyl) atom <u>trans</u> to the carbene ligand is 2.08(2) Å from the Pt atom. This distance differs from that of 2.147(11) observed in Chapter 2 by 2.9σ.

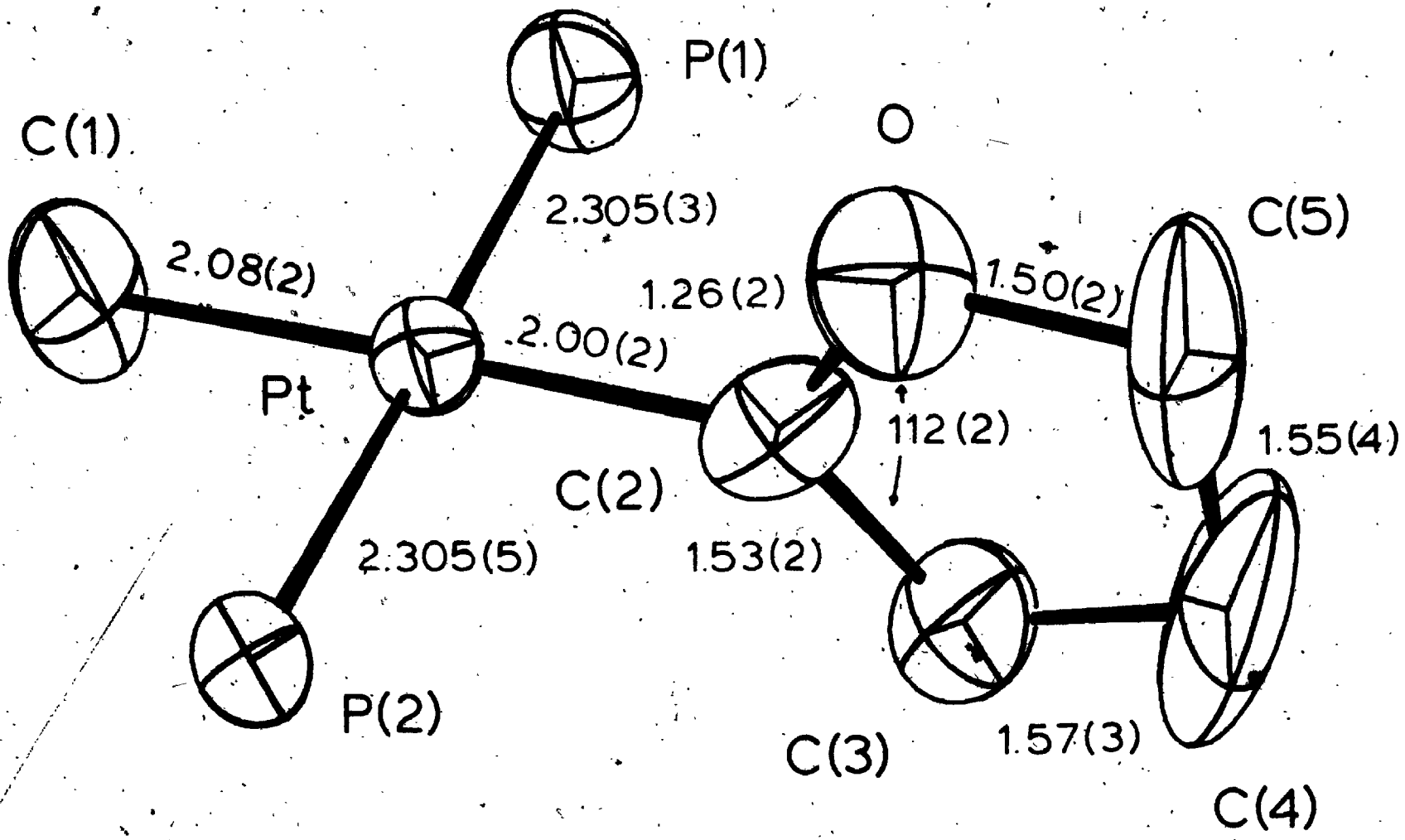

Fig. 3.3

The Carbene Ligand and the Inner Coordination Sphere of the Metal Atom

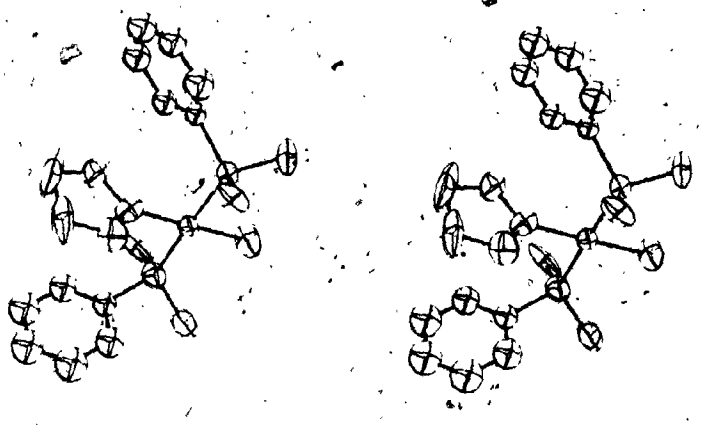

Fig. 3.4

A Stereoview of the Cation.

TABLE 3.8

Selected Intramolecular Bond Distances and Angles

Distances(Å)		Angles(deg.)	
Metal Atom Inner Coordination Sphere			
Pt-P(1)	2.305(5)	P(1)-Pt-P(2)	178.5(2)
Pt-P(2)	2.305(5)	C(1)-Pt-C(2)	179.0(8)
Pt-C(1)	2.08(2)	C(1)-Pt-P(1)	86.6(7)
Pt-C(2)	2.00(2)	C(1)-Pt-P(2)	90.3(7)
		C(2)-Pt-P(1)	92.3(6)
		C(2)-Pt-P(2)	88.9(6)
Phosphine Ligands			
P(1)-C(11)	1.82(2)	Pt-P(1)-C(11)	114.4(7)
P(1)-C(12)	1.81(2)	Pt-P(1)-C(12)	118.6(8)
P(1)-1C(1)	1.83(1)	Pt-P(1)-1C(1)	111.9(5)
P(2)-C(21)	1.84(2)	Pt-P(2)-C(21)	112.6(6)
P(2)-C(22)	1.80(2)	Pt-P(2)-C(22)	118.8(7)
P(2)-2C(1)	1.82(1)	Pt-P(2)-2C(1)	109.6(7)
		C(11)-P(1)-C(12)	102(1)
		C(11)-P(1)-1C(1)	105.7(9)
		C(12)-P(1)-1C(1)	103(1)
		C(21)-P(2)-C(22)	104(1)
		C(21)-P(2)-2C(1)	105.5(8)
		C(22)-P(2)-2C(1)	105(1)
Carbene Ligand			
C(2)-O	1.26(2)	Pt-C(2)-O	122(2)
C(2)-C(3)	1.53(2)	Pt-C(2)-C(3)	125(1)
C(3)-C(4)	1.57(3)	C(2)-O-C(5)	113(2)
C(4)-C(5)	1.55(4)	C(2)-C(3)-C(4)	105(2)
O-C(5)	1.50(2)	C(3)-C(4)-C(5)	102(2)
		C(4)-C(5)-O	106(2)
		C(3)-C(2)-O	112(2)

The cation has distorted square planar coordination about the Pt atom. The equatorial plane is formed by the Pt, two phosphine P atoms, the C(methyl) and C(carbene) atoms. A weighted least-squares plane (Table 3.9) shows that the atoms P(1) and P(2) deviate most from the plane, being 0.021(6) and 0.015(5) Å below the plane respectively. The P(1)-Pt-P(2) angle is 178.5(2)° and the C(1)-Pt-C(2) angle is 179.0(8)°. The mean P-Pt-C angle is 90.03(8)°. Thus, the distortion of the square plane is only slight.

The phosphine P atoms lie 2.305(5) Å to either side of the Pt atom. The orientation of the phosphine ligands is similar to that in the corresponding aminocarbene complex (Chapter 2) where both phenyl rings occupy the carbene side of the equatorial plane in a 'lopsided' arrangement of the cation. One ring lies well above the square plane of the Pt atom, and one well below. This constrains one of the P-C(methyl) bonds in each phosphine to lie almost parallel to the equatorial plane and the other to lie nearly perpendicular to it. Both phenyl rings are oriented nearly perpendicular to the square plane; the angles between the planes being 85° for Ph-1 and 93° for Ph-2. As in the similar aminocarbene complex (Chapter 2) the phenyl rings are bent slightly towards the carbene ligand. The angles P(1)-1C(1)-1C(4) and P(2)-2C(1)-2C(4) are 175.0(8) and 174.9(7) respectively. No other significant distortion of the phenyl rings is observed. The angles

TABLE 3.9

Weighted Least-Squares Planes

Atom	Deviation from Plane(Å)
Atoms included: Pt, P(1), P(2), C(1), C(2)	
Equation of Plane: 14.09x - 7.240y - 2.858z = -3.734	
Pt	0.001(1)
P(1)	-0.021(6)
P(2)	-0.015(5)
C(1)	0.01(3)
C(2)	0.01(2)
Atoms included: C(2), O, C(3), C(4), C(5)	
Equation of Plane: 6.850x + 17.01y - 9.00z = 3.527	
C(2)	0.02(2)
O	0.00(1)
C(3)	-0.04(2)
C(4)	-0.13(4)
C(5)	-0.03(2)

P(1)-1C(1)-1C(2) and P(1)-1C(1)-1C(6) are 118(1) and 122(1)° respectively. Corresponding angles about atom 2C(1) are 118(1) and 121(1)°.

As observed previously (92, 93, 96), the organic substituents on the phosphine ligands are bent back away from the metal atom to a considerable extent, resulting in a distorted tetrahedral geometry about the P atoms. The Pt-P-C angles vary from 109.6(7)° to 118.8(7)° and the average is 114(2)°. The C-P-C angles vary from 102(1)° to 105.7(9)° with a mean value of 104.2(6)°. Corresponding angles in the aminocarbene complex (Chapter 2) have mean values of 114.4(7)° and 103.4(5)°. All P-C distances are crystallographically equivalent and the mean value is 1.820(6) Å compared to 1.805(6) Å in the aminocarbene complex. The oxycarbene ligand is present as an almost planar five membered ring coordinated through the C(sp^2) atom. A weighted least-squares plane calculated through the carbene ligand is shown in Table 3.9. C(4) is farthest from the plane, being 0.13(4) Å above it. This plane is at an angle of 87.3(6)° to the square plane of the Pt atom.

The large thermal ellipsoids representing atoms C(4) and C(5) give evidence of considerable motion in that region of the carbene ligand. Such motion may be the result of a strained five membered ring.

The Pt-C(sp^2) distance is 2.00(2) Å, significantly shorter (3.3σ) than that of 2.079(13) Å observed in trans-[Pt(Me—NMe$_2$)Me(PMe$_2$Ph)$_2$]PF$_6$ (Chapter 2). The

$C(sp^2)$-O bond length is 1.26(2) Å, compared with 1.32(3) Å in the complex cis-Pt{C(NHPh)(OEt)}Cl_2PEt_3 (65). This short bond distance is similar to the C—N distance observed in the aminocarbene complex (Chapter 2). An O-C(5) bond length of 1.50(2) Å is observed. This agrees well with the mean value of 1.51(4) Å obtained for the cyclic carbene ligand in the complex cis-Mn($\overline{COCH_2CH_2O}$)Cl(CO)$_4$ (99). The C(2)-C(3) distance of 1.53(2) Å is equivalent to the value of 1.526(18) Å observed in Chapter 2. The mean $C(sp^3)$-$C(sp^3)$ bond distance in the carbene ring is 1.56(1) Å. The value obtained for cis-Mn($\overline{COCH_2CH_2O}$)Cl(CO)$_4$ (99) is 1.53(4) Å. None of the C-C bond lengths around the carbene ring are significantly different.

Of the three angles around C(2), Pt-C(2)-O and Pt-C(2)-C(3) have values of 122(2) and 125(1)° respectively. These exceed the expected 120° angle for sp^2 hybridization, and the angle within the ring, C(3)-C(2)-O, is only 112(2)°. The cyclic nature of the ring does impose some strain upon the system. This is further displayed by the angles about the $C(sp^3)$ atoms which are all less than the ideal value of 109.47°. The average value of these three angles is 104.3(9)°. The angle C(2)-O-C(5) is 113(2)°. The corresponding angle about the O atom in Cr(PhC—OMe)(CO)$_5$ (47), where a methoxyphenylcarbene ligand with trans stereochemistry is present, is 121(2)°. Thus, the cyclic nature of the carbene ligand tends to constrict this angle as well. The sp^2 hybridization at C(2) and O is best observed from

the least-squares plane although the carbene ligand (Table 3.9). C(4) is the only atom in the carbene ligand not bonded to C(2) or O, and is the only one that deviates significantly (3.3σ) from the least-squares plane. This is also the atom which shows the greatest thermal motion as observed from the large thermal elipsoids in Figs. 3.2-3.4.

The C(methyl) atom <u>trans</u> to the carbene ligand is 2.08(2) Å from the Pt atom. This distance differs from that of 2.147(11) observed in Chapter 2 by 2.9σ.

3.5 Discussion

The overall structure of this compound is very similar to that of the aminocarbene complex in Chapter 2. Both cations are square planar and the carbene ligands lie very nearly perpendicular to the equatorial plane of the metal atom. The orientation of the phosphine ligands is also similar.

The Pt-C(carbene) distance is significantly shorter than observed in the previous chapter. The Pt-C(carbene) bond of 2.00(2) Å in the alkoxycarbene complex is shorter than that of 2.079(13) Å in the aminocarbene cation by 3.3σ. A factor which may be responsible for this difference in Pt-C(sp^2) bond lengths is that oxygen is more electronegative than nitrogen and hence a poorer nucleophile. Thus, alkoxy-substituents do not stabilize the electron deficient C(sp^2) atom as well as alkylamino ones, and π bonding from the metal atom to the vacant p_z orbital of C(carbene) may be postulated. Such an effect would tend to shorten the Pt-C(sp^2) bond even though the strong trans influence of the methyl group is still present. Thus, the Pt-C(sp^2) distance is comparable to that of 2.029(11) Å observed for the purely σ bond in trans-Pt(MeC=N-p-C_6H_4Cl)$I(PEt_3)_2$ (96) where the weak trans influence ligand I^- lies opposite C(sp^2).

There exists further data which tends to favour significant metal-ligand π interaction for alkoxycarbene Pt(II) complexes. A spectroscopic technique which is very

sensitive to differences in bonding about C atoms is ^{13}C NMR. Substantial differences are observed in the C(carbene) resonances, and in the $^{1}J_{Pt-C(carbene)}$ and $^{1}J_{Pt-C(methyl)}$ coupling constants for complexes of the type trans-$[PtLMe(AsMe_3)_2]PF_6$, where L = alkoxycarbene or alkylaminocarbene (98). Such changes have been attributed to differences in π bonding about the C(sp^2) atom in alkoxy- and alkylaminocarbene systems. Similar results have been observed in the chemical shifts of C(carbene) for the carbene complexes $Cr(PhC{=}{-}OMe)(CO)_5$ and $Cr(MeC{=}{-}NEt_2)(CO)_5$ (100). The chemical shift for C(carbene) in the alkylaminocarbene complex is upfield from the alkoxycarbene value by approximately 60 ppm. This has been attributed to greater dπ-pπ interaction in the alkoxycarbene systems. This argument is supported by the X-ray crystal structures of these two complexes where the Cr-C(carbene) bond length increases from 2.04(3) Å in the alkoxycarbene system (47) to 2.16(1) Å in the alkylaminocarbene complex (50). The bond lengths differ by 3.8σ. These results parallel the spectral and crystallographic data in the square planar Pt complexes.

The carbene C(sp^2)-heteroatom distances in the two Pt complexes examined thus far are consistently shorter than those in the two Cr complexes by approximately 2.5σ. Although the distances are not significantly different, the trend implies that more electron density is required of the heteroatoms in the form of pπ-pπ interactions in the Pt

complexes. The Pt(II) atom is not capable of as much $d\pi$-$p\pi$ back donation as is the zero valent Cr atom. This will be further discussed in Chapter 7. Nonetheless, significant metal-ligand bonding appears to be present in the alkoxycarbene complex being discussed.

Three resonance structures are generally drawn for carbene ligands of this type.

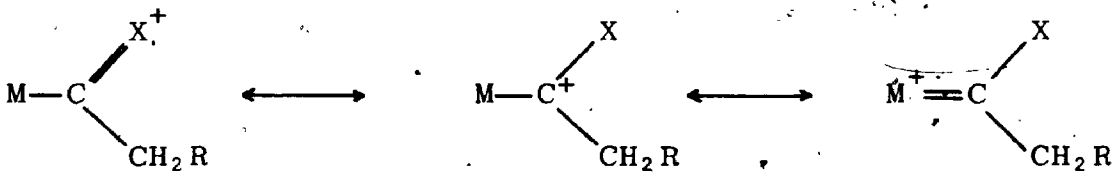

I II III

X = alkylamino, alkoxy-

R = H, alkyl, aryl

Structural data tend to indicate that the aminocarbene complex in Chapter 2 favours structure I, as does the alkoxycarbene complex in this chapter, but with a significant contribution from III. Thus, the carbene ligand in the complex trans-$[Pt(\overline{CH_2C{=}{=}OCH_2CH_2})Me(PMe_2Ph)_2]PF_6$ may be referred to as a metal stabilized carbonium ion.

The Pt-C(sp^3) bond length of 2.08(2) Å to the methyl ligand trans to carbene is not significantly different from that of 2.147(11) Å observed in Chapter 2. These bond lengths differ by 2.9σ. A summary of available Pt(II)-C(sp^3) bond lengths for square planar complexes is presented in Table 3.10. Clearly, a close comparison of bond length data with regard to trans influence is difficult because of the large estimated standard deviations on the bond distances.

TABLE 3.10

Platinum II-Carbon(sp^3) Bond

Lengths in Square Planar Complexes

Complex	Pt-C(sp^3)(Å)	Ligand trans to C(sp^3)	Reference
trans-$PtMeCl(PMePh_2)_2$	2.07(1)	Cl^-	101
trans-$Pt(CH_2SiMe_3)Cl(PMe_2Ph)_2$	2.079(14)	Cl^-	95
trans-$[PtMe(\overline{CH_2C{=}{=}OCH_2CH_2})(PMe_2Ph)_2]PF_6$	2.08(2)	$\overline{CH_2C{=}{=}OCH_2CH_2}$	This Chapter
trans-$[PtMe(MeC{\equiv}CMe)(PMe_2Ph)_2]PF_6$	2.11(2)	$MeC{\equiv}CMe$	93
trans-$[PtMe(MeC{=}{=}OMe)(PMe_2Ph)_2]PF_6$	2.13(2)	$MeC{=}{=}OMe$	92
trans-$[PtMe(MeC{=}{=}NMe_2)(PMe_2Ph)_2]PF_6$	2.147(11)	$MeC{=}{=}NMe_2$	Chapter 2
Sum of the covalent radii	2.08		94

Of the six structures shown in Table 3.10, the Pt-C(sp^3) bond lengths for the first five are not significantly different. But, for the complexes where lower standard deviations are obtained, the expected trend is observed. In the complex examined in Chapter 2, the bond length of 2.147(11) Å is longer by 3.8σ and 5.1σ than that in trans-$Pt(CH_2SiMe_3)Cl(PMe_2Ph)_2$ (95) and trans-$PtMeCl(PMe_2Ph)_2$ (101) respectively. The complex with the longer bond length has an aminocarbene ligand trans to the C(sp^3) atom, whereas the short distances are observed when Cl^- is trans to C(sp^3). A comparison of Pt-C(sp^2) bond length data will be made in the final section of this thesis.

An account of this work has been published (102).

CHAPTER 4

THE CRYSTAL AND MOLECULAR STRUCTURE OF TRANS-CHLORO(3-HYDROXYPROPYL-N,N-DIMETHYLAMINOCARBENE)BIS(DIMETHYLPHENYLPHOSPHINE)PLATINUM(II)HEXAFLUOROPHOSPHATE, Trans-$[Pt\{HO(CH_2)_3C{=}N(CH_3)_2\}Cl\{P(CH_3)_2C_6H_5\}_2]PF_6$.

4.1 Introduction

The complex containing the cyclic alkoxycarbene ligand, trans-$[Pt(\overline{CH_2C{=}{=}OCH_2CH_2})Me(PMe_2Ph)_2]PF_6$, whose X-ray crystal structure is discussed in Chapter 3, reacts readily with dimethylamine in dichloromethane solution to give an interesting product (64).

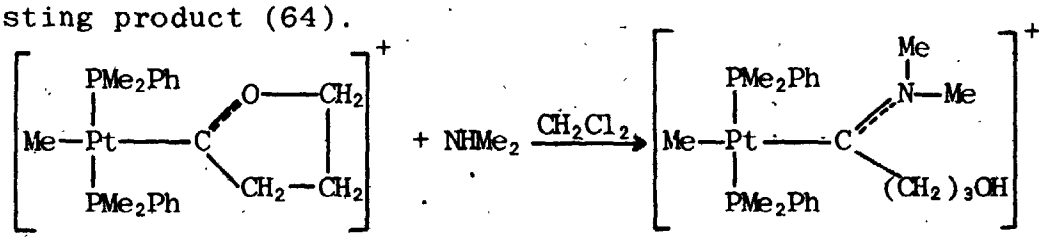

I II

As with non-cyclic alkoxycarbene ligands, dimethylamine displaces the alkoxy-substituent to form an aminocarbene. When this reaction is performed on I, the carbene ring is cleaved at the C-O bond, and a 3-hydroxypropyl-N,N-dimethylamino carbene ligand is formed (complex II).

The new product (II) has a methyl ligand trans to the carbene. We have found that limited information about the trans influence of the carbene ligands being studied can be obtained from Pt-C(methyl) bond lengths (Chapter 3). However,

Pt-Cl bond distances have been utilized with reasonable success as a probe for the determination of crystallographic trans influence of various ligands, and more specifically of 'carbon donor' ligands (68). Since Cl is a much heavier atom than C, its position can be determined more accurately by X-ray diffraction methods. Therefore, Pt-Cl bond lengths are much more sensitive as indicators of trans influence than the Pt-C distances.

Clark et al. have observed that when carbene complexes such as I and II are reacted with HCl, the carbene ligand is left unchanged, but the methyl at the trans coordination site is displaced to give the corresponding chloro complex (64).

$$\text{trans-}[PtMe(carbene)(PMe_2Ph)_2]PF_6 + HCl \longrightarrow \text{trans-}[PtCl(carbene)(PMe_2Ph)_2]PF_6 + CH_4$$

Thus, a ligand of very strong trans influence is replaced by one of very weak trans influence. The full chemical significance of this will be realized in Chapter 5.

When the above reaction is performed with complex II, trans-$[Pt\{HO(CH_2)_3C{=}{=}NMe_2\}Cl(PMe_2Ph)_2]PF$ is obtained. An X-ray crystal structure determination of this compound was undertaken. Since a chloro ligand lies trans to carbene in this complex, a more accurate estimate of the trans influence of the tertiary carbene ligand should be possible. The trans influence of this ligand can be compared to those of other types of tertiary carbene ligands. Also, evaluation of the Pt-C(carbene) bond, and of the geometry of the carbene

ligand with respect to previously observed data, should help clarify bonding trends in complexes of this type.

4.2 Experimental

The preparation of the complex is described in detail in Chapter 5. Spectral and physical data are also given since they have not been reported elsewhere.

A colourless sample of the compound was prepared and recrystallized from a dichloromethane/ether mixture to give irregular octahedral blocks with well developed faces. The crystal data are presented in Table 4.1.

A photographic study revealed the crystals to be orthorhombic. The observed systematic absences are $0k\ell$, $k + \ell \neq 2n$; $h0\ell$, $h \neq 2n$. These extinctions are consistent with those for the centrosymmetric space group Pnam, an alternate setting of Pnma (D_{16}^{2h}, No. 62), and for the acentric space group $Pna2_1$ (C_{2v}^{9}, No. 33) (76). For Pnam there are 8 equivalent positions of site symmetry 1 in each unit cell, and 4 with site symmetry m, while for $Pna2_1$ there are 4 with no imposed symmetry. The density and unit cell volume indicate the presence of four formula units per cell. The presence of the long alcoholic group bonded to C(carbene) minimizes the possibility of the presence of a mirror plane through Cl, Pt and the carbene ligand, so m site symmetry was considered unlikely. The structure solution was initiated and successfully completed in $Pna2_1$.

The conditions for intensity data collection are presented in Table 4.2. Since the space group $Pna2_1$ is noncentrosymmetric and atoms displaying large anomalous dispersion effects are present (Pt, P, Cl), Friedel's law breaks down.

TABLE 4.1

Crystal Data for Trans-$[Pt\{HO(CH_2)_3C{=}NMe_2\}Cl(PMe_2Ph)_2]PF_6$

$C_{22}H_{35}ClF_6NOP_3Pt$	f.w. = 767.0
Analysis found (calculated)	C, 34.64 (34.45); H, 4.53 (4.60); N, 1.74 (1.83)
Crystal description	irregular octahedral blocks
Systematic absences	$0k\ell$, $k + \ell \neq 2n$; $h0\ell$, $h \neq 2n$
Laue symmetry	mmm
Crystal system	orthorhombic
Space group	$Pna2_1$
Equivalent positions (4)	$x, y, z; \bar{x}, \bar{y}, \frac{1}{2} + z; \frac{1}{2} - x, \frac{1}{2} + y, \frac{1}{2} + z; \frac{1}{2} + x, \frac{1}{2} - y, z$
Cell constants	$a = 14.4032(19)$ Å $\alpha = 90.0°$ $b = 12.6309(18)$ Å $\beta = 90.0°$ $c = 16.1508(22)$ Å $\gamma = 90.0°$
Cell volume	2938 Å^3
Wavelength used for cell determination	1.54056 Å
Temperature at which cell was determined	23°C
Method of density determination	flotation ($C_2H_4Br_2/CCl_4$)
Density (observed) (calculated)	1.75(1) g cm^{-3} 1.73 g cm^{-3}
Z	4
Symmetry constraints	none

TABLE 4.2

Experimental Conditions for Data Collection

Radiation	Cu Kα
Wavelength	1.54056 Å
Filter	pre-filtered, Ni foil (0.018mm)
Mean ω scan width at half height (reflections)	0.06° (200, 020, 002)
Reflections centered; in 2θ range	14; 34° < 2θ < 72°
Scan range a) low angle side of 2θ	0.70°
b) high angle side of 2θ	0.70°
Scan rate	2.0° min^{-1}
Stationary background count time	10 sec
% available Bragg intensity obtained for a given reflection	80%
Take-off angle	1.8°
Tube KV; mA	40; 14
Collimator size	1.0mm
Crystal-counter distance	32cm
Crystal-aperture distance	30cm
Aperture dimensions	5mm x 5mm
2θ range	2.5° < 2θ < 125°
Shells (No; high angle limit)	4; 60°, 90°, 105°, 125°
Index limits	$0 \leq h \leq 16$, $0 \leq k \leq 14$, $-18 \leq \ell \leq 18$
No. of data collected	5296
p value	0.03
No. of reflections with $I > 3\sigma(I)$	3442
μ (Cu Kα)	113.01 cm^{-1}
Crystal faces	$\{111\}$, $(00\bar{1})$, $(0\bar{1}1)$, $(01\bar{1})$, $(0\bar{1}\bar{1})$, $(\bar{1}\bar{1}0)$, (110), $(\bar{1}10)$
Crystal dimensions	0.22mm x 0.17mm x 0.18mm
Absorption correction	analytical
Transmission coefficients a) minimum	0.261
b) maximun	0.407

This requires that $hk\ell$ and $\bar{h}k\bar{\ell}$ data be measured. Point group symmetry predicts that $F_{(\bar{h}k\bar{\ell})} = F_{(hk\ell)}$. It was found to be more convenient in terms of orientations of the goniostat to obtain the intensities of the $hk\ell$ data rather than those of the equivalent $\bar{h}k\bar{\ell}$ reflections.

5296 intensities were recorded using CuKα radiation out to a 2θ value of 125°. The five standard reflections (200, 110, 020, 002, and 00$\bar{2}$), measured after every 150 data recorded, increased slightly in intensity. The mean increase was 10(1)%. No correction was applied to the data to account for this increase. All data were processed and 3442 were found to have $I > 3\sigma(I)$. The structure solution was based on these reflections only. An optical goniometric study revealed that the crystal had fifteen faces (Table 4.1). The crystal was measured and an absorption correction was performed on all data with $I > 0$. The minimum and maximum absorption coefficients differed by 56%. A diagram of the data crystal is presented in Fig. 4.1.

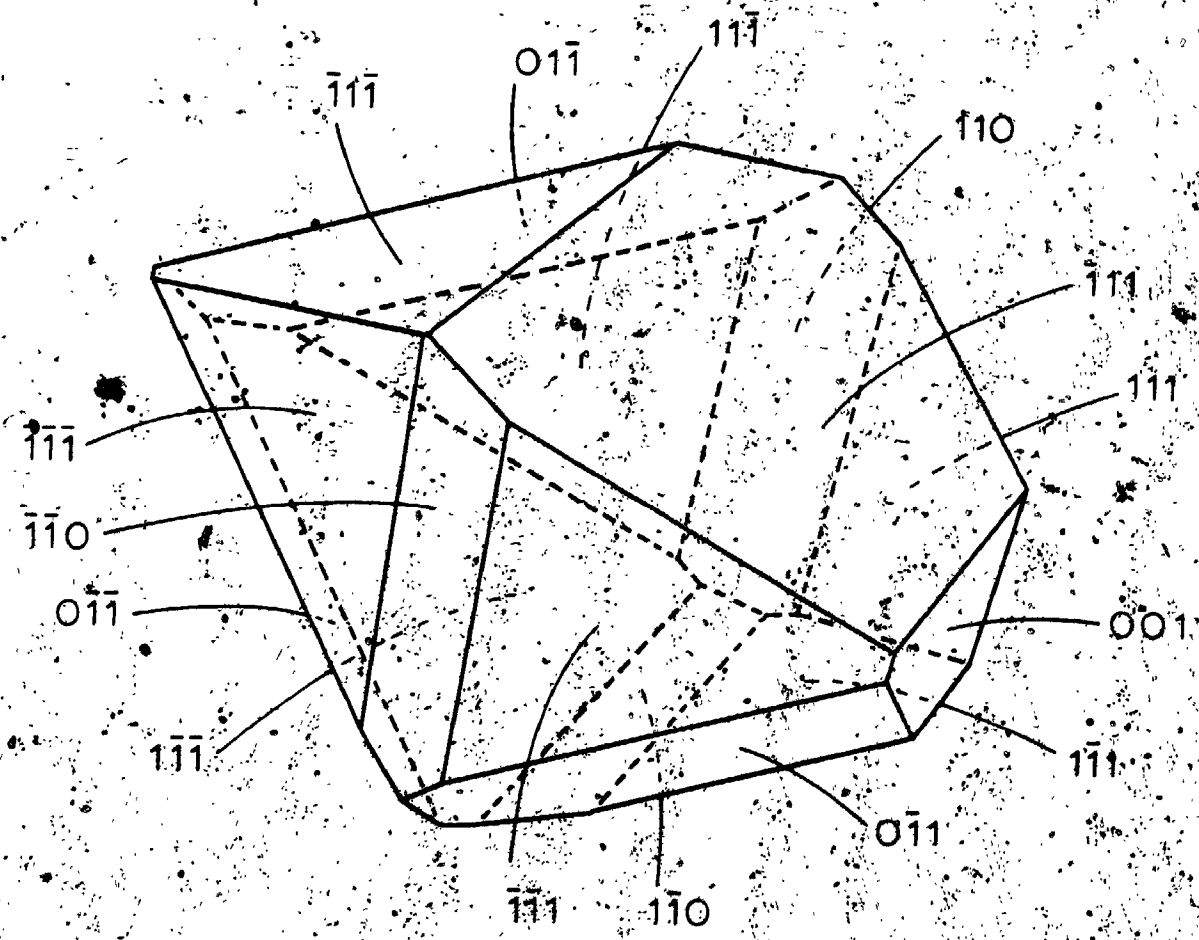

Fig. 4.1

A Drawing of the Data Crystal

Faces with dotted edges are hidden from view.

4.3 Structure Solution and Refinement

From a three dimensional Patterson function the positional parameters of the Pt atom were obtained. These values, together with an overall scale factor were varied in two cycles of least-squares refinement. Agreement factors of $R_1 = 0.232$ and $R_2 = 0.293$ resulted.

Remaining non-hydrogen atom positions were readily determined from successive least-squares refinements and difference Fourier syntheses. The orientation of the cations in the unit cell was found to be such as to preclude m symmetry as required by Pnam, so the choice of Pna2$_1$ as the correct space group was confirmed. As a further test for the presence of a centre of symmetry, values of E, the normalized structure factors were calculated, and the calculated distribution of E values was compared to theoretical calculations for centric and acentric crystals. This operation was performed employing the program FAME. The results were inconclusive as to the presence of a center of symmetry.

The phosphine-phenyl rings were refined as rigid groups with D_{6h} symmetry, and a rigid group of O_h symmetry was calculated for the six F atoms of the anion. Two cycles of least-squares were calculated with isotropic non-group atom temperature factors and overall group thermal parameters being varied, together with positional parameters and an overall scale factor. The isotropic temperature factor of the F6 rigid group increased to about 26 Å^2. Disorder was

suspected, and an examination of electron density maps over the region of the anion confirmed these suspicions. A disorder model analogous to that in Chapter 2 was applied and refined in subsequent least-squares cycles.

As was mentioned above, the space group $Pna2_1$ is non-centrosymmetric and atoms exhibiting large anomalous scattering effects are present. Because of this, two enantiomorphous orientations of the structure are possible, one related to the other by reflection in [001] or by inversion through the origin. Two cycles of full matrix least-squares calculations were performed on each orientation to determine which was the correct one. The same parameters were varied in each case. All non-group atoms of the cation were allowed to vibrate anisotropically. Individual isotropic thermal parameters were varied for phenyl ring rigid groups and overall group temperature factors were calculated for the F6 rigid groups. The P atom of the anion was refined as an atom undergoing isotropic thermal motion. The final agreement factors were considerably different for the two calculations. The values of R_1 and R_2 for the original orientation in which the structure was solved were 0.051 and 0.060 respectively. The second model converged at $R_1 = 0.060$ and $R_2 = 0.074$ Application of Hamilton's R factor significance test (103) to the R_2 values showed that the second orientation could be rejected at the 0.005 significance level. However, no significant differences in geometries were observed for the two models, and only small differences in the heavy atom

thermal parameters were present.

As a further check as to which orientation is correct, the relative magnitudes of the observed and calculated structure factors of the reflections $hk\ell$ and $hk\bar{\ell}$ for both models were compared using the program BIJVOET. For the first model it was found that the relative magnitudes of $F_{hk\ell}$ and $F_{hk\bar{\ell}}$ were the same for the observed and calculated structure factors 87% of the time for the 95 pairs of reflections where $F_{c(hk\ell)}$ and $F_{c(hk\bar{\ell})}$ differed by more than 10%. Of the 80 Friedel pairs differing in F_c by more than 10% in the second model, only 18% showed the same relative magnitudes for F_o and F_c.

Both the R factor significance test and examination of the relative magnitudes of the structure factors of the Friedel pairs confirm that the first model is correct, so the structure refinement was completed in this 'hand'.

The contributions to F_c of the thirty-four H atoms were included in the final least-squares cycles. The positional parameters were calculated from the program HYDRA, and thermal parameters were calculated to be 1.0 $\AA^2$ larger than those of the atom to which each H atom is bonded. Ten phenyl H atom positions were obtained utilizing the known geometry of the ring and a C-H distance of 0.95 Å. Positional parameters for the six methylene H atoms of the carbene ligand were calculated from ideal tetrahedral geometry. A C-H distance of 1.00 Å was assumed. Positions for the six methyl groups were obtained as described in Chapter 2. The methyl C-H distance

is 1.00 Å. Definite evidence for the H atom bonded to O was not observed in the electron density maps, so structure factors were not calculated for this atom.

The final two cycles of full matrix least-squares refinement employed 3421 observations with 187 parameters being varied. The conditions and results of the calculations are given in Table 4.3. Final agreement factors of $R_1 = 0.047$ and $R_2 = 0.054$ were obtained. A statistical examination of the structure factors showed no unusual trends, and no evidence for the presence of secondary extinction was detected.

Final positional and thermal parameters of the non-group atoms are presented in Table 4.4. Rigid group positional and orientation parameters are given in Table 4.5, and derived positional and thermal parameters of rigid group atoms are given in Table 4.6. Calculated H atom positional and thermal parameters are shown in Table 4.7, and a list of $10|F_o|$'s $10|F_c|$ in electrons is presented in Appendix III.

TABLE 4.3

Conditions and Results of Final Full Matrix Least-Squares Calculations

Observations	3421
Variables	187
Ratio (observations/variables)	18.3
Rigid Groups	4
Disorder models (No.; entities)	1; PF_6 anion
Non-group atoms	17
a) Anisotropic	16
b) Isotropic	1
H atoms included; No. (type)	34; 18(methyl), 6(methylene), 10(phenyl)
Extinction coefficient	not refined
Maximum value of (parameter shift/ standard deviation)	1.81
Agreement factors: R_1	0.047
R_2	0.054
Final error on an observation of unit weight	1.75
Final difference Fourier synthesis:	
a) Position of largest peak	(0.269, 0.229, -0.0358)
b) Electron density	1.37(13)e $\AA^{-3}$
c) Associated with	disordered PF_6 anion

TABLE 4.4

Individual Atom Positional and Thermal Parameters

Atom	x	y	z	U_{11}[a]	U_{22}	U_{33}	U_{12}	U_{13}	U_{23}
Pt	0.10441(4)[b]	0.05172(4)	0.2500	548(3)	535(3)	330(2)	24(3)	-124(5)	-101(5)
P(1)	0.2249(2)	-0.0689(3)	0.2431(5)	586(19)	713(23)	374(22)	95(18)	-142(28)	-38(29)
P(2)	-0.0071(3)	0.1818(3)	0.2661(2)	678(24)	535(20)	370(29)	49(19)	25(19)	-97(18)
Cl	0.1881(4)	0.1350(4)	0.3571(3)	1287(47)	1080(40)	966(36)	190(37)	-660(35)	-537(32)
P(3)	0.4534(4)	0.0642(5)	-0.0674(4)	.093(2)[c]					
C(11)	0.2436(14)	-0.1388(14)	0.3419(9)	1189(163)	750(122)	380(84)	154(125)	-346(97)	139(80)
C(12)	0.3338(11)	-0.005(2)	0.2228(11)	467(96)	1483(157)	811(152)	-104(107)	-88(85)	63(112)
C(21)	0.0408(11)	0.3101(11)	0.2365(13)	876(108)	713(97)	535(136)	-24(84)	-40(106)	-56(97)
C(22)	-0.0473(14)	0.1963(15)	0.3706(10)	1031(153)	987(148)	463(94)	47(122)	293(99)	-247(92)
C(1)	0.0351(9)	-0.0175(11)	0.1592(7)	346(78)	518(91)	302(64)	163(68)	-25(57)	-83(58)
N	-0.0248(8)	-0.0924(9)	0.1702(7)	392(70)	652(82)	425(69)	-210(66)	53(56)	-131(58)
C(2)	-0.0486(10)	-0.1307(11)	0.255(2)	787(99)	692(95)	843(111)	-239(81)	23(175)	316(159)
C(3)	-0.0766(10)	-0.1394(14)	0.1028(11)	422(101)	795(122)	823(118)	-265(86)	-64(84)	-210(99)
C(4)	0.0533(9)	0.0164(11)	0.0702(8)	338(80)	499(88)	444(77)	8(67)	58(62)	33(63)
C(5)	0.1205(11)	0.1058(13)	0.0556(9)	598(111)	777(108)	461(81)	25(92)	-53(80)	19(78)
C(6)	0.1334(13)	0.1319(15)	-0.0354(10)	850(140)	770(120)	517(93)	-18(103)	25(90)	-62(86)
O	0.1704(8)	0.0464(11)	-0.0807(7)	724(80)	1412(117)	554(65)	-193(92)	90(59)	-163(76)

[a] The U_{ij}'s are the thermal parameters in terms of mean-square amplitudes of vibration in $Å^2$. Values are given as $U \times 10^4$. The expression for the thermal ellipsoid is given in Appendix II.

[b] Numbers in parentheses given here and in other tables are estimated standard deviations in the least significant digits.

[c] Isotropic thermal parameters are given as U_{iso} in $Å^2$.

TABLE 4.5

Rigid Group Parameters

Group	x_g[a]	y_g	z_g	δ	ε	η	Multiplicity
Ph-1	0.1908(5)	-0.2448(6)	0.1031(5)	2.372(9)	-2.460(7)	1.248(10)	
Ph-2	-0.1851(5)	0.1394(6)	0.1535(5)	-0.581(9)	2.329(6)	1.012(9)	
1-F6	0.4537(10)	0.0582(12)	-0.0628(10)	-0.201(14)	-3.331(13)	-0.449(14)	0.51(2)
2-F6	0.4507(10)	0.0706(13)	-0.0698(10)	-2.477(15)	3.185(13)	2.647(14)	0.49(2)

[a] x_g, y_g, and z_g are the fractional coordinates of the group origin, and δ, ε, and η (radians) are the group orientation angles.

TABLE 4.6

Derived Group Atom Positional and Thermal Parameters

	Atom	x	y	z	B(Å^2)	
Ph-1						
	1C(1)[a]	0.2089(8)	-0.1732(9)	0.1665(6)	4.6(4)	
	1C(2)	0.2451(8)	-0.1558(8)	0.0877(8)	5.6(4)	
	1C(3)	0.2269(9)	-0.2274(10)	0.0243(5)	7.2(5)	
	1C(4)	0.1726(9)	-0.3165(9)	0.0396(7)	7.3(5)	
	1C(5)	0.1365(8)	-0.3339(8)	0.1184(8)	6.7(5)	
	1C(6)	0.1546(8)	-0.2623(10)	0.1819(6)	5.9(4)	
Ph-2						
	2C(1)	-0.1096(6)	0.1640(8)	0.2038(6)	4.1(3)	
	2C(2)	-0.1790(8)	0.0968(8)	0.2329(5)	5.9(4)	
	2C(3)	-0.2544(7)	0.0721(8)	0.1826(7)	6.6(4)	
	2C(4)	-0.2606(7)	0.1147(9)	0.1033(7)	5.9(4)	
	2C(5)	-0.1913(8)	0.1820(9)	0.0742(5)	5.9(4)	
	2C(6)	-0.1158(7)	0.2066(8)	0.1245(6)	5.6(4)	
1-F6						
	1F(1)	0.5488(12)	0.026(2)	-0.105(2)		
	1F(2)	0.3587(12)	0.091(2)	-0.0211(15)		
	1F(3)	0.432(2)	-0.0622(13)	-0.044(2)		
	1F(4)	0.475(2)	0.1786(13)	-0.0812(15)	B(group) = 13.8(8)	
	1F(5)	0.403(2)	0.048(2)	-0.1494(11)		
	1F(6)	0.504(2)	0.068(2)	0.0237(11)		
2-F6						
	2F(1)	0.5253(14)	0.141(2)	-0.023(2)		
	2F(2)	0.3761(15)	0.001(2)	-0.116(2)		
	2F(3)	0.383(2)	0.169(2)	-0.074(2)		
	2F(4)	0.518(2)	-0.028(2)	-0.066(2)	B(group) = 13.8(8)	
	2F(5)	0.407(2)	0.038(2)	0.0162(12)		
	2F(6)	0.494(2)	0.103(2)	-0.1559(12)		

[a] Ring C atoms are numbered sequentially. 1C(1) is bonded to P(1).

TABLE 4.7

Derived Hydrogen Atom Positional and Thermal Parameters

Atom	x	y	z	B(Å²)[a]
	Methyl Hydrogen Atoms			
H1C(11)	0.1950	-0.1956	0.3478	7.13
H2C(11)	0.3064	-0.1718	0.3416	7.13
H3C(11)	0.2380	-0.0876	0.3884	7.13
H1C(12)	0.3750	-0.0541	0.1911	8.13
H2C(12)	0.3225	0.0606	0.1893	8.13
H3C(12)	0.3640	0.0145	0.2763	8.13
H1C(21)	0.1050	0.3164	0.2604	6.94
H2C(21)	0.0417	0.3168	0.1764	6.94
H3C(21)	0.0006	0.3673	0.2621	6.94
H1C(22)	0.0070	0.2085	0.4082	7.36
H2C(22)	-0.0907	0.2580	0.3741	7.36
H3C(22)	-0.0806	0.1303	0.3880	7.36
H1C(2)	-0.1174	-0.1269	0.2625	7.10
H2C(2)	-0.0276	-0.2060	0.2603	7.10
H3C(2)	-0.0168	-0.0859	0.2967	7.10
H1C(3)	-0.1084	-0.0824	0.0706	6.43
H2C(3)	-0.0330	-0.1790	0.0659	6.43
H3C(3)	-0.1240	-0.1894	0.1259	6.43
	Methylene Hydrogen Atoms			
H1C(4)	0.0768	-0.0469	0.0392	4.36
H2C(4)	-0.0082	0.0381	0.0454	4.36
H1C(5)	0.0962	0.1701	0.0841	5.98
H2C(5)	0.1814	0.0853	0.0793	5.98
H1C(6)	0.0712	0.1496	-0.0602	6.75
H2C(6)	0.1758	0.1928	-0.0410	6.75
	Phenyl Hydrogen Atoms[b]			
H1C(2)	0.2818	-0.0956	0.0778	6.71
H1C(3)	0.2509	-0.2157	-0.0292	8.18
H1C(4)	0.1595	-0.3655	-0.0036	8.01
H1C(5)	0.0990	-0.3954	0.1290	7.36
H1C(6)	0.1299	-0.2753	0.2360	6.82
H2C(2)	-0.1741	0.0677	0.2872	6.91
H2C(3)	-0.3009	0.0254	0.2027	7.48
H2C(4)	-0.3115	0.0968	0.0691	6.91
H2C(5)	-0.1954	0.2104	0.0202	7.00
H2C(6)	-0.0686	0.2528	0.1047	6.46

[a] The isotropic thermal parameters for the H atoms are 1.0Å² greater than those of the atoms to which they are bonded.

[b] Phenyl H atoms are numbered sequentially. H1C(2) is bonded to R1C(2), H1C(3) is bonded to R1C(3), etc.

4.4 Description of the Structure

Crystals of the complex result from the packing of discrete ions. The nearest anion-cation approach is 2.93 Å, which is the distance between O and 1F(2). This distance agrees quite well with those of 3.18 Å and 3.08 Å observed in Chapters 2 and 3. Once again disorder of the anion is observed with each possible orientation being equally populated. The disorder multiplicity parameter refined to a value of 0.51(2). The octahedral anion has an almost ideal geometry. The mean P-F bond length is 1.58(2) Å and the mean F-P-F angles are 89.9(6)° and 174.2(7)° for cis and trans F atoms respectively.

An ORTEP diagram of the square planar cation with the atom labelling scheme is presented in Fig. 4.2. A view of the carbene ligand and inner coordination sphere of the Pt atom is given in Fig. 4.3 and an overall stereoview of the cation is shown in Fig. 4.4. Intramolecular bond distances and angles together with their estimated standard deviations are listed in Table 4.8.

The square plane of the metal atom is slightly distorted, since the P(1)-Pt-P(2) angle for the trans phosphines is only 174.3(2)°. The phosphine ligands are bent back away from the carbene ligand. The mean C(1)-Pt-P angle is 92.9(2)° and the average Cl-Pt-P angle is 87.2(3)°. A weighted least-squares plane calculated through Pt, Cl, P(1), P(2) and C(1) is shown in Table 4.9. Atom P(1) lies 0.020(6) Å above this plane and is farthest from it. None

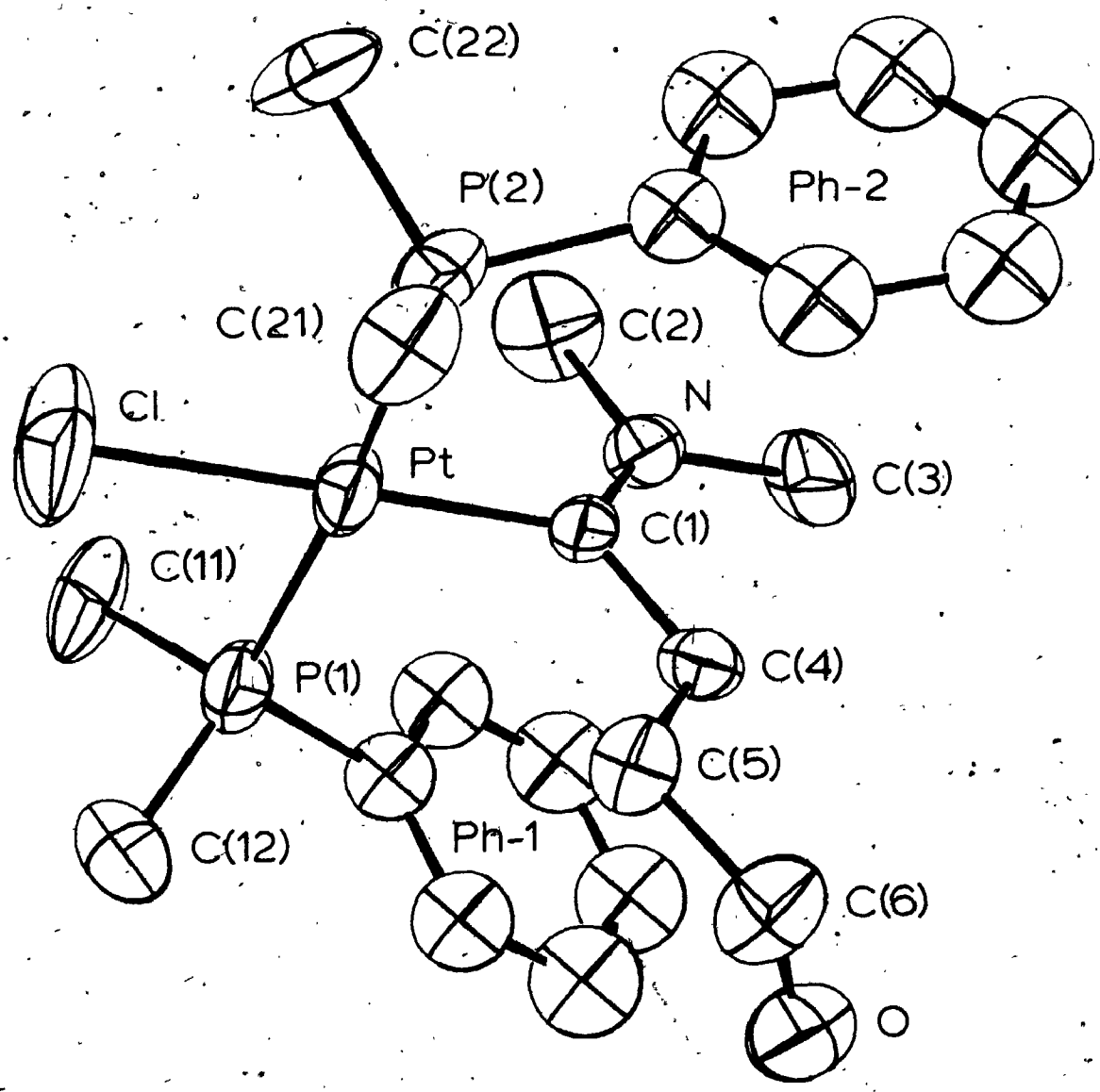

Fig. 4.2

An ORTEP View of the Cation Showing the Atom Numbering Scheme . Ellipsoids are drawn at the 50% probability level.

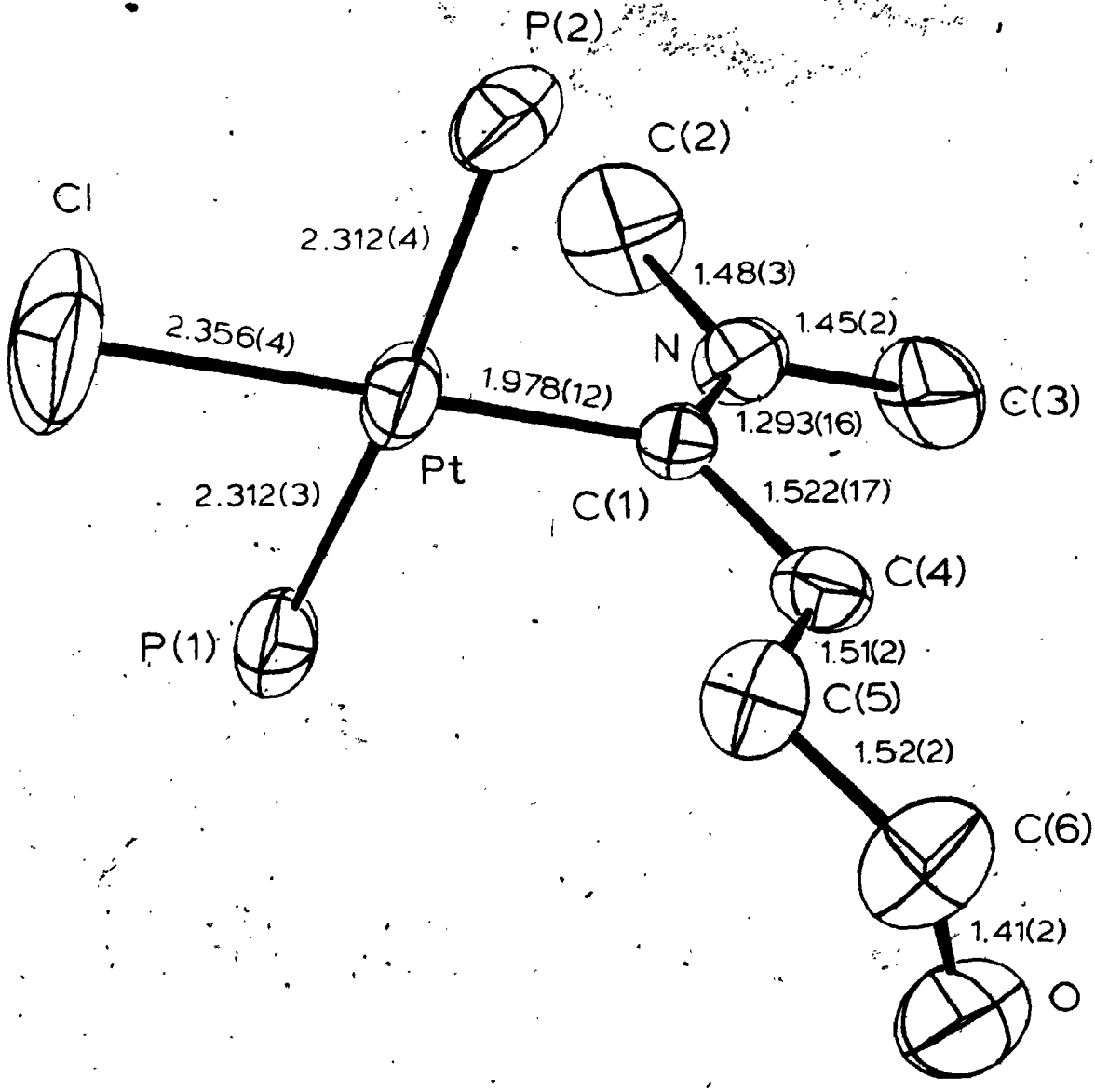

Fig. 4.3

The Carbene Ligand and the Inner Coordination Sphere of the Metal Atom

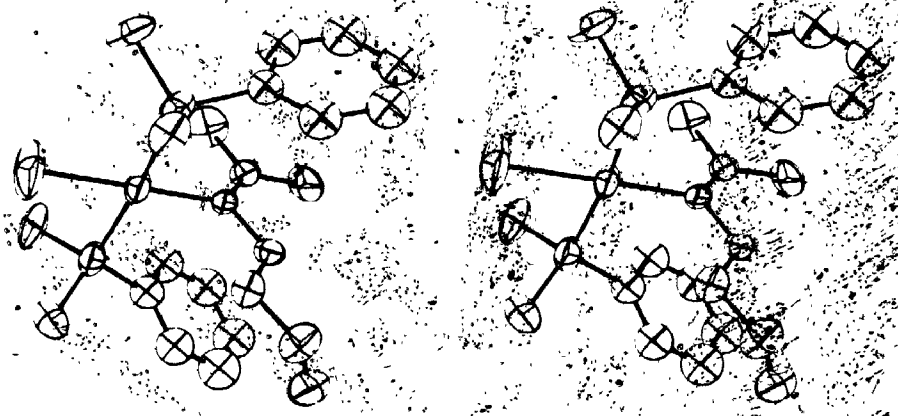

Fig. 4.4

A Stereoview of the Cation

TABLE 4.8

Selected Intramolecular Bond Distances and Angles

Distances(Å)		Angles(deg)	
Metal Atom Inner Coordination Sphere			
Pt-P(1)	2.312(3)	P(1)-Pt-P(2)	171.3(2)
Pt-P(2)	2.312(4)	Cl-Pt-C(1)	179.4(4)
Pt-Cl	2.356(4)	Cl-Pt-P(1)	86.9(2)
Pt-C(1)	1.978(12)	Cl-Pt-P(2)	87.5(2)
		C(1)-Pt-P(1)	93.0(4)
		C(1)-Pt-P(2)	92.7(4)
Phosphine Ligands			
P(1)-C(11)	1.842(15)	Pt-P(1)-C(11)	112.6(7)
P(1)-C(12)	1.792(17)	Pt-P(1)-C(12)	111.8(7)
P(1)-1C(1)	1.822(12)	Pt-P(1)-1C(1)	114.5(4)
P(2)-C(21)	1.825(15)	Pt-P(2)-C(21)	109.8(5)
P(2)-C(22)	1.795(15)	Pt-P(2)-C(22)	113.7(7)
P(2)-2C(2)	1.801(10)	Pt-P(2)-2C(1)	114.7(4)
		C(11)-P(1)-C(12)	104.1(9)
		C(11)-P(1)-1C(1)	105.1(7)
		C(12)-P(1)-1C(1)	108.0(7)
		C(21)-P(2)-C(22)	106.1(9)
		C(21)-P(2)-2C(1)	108.4(6)
		C(22)-P(2)-2C(1)	107.6(6)
Carbene Ligand			
C(1)-N	1.293(16)	Pt-C(1)-N	123.9(9)
C(1)-C(4)	1.522(17)	Pt-C(1)-C(4)	119(1)
N-C(2)	1.484(20)	N-C(1)-C(4)	117(1)
N-C(3)	1.447(17)	C(1)-N-C(2)	121(1)
C(4)-C(5)	1.505(20)	C(1)-N-C(3)	123(1)
C(5)-C(6)	1.518(20)	C(2)-N-C(3)	116(1)
C(6)-O	1.409(19)	C(1)-C(4)-C(5)	118(1)
		C(4)-C(5)-C(6)	113(1)
		C(5)-C(6)-O	112(1)

TABLE 4.9

Weighted Least-Squares Planes

Atom	Deviation from Plane(Å)
Atoms included: Pt, Cl, P(1), P(2), C(1)	
Equation of Plane: 6.763x + 7.207y - 10.88z = -1.641	
Pt	-0.0002(4)
Cl	0.000(7)
P(1)	0.020(6)
P(2)	0.008(4)
C(1)	0.020(14)
Atoms included: C(1), N, C(2), C(3), C(4)	
Equation of Plane: 10.31x - 8.759y - 1.355z = 0.3068	
C(1)	-0.008(12)
N	0.016(12)
C(2)	-0.008(16)
C(3)	-0.014(18)
C(4)	0.003(13)
C(5)	-0.067
C(6)	-0.039
O	1.15

of the other atoms deviate significantly from the plane. The Cl-Pt-C(1) angle is 179.4(4)°.

The dimethylphenylphosphine ligand orientations and geometries are similar to those observed in Chapters 2 and 3. Again the phenyl rings lie on the carbene side of the square plane and virtually perpendicular to it. The angles between the normals to the planes are 94° and 92° for Ph-1 and Ph-2 respectively. As before, the rings are significantly bent in towards the carbene ligand. The P(1)-1C(1)-1C(4) and P(2)-2C(1)-2C(4) angles are 173.6(7)° and 173.7(7)°. Bond angles about 1C(1) and 2C(1) are nearly ideal, for P(1)-1C(1)-1C(2) and P(1)-1C(1)-1C(6) have values of 117.4(8)° and 122.3(9)° respectively, and the corresponding angles about 2C(1) are 118.4(7)° and 121.2(7)°. The geometry about the phosphorus atoms is approximately tetrahedral. The mean Pt-P-C angle is 112.8(8)° and the average C-P-C angle has a value of 106.5(7)°. An average P-C bond length of 1.813(8) Å is observed. These values are consistent with those obtained in Chapters 2 and 3. The phosphine P atoms are equidistant from the metal atom being 2.312(4) Å from it.

The weighted least-squares plane of the carbene ligand (Table 4.9), defined as that containing C(sp^2), N and the atoms C(4), C(2) and C(3) to which they are bonded, lies at an angle of 90.2° to the coordination plane of the metal atom. The N atom is farthest from this plane and lies 0.016(12) Å above it. The carbene ligand can be written as

$RCH_2C{=}NMe_2$, where R is an ethanolic substituent. Of the atoms making up this group, C(5) and C(6) lie only slightly below the carbene plane, and O is 1.15 Å above it.

The Pt-C(sp^2) bond distahce is 1.978(12) Å and is shorter by 5.6σ than that of 2.079(13) Å observed for the aminocarbene complex in Chapter 2. Within the carbene ligand, the C(sp^2)-N bond length is 1.293(16) Å. This is not significantly longer than that of 1.266(15) Å observed in Chapter 2 in that the bond lengths differ by 1.2σ. The mean N-C(methyl) distance is 1.465(15) Å and the C(sp^2)-C(4) bond length is 1.505(20) Å. These values are crystallographically equivalent to those obtained in Chapter 2. The angles about the C(carbene) atom have a mean value of 120(2)°. The mean C(1)-N-C(methyl) angle is 122(1)° and the C(2)-N-C(3) angle is 116(1)°. Coplanarity of C(1), N, C(2), C(3) and C(4) as well as the magnitude of the angles about C(1) and N are indicative of sp^2 hybridization. The smaller C(2)-N-C(3) angle may be due to some sp^3 character in the N atom. This is not surprising since C(1) and N are not related by a formal double bond. The C(sp^3)-N-C(sp^3) angle for the dimethylamino-substituent in Chapter 2 was 113(1)°.

The mean C(sp^3)-C(sp^3) bond length in the alcoholic substituent is 1.511(7) Å. A value of 1.54 Å is predicted from the sum of the covalent radii (94). The mean angle about the C(sp^3) atoms of this group is 114(3)°, a value larger than that of 109.47° expected in an ideal tetrahedral

situation. The oxygen atom of the hydroxyl group and C(6) are separated by a bond of 1.409(19) Å. An accepted C-O single bond length is 1.43 Å (88).

The Cl^- ligand is located <u>trans</u> to the carbene and a Pt-Cl bond of 2.356(4) Å is observed. This value is crystallographically equivalent to those of 2.362(3) and 2.361(5) Å obtained for <u>cis</u>-$PtCl_2\{C(NPhCH_2)_2\}PEt_3$ (71) and <u>cis</u>-$PtCl_2\{C(OEt)NHPh\}PEt_3$ (69) respectively. In these complexes carbene ligands also lie opposite Cl^-.

4.5 Discussion

Pt-Cl bond lengths are useful for determining the trans influence of the ligand in the opposite coordination site (68). For example, the Pt-Cl bond length of 2.276(1) Å in cis-$PtCl_2(CO)PPh_3$ (104) is shorter than that of 2.371(3) in trans-$PtMeCl(PPh_2Me)_2$ (101) by 31.7σ. In the former complex the Cl^- ligand lies opposite CO, a ligand of very weak trans influence, whereas in the latter Cl^- is opposite methyl, a strong trans influence ligand.

In this study, the Pt-Cl bond length is 2.356(4) Å. This is 3.0σ shorter than that where Cl^- is trans to a methyl ligand and 20.0σ longer than that where Cl^- is trans to CO. The carbene ligand displays a trans influence almost as large as that of the methyl ligand. Equivalent Pt-Cl bond lengths of 2.362(3) and 2.361(5) Å have been obtained for the complexes cis-$PtCl_2\{C(NPhCH_2)_2\}PEt_3$ (71) and cis-$PtCl_2\{C(OEt)NHPh\}PEt_3$ (69) respectively where different types of tertiary carbene ligands lie opposite Cl^-. Thus, the trans influences of the different types of tertiary carbene ligands are similar, suggesting that the nature of the Pt-C(sp^2) bonds is also similar.

The Pt-C(carbene) distance of 1.978(12) Å is equivalent to those of 2.009(13) and 1.962(18) Å obtained for cis-$PtCl_2\{C(NPhCH_2)_2\}PEt_3$ (71) and cis-$PtCl_2\{C(OEt)NHPh\}PEt_3$ (69) respectively, but is shorter by 5.6σ than that observed for the similar aminocarbene complex in Chapter 2, where methyl lies opposite carbene. Thus replacing a strong trans

influence ligand by a weaker one results in a significant shortening of the metal-carbene bond. A similar effect can be induced by replacing the amino-substituent on the carbene ligand with an oxy- one, as in Chapter 3. This results in the observation of significant metal carbene $d\pi$-$p\pi$ interaction owing to the greater electronegativity of O over N. It has been shown in Chapter 2 that although the carbene ligand lies approximately perpendicular to the square plane of the metal atom, metal-ligand π bonding is virtually nonexistent in the aminocarbene systems. This has also been concluded from X-ray photo-electron studies on other Pt(II) aminocarbene compounds (105). Thus the 'shortened' Pt-Cl(carbene) bond is a result of the weak trans influence of Cl^-.

CHAPTER 5

PREPARATION OF COMPLEXES FOR X-RAY CRYSTALLOGRAPHIC EXAMINATION

5.1 Introduction

An examination of current literature revealed that X-ray crystallographic structure determinations have been performed in several square-planar carbene complexes of Pt(II) (35, 69, 71, 72). These are in addition to the experiments performed in our laboratories (92, Chapter 2, Chapter 3, Chapter 4). Comparison of the results obtained in Chapters 2, 3, and 4 with those from the other structural studies proved difficult since the environments of the carbene ligands in the other complexes vary considerably; moreover, the nature of the carbene ligand itself differs greatly. Thus it became evident that a great deal of valuable information could be obtained about these systems if complexes containing more than one type of carbene ligand in similar environments could be prepared. Also, compounds containing various carbene ligands together with other related ligands of varying C—N bond order would be extremely useful for X-ray structural studies. Since we had already performed four experiments on square-planar Pt(II) complexes containing mutually <u>trans</u> dimethylphenylphosphine ligands, it was regarded as advantageous to retain this basic environment in

the new compounds. Accordingly, complexes of the form <u>trans</u>-$[PtLL'(PMe_2Ph)_2]^{n+}$ were prepared. L and L' are combinations of the following types of ligands.

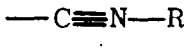

isocyanide

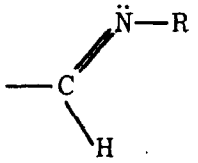

formimidoyl

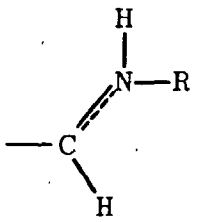

secondary carbene (2a)

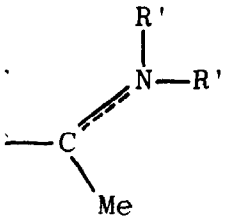

3b

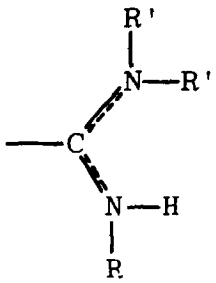

3a

tertiary carbenes

R = p-tolyl

R' = H, methyl

5.2 Complexes Obtained from Isocyanide Insertion Reactions

Isocyanide insertion reactions are quite well known for square planar Pt(II) systems (19, 61, 106-109). Among these, the insertions of isocyanide molecules into Pt-R(R=Me,Ph) bonds resulting in the formation of 'imidoyl' ligands (106-108) have been reported for systems containing trans phosphine ligands. The resulting complexes are of the form trans-$[MRXL_2]$ where X = halide, L = phosphine and R is an 'imidoyl' ligand.

Christian and Clark have reported reactions involving the insertion of isocyanide into Pt-H bonds in square planar trans-bis-triethylphosphine complexes of Pt(II) (19) to give products containing formimidoyl ligands. Protonation of these ligands results in the formation of secondary carbenes. The reaction scheme is presented in Fig. 5.1. It seemed probable that this reaction sequence could be extended to the bis-dimethylphenylphosphine system to give the corresponding formimidoyl and secondary carbene compounds. On the premise that these complexes could be obtained, the following reaction sequence was proposed:

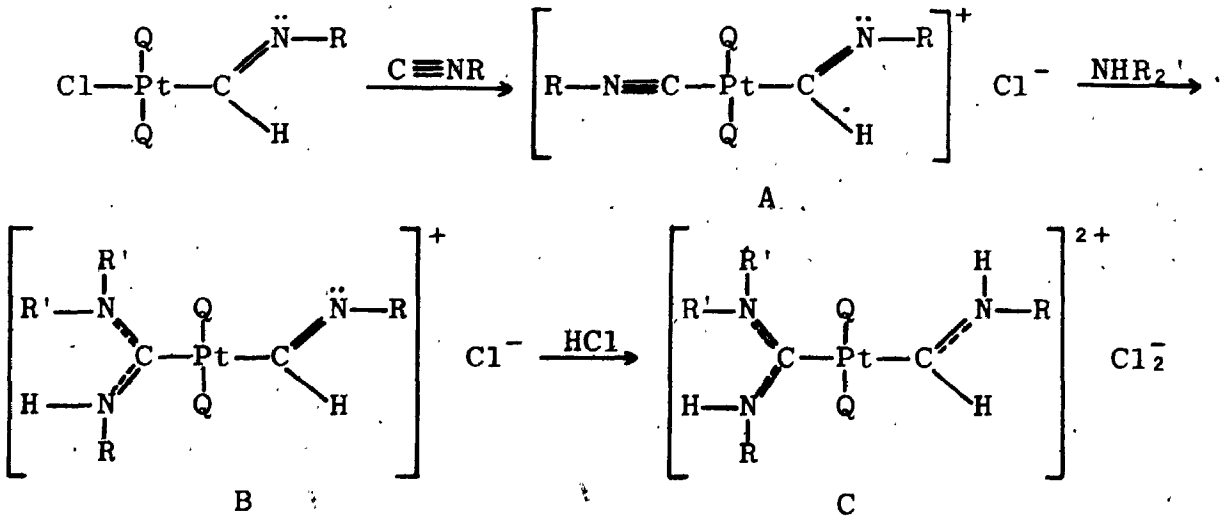

R = p-tolyl, Q = PMe_2Ph, R' = H, alkyl, aryl

Fig. 5.1

Preparation of Secondary Carbene Complexes from Isocyanide Insertion Products

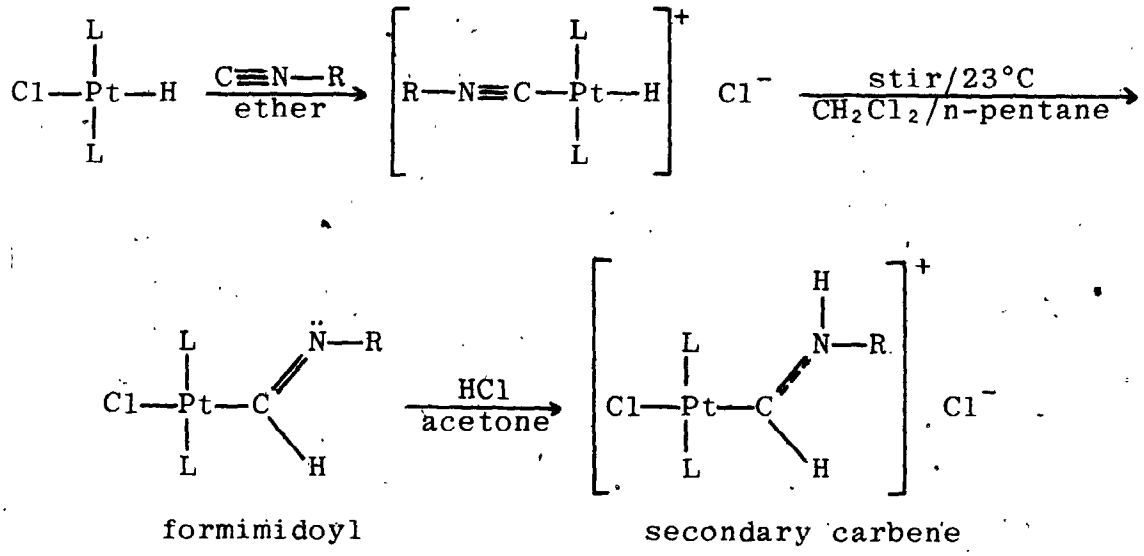

formimidoyl

secondary carbene

R = p-tolyl, L = PEt_3

The three cationic systems above would be interesting complexes for crystallographic studies. A has a formimidoyl ligand trans to isocyanide; or, if the formimidoyl is protonated, secondary carbene trans to isocyanide. Complex B has formimidoyl trans to a tertiary carbene, and if protonated to give compound C, then both a secondary and tertiary carbene ligand would be present in the same complex.

i. Preparation

The syntheses of the desired complexes were not as straight forward as expected. When a very dilute solution of p-tolylisocyanide (0.01M) was added dropwise to a suspension of trans-$PtHCl(PMe_2Ph)_2$ at room temperature, the solution immediately turned a deep red colour. The source of the colouration was not identified, but this byproduct was difficult to separate from the desired complex. The reaction went with poor yield. If the reaction mixture was cooled to -80°C, the reaction proceeded cleanly in good yield. Slight red colouration occurred as the reaction mixture was warmed to room temperature. The cationic product was found to be very hygroscopic and so the insertion reaction to yield B was performed as quickly as possible. Some red discolouration persisted throughout the insertion reaction, but pale yellow crystals of $Pt(CH{=}N\text{-}p\text{-}tolyl)Cl(PMe_2Ph)_2$ could be obtained after lengthy workup.

It was found that the formimidoyl complex B is readily protonated with HCl to give the secondary carbene species

trans-[Pt(CH==NH-p-tolyl)Cl(PMe_2Ph)$_2$]Cl. This compound could easily be recrystallized to give clean colourless crystals. The protonation could then be reversed with triethylamine to give back the formimidoyl complex with no red discolouration. This proved useful in obtaining a pure formimidoyl product. Either the secondary carbene or the formimidoyl complex could be reacted with isocyanide. The strong trans effect of the formimidoyl and carbene ligands allows facile diplacement of the chloride ligand by isocyanide. 1,2 addition of p-toluidine across the isocyanide ligand produced the desired tertiary carbene complexes (B, C). Deprotonation of the secondary carbene ligand could be performed at any step of the synthesis. Since the secondary carbene complexes proved to be easier to handle, if a formimidoyl product was desired, the deprotonation reaction was performed last.

In order to obtain the cationic complexes in pure crystalline form, the Cl^- anions were often exchanged for PF_6^- using $AgPF_6$. The hexafluorophosphate salts were sometimes easier to crystallize.

ii. Characterization and Discussion

a. Infrared and Analytical Data

The isocyanide, formimidoyl, and carbene ligands all show strong characteristic bands in the infrared spectrum. These bands are due to the C — N vibrations of the various ligands. A summary of the IR spectral data for complexes I - VI is presented in Table 5.1.

TABLE 5.1

Infrared Data for Complexes I - VI (cm^{-1})[a]

Complex[b]	ν(C≡N)	ν(C=N)	ν(C···N)	ν(C-H) (formimidoyl)	ν(N-H)	δ(N-H)	ν(P-F)
I $[Pt(C{\equiv}NR)HQ_2]Cl$[c]	2195 vs						
II $Pt(CH{=}NR)ClQ_2$[c]		1550 s					
III $[Pt(CH{=}NHR)ClQ_2]Cl$			1575 s		2745 s(br)	1633 s	
IV $[Pt(CH{=}NHR)(C{\equiv}NR)Q_2](PF_6)_2$	2225 vs.		1570 s		3290 s	1620 s	835 vs(br)
V $[Pt(CH{=}NHR)\{C(NHR)_2\}Q_2]Cl_2$			1535 s(br)		3260 vs	1615 s	
VI $[Pt(CH{=}NR)\{C(NHR)_2\}Q_2]PF_6$		1540 s(br)	1540 s(br)	2728 s(br)	3770 s, 3300 s(br)	1600 s(br)	835 vs
$[Pt(CH{=}NR)\{C(NHR)_2\}Q_2]Cl$		1540 s(br)	1540 s(br)	2730 m	3265 s(v br)	1610 s, 1590 s	

[a] IR spectra were measured as nujol mulls unless otherwise stated.

[b] R = p-tolyl, Q = PMe_2Ph; all complexes here and in other tables have trans stereochemistry.

[c] recorded in dichloromethane.

For the isocyanide complexes I and IV, the $\nu(C\equiv N)$ stretch occurs at approximately 2200 cm^{-1}; a substantial increase from the value of 2125 cm^{-1} for the uncoordinated ligand. Such a shift in $\nu(C\equiv N)$ is characteristic for cationic systems (110). When the insertion reaction is performed to give the formimidoyl ligand, or when addition of amine across the isocyanide occurs to form a tertiary carbene complex, the $\nu(C\equiv N)$ stretch is replaced by a weaker, broader band due to $\nu(C=N)$ or $\nu(C=\!=N)$ in the frequency range 1500-1600 cm^{-1}. Protonation of the formimidoyl ligand to give secondary carbene results in only a slight shift in the $\nu(C=N)$ band. The secondary and tertiary carbene ligands show N-H stretching and deformation bands at frequencies of approximately 3300 cm^{-1} and 1600 cm^{-1} respectively. The complex <u>trans</u>-[Pt(CH=NH-p-tolyl)$(PMe_2Ph)_2$]Cl is anomalous in that ν(N-H) occurs at 2745 cm^{-1}. For the corresponding triethylphosphine complex a similar effect was observed and the ν(N-H) band was observed at 2575 cm^{-1} (61). The absence of a band at 3300 cm^{-1}, and D_2O exchange studies on the triethylphosphine system show that this low frequency band is indeed due to ν(N-H). An explanation of the low frequency at which this vibration is observed may be that some hydrogen bonding occurs between the carbene proton and the Cl^- anion. When the Cl^- anion is exchanged for ClO_4^- in the triethylphosphine complex, four ν(N-H) bonds are observed in the frequency range 3100 - 3250 cm^{-1}. The presence of several ν(N-H) bands is considered to be the result of perchlorate association with the carbene H atom (61).

The solid state spectra for the formimidoyl complexes have a ν(C-H) (formimidoyl) stretch at about 2730 cm^{-1}. Similar behavior is observed for the formimidoyl ligands of the triethylphosphine complexes (109) as well as for the electronically similar formyl ligand in $[Fe(HCO)(CO)_5]^-$ (111).

In the complexes containing a PF_6^- anion, a very strong ν(P-F) band at 835 cm^{-1} is observed.

Analytical and physical data for these complexes are presented in Table 5.2.

b. ^1H NMR Spectra

^1H NMR data for the complexes II to VI are presented in Table 5.3.

The formimidoyl and secondary carbene ligands show characteristic downfield resonances in their ^1H NMR spectra. Signals at about δ 10.5 are due to the proton bonded to the $C(sp^2)$ atom. The spectrum of this atom is expected to be a triplet as a result of spin-spin coupling with ^{31}P of the two phosphine ligands. Satellite resonances with the same structure, but of about one-quarter intensity due to coupling with ^{195}Pt ($I = \frac{1}{2}$, natural abundance 33.8%) should also be present. Two overlapping sets of such 'triplet of triplets' resonances are observed for the complexes trans-Pt(CH=N-p-tolyl)Cl$(PMe_2Ph)_2$ and trans-$[Pt(CH{=}{=}NH\text{-}p\text{-}tolyl)Cl(PMe_2Ph)_2]Cl$. Similar spectra have been observed for the analogous triethylphosphine complexes, which have been studied extensively. In these compounds the two sets of downfield signals observed

TABLE 5.2

Analytical and Physical Data[a]

Complex[b]	Analysis: found (calculated) (%) C	H	N	Melting Point (°C)
II $Pt(CH{=}NR)ClQ_2$	46.29 (46.12)	4.81 (4.84)		133–135
III $[Pt(CH{=}NHR)ClQ_2]PF_6$	37.34 (37.39)	3.98 (4.05)	2.02 (1.82)	198–199
IV $[Pt(CH{=}NHR)(C{\equiv}NR)Q_2](PF_6)_2$	38.52 (38.50)	3.87 (3.84)	2.82 (2.81)	171–172
V $[Pt(CH{=}NHR)\{C(NHR)_2\}Q_2]Cl_2$	52.76 (52.88)	5.29 (5.35)	4.66 (4.74)	184–186
VI $[Pt(CH{=}NR)\{C(NHR)_2\}Q_2]PF_6$	48.27 (48.85)	4.73 (4.84)		196–197
$[Pt(CH{=}NR)\{C(NHR)_2\}Q_2]Cl\cdot CH_2Cl_2$	51.68 (51.43)	5.11 (5.18)	4.46 (4.50)	170–172

[a] All compounds were colourless.

[b] R = p-tolyl, Q = PMe_2Ph.

TABLE 5.3

^{1}H NMR Chemical Shifts[a] and Coupling Constants[b]

Complex[c]	Phosphine Methyl Protons			Formimidoyl Proton				p-Tolyl Methyl	Other ^{1}H NMR Signals
	$\delta(CH_3)$	J_{P-H}[d]	$^3J_{Pt-H}$	$\delta(CH)$	$^2J_{PtCH}$	$^3J_{PPtCH}$	$^3J_{HCNH}$	$\delta(CH_3)$	
II $Pt(CH{=}NR)ClQ_2$	1.82 1.76	6.8 7.0	29.0 29.0	10.57, 10.46(1:1)[e]	78.0, 74.0	5.0, 5.5		2.23	δ(phenyl) 6.8-7.9
III $[Pt(CH{=}NHR)ClQ_2]Cl$	1.90[f] 1.84	7.2 7.2	30.0 30.4	11.30, 10.66(4:7)	37.5, 49.5	5.4	10.0, 17.5	2.26	δ(phenyl) 6.7-7.9
IV $[Pt(CH{=}NHR)(C{\equiv}NR)Q_2](PF_6)_2$	1.97 2.05	8.3 8.0	33.5 33.5	10.91	33.5	5.6	16.0	2.27(br)	δ(phenyl) 6.4-7.9
V $[Pt(CH{=}NHR)(C(NHR)_2)Q_2]Cl_2$	1.84 1.82	7.2 7.2	32.4 32.2	10.60	32.2	5.5	15.4	2.31, 2.36	δ(phenyl) 6.4-8.0 δ(N-H) 12.29, ^3J(PtCNH)~45
VI $[Pt(CH{=}NR)(C(NHR)_2)Q_2]Cl$	1.72 1.71	6.8 6.8	32.0 32.0	10.21	32.0	6.5		2.30, 2.23	δ(phenyl) 6.4-8.2 δ(N-H) 12.17, ^3J(PtCNH) 46.0

[a] In ppm (±0.01) (downfield positive) from TMS

[b] In Hz.

[c] R = p-tolyl, Q = PMe_2Ph.

[d] $^2J_{P-H} + {}^4J_{P-H}$ is quoted. See references 114 and 115.

[e] Numbers in brackets are ratios of isomers.

[f] Other resonances were complex and could not be interpreted.

are due to syn/anti isomerism in the formimidoyl complex, and due to cis/trans isomerism of the secondary carbene ligand (61, 109).

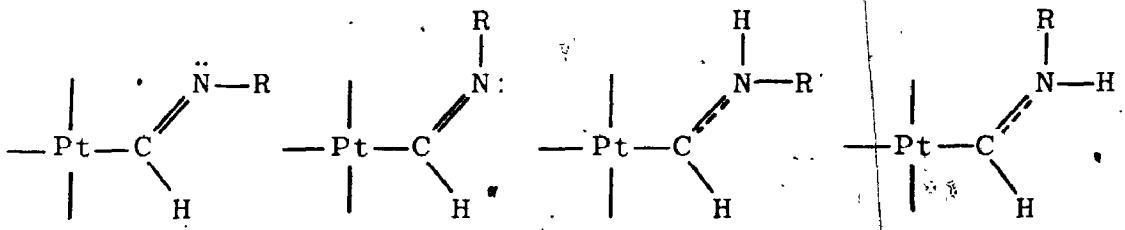

syn anti trans cis

formimidoyl secondary carbene

The relative magnitudes of these downfield resonances, and thus the relative multiplicities of each isomer present were found to be solvent dependent for the complex trans-$Pt(CH{=}N\text{-}p\text{-}tolyl)Cl(PEt_3)_2$ (61). This, in conjunction with the fact that the ortho protons of the p-tolyl phenyl ring show a large downfield shift (~1.2 ppm) with respect to the free ligand in these and related complexes (69, 109, 112), was used to assign the resonance at lower field to the anti isomer. The coupling constants $^2J_{PtCH}$ and $^3J_{PPtCH}$ were found to be smaller for the anti than for the syn isomer. For the complex trans-$Pt(CH{=}N\text{-}p\text{-}tolyl)Cl(PMe_2Ph)_2$ (II) the two isomers are present in equal amounts in $CDCl_3$ solution; moreover, the p-tolyl phenyl ring resonances are complicated by the presence of the phosphine phenyl proton signals. The coupling constants to Pt and P for the formimidoyl proton resonances at lower field are smaller than those

for the higher field signal, so by analogy with the triethylphosphine compound the signal at lower field was assigned to the anti isomer.

The secondary carbene ligands of the complexes trans-[Pt(CH=NH-p-tolyl)ClL$_2$]Cl; L = PMe_2Ph, PEt_3 show downfield signals similar to those of the formimidoyl ligand, and assignment of the signals at lower field to the cis isomer were made in the same manner. The ratio of carbene isomers cis:trans for the complex trans-[Pt(CH=NH-p-tolyl)Cl(PMe_2Ph)$_2$]Cl (III) in $CDCl_3$ is about 4:7. An added feature of the downfield spectrum of the secondary carbene complexes is that strong coupling $^3J_{HCNH}$ is observed. Such long range coupling is similar to that observed in vinylic systems, where the coupling constants for the trans isomers are generally larger than those for the cis ones (113). Thus, the magnitude of $^3J_{HCNH}$ can be used as a check on the assignment of the downfield C(sp^2)-H signals to the cis and trans isomers. The trans isomer is dominant for the complex III, and for complexes IV and V the cis isomers of the secondary carbene ligand are virtually non-existent.

The complex trans-[Pt(CH=N-p-tolyl){C(NH-p-tolyl)$_2$}(PMe_2Ph)$_2$]Cl (VI) shows only one downfield resonance due to C(sp^2)-H of the formimidoyl ligand. This implies that either free rotation occurs about the C=N bond, or that only the more stable isomer is present. The carbene ligand trans to the formimidoyl ligand is a good σ donor, as are

the phosphine ligands. An electron rich Pt atom could result in a polarized transition state where the barrier to rotation about the C=N bond is lowered:

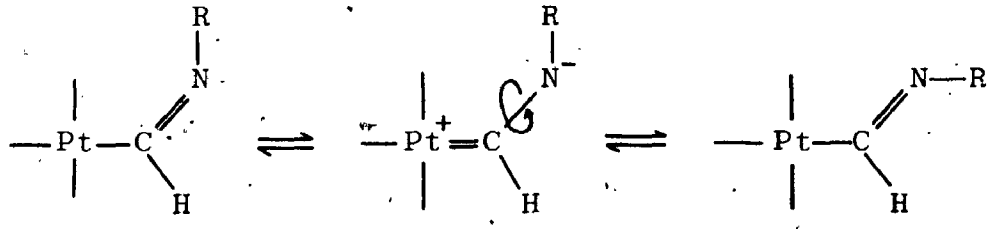

anti syn

Rapid rotation could result in an NMR signal averaged over the syn and anti isomers. The complex trans-Pt{C(OMe)-N-p-tolyl}(CH=N-p-tolyl)(PEt_3)$_2$ also showed only one downfield signal in its ^1H NMR spectrum (109), even on cooling to -80°C. This observation suggests the presence of only the thermodynamically stable isomer of the formimidoyl ligand in these complexes.

The N-H signals of the secondary carbene ligand are not observed in the $CDCl_3$ solution spectra. Broad resonances due to the tertiary carbene ligands are observed (δ~12) in the spectra of compounds V and VI. These signals appear as singlets with ^{195}Pt satellites, $^3J_{PtCNH}$ ~46 Hz.

The stereochemistry of the complexes may be determined from the resonances of the phosphine methyl groups. In a simple situation where trans-dimethylphenylphosphine ligands are present, and all methyl groups are equivalent, a triplet signal resulting from coupling to ^{31}P (114, 115) with ^{195}Pt satellites is observed. In more complex situations, where the methyl protons are non-equivalent,

several overlapping 'triplet of triplets' signals are observed. Magnetic inequivalence of the methyl protons may be a result of the absence of a mirror plane of symmetry perpendicular to and bisecting the P-Pt-P axis, or due to restricted rotation about the Pt-C(sp^2), C=N or C≡≡N bonds, resulting in the presence of isomers (116).

An account of some of this work has been published in conjunction with the results obtained from the analogous triethylphosphine complexes (61, 109).

5.3 Complexes Obtained from Acetylenic Intermediates

A second route to complexes for X-ray crystallographic studies emerged from work reported by Chisholm and Clark (63, 64). Addition of $AgPF_6$ to a methanolic solution of trans-$PtMeCl(PMe_2Ph)_2$ resulted in precipitation of AgCl to give the solvated cationic species trans-$[PtMeS(PMe_2Ph)_2]PF_6$, S = solvent. Addition of terminal acetylenes to methanolic solutions of the solvated cation produces oxy-carbene species, with the carbene ligand trans to a methyl ligand (63). Reaction of the carbene complex with some primary and secondary amines produced the corresponding aminocarbene complexes. As discussed in Chapter 4, further reaction with HCl resulted in replacement of the methyl ligand with chloride. In these complexes the aminocarbene ligand occupies a coordination site trans to chloride. Since the carbene exerts a strong trans influence, these chloro-complexes seemed the logical precursors for new systems. A reaction route was proposed:

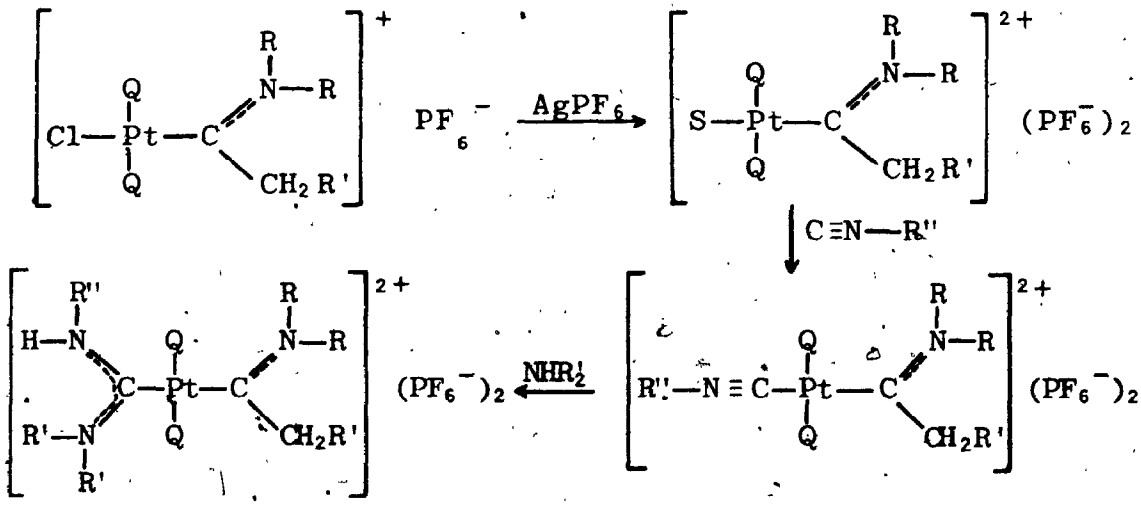

S = solvent; Q = PMe_2Ph; R = H, alkyl; R' = H, alkyl, aryl; R'' = alkyl, aryl

Such a scheme would give complexes containing tertiary carbene ligands trans to isocyanide, as well as bis-carbene complexes containing different types of tertiary carbene ligands.

i. Preparation

Attempts to prepare the solvated dicationic species at room temperature proved futile. Addition of $AgPF_6$ to acetone or methanol solutions of trans-$[Pt(MeC{=}{=}NMe_2)Cl(PMe_2Ph)_2]PF_6$ resulted in precipitation of AgCl, followed by rapid decomposition of the compound in solution. This occurred even if the isocyanide was added prior to $AgPF_6$.

The desired isocyanide complex could readily be obtained by cooling an acetone solution of starting material to -80°C. Addition of isocyanide and then $AgPF_6$ gave no reaction, but on warming the solution slowly to room temperature, a precipitate of AgCl formed and the solution turned a pale yellow colour. The stable dicationic complex trans-$[Pt(C{\equiv}N\text{-}p\text{-}tolyl)(MeC{=}{=}NMe_2)(PMe_2Ph)_2](PF_6)_2$ was easily isolated. Reaction of this complex with $NHMe_2$ in dichloromethane solution gave the desired bis-carbene complex trans-$[Pt\{C(NH\text{-}p\text{-}tolyl)(NMe_2)\}(MeC{=}{=}NMe_2)(PMe_2Ph)](PF_6)_2$. These reactions could readily be repeated with starting materials containing the carbene ligands $MeC{=}{=}NHMe$ and $HO(CH_2)_3C{=}{=}NMe_2$.

ii. Characterization and Discussion

a. Infrared and Analytical Data

Infrared data for the series of isocyanide-carbene and bis-carbene complexes are summarized in Table 5.4. The preparation of compounds similar to trans-$[Pt\{HO(CH_2)_3-C{=}{=}NMe_2\}Cl(PMe_2Ph)_2]PF_6$ (VII) has been described previously (64), however no spectral results have been presented for this particular complex. These are therefore included with the data presented here.

As with the formimidoyl and secondary carbene species described earlier, the infrared spectra of the present complexes are very informative with respect to the isocyanide and carbene ligands. In all cases the starting materials were monocarbene compounds similar to VII. These complexes show a strong single band at about 1590 cm^{-1} corresponding to $\nu(C{=}{=}N)$ of the carbene ligand. Upon reaction with isocyanide, a strong $\nu(C{\equiv}N)$ band appears at about 2220 cm^{-1}. This represents an increase in the isocyanide stretching frequency from that of the free ligand of 95 cm^{-1}. Reaction of $NHMe_2$ with the isocyanide complexes results in disappearance of the strong $\nu(C{\equiv}N)$ stretch, and in the appearance of a second $\nu(C{=}{=}N)$ carbene band at about 1550 cm^{-1}. This band is at slightly lower frequency, and is broader than the one due to the other carbene ligand.

Other new bands are also observed at 3150-3400 cm^{-1}, and at about 1620 cm^{-1}. These correspond to stretching and deformation vibrations of the N-H bond of the p-tolylamino

TABLE 5.4

Infrared Data for Complexes VII to XIII (cm^{-1})[a]

Complex[b]	ν(C≡N)	ν(C=N)	ν(N-H)	δ(N-H)	ν(O-H)	ν(P-F)
VII $[Pt\{HO(CH_2)_3C=NMe_2\}ClQ_2]PF_6$		1576 s			3586 s	840 vs(br)
VIII $[Pt(C\equiv NR)(MeC=NHMe)Q_2](PF_6)_2$	2226 vs	1627 s	3328 s	1630 s[c]		841 vs(br)
IX $[Pt(C\equiv NR)(MeC=NMe_2)Q_2](PF_6)_2$	2218 vs	1623 s				842 vs(br)
X $[Pt(C\equiv NR)\{HO(CH_2)_3C=NMe_2\}Q_2](PF_6)_2$	2221 vs	1592 s			3602 s	841 vs(br)
XI $[Pt\{C(NHR)(NMe_2)\}(MeC=NHMe)Q_2](PF_6)_2$		1557 vs, 1609 s	3386 s, 3260 m(br) 3172 s(br)	1627 s		847 vs(br)
XII $[Pt\{C(NHR)(NMe_2)\}(MeC=NMe_2)Q_2](PF_6)_2$		1554 vs, 1602 s	3266 m	1608 s[c]		841 vs(br)
XIII $[Pt\{C(NHR)(NMe_2)\}\{HO(CH_2)_3C=NMe_2\}Q_2](PF_6)_2$		1558 vs, 1576 s	3380 m, 3355 s	1610 s	3600 s	844 vs(br)

[a] All IR spectra were recorded as nujol mulls.

[b] Q = PMe_2Ph, R = p-tolyl.

[c] Shoulder on C=N band.

substituent of the new tertiary carbene ligand —C(NH-p-C_6H_4Me)-(NMe_2). Three ν(N-H) stretching frequencies have been observed for complex IX, and two for VIII although only two N-H bonds should occur in the former, and one in the latter. Similar effects have been previously observed in solid state IR spectra of Pt(II) carbene complexes (61, 117). Such observations are attributed to hydrogen bonding and solid state effects.

Compounds containing the carbene ligand —C{$(CH_2)_3OH$}(NMe_2) show a characteristic ν(O-H) stretch at about 3600 cm^{-1}.

Analytical and Physical data for these complexes are given in Table 5.5.

b. ^1H NMR Spectra

The ^1H NMR spectra of these complexes are quite complicated. A summary of the data obtained is presented in Table 5.6. The assignments of the resonances due to the carbene ligands were made mainly by comparison with similar systems (118, 119, 120).

Clark and coworkers have performed extensive ^1H and ^{13}C NMR experiments on carbene complexes of the type trans-[Pt(MeC---NMe_2)MeL_2]PF_6, L = PMe_2Ph, $AsMe_3$(118), and Moser and Fischer have examined Cr(MeC---NMe_2)$(CO)_5$ (120). In both systems the expected three resonances due to methyl protons of the methyl-N,N-dimethylaminocarbene ligand were observed. In the Pt complexes they occurred at δ 2.40, 3.23, and 3.63. The same signals for the Cr complex were observed at δ 2.69, 3.23, and 3.30. These resonances have been

TABLE 5.5

Analytical and Physical Data[a]

	Complex[b]	Analysis, found (calculated) (%)			Melting Point (°C)
		C	H	N	
VII	$[Pt\{HO(CH_2)_3C{=}NMe_2\}ClQ_2](PF_6)$	34.64 (34.45)	4.53 (4.60)	1.74 (1.83)	195–196
VIII	$[Pt(C{\equiv}NR)(MeC{=}NMe)Q_2](PF_6)_2$	34.79 (34.66)	3.70 (3.88)	3.02 (2.99)	214–216
IX	$[Pt(C{\equiv}NR)(MeC{=}NMe_2)Q_2](PF_6)_2$	35.11 (35.42)	4.22 (4.03)	2.87 (2.95)	204–206
X	$[Pt(C{\equiv}NR)\{HO(CH_2)_3C{=}NMe_2\}Q_2](PF_6)_2$	36.45 (36.26)	4.02 (4.26)	2.91 (2.82)	208–209
XI	$[Pt\{C(NHR)(NMe_2)\}(MeC{=}NMe)Q_2](PF_6)_2$	35.30 (35.52)	4.20 (4.42)	4.12 (4.29)	217–218
XII	$[Pt\{C(NHR)(NMe_2)\}(MeC{=}NMe_2)Q_2](PF_6)_2$	36.04 (36.23)	4.51 (4.56)	3.82 (4.22)	238–239
XIII	$[Pt\{C(NHR)(NMe_2)\}\{HO(CH_2)_3C{=}NMe_2\}Q_2](PF_6)_2$	37.03 (37.00)	4.93 (4.76)	3.87 (4.04)	207–209

[a] All compounds were colourless

[b] R = p-tolyl, Q = PMe_2Ph.

TABLE 5.6

^{1}H NMR Chemical Shifts[a] and Coupling Constants[b]

Complex[b]	Phosphine Methyl Protons $\delta(CH_3)$	J_{P-H}[d]	$^3J_{Pt-H}$	p-Tolyl Methyl $\delta(CH_3)$	$-C(NMe_1Me_2)(NH\text{-}p\text{-}tolyl)$		Other ^{1}H NMR Signals	
VII $[Pt(HO(CH_3)_2C{=}NMe_2)Cl_2]PF_6$	1.96	7.0	29.4		$\delta(Me_1)$ 3.82, $^3J_{Pt-H}$ 12.0		$\delta(CH_2OH)$ 3.52	
	1.97	7.0	29.0		$\delta(Me_2)$ 2.79, $^3J_{Pt-H}$ 9.7		δ(phosphine, C_6H_5) 7.4-7.9	
VIII[e] $[Pt(C{\equiv}NR)(MeC{=}NMe)Q_2](PF_6)_2$	2.26	8.3	33.0	2.34	$\delta(Me_1)$ 3.40, $^3J_{Pt-H}$ 9.0, $^5J_{HCCNCH}$ 0.7		δ(p-tolyl, C_6H_4) 7.26 δ(phosphine, C_6H_5) 7.4-8.0	Isomer ratio 4:1
					$\delta(Me_2)$ -2.31			
VIII[f]					$\delta(Me_2)$ 3.08, $^3J_{Pt-H}$ ~9			
IX $[Pt(C{\equiv}NR)(MeC{=}NMe_2)Q_2](PF_6)_2$	2.26	8.5	34.0	2.37	$\delta(Me_1)$ 3.55, $^3J_{Pt-H}$ 9.0, $^5J_{HCCNCH}$ ~1		δ(p-tolyl, C_6H_4) 7.30	
	2.25	8.5	34.0		$\delta(Me_2)$ 3.21, $^3J_{Pt-H}$ 8.0		δ(phosphine, C_6H_5) 7.4-8.0	
					$\delta(Me_1)$ 2.71			
X $[Pt(C{\equiv}NR)(HO(CH_3)_2C{=}NMe_2)Q_2](PF_6)_2$	2.29	8.0	33.2	2.33	$\delta(Me_1)$ 3.74, $^3J_{Pt-H}$ 10.0		δ(p-tolyl, C_6H_4) 7.30 δ(phosphine, C_6H_5) 7.5-8.1 $\delta(CH_2OH)$ 3.56, δ(OH) 2.80	
					$\delta(Me_2)$ 3.36, $^3J_{Pt-H}$ 9.5			
XI[e] $[Pt(C(NHR)(NMe_2))(MeC{=}NMe)Q_2](PF_6)_2$	1.92[g]	7.3	32.4	2.38	$\delta(Me_1)$ 3.29, $^3J_{Pt-H}$ 9.7, $^5J_{HCCNCH}$ ~0	$\delta(Me_1)$ 3.62, $^3J_{Pt-H}$ 5.6	δ(phenyl) 7.2-8.0	
					$\delta(Me_2)$ 2.22, $^3J_{Pt-H}$ 20.2	$\delta(Me_2)$ 3.08, $^3J_{Pt-H}$ 4.1, $^5J_{PH}$ ~2		
XI[f]				2.35	$\delta(Me_1)$ 2.96, $^3J_{Pt-H}$ 9	$\delta(Me_1)$ 3.88, $^3J_{Pt-H}$ 5.1		Isomer ratio 2:1
					$\delta(Me_2)$ 2.23, $^3J_{Pt-H}$ 21.0	$\delta(Me_2)$ 3.18, $^3J_{Pt-H}$ 4.1, $^5J_{PH}$ ~1.5		
XII[e] $[Pt(C(NHR)(NMe_2))(MeC{=}NMe_2)Q_2](PF_6)_2$	1.98[g]	6.8	32.7	2.34	$\delta(Me_1)$ 3.23, $^3J_{Pt-H}$ 9.0, $^5J_{HCNCH}$ ~1	$\delta(Me_1)$ 3.96, $^3J_{Pt-H}$ 4.7	δ(phenyl) 7.2-8.0	
					$\delta(Me_2)$ 3.14, $^3J_{Pt-H}$ 6.0, $^5J_{HCNCH}$ ~1	$\delta(Me_2)$ 3.31, $^3J_{Pt-H}$ 9.0	δ(N-H) 9.0	Isomer ratio 3:2
					$\delta(Me_1)$ 2.40, $^3J_{Pt-H}$ 17.8			
XII[f]	1.97[g]	7.0	33.0			$\delta(Me_1)$ 3.71, $^3J_{Pt-H}$ 5.2		
						$\delta(Me_2)$ 2.92, $^3J_{Pt-H}$ ~8		
XIII $[Pt(C(NHR)(NMe_2))(HO(CH_3)_2C{=}NMe_2)Q_2](PF_6)_2$	1.93	7.0	33.0	2.34		$\delta(Me_1)$ 3.80, $^3J_{Pt-H}$ ~6	δ(carbene, CH_3) 3.0-3.5 $\delta(CH_2OH)$ ~3.53 δ(OH) 2.84 δ(carbene, CCH_2CH_2) 2.54 δ(phenyl) 7.2-7.9 δ(NH) 9.05	

[a] In ppm (± 0.01) (downfield positive) from TMS.

[b] In Me_2.

[c] Q = Me_2PhP, R = p-tolyl.

[d] $^2J_{P-H} + {}^4J_{P-H}$ is quoted. See references 114 and 115.

[e] Major isomers.

[f] Minor isomers.

[g] Other resonances were complex and could not be interpreted.

assigned to the same protons in both systems:

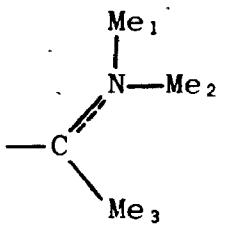

The signal at highest field has been assigned to the H atoms of Me_3 while that at lowest field to Me_1 which lies *trans* to Me_3. The third resonance is due to the *cis* amino-methyl protons, Me_2. Long range coupling $^5J_{HCCNCH}$ between carbene protons is often observed with *trans* coupling being greater than *cis*. In the Pt complexes, coupling to ^{195}Pt is observed for all three methyl resonances.

The complex *trans*-$[Pt(MeC{=}NMe_2)(C{\equiv}N\text{-}p\text{-}tolyl)(PMe_2Ph)_2](PF_6)_2$ (IX) contains the same aminocarbene ligand, and the same carbene methyl resonances are observed at δ 2.31, 3.21, and 3.55. For complexes VII and X which also contain a dimethylamino-substituent, the methyl proton resonances were assigned similarly with the low field signal being due to Me_1 and that at higher field to Me_2. Complex VIII contains the methyl-N-methylaminocarbene ligand. A downfield amino-methyl signal is observed at δ 3.40, and a second resonance of about one-quarter the intensity of the first is observed at δ 3.08. This implies the presence of two isomers of the carbene ligand. A similar effect was observed for the compound *trans*-$[Pt(MeC{=}NHMe)Me(AsMe_3)_2]PF_6$ (118). On the basis of the above assignments for the dimethylamino-substituents, the major resonance at lower field is thought

to be due to the trans isomer and the other to the cis:

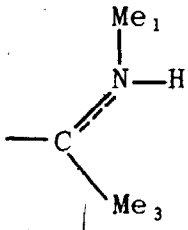

trans

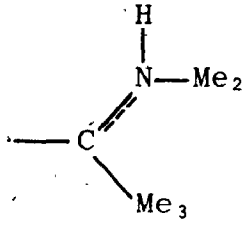

cis

Preliminary X-ray crystallographic results for the complex trans-$[Pt(MeC{=}NHMe)Cl(PMe_2Ph)_2]PF_6$ (121) indicate that the carbene ligand is present in the solid state as the trans isomer only. Thus the trans configuration does seem to be the more stable one in these complexes. The resonance due to the Me_3 protons overlaps with the p-tolyl methyl and phosphine methyl signals and is not clearly observed. This is true for several of the complexes in Table 5.6.

The spectra of the bis-carbene compounds XI, XII, and XIII are complex in the region of the carbene amino-methyl signals where resonances due to as many as four such methyl groups occur. Further complications arise from the presence of isomers. The complex trans-$[Pt\{C(NH\text{-}p\text{-}tolyl)(NMe_2)\}(MeC{=}NHMe)(PMe_2Ph)_2](PF_6)_2$ (XI) can have up to four isomers as a result of restricted rotation about the C=N bonds giving the carbene ligand isomers:

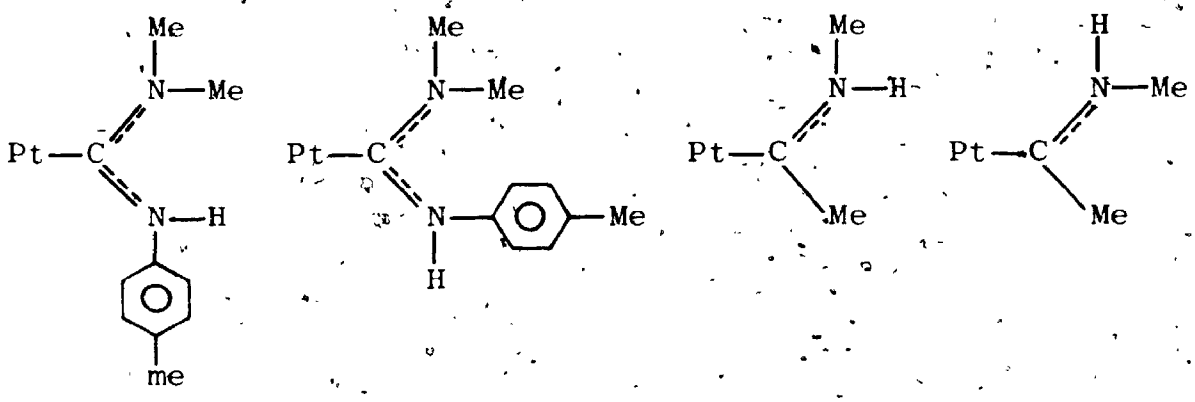

trans cis trans cis

A B

Evidence of such isomerism is present in the ^{1}H NMR spectrum. The amino-methyl protons of carbene ligand A should be coupled only to ^{195}Pt and possibly to ^{31}P of the phosphine ligands. The corresponding methyl H atoms of ligand B can couple to the amino-protons and also to the protons of the methyl bonded to $C(sp^2)$, as well as to ^{195}Pt and ^{31}P. Six downfield methyl signals due to amino-methyl groups are observed. Three of the signals are approximately twice the magnitude of the other three. Clearly, more than one isomer is present. Of the six signals, two at δ 3.88 and 3.62 are sharp triplets showing coupling to ^{195}Pt only. Two more resonances at δ 3.18 and 3.08 were 'triplet of triplets' signals showing coupling to ^{195}Pt and ^{31}P. Since no H-H coupling was observed for these four signals, they were assigned to the two isomers of A. The remaining two resonances at δ 3.29 and 2.96, also present in a 2 to 1 ratio, are broad and show evidence of long-range H-H coupling. These are believed to be the amino-methyl proton signals of

carbene B. As with complex IX, the low field signal is thought to be due to the trans isomer. Broad signals at δ ~2.22 are due to the methyl bonded to C(sp^2) in carbene B.

Four isomers of this complex are possible due to the presence of cis and trans isomers of the two carbene ligands. Only two isomers will occur however, if the stereochemistries of carbenes A and B are sterically dependent on one another. For example, the cis form of B may be favoured to occur with the trans form of A. The assignments of the signals for complex XII were made in the same manner as those of XI. Two isomers of this complex are present due to isomerization of carbene A, since the cis and trans isomers are not possible for the methyl-N,N-dimethylaminocarbene ligand. Only one broad resonance is observed for each amino-methyl group of this ligand. Furthermore these methyl groups seem to be coupled to one another $^4J_{HCNCH}$ ~1 Hz, since no long range coupling to the methyl group bonded to C(sp^2) is observed. This resonance appears as a sharp singlet with ^{195}Pt satellites at δ 2.40 ($^3J_{Pt-H}$ 17.8 Hz). Such long-range coupling of the amino-methyl groups is not usually observed in complexes containing this carbene ligand.

Only one isomer of the complex XIII seems to be present. One sharp singlet with ^{195}Pt satellites is observed for the downfield carbene methyl resonance at δ 3.80. This complex contains two bulky carbene ligands, so the presence of two isomers of carbene A may be sterically unfavourable. Determination of the trans stereochemistry of all complexes

came from examination of the phosphine methyl signals as described for the complexes II-VI. As in those compounds overlapping 'triplet of triplets'' methyl signals due to magnetically inequivalent phosphine methyl groups are often observed.

Resonances due to the phenyl protons of the phosphine ligands and p-tolyl phenyl protons were observed at δ 7-8. For the isocyanide complexes VIII, IX, and X the resonance due to the p-tolyl phenyl H atoms occurs at slightly higher field than that of the phosphine phenyl protons. In the bis-carbene compounds the two phenyl signals collapse into a broad multiplet.

Having prepared and characterized a series of complexes, it was then necessary to obtain cystalline samples of suitable quality for structural examination. This proved to be no simple matter!

5.4 Crystals for X-ray Crystallographic Examination

The secondary carbene and formimidoyl complexes were difficult to obtain in pure form, and the complex trans-[Pt{C(NH-p-tolyl)$_2$}(CH=N-p-tolyl)(PMe$_2$Ph)$_2$]Cl (VI) persisted in forming as a microcrystalline precipitate, even when the anion was exchanged for PF_6^- or ClO_4^-. The protonated form of this complex (V) displayed similar behavior. Efforts to obtain suitable crystals of these complexes were unsuccessful, thus precluding their study by single crystal techniques.

The second series of complexes was more easily obtained in crystalline form. The complexes trans-[Pt{C(NH-p-tolyl)-(NMe$_2$)}(MeC$\equiv$NMe$_2$)(PMe$_2$Ph)$_2$](PF$_6$)$_2$ (XII) and trans-[Pt(C$\equiv$N-p-tolyl)(MeC$\equiv$NMe$_2$)(PMe$_2$Ph)$_2$](PF$_6$)$_2$ (IX) were selected for examination. Both complexes gave the good single crystals required. From ^{1}H NMR data, complex XIII, which seems to be present as only one isomer, would be a more desirable compound for the experiment. However only thin, feathery crystals could be obtained. The presence of two isomers in solution for compound XII was carefully considered, and it was decided that even if cis and trans isomers of the carbene ligand —C(NH-p-tolyl)(NMe$_2$) were observed in the solid state, the resultant disorder could easily be refined without seriously affecting the remainder of the structure. In such a situation, disorder would result in the presence of two non-overlapping p-tolyl substituents. Since the structure of a phenyl ring is well known and rigid group refinement of this entity is common practice, such disorder could readily

be accounted for.

Accordingly the structural investigation of VII is presented in Chapter 6 and that of IX in Chapter 7.

5.5 Experimental

All reactions were carried out under nitrogen and 'spectro' grade solvents were used without further purification. K_2PtCl_4 was kindly supplied by Dr. H.C. Clark.

Infrared spectra were recorded on a Perkin Elmer 621 spectrophotometer as nujol suspensions between NaCl plates.

^1H nuclear magnetic resonance spectra were recorded on a Varian Associates HA-100 spectrometer at 100 MHz using tetramethylsilane as internal lock.

The author is grateful to Heather Schroeder for recording the ^1H NMR spectra.

Microanalyses were obtained from Chemalytics Inc., Tempe, Arizona. Values are tabulated in Tables 5.2 and 5.5.

Several of the compounds were prepared by the same general method, so in these instances only an example preparation will be described.

i. Preparation of Ligands

a. PMe_2Ph (122)

A solution of Grignard reagent was prepared by the dropwise addition of 54 ml of methyl iodide to 20g of magnesium stirred in 500 ml of anhydrous diethyl ether. The resultant solution was left to stir for 30 min and was placed in an ice bath. 50 ml of dichlorophenylphosphine in 150 ml of anhydrous ether was added carefully drop by drop. The mixture was left to stir for 30 min. Excess

Grignard reagent was hydrolized with ice cold saturated ammonium chloride solution. The ether layer was removed and the aqueous layer was washed with three 20 ml aliquots of ether. The ether layer was washed with three 20 ml aliquots of water. The diethyl ether was removed under reduced pressure and the product was purified by fractional distillation. Yield was 28g (55%).

b. $p\text{-}C{\equiv}N\text{-}C_6H_4\text{-}Me$ (123)

27g of p-tolylformamide, 65g of triphenylphosphine, 31g of carbontetrachloride and 4g of triethylamine were dissolved in 250 ml of methylene chloride. The mixture was refluxed for 3 hr. Dichloromethane and carbontetrachloride were recovered under reduced pressure. The residue was extracted with 30-60 petroleum ether (250 ml). The petroleum ether was then extracted with 100 ml of water. The aqueous layer was washed with 20 ml of petroleum ether and the organic layer was dried over $CaCl_2$ and filtered. Solvent was removed under reduced pressure, and the product was purified by fractional distillation. Yield was 15.6g (67%).

ii. Preparation of Starting Materials

a. Cis-$PtCl_2(PMe_2Ph)_2$

1.95g of PMe_2Ph was added to 3.0g of K_2PtCl_4 dissolved in 50 ml of water. A beige precipitate formed immediately and the solution was left to stir for 1 hr. The solid was filtered and washed first with 25 ml ethanol and then with

25 ml diethyl ether. After air drying, the solid was placed in a flask and enough β-methoxyethanol was added to just cover it. The flask was swirled in a water bath (85°C) until the solid dissolved, and the solution was refrigerated at -15°C for 12 hrs. The product was filtered and washed with diethyl ether. Yield was 3.5g (89%).

b. Trans-$PtHCl(PMe_2Ph)_2$

A modification of the method described by Howard (124) was employed in the preparation of this complex.

To a solution of 0.514g of cis-$PtCl_2(PMe_2Ph)_2$ in tetrahydrofuran was added dropwise 0.036g of $NaBH_4$ in 15 ml of warm absolute ethanol. The reaction mixture became yellow-brown as this reagent was added. Solvent was removed under reduced pressure. The residual solid was dissolved in a minimum amount of benzene and chromatographed on a florisil column. 30-60 petroleum ether was added until the solution became cloudy. The mixture was chilled at -15°C for 4 hr. Colourless plate shaped crystals were filtered, washed with diethyl ether and air dried. Yield was 0.39 g (76%).

c. Cis-$PtMe_2(PMe_2Ph)_2$ (125, 126)

To a solution of 3.5g of cis-$PtCl_2(PMe_2Ph)_2$ in 50 ml of anhydrous diethyl ether was added 12 ml of a 2.08 M solution of methyl lithium in diethyl ether. The solution immediately turned pale yellow. After stirring for 1 hr

the excess methyl lithium was hydrolized with ice cold saturated ammonium chloride solution. The ether layer was removed and the aqueous layer was washed with 20 ml of ether. After washing the organic layer with 20 ml of water, it was dried over magnesium sulfate and filtered. Ether was removed under reduced pressure, and the product was dried under vacuum. Yield was 3.0g (93%).

d. Trans-$PtMeCl(PMe_2Ph)_2$ (125)

To a solution of 3.5g of cis-$PtMe_2(PMe_2Ph)_2$ in 20 ml of ether was added 512 µl of acetyl chloride. A white precipitate appeared after several minutes of vigourous stirring. The solution was chilled at -15°C for 6 hr. The ether was then decanted, and the solid was refluxed in methanol for 1 hr. This solution was refrigerated at -15°C for 12 hr. The large crystals were filtered and washed with diethyl ether. Yield was 3.16g (87%).

e. Trans-$[Pt(\overline{CH_2C{=}{=}OCH_2CH_2})Me(PMe_2Ph)_2]PF_6$ (18)

0.500g of trans-$PtMeCl(PMe_2Ph)_2$ was dissolved in 50 ml of methanol at 40°C under a nitrogen atmosphere. Addition of 0.242g of $AgPF_6$ in 10 ml of methanol resulted in immediate formation of a AgCl precipitate. The solution was stirred for 10 min and AgCl was removed by centrifugation to give a colourless solution. On addition of 79 µl of $CH{\equiv}CCH_2CH_2OH$ the solution became pale yellow. After stirring for 15 min the solvent was removed under reduced pressure until a

crystalline precipitate was observed. 20 ml of diethyl ether was added and the solution was chilled at -15°C for 6 hr. The crystals were filtered, washed with ether and air dried.

Subsequent recrystallization from methanol-ether solution gave colourless crystals of product. Yield was 0.47g (70%).

f. Trans-$[Pt\{HO(CH_2)_3C{=}{=}{=}NMe_2\}Me(PMe_2Ph)_2]PF_6$ (19)

0.470g of trans-$[Pt(\overline{CH_2C{=}{=}{=}OCH_2CH_2})Me(PMe_2Ph)_2]PF_6$ was dissolved in 10 ml of well stirred dichloromethane. Dimethylamine was bubbled into the solution for 2 min and vigourous stirring was continued for 15 min. The solvent was removed under reduced pressure to give a pale yellow oil. A fine white precipitate formed upon thorough trituration with diethyl ether. The product was dried under vacuum. Yield was 0.48g (96%).

g. Trans-$[Pt\{HO(CH_2)_3C{=}{=}{=}NMe_2\}Cl(PMe_2Ph)_2]PF_6$ (19)

To a solution of 0.392g of trans-$[Pt\{HO(CH_2)_3C{=}{=}{=}NMe_2\}Me(PMe_2Ph)_2]PF_6$ in a mixture of 10 ml of dichloromethane and 15 ml of methanol, was added 40 µl of acetyl chloride. The solution was stirred for 5 min and the solvent removed under reduced pressure. The resultant white precipitate was washed with diethyl ether and dried under vacuum. Yield was 0.38g (95%).

iii. Preparation of New Complexes

a. Trans-[Pt(C≡N-p-tolyl)H(PMe_2Ph)$_2$]Cl

A suspension of 0.487g of trans-PtHCl(PMe_2Ph)$_2$ in 40 ml of diethyl ether was chilled to -80°C. While the solution was being stirred vigourously, 0.15g of p-tolylisocyanide in 25 ml of diethyl ether was slowly added. The resultant mixture was stirred for 20 min and slowly warmed to room temperature. The solvent was decanted from the pale yellow precipitate, which was washed with 20 ml of diethyl ether and dried under vacuum. Since it was found to be very hygroscopic, the product was used immediately after preparation. Approximate yield was 90%.

b. Trans-Pt(CH=N-p-tolyl)Cl(PMe_2Ph)$_2$

Approximately 0.45g of trans-[Pt(C≡N-p-tolyl)H(PMe_2Ph)$_2$]Cl was dissolved in 15 ml of dichloromethane to give a bright red solution. N-pentane (~5 ml) was added until the solution was saturated with the complex. This solution was left to stir for 15 hr, during which time the colour became orange. Removal of solvent under reduced pressure gave a viscous oil. Thorough washing with diethyl ether and n-pentane gave a yellow-brown flocculent precipitate. Some pale yellow crystals were obtained by recrystallization from dichloromethane-diethyl ether solution.

A better method of purification involved preparation of the secondary carbene complex trans Pt(CH=NH-p-tolyl)-

$Cl(PMe_2Ph)_2]Cl$.

c. Trans-$[Pt(CH{=}NH\text{-}p\text{-}tolyl)Cl(PMe_2Ph)_2]Cl$

To an acetone solution of trans-$Pt(CH{=}N\text{-}p\text{-}tolyl)(PMe_2Ph)_2$ was added 0.2 ml of concentrated HCl in 5 ml of acetone. The solution was stirred for 5 min and the solvent removed under reduced pressure. Recrystallization from dichloromethane-ether solution gave colourless crystals. Yield was 0.42g (~90%). This carbene product was readily deprotonated by addition of about a 10 fold excess of triethylamine to a dichloromethane solution of the complex. The solution was chromatographed on a florisil column and the solvent of the resultant solution was removed under reduced pressure to give a pale yellow oil. Washing with diethyl ether gave pale yellow precipitate. Recrystallization from dichloromethane-diethyl ether solution gave colourless crystals (0.37g).

The PF_6 salt of the secondary carbene complex could be prepared readily by anion exchange using $AgPF_6$ (1 equivalent) in acetone solution.

d. Trans-$[Pt(CH{=}NH\text{-}p\text{-}tolyl)(C{\equiv}N\text{-}p\text{-}tolyl)(PMe_2Ph)_2]Cl_2$

To 0.345g of trans-$[Pt(CH{=}NH\text{-}p\text{-}tolyl)Cl(PMe_2Ph)_2]Cl$ in 20 ml of dichloromethane was slowly added 0.061g of p-tolyl-isocyanide in 10 ml of the solvent. Stirring was continued until the smell of the isocyanide dissipated. Diethyl ether was added (~15 ml) and the solution was chilled at -15°C for

6 hr to give colourless needle shaped crystals. Yield was 0.34g (84%).

e. Trans-$[Pt\{C(NH\text{-}p\text{-}tolyl)_2\}(CH{=}{=}NH\text{-}p\text{-}tolyl)(PMe_2Ph)_2]Cl_2$

To a solution of trans-$[Pt(C{\equiv}N\text{-}p\text{-}tolyl)(CH{=}{=}NH\text{-}p\text{-}tolyl)(PMe_2Ph)_2]Cl_2$ (0.307g) in 30 ml of dichloromethane was added approximately a 5 fold excess of p-toluidine (0.2g). The solution was stirred for 16 hr and the solvent removed under reduced pressure. The solid was washed thoroughly with diethyl ether to remove the excess p-toluidine. Microcrystalline product was obtained on recrystallization from dichloromethane-diethyl ether solution. Yield was 0.28g (81%).

f. Trans-$[Pt\{HO(CH_2)_3C{=}{=}NMe_2\}(C{\equiv}N\text{-}p\text{-}tolyl)(PMe_2Ph)_2](PF_6)_2$

A colourless solution of 0.308g of trans-$[Pt\{HO(CH_2)_3C{=}{=}NMe_2\}Cl(PMe_2Ph)_2]PF_6$ in 30 ml of acetone was chilled to -80°C. 0.048g of p-tolylisocyanide in 10 ml of acetone was added, followed by 0.103g of $AgPF_6$ in 10 ml of acetone. The solution was stirred and slowly warmed to room temperature. During this time a thick precipitate of AgCl formed, and the solution became pale yellow in colour. The precipitate was collected by centrifugation and the solvent was removed under reduced pressure. The resultant oil was washed with diethyl ether to give a pale yellow solid. Recrystallization from acetone-diethyl ether solution gave needle shaped crystals of the desired product. Yield was 0.31g (76%).

g. Trans-[Pt{HO(CH$_2$)$_3$C$\overline{---}$NMe$_2$}{C(NH-p-tolyl)(NMe$_2$)}-(PMe$_2$Ph)$_2$](PF$_6$)$_2$

Dimethylamine was bubbled into a solution of 0.256g of trans-[Pt{HO(CH$_2$)$_3$C$\overline{---}$NMe$_2$}(C≡N-p-tolyl)(PMe$_2$Ph)$_2$](PF$_6$)$_2$ in 15 ml of acetone for 2 min. The solution changed from colourless to pale yellow. Stirring was continued for 1 hr and the solution became colourless again. Solvent was removed on a rotary evaporator and the residue was washed with diethyl ether. Recrystallization from acetone/diethyl ether solution gave feathery crystals of product. Yield was 0.25g (95%).

CHAPTER 6

THE CRYSTAL AND MOLECULAR STRUCTURE OF TRANS-PARA-TOLYLISOCYANIDE(METHYL-N,N-DIMETHYLAMINOCARBENE)BIS-(DIMETHYLPHENYLPHOSPHINE)PLATINUM(II)HEXAFLUOROPHOSPHATE. Trans-$[Pt\{CH_3C{=}N(CH_3)_2\}(C{\equiv}N\text{-}p\text{-}C_6H_4CH_3)\{P(CH_3)_2C_6H_5\}_2](PF_6)_2$

6.1 Introduction

Comparison of the bonding of isocyanide ligands and of the carbene ligands in this work can be made quite readily as is evident from the following resonance forms.

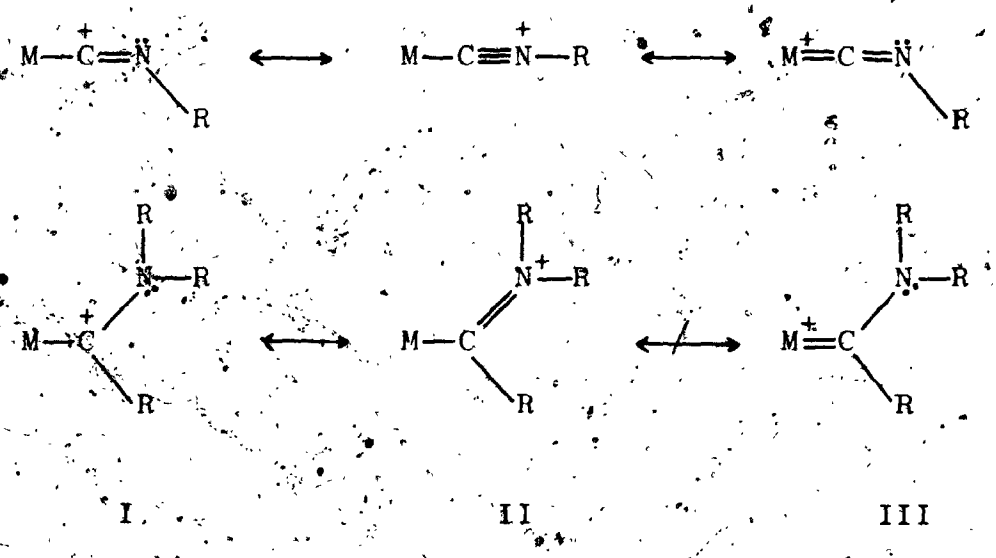

I II III

Both ligands contain an apparently electron deficient C atom coordinated to the metal. This C atom can be stabilized by electron donation from the nucleophilic N atom and by π back donation from the metal atom. In cationic systems such as these of divalent Pt, the metal atom itself is 'electron deficient', hence, as seems to be the case with

aminocarbene complexes (Chapter 3), the second resonance form (II) is considered to be the major contributor. Infrared spectral data are in agreement with this since the C-N stretching frequency of the isocyanide ligand increases on coordination to metal atoms of high formal oxidation state (Chapter 5). For the title complex, an increase of 93 cm^{-1} is observed.

Spectral and chemical data give a good insight as to the nature of the M-C(isocyanide) bond. It has been established that the isocyanide ligand is a poorer π acceptor than carbon monoxide (127-130), and a better π acceptor than carbene (105). Chemical evidence also indicates that isocyanide ligands are weaker σ donors than carbenes (127).

X-ray structural studies have been completed on several square planar Pt(II) isocyanide complexes (34, 72, 131, 132). It has been determined that isocyanide ligands have a weak trans influence, comparable to that of Cl^- or carbon monoxide (131, 132). In the complex trans-$[Pt(C{\equiv}N\text{-}p\text{-}C_6H_4Me)(MeC{=}{=}NMe_2)(PMe_2Ph)_2](PF_6)_2$ the isocyanide ligand occupies a coordination site trans to the carbene ligand. The X-ray crystal structure determination of this complex was undertaken to further examine the bonding of the carbene ligand in a situation where it is opposite a ligand of weak trans influence. This complex also offers a good opportunity to study the coordination and geometry of the isocyanide ligand, whose mode of bonding to the metal atom is probably

quite similar to that of the carbene ligand. Since both ligands are in similar environments, close comparison of their respective σ donor and π acceptor capabilities should be possible.

When dimethylamine is bubbled into a solution of this complex, 1,2 addition occurs across the C≡N bond of the isocyanide ligand to give a bis-carbene compound. The crystal structure investigation of this complex is presented in Chapter 7.

6.2 Experimental

A sample of the complex was obtained by following the preparative route detailed in Chapter 5. Colourless prisms with well developed faces were obtained by recrystallization from acetone/diethyl ether. Preliminary photographic examination indicated an orthorhombic space group with systematic absences $0k\ell$, $k + \ell \neq 2n$; $hk0$, $h \neq 2n$. These are consistent only with the space groups $Pnma$ (D_{16}^{2h}, No. 62) and $Pn2_1a$, an alternate setting of $Pna2_1$ (C_{2v}^{9}, No. 33) (76). Since there are four formula units per unit cell, m site symmetry must be present if Pnma is the correct space group, while 1 site symmetry is required for $Pn2_1a$. The non-centrosymmetric space group $Pn2_1a$ was initially chosen, due to the acentric habit of the crystals as determined from optical goniometric measurements. The Crystal data are presented in Table 6.1.

The intensities of 5132 reflections were measured with Cu Kα radiation. As was discussed in Chapter 4, $F_{hk\ell} \neq F_{h\bar{k}\ell}$ for the polar space group $Pn2_1a$ when anomalous scattering effects are significant. Thus $hk\ell$ reflections were measured out to a 2θ angle of 120° and the Friedel pairs were collected to a 2θ of 105°. The four standard reflections (400, 020, 020, 004) were monitored throughout the period of data collection. Their intensities showed only random fluctuations of approximately 3%. The conditions of data collection are summarized in Table 6.2

All data were processed. The 4035 data with $I > 3\sigma(I)$

TABLE 6.1

Crystal Data for Trans-$[Pt(MeC{=}NMe_2)(C{\equiv}N\text{-}p\text{-}C_6H_4Me)(PMe_2Ph)_2](PF_6)_2$

$C_{28}H_{38}F_{12}N_2P_4Pt$	f.w. = 949.6
Analysis found (calculated)	C, 35.11 (35.42); H, 4.22 (4.03); N, 2.87 (2.95)
Crystal description	colourless prisms
Systematic absences	$0k\ell$, $k + \ell \neq 2n$; $hk0$, $h \neq 2n$
Laue Symmetry	mmm
Crystal system	orthorhombic
Space group	$Pn2_1a$
Equivalent positions (4)	x, y, z; $\bar{x}, \frac{1}{2} + y, \bar{z}$; $\frac{1}{2} - x, \frac{1}{2} + y, \frac{1}{2} + z$; $\frac{1}{2} + x, y, \frac{1}{2} - z$
Cell constants	a = 17.071(3)Å α = 90.0° b = 16.503(2)Å β = 90.0° c = 12.573(2)Å γ = 90.0°
Cell volume	3542 Å^3
Wavelength used for cell determination	1.54056 Å
Temperature at which cell was determined	21°C
Method of density determination	flotation($C_2H_4Br_2/CCl_4$)
Density (observed) (calculated)	1.79(1)g cm^{-3} 1.79g cm^{-3}
Z	4
Symmetry constraints	none

TABLE 6.2

Experimental Conditions for Data Collection

Radiation		Cu Kα
Wavelength		1.54056
Filter		pre-filtered, Ni foil (0.018mm)
Mean ω scan width at half height (reflections)		0.13° (400, 020, 004)
Reflections centered in 2θ range		24; 20° < 2θ < 65°
Scan range	a) low angle side of 2θ	-0.75°
	b) high angle side of 2θ	0.75°
Scan rate		2.0° min^{-1}
Stationary background count time		10 sec
% available Bragg intensity obtained for a given reflection		80%
Take-off angle		1.5°
Tube KV; mA		40; 14
Collimator size		1.0mm
Crystal-counter distance		32cm
Crystal-aperture distance		30cm
Aperture dimensions		5mm x 5mm
2θ range		2.5° < 2θ ≤ 105°
Shells (No; high angle limit)		4; 60°, 90°, 105°, 120°
Index limits		$0 \leq h \leq 19$, $-16 \leq k \leq 18$; $0 \leq \ell \leq 14$
No. of data collected		5132
p value		0.02
No. of reflections with $I_o > 3\sigma(I)$		4035
μ (Cu Kα)		94.27cm^{-1}
Crystal faces		$(011),(01\bar{1}),(\bar{2}\bar{1}\bar{1}),(2\bar{1}\bar{1}),(\bar{2}11),(2\bar{1}1)$
Crystal dimensions		0.29mm x 0.21mm x 0.18mm
Absorption correction		analytical
Transmission coefficients	a) minimum	0.283
	b) maximum	0.417

were used in the solution and refinement of the structure. An optical goniometric study was performed on the data crystal and the dimensions were measured (Table 6.1). A diagram of the crystal is shown in Fig. 6.1. Upon successful solution of the structure, all data with $I > 0$ were corrected for absorption. The maximum and minimum transmission coefficients were found to differ by 47%.

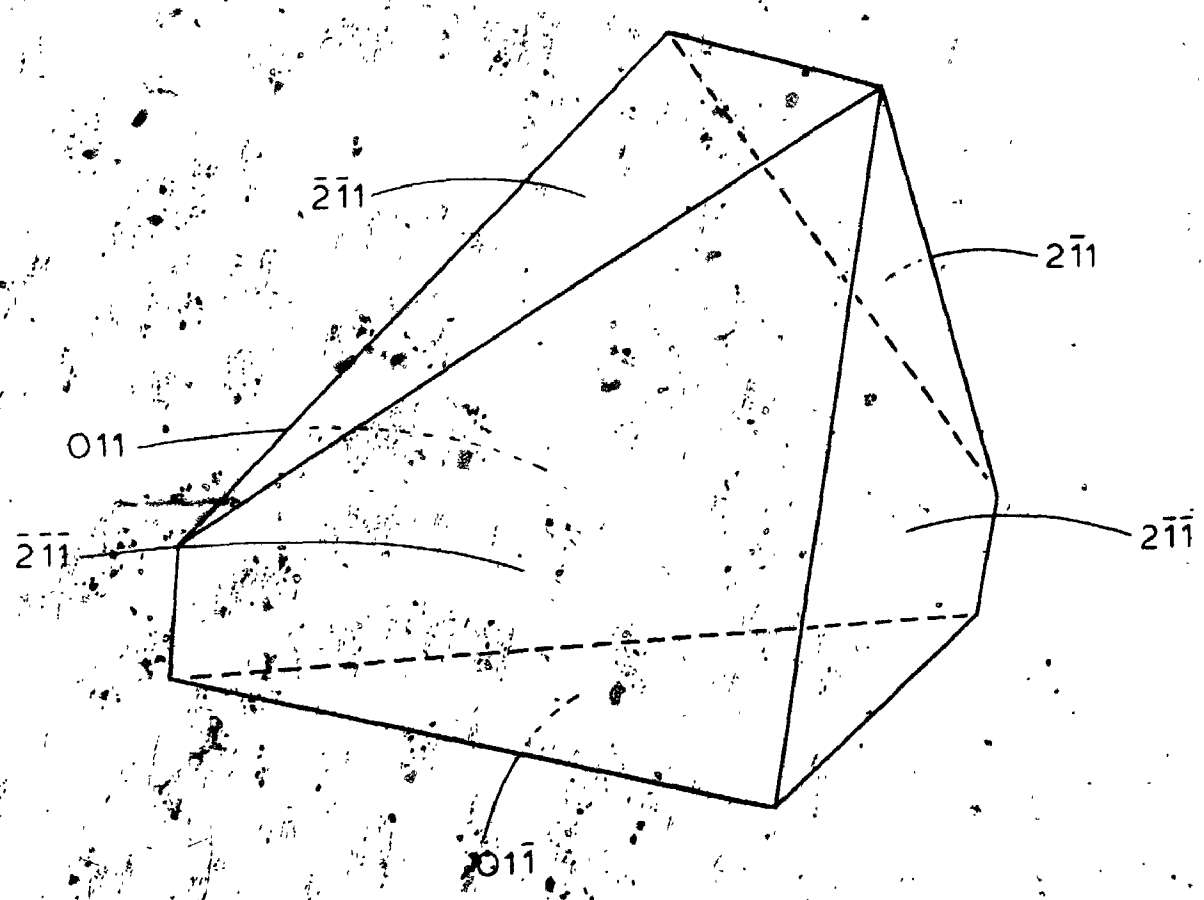

Fig. 6.1

A Drawing of the Data Crystal

Faces with dotted edges are hidden from view.

6.3 Structure Solution and Refinement

A three dimensional Patterson synthesis yielded positional parameters for the Pt and two phosphine P atoms. The positions of these atoms, and an overall scale factor were varied in two cycles of least-squares calculations. The agreement factors obtained were $R_1 = 0.255$ and $R_2 = 0.321$. The positions of the remaining non-hydrogen atoms were readily obtained from difference Fourier syntheses.

At this point it became obvious that the acentric space group was the correct one, since the orientation of the ions in the unit cell is such that no m site symmetry, as required by Pnma, is possible. As a further test of the presence or absence of a center of symmetry, normalized structure factors were calculated, and their distributions compared to theoretical ones for centric and acentric crystals. The calculations were performed using the program FAME, and, as was the case in Chapter 4, the results were inconclusive. The structure was successfully refined in $Pn2_1a$.

The phenyl rings were varied as rigid groups with D_{6h} symmetry in least-squares cycles. The six F atoms of each anion were formulated into rigid groups of O_h symmetry (Chapter 2). Least-squares refinement was performed on all non-hydrogen atoms. All non-group atoms except those of the carbene ligand and the P atoms of the anions were refined as anisotropic atoms. Individual isotropic group atom thermal parameters were varied. Two least-squares

cycles converged the refinement. Agreement factors $R_1 = 0.051$ and $R_2 = 0.059$ were obtained.

The resulting least-squares parameters and geometry were examined carefully. No evidence of the disorder of the PF_6 anions was present. The geometry of the carbene ligand revealed some interesting discrepancies. The $C(sp^2)$-N separation in the carbene ligand was found to be 1.19 Å. This distance was considerably shorter than those of 1.266(15) Å and 1.293(16) Å observed in Chapters 2 and 4 respectively and was similar to the C-N separation of 1.18 Å in the isocyanide ligand. The isocyanide C-N bond length was close to that of 1.16(1) Å (88), the accepted value for a C-N triple bond in an isocyanide ligand. Thus, the carbene C-N distance is anomalous, since the bond length indicates the presence of approximate triple bond character when a bond order of less than 2 is expected. The infrared data for this complex do not predict unusual bonding in the carbene ligand, in that characteristic ν(C---N) carbene and ν(C≡N) isocyanide stretches at 1623 cm^{-1} and 2218 cm^{-1} respectively are observed. A large distortion of the equatorial plane of the metal atom was observed at the carbene ligand. The C(isocyanide)-Pt-C(carbene) angle was 167°. Isotropic thermal parameters of the carbene ligand atoms were not overly large (4-8 $Å^2$), but attempts to refine the atoms anisotropically failed and non-positive definite temperature factors resulted for two of the C(methyl) atoms. A difference Fourier synthesis over the unique

region of the unit cell revealed the presence of a major residual peak near the position of the carbene nitrogen atom. The electron density of this peak was about 1.7 eA^{-3}. The above observations are reminiscent of those encountered during refinement of the structure of trans-[Pt(MeC=OMe)-Me(PMe_2Ph)$_2$]PF_6 (92) where the carbene ligand was found to be disordered.

In order to investigate the possibility of disorder, the contributions of the carbene ligand atoms were removed from the least-squares calculations, and an electron density map was calculated through the plane of the carbene ligand. (Fig. 6.2) Five major peaks characteristic of the methyl-N,N-dimethylaminocarbene are present. Closer scrutiny of the isopleths in the diagram reveals the presence of a distinct shoulder close to the peak due to the N atom, and a similar but less obvious shoulder is present at the electron density resulting from the C(sp^2) atom. The shoulders have approximately half the intensity of the major peaks. It was found that a disorder model resulting from 180° rotation about the Pt-C(sp^2) bond, accompanied by a significant translation of the C atom out of the square plane could readily accommodate the observed electron density. The model requires that the C(methyl) atoms of the disordered ligand occupy the same three electron density peaks. Such rotational-translational ligand disorders are not unknown in square planar complexes of divalent Pt (92, 133). The disorder calculations were performed in the same manner as

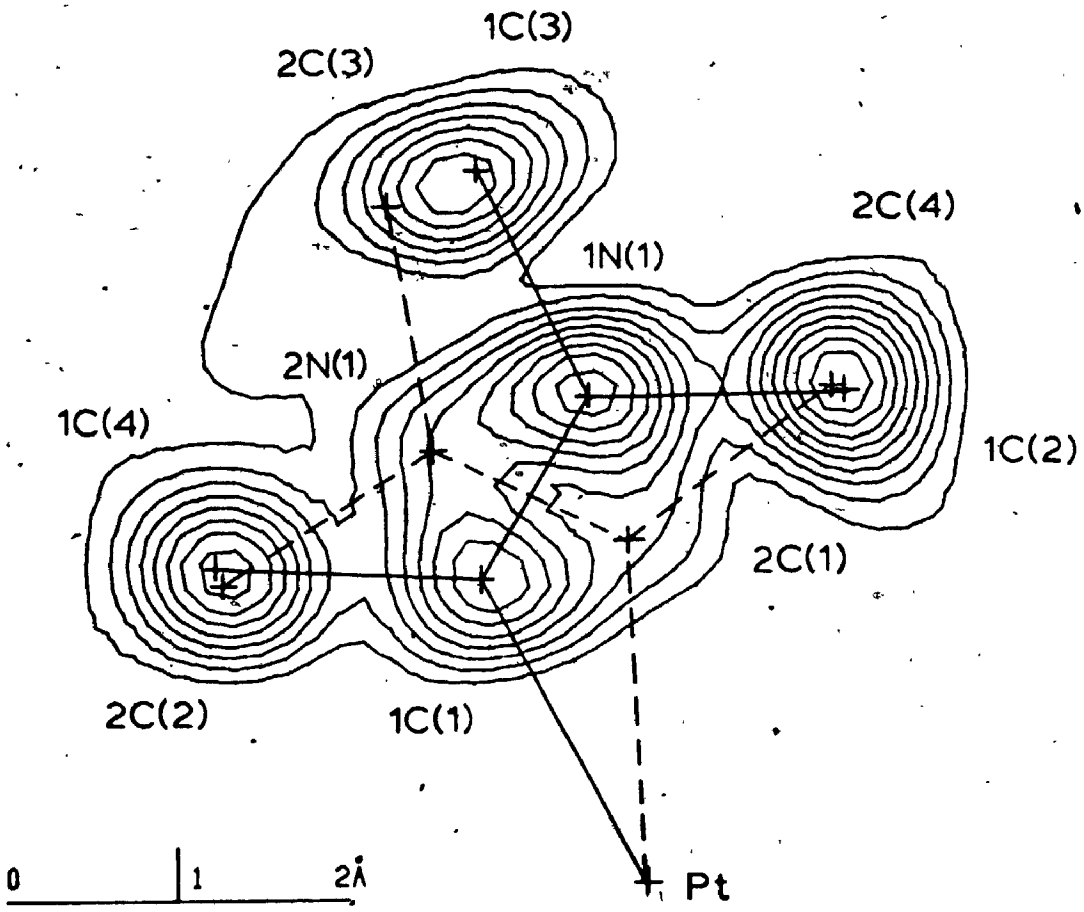

Fig. 6.2

An Electron Density Map Calculated Through the Plane of the Carbene Ligand

Contours are drawn at intervals of 0.5 $e\text{Å}^{-3}$.

Superimposed on the map are the final positions for the

atoms of the disordered ligand.

for the PF_6 disorder in Chapter 2. Two rigid groups were formulated. Rigid group orientation parameters and an isotropic temperature factor were varied for each group. Also refined was a group multiplicity parameter. The rigid group geometry of the methyl-N,N-dimethylaminocarbene was the same as that obtained for the ordered ligand in the structural examination in Chapter 2, where the carbene ligand is in a similar environment. Thus the rigid groups were calculated to be planar and to have the geometry shown in Fig. 6.3. The carbene disorder was refined successfully.

In space group $Pn2_1a$ two enantiomorphous orientations of the complex are possible, one related to the other by reflection in [010] or by inversion through the origin. Two cycles of least-squares refinement were calculated on each orientation, and the same parameters were varied in each case. The C atoms of the p-tolyl phenyl ring, where rigid group constraints had been removed were refined as isotropic atoms. Remaining non-group atoms of the cation were refined anisotropically. Individual isotropic group atom thermal parameters were varied for rigid groups not associated with disorder. The agreement factors obtained were $R_1 = 0.046$ $R_2 = 0.055$ for one solution and $R_1 = 0.058$ $R_2 = 0.072$ for the second. No significant differences in the geometry of the complex were observed, but some thermal parameters were found to be significantly different in the two solutions. Application of Hamilton's

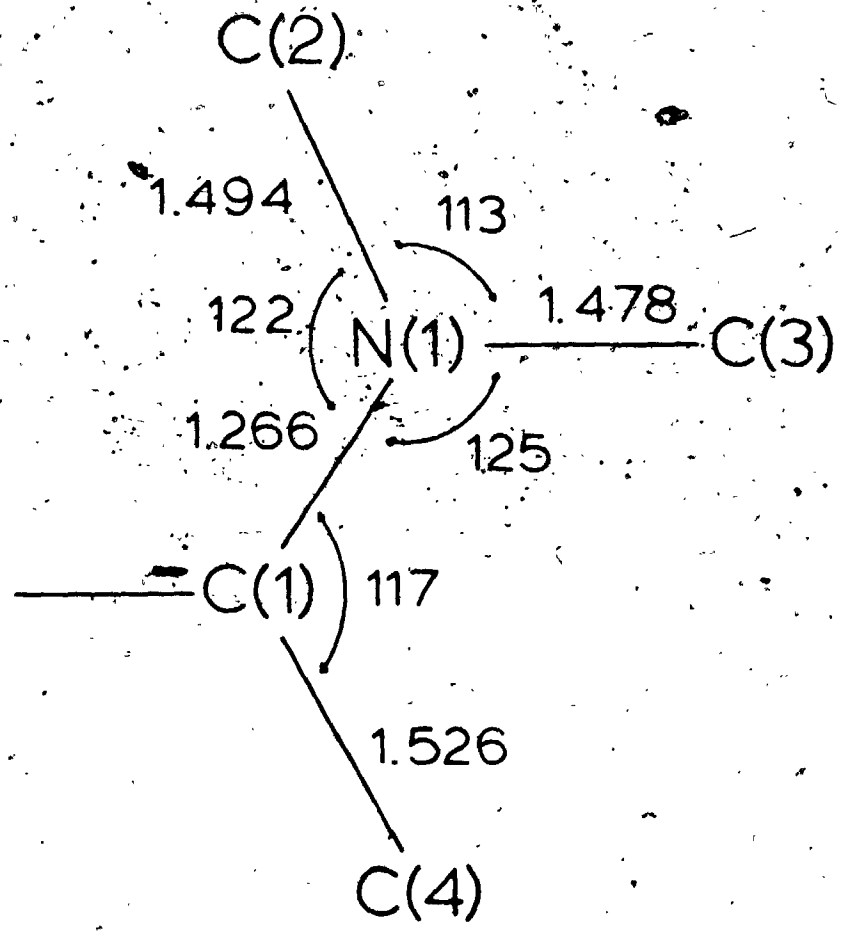

Fig. 6.3

Rigid Group Geometry for the Carbene Ligand

significance test (103) to the weighted agreement factors showed that the second solution could be rejected at a probability level of less than 0.005. The relative magnitudes of those $F_{c(hk\ell)}$ and $F_{c(\bar{h}k\bar{\ell})}$ which differed by more than 10% were compared to the relative magnitudes of the observed values for each solution. For the first model 89% of the 178 Friedel pairs showed the same trends for F_o and F_c. For the second solution only 8% of the Friedel pairs showed the same relationship for the observed and calculated structure amplitudes. The first solution was therefore selected as the correct one.

Hydrogen contributions to F_c were calculated as described in Chapter 2. All H atoms were located, except those of the carbene ligand. Little evidence for the methyl H atoms of this disordered ligand was present, so it was decided that their inclusion in the calculation of F_c was unwarranted. The remaining H atom positions were obtained using the program HYDRA. The methyl C-H distance is 1.0 Å and the phenyl C-H separation is 0.95 Å. H atom temperature factors were set to be 1.0 $Å^2$ larger than those of the C atoms to which they are bonded.

The conditions and results of the final cycles of full matrix least-squares are given in Table 6.3. P atoms of the anions and C atoms of the p-tolyl phenyl ring were allowed to vibrate isotropically whereas the remaining non-group atoms were allowed to undergo anisotropic thermal motion. Individual isotropic group atom temperature factors

3 4

OF/DE

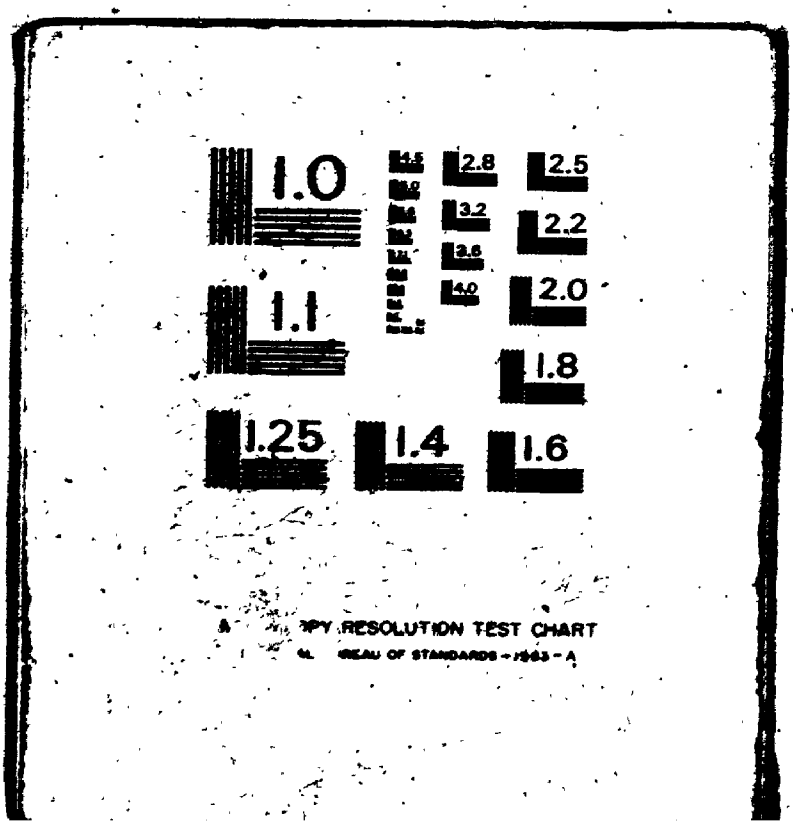
1.0
1.1
1.25
1.4
1.6
1.8
2.0
2.2
2.5
2.8
3.2
3.6
4.0
RESOLUTION TEST CHART
BUREAU OF STANDARDS - 1963 - A

TABLE 6.3

Conditions and Results of Final Full Matrix Least-Squares Calculations

Observations	4025
Variables	185
Ratio (observations/variables)	21.8
Rigid groups	6
Disorder models (No; entities)	1; MeC—NMe_2
Non-group atoms	18
a) Anisotropic	10
b) Isotropic	8
H atoms included; No. (type)	29; 15(methyl), 14(phenyl)
Extinction coefficient	not refined
Maximum value of (parameter shift/ standard deviation)	0.13
Agreement factors: R_1	0.0421
R_2	0.0476
Final error on an observation of unit weight	2.57 electrons
Final difference Fourier synthesis:	
a) Position of largest peak	(0.333, 0.216, -0.165)
b) Electron density	1.35(8)e $Å^{-3}$
c) Associated with	disordered carbene

were varied for ordered rigid groups. The final agreement factors were $R_1 = 0.042$ and $R_2 = 0.048$. An analysis of the structure factors in terms of the magnitudes of F_o, $\lambda^{-1}\sin\theta$, Miller indices, and diffractometer setting angles showed no abnormal trends. A final electron density map calculated over the unique region of the unit cell showed that the largest residual peak has an electron density of 1.35(8) and is associated with a methyl group of the disordered carbene ligand. The next largest peak has an electron density of 1.13(8) $e\text{Å}^{-3}$. This peak is in the vicinity of a phosphine phenyl ring.

In Table 6.4 are presented the final atomic positional and thermal parameters. In Table 6.5 are listed the rigid group parameters and the derived group atom positional and thermal parameters are shown in Table 6.6. Derived positional and thermal parameters for the H atoms are given in Table 6.7. A list of the structure factors given as $10\,|F_o|$ and $10\,|F_c|$ (electrons) appears in Appendix 3.

TABLE 6.4

Individual Atom Positional and Thermal Parameters

Atom	x	y	z	U_{11}[a]	U_{22}	U_{33}	U_{12}	U_{13}	U_{23}
Pt	0.15336(3)[b]	0.1000	-0.10946(3)	580(3)	284(2)	421(2)	-39(6)	-60(2)	-6(5)
P(1)	0.0871(2)	0.0993(4)	-0.2718(2)	601(16)	376(12)	444(15)	-59(35)	-47(13)	-107(35)
P(2)	0.2203(2)	0.0976(4)	0.0526(2)	689(18)	364(14)	479(14)	-137(35)	-86(14)	36(36)
P(3)	-0.1656(2)	-0.0670(2)	-0.2178(3)	0.0623(9)[c]					
P(4)	0.0378(2)	-0.0610(2)	0.3045(3)	0.0605(9)					
C(11)	-0.0100(8)	0.1383(7)	-0.2585(11)	603(87)	738(85)	593(83)	68(67)	75(72)	-11(68)
C(12)	0.0749(10)	-0.0000(8)	-0.3264(11)	1165(126)	466(75)	542(83)	-26(82)	-231(89)	7(68)
C(21)	0.1574(9)	0.1333(8)	0.1594(11)	940(108)	776(95)	523(74)	-216(85)	-72(87)	16(66)
C(22)	0.2500(9)	-0.0017(8)	0.0933(12)	961(112)	451(73)	804(103)	-79(77)	-408(91)	197(74)
N(2)	0.1044(8)	-0.0798(7)	-0.0783(9)	854(89)	310(57)	547(74)	-69(56)	-13(64)	193(50)
C(5)	0.1241(7)	-0.0136(7)	-0.0883(9)	535(76)	431(76)	423(75)	90(61)	-120(58)	-24(58)
C(6)	0.0769(11)	-0.4223(6)	-0.0589(13)	1458(149)	213(95)	983(114)	-219(74)	-244(110)	97(62)
R3C(1)[d]	0.0946(7)	-0.1646(7)	-0.0697(10)	0.049(3)					
R3C(2)	0.1154(7)	-0.2053(8)	0.0216(10)	0.057(3)					
R3C(3)	0.1097(7)	-0.2890(7)	0.0243(10)	0.051(3)					
R3C(4)	0.0817(8)	-0.3309(8)	-0.0617(11)	0.054(3)					
R3C(5)	0.0608(9)	-0.2889(9)	-0.1515(12)	0.074(4)					
R3C(6)	0.0647(8)	-0.2059(8)	-0.1559(11)	0.066(4)					

[a] The Uij's are the thermal parameters in terms of mean-square amplitudes of vibration in $\AA^2$. Values are given as U x 10^4. The expression for the thermal ellipsoid is given in Appendix II.

[b] Numbers in parentheses given here and in other tables are estimated standard deviations in the least significant digits.

[c] Isotropic thermal parameters are given as U_{11} in $\AA^2$.

[d] Ring C atoms are numbered sequentially. R3C(1) is bonded to N(2).

TABLE 6.5

Rigid Group Parameters

Group	x_g [a]	y_g	z_g	δ	ε	η	Multiplicity
Ring-1	0.1609(3)	0.2019(4)	-0.4637(5)	-2.647(6)	2.788(5)	0.951(6)	
Ring-2	0.3732(3)	0.2093(4)	0.0574(4)	0.623(5)	3.261(5)	3.144(6)	
1-F6	-0.1660(3)	-0.0678(3)	-0.2163(4)	1.817(4)	2.699(4)	-3.138(4)	
2-F6	0.0377(3)	-0.0605(3)	0.3026(3)	1.752(3)	2.900(4)	3.156(4)	
Car-1	0.2048(6)	0.2114(5)	-0.1457(9)	-2.082(7)	2.719(7)	-2.891(11)	0.68(2)
Car-2	0.1611(14)	0.2259(14)	-0.112(2)	1.36(2)	-2.49(2)	-0.02(3)	0.32(2)

[a] x_g, y_g, and z_g are the fractional coordinates of the group origin, and δ, ε, and η (radians) are the group orientation angles.

TABLE 6.6

Derived Group Atom Parameters

	Atom	x	y	z	B(Å²)	
Ring-1						
	R1C(1)[a]	0.1302(5)	0.1577(5)	-0.3791(6)	3.8(2)	
	R1C(2)	0.1770(5)	0.1195(4)	-0.4546(7)	4.9(3)	
	R1C(3)	0.2077(5)	0.1636(6)	-0.5392(6)	6.4(4)	
	R1C(4)	0.1917(6)	0.2461(6)	-0.5482(7)	7.2(4)	
	R1C(5)	0.1448(6)	0.2843(4)	-0.4728(8)	6.1(3)	
	R1C(6)	0.1141(5)	0.2402(5)	-0.3882(7)	5.2(3)	
Ring-2						
	R2C(1)	0.3070(4)	0.1602(5)	0.0571(7)	3.8(2)	
	R2C(2)	0.2992(4)	0.2437(5)	0.0687(7)	4.0(2)	
	R2C(3)	0.3654(5)	0.2929(4)	0.0690(7)	5.1(3)	
	R2C(4)	0.4395(4)	0.2585(5)	0.0577(8)	5.7(3)	
	R2C(5)	0.4472(4)	0.1750(5)	0.0461(8)	5.6(3)	
	R2C(6)	0.3810(5)	0.1258(4)	0.0458(7)	4.9(3)	
1-F6						
	1F(1)	-0.1433(4)	-0.1606(3)	-0.2166(6)	9.9(3)	
	1F(2)	-0.1887(4)	0.0250(3)	-0.2159(6)	11.0(3)	
	1F(3)	-0.0849(3)	-0.0467(4)	-0.1625(6)	9.0(3)	
	1F(4)	-0.2471(3)	-0.0889(5)	-0.2701(6)	11.5(3)	
	1F(5)	-0.2044(4)	-0.0781(5)	-0.1027(4)	10.6(3)	
	1F(6)	-0.1277(5)	-0.0575(5)	-0.3298(4)	12.2(4)	
2-F6						
	2F(1)	0.0546(4)	-0.1547(3)	0.3008(6)	9.0(3)	
	2F(2)	0.0207(4)	0.0336(3)	0.3043(5)	7.0(2)	
	2F(3)	0.1261(3)	-0.0438(4)	0.3326(6)	12.4(4)	
	2F(4)	-0.0507(3)	-0.0773(4)	0.2725(6)	10.4(3)	
	2F(5)	0.0162(4)	-0.0660(4)	0.4246(4)	10.1(3)	
	2F(6)	0.0592(4)	-0.0551(4)	0.1805(4)	10.4(3)	
Car-1						
	1C(1)	0.2048(6)	0.2114(5)	-0.1457(9)		
	1N(1)	0.1719(5)	0.2782(5)	-0.1242(7)		
	1C(2)	0.0954(7)	0.2818(9)	-0.0693(13)	B(group) = 3.5(2)	
	1C(3)	0.2045(8)	0.3598(5)	-0.1503(13)		
	1C(4)	0.2838(7)	0.2148(8)	-0.2026(12)		
Car-2						
	2C(1)	0.1611(14)	0.2259(14)	-0.112(2)		
	2N(1)	0.2170(11)	0.2576(11)	-0.164(2)		
	2C(2)	0.272(2)	0.208(2)	-0.228(3)	B(group) = 4.0(6)	
	2C(3)	0.235(2)	0.3462(11)	-0.167(3)		
	2C(4)	0.108(2)	0.283(2)	-0.049(3)		

[a] Ring C atoms are numbered sequentially. R1C(1) is bonded to P(1)

TABLE 6.7

Derived Hydrogen Atom Positional and Thermal Parameters

Atom	x	y	z	B(Å²)[a]
	Methyl Hydrogen Atoms			
H1C(11)	0.0074	0.1956	-0.2329	6.08
H2C(11)	-0.0369	0.1364	-0.3291	6.08
H3C(11)	-0.0396	0.1046	-0.2060	6.08
H1C(12)	0.0407	-0.0327	-0.2788	6.73
H2C(12)	0.0503	0.0045	-0.3986	6.73
H3C(12)	0.1274	-0.0265	-0.3333	6.73
H1C(21)	0.1869	0.1291	0.2284	6.88
H2C(21)	0.1431	0.1909	0.1459	6.88
H3C(21)	0.1096	0.0989	0.1626	6.88
H1C(22)	0.2056	-0.0287	0.1312	6.81
H2C(22)	0.2647	-0.0341	0.0291	6.81
H3C(22)	0.2961	0.0027	0.1421	6.81
H1C(6)	0.0213	-0.4395	-0.0691	7.90
H2C(6)	0.1099	-0.4450	-0.1178	7.90
H3C(6)	0.0967	-0.4422	0.0110	7.90
	Phenyl Hydrogen Atoms			
H1C(2)	0.1880	0.0628	-0.4486	5.83
H1C(3)	0.2400	0.1376	-0.5914	7.47
H1C(4)	0.2129	0.2769	-0.6063	8.19
HIC(5)	0.1339	0.3414	-0.4786	7.08
H1C(6)	0.0819	0.2666	-0.3359	6.31
H2C(2)	0.2481	0.2674	0.0766	5.01
H2C(3)	0.3602	0.3504	-0.0772	6.01
H2C(4)	0.4852	0.2922	0.0581	6.70
H2C(5)	0.4982	0.1511	0.0384	6.67
H2C(6)	0.3861	0.0681	0.0378	5.79
H3C(2)	0.1332	-0.1756	0.0831	5.49
H3C(3)	0.1262	-0.3180	0.0866	5.07
H3C(5)	0.0431	-0.3178	-0.2129	6.94
H3C(6)	0.0468	-0.1769	-0.2176	6.25

[a] The isotropic thermal parameters for the H atoms are 1.0Å² greater than those of the atoms to which they are bonded.

[b] Phenyl H atoms are numbered sequentially. H1C(2) is bonded to R1C(2), H1C(3) is bonded to R1C(3), etc.

6.4 Description of the Structure

The unit cell contains distinct anionic and cationic components present in a two to one ratio. The nearest anion-cation separations are 3.09 Å between 1F(4) and C(5); and 2.99 Å between 2F(3) and 2C(3). These distances are of the magnitude expected if no significant anion-cation interactions occur.

The two PF_6 anions show little deviation from ideal geometry (90, 91). The mean P-F distance is 1.580(7) Å. Mean F-P-F angles have values of 90.0(2)° for cis F atoms and 178.6(4)° for those in mutually trans positions.

An ORTEP diagram of the cation showing the atom labelling scheme is presented in Fig. 6.4. In Fig. 6.5 are shown the inner coordination sphere of the metal atom and the two orientations of the disordered carbene ligand. A stereoview of the cation is given in Fig. 6.6, and selected bond distances and angles are listed in Table 6.8.

The doubly charged cation has distorted square planar geometry about the Pt atom. The two phosphine ligands occupy mutually trans coordination sites while the remaining two positions in the square plane are occupied by the isocyanide and carbene ligands. Distortion of the square plane occurs at the carbene ligand where the C(sp^2) atoms of the carbene rigid groups lie to opposite sides of the equatorial plane. Calculation of a weighted least-squares plane through the atoms Pt, P(1), P(2) and C(5) (Table 6.9), shows that of these atoms C(5) lies farthest from the plane,

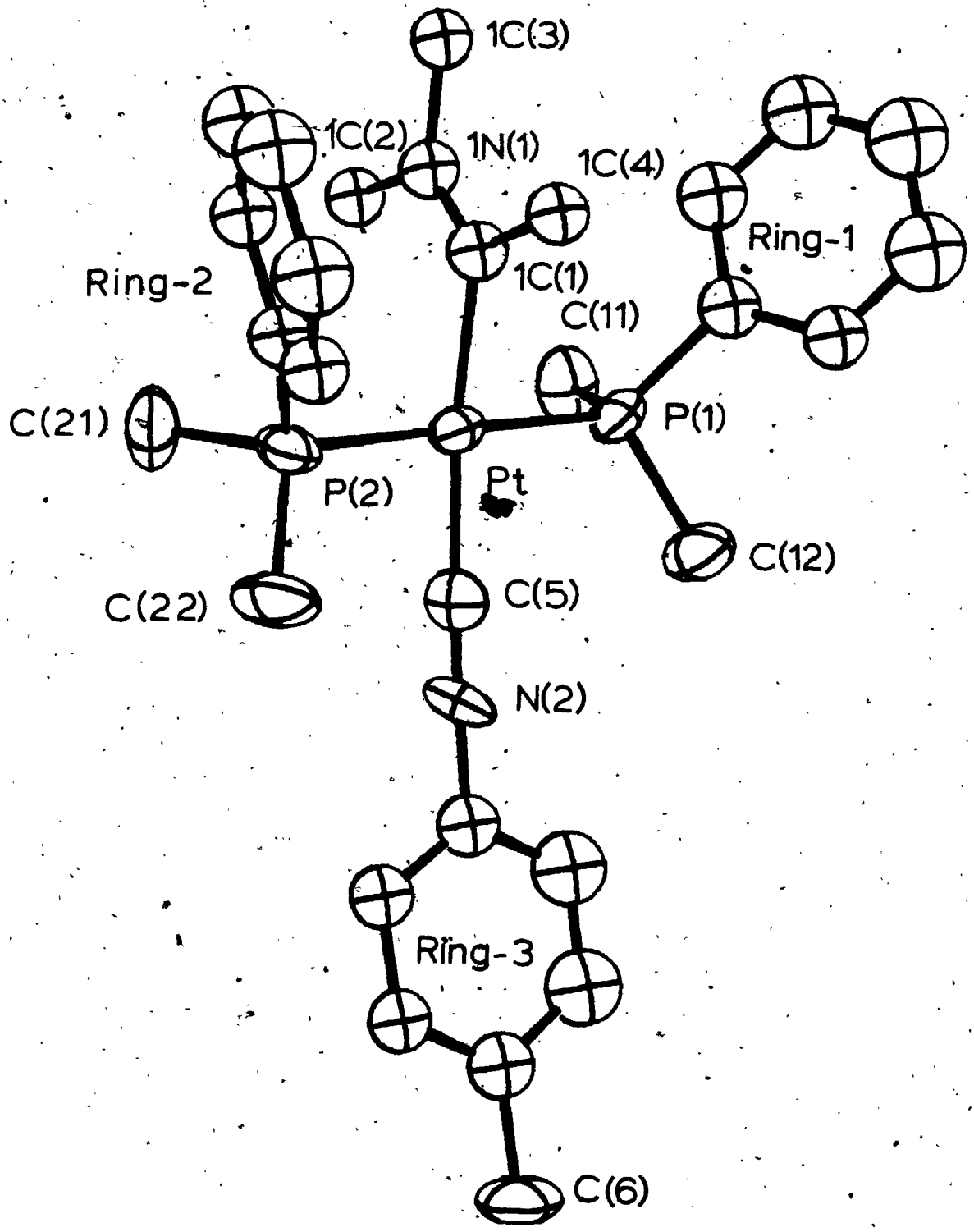

Fig. 6.4

ORTEP View of the Cation Showing the Atom Numbering Scheme

50% probability ellipsoids are drawn.

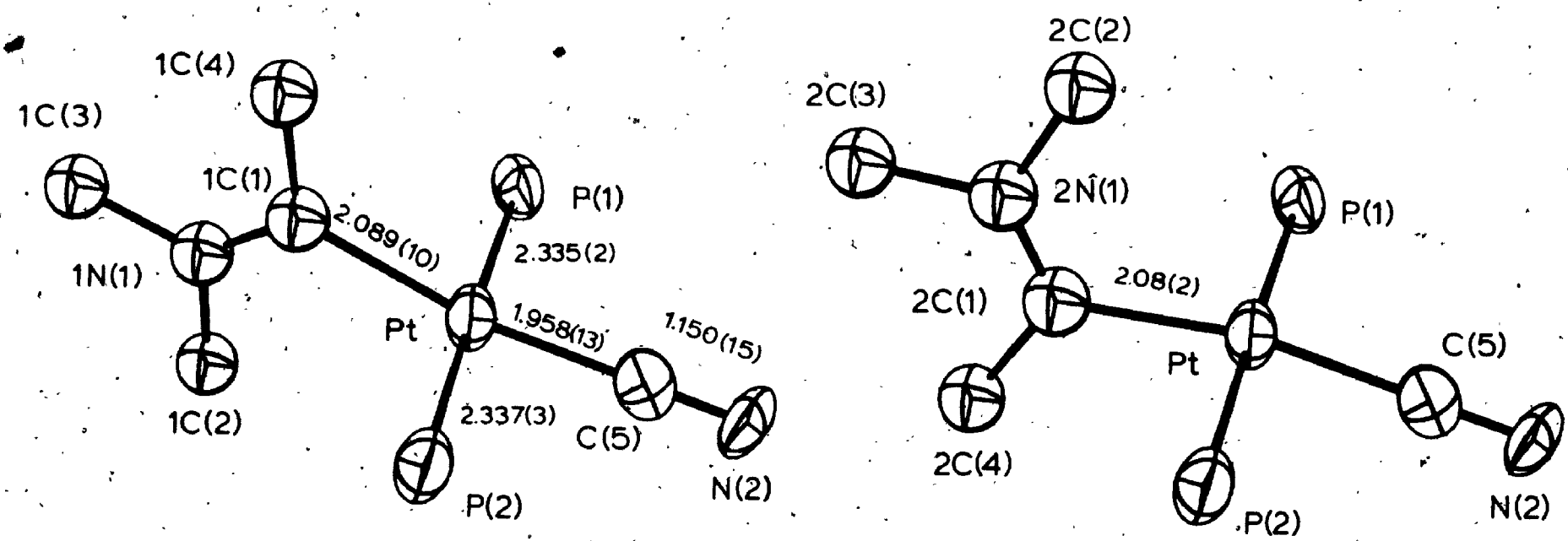

Fig. 6.5

The Carbene Ligand and the Inner Coordination Sphere of the Metal Atom. The two final orientations of the disordered carbene ligand are shown.

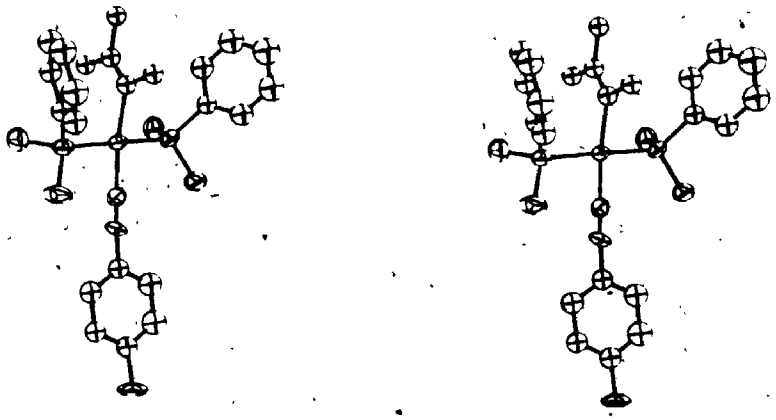

Fig. 6.6

A Stereoview of the Cation

TABLE 6.8

Selected Intramolecular Bond Distances and Angles

Distances(Å)		Angles(deg.)	
Metal Atom Inner Coordination Sphere			
Pt-P(1)	2.335(2)	P(1)-Pt-P(2)	178.7(2)
Pt-P(2)	2.337(3)	C(5)-Pt-1C(1)	168.5(4)
Pt-1C(1)	2.089(10)	C(5)-Pt-2C(1)	166.9(8)
Pt-2C(1)	2.08(2)	1C(1)-Pt-P(1)	90.0(3)
Pt-C(5)	1.958(13)	2C(1)-Pt-P(1)	91.1(7)
		1C(1)-Pt-P(2)	90.0(3)
		2C(1)-Pt-P(2)	90.1(7)
		C(5)-Pt-P(1)	89.4(4)
		C(5)-Pt-P(2)	89.4(4)
Phosphine Ligands			
P(1)-C(11)	1.785(14)	Pt-P(1)-C(11)	111.5(5)
P(1)-C(12)	1.790(14)	Pt-P(1)-C(12)	113.3(5)
P(1)-R1C(1)	1.813(9)	Pt-P(1)-R1C(1)	116.8(3)
P(2)-C(21)	1.818(16)	Pt-P(2)-C(21)	110.4(5)
P(2)-C(22)	1.789(14)	Pt-P(2)-C(22)	113.8(5)
P(2)-R2C(1)	1.805(9)	Pt-P(2)-R2C(1)	114.7(3)
		C(11)-P(1)-C(12)	104.9(7)
		C(11)-P(1)-R1C(1)	104.8(5)
		C(12)-P(1)-R1C(1)	104.4(6)
		C(21)-P(2)-C(22)	104.7(7)
		C(21)-P(2)-R2C(1)	106.0(6)
		C(22)-P(2)-R2C(1)	106.4(6)
Isocyanide Ligand			
C(5)-N(2)	1.150(15)	Pt-C(5)-N(2)	177(1)
N(2)-R3C(1)	1.414(16)	C(5)-N(2)-R3C(1)	170(1)
C(6)-R3C(4)	1.510(19)	N(2)-R3C(1)-R3C(2)	121(1)
R3C(1)-R3C(2)	1.376(16)	N(2)-R3C(1)-R3C(6)	118(1)
R3C(2)-R3C(3)	1.386(17)	R3C(2)-R3C(1)-R3C(6)	121(1)
R3C(3)-R3C(4)	1.370(17)	R3C(1)-R3C(2)-R3C(3)	119(1)
R3C(4)-R3C(5)	1.372(18)	R3C(2)-R3C(3)-R3C(4)	121(1)
R3C(5)-R3C(6)	1.372(18)	R3C(3)-R3C(4)-R3C(5)	119(1)
R3C(6)-R3C(1)	1.379(17)	R3C(3)-R3C(4)-C(6)	120(1)
		R3C(5)-R3C(4)-C(6)	121(1)
		R3C(4)-R3C(5)-R3C(6)	122(1)
		R3C(5)-R3C(6)-R3C(1)	119(1)

TABLE 6.9

Weighted Least-Squares Planes

Atom	Deviation from Plane(Å)
Atoms included: Pt, P(1), P(2), C(5)	
Equation of Plane: 14.27x - 4.742y - 5.877z = 2.358	
Pt	-0.0004(4)
P(1)	0.011(3)
P(2)	0.015(4)
C(5)	-0.003(13)
1C(1)	0.42
2C(1)	-0.48
Atoms included: N(2), C(5), C(6), R3C(1), R3C(2), R3C(3), R3C(4), R3C(5), R3C(6)	
Equation of Plane: 15.84x + 2.092y - 4.414z = 2.226	
N(2)	-0.060(13)
C(5)	0.158(13)
C(6)	0.134(19)
R3C(1)	-0.077(12)
R3C(2)	-0.065(13)
R3C(3)	0.008(12)
R3C(4)	0.032(13)
R3C(5)	0.011(15)
R3C(6)	-0.082(14)
Atoms included: R3C(1), R3C(2), R3C(3), R3C(4), R3C(5), R3C(6)	
Equation of Plane: 15.89x - 1.353y - 4.476z = 2.024	
R3C(1)	0.013(12)
R3C(2)	-0.009(13)
R3C(3)	0.001(12)
R3C(4)	-0.002(13)
R3C(5)	0.012(15)
R3C(6)	-0.019(14)

being 0.013(3) Å above it. Atoms 1C(1) and 2C(1) lie 0.40 Å below and 0.48 Å above this plane respectively. Such distortion seems to be characteristic of square planar systems where ligand disorder of this kind occurs (92, 133). The mean C-Pt-C angle is 167.7(8)° and the mean P-Pt-C(sp^2) angle is 90.5(3)°. No large distortions occur with respect to the other ligands. The mean P-Pt-C(5) angle is 89.445(5)° and the P-Pt-P angle is 178.7(2)°.

An eclipsed configuration is observed for the two phosphine ligands. Both phosphine phenyl rings lie on the same side of the Pt atom as the carbene ligand. The angles between the normals to the planes of the phenyl rings and the equatorial plane of the metal atom are 54° and 79° for Ring-1 and Ring-2 respectively. The former angle is considerably smaller than observed in previous structures. In earlier chapters of this work the phenyl rings of the phosphine ligands have been found to lie approximately perpendicular to the equatorial plane, with the mean angle being 83(3)°.

Only slight deviation from ideal phenyl ring geometry is observed with respect to the P-C(phenyl) bonds. The P(1)-R1C(1)-R1C(4) and P(2)-R2C(1)-R2C(4) angles are 178.0(5)° and 178.2(4)°, where a value of 180° is considered ideal. For both phenyl rings the distortion is such that they are bent slightly towards the carbene ligand. No other significant deviations occur at atoms R1C(1) and R2C(1). The P(1)-R1C(1)-R1C(2) and P(1)-R1C(1)-R1C(6)

angles are 119.9(6)° and 120.0(6)° respectively. The corresponding angles about R2C(1) are 119.5(6)° and 120.5(6)°.

The phosphine P atoms are an average distance of 2.336(1) Å from the metal atom and have approximately tetrahedral geometries, with the organic substituents bonded to P compressed toward one another to a small extent. The mean Pt-P-C angle is 113.4(9)° and the average C-P-C angle is 105.2(3)°. A mean P-C bond length of 1.800(6) Å is observed. These angles and distances agree well with those observed in foregoing chapters.

The carbene ligand disorder is defined in terms of two superimposed rigid groups related to one another by 180° rotation about the Pt-C(sp^2) vector and by translation out of the square plane so that the C(sp^2) atoms are approximately equal distances above and below this plane. A rigid group disorder parameter was refined so that the sum of the multiplicities of the carbene groups always equalled 1.0. The final value obtained for this parameter is 0.68(2). Thus one orientation of the carbene ligand (that of Car-1) is favoured by about two to one. This is in agreement with the magnitudes of the regions of electron density corresponding to C(sp^2) and N for Car-1 and Car-2, as observed in Fig. 6.2.

The planes of Car-1 and Car-2 intersect the square plane of the Pt atom at angles of 77° and 68° respectively. Thus the methyl-N,N-dimethylaminocarbene ligand does not lie perpendicular to the equatorial plane of the metal atom

as it does for the complex in Chapter 2. The mean Pt-C(sp^2) distance is 2.086(3) Å. This is crystallographically equivalent to the value of 2.079(13) obtained in Chapter 2.

Angles about the C(carbene) atom are characteristic of sp^2 hybridization; the mean values of the angles Pt-1C(1)-1N(1) and Pt-2C(1)-2N(1) is 120(2)° and that of Pt-1C(1)-1C(4) and Pt-2C(1)-2C(4) is 122(2)°.

The isocyanide ligand C atom occupies a coordination site trans to the carbene ligand and is 1.958(13) Å from the Pt atom. This compares well with the Pt-C bond length of 1.968(9) Å in the dicationic complex trans[Pt(C≡NMe)$_2$-{C(NHMe)(SEt)}$_2$](PF$_6$)$_2$ (72). The isocyanide ligand is approximately planar. Weighted least-squares planes are shown in Table 6.9. One plane is calculated through all non hydrogen atoms of the isocyanide. The C(sp) atom and the p-tolyl C(methyl) atom are most distant from the plane, being 0.158(13) Å and 0.134(19) Å above it. A second least-squares plane is calculated through the p-tolyl phenyl ring C atoms. No C atom is a significant distance from the plane. The phenyl ring plane intersects that of the metal atom at an angle of 14.5°. The mean C-C distance within the ring is 1.376(2) Å and is slightly shorter than the accepted value of 1.392 Å (88). A mean C-C-C angle of 120.0(5)° is observed. The p-tolyl methyl group is 1.510(19) Å from atom R3C(4) and the mean of angles C(6)-R3C(4)-R3C(3) and C(6)-R3C(4)-R3C(5) is 120.5(2)°. On the opposite side of the phenyl ring, the R3C(1)-N(2) distance is

1.414(16) Å. An equivalent value of 1.37(2) Å is observed for the N-C(phenyl) separation in the complex trans-$PtCl_2(C{\equiv}NPh)_2$ (132).

The isocyanide C(5)-N(2) distance is 1.150(15) Å. This compares well with the mean value of 1.17(2) Å observed in trans-$PtCl_2(C{\equiv}NPh)_2$ (6). The isocyanide ligand is approximately linear with respect to the Pt atom, with the Pt-C(5)-N(2) angle being 177(1)°, however the ligand is bent slightly with respect to the p-tolyl group for the C(5)-N(2)-R3C(1) angle is 170(1)°.

6.5 Discussion

It has been observed that the carbene disorder is the result of not only 180° rotation about the Pt-C(sp^2) bond, but that translation of the ligand out of the square plane also occurs. When this effect was first observed in the structure determination of trans-[Pt(MeC=OMe)-$Me(PMe_2Ph)_2$]PF_6 (92) it was thought that the large distortion of the equatorial plane might possibly be the result of an inadequate disorder model. A second occurence of such a disorder together with the presence of a similar effect in the solid state structure of trans-$Pt(CH=CH_2)Cl(PEt_2Ph)_2$ (133), where the vinyl ligand is disordered, tends to indicate that the distortion of the square plane is a real phenomenon. Furthermore the small group thermal parameters observed for Car-1 and Car-2 (3.5(2) and 4.0(6)) indicate that the model is a good approximation of the actual disorder. The distortion of the equatorial plane can be explained in terms of packing effects. If the two isomers are considered separately, and if no distortion of the square plane is postulated, then clearly in one isomer the carbene ligand occupies a larger region of space above the equatorial plane than below, and vice versa for the second isomer:

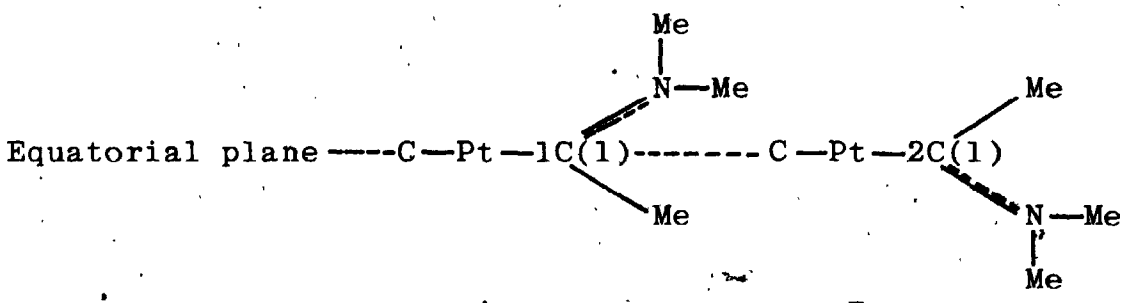

A B

Hence the spatial requirements of the two isomers are different, and they might be expected to form different crystal lattices. If distortion of the equatorial plane is implemented such that 1C(1) of isomer A is moved to a position below the equatorial plane, 2C(1) of B is moved to a position above the plane, and the remaining carbene ligand atoms of both isomers are shifted correspondingly, then the isomers occupy the same regions of space as shown in Fig. 6.2. Thus through a distortion of the equatorial plane of the metal atom, the two isomers can occupy the same lattice.

As noted earlier, the planes of the carbene rigid groups do not lie perpendicular to the square plane of the metal atom. The mean angle of intersection of the planes is 72.5°. A perpendicular orientation is required if significant in-plane π bonding between the C(sp^2) $2p_z$ and the Pt $5d_{xy}$ orbitals is to occur. In Chapter 3 it was concluded that metal-carbene π bonding is not an important factor in the metal-carbene bond in <u>trans</u>-[Pt(MeC$\equiv$NMe$_2$)-Me(PMe$_2$Ph)$_2$]PF_6. In the compound being examined here, the methyl ligand <u>trans</u> to the carbene has been replaced by the isocyanide ligand, which is not only a poorer σ donor than methyl, but is also capable of π interaction with the metal atom. Even less electron density should be available for π back-bonding to the carbene ligand than in the complex in Chapter 2, so metal-carbene π interactions should be smaller. The orientation of the carbene ligand is such

that no significant π bonding interactions can be present in the Pt-C(sp^2) bond.

The mean Pt-C(carbene) distance of 2.086(3) Å is indicative of a situation where little π bonding occurs, but does not reflect a weak trans influence for the isocyanide ligand. The Pt-C(sp^2) bond length in Chapter 4 where a chloride ligand is trans to carbene is 1.978(12) Å. The chloride exerts a weak trans influence as is expected for the isocyanide ligand (67, 131, 132), but the Pt-C(carbene) bond lengths differ by 9.0 σ. The Pt-C(sp^2) distance observed in Chapter 2 where methyl, a strong trans influence ligand, is opposite carbene is 2.079(13) Å. If a shift of the carbene ligand which causes C(carbene) to move ~ 0.45 Å out of the square plane of the Pt atom can be attributed to packing forces as discussed above, then a much smaller lengthening of the Pt-C(sp^2) bond could also result from these effects. Inaccuracies in the disorder model could also affect the Pt-C(sp^2) bond.

There is only little evidence of the strong trans influence of the carbene ligand in the Pt-C(isocyanide) bond length of 1.958(13) Å. This distance is 3.1 σ longer than that of 1.83(4) found in cis-$Pt(C{\equiv}NEt)Cl_2PEt_2Ph$ (131) and is 3.0 σ longer than the mean distance of 1.896(16) Å observed in cis-$Pt(C{\equiv}NPh)_2Cl_2$ (132). In both these complexes Cl^- lies opposite the isocyanide ligands. The Pt-C(isocyanide) distance is equivalent to that of 1.968(9) Å observed in trans-$[Pt(C{\equiv}NMe)_2\{C(NHMe)SEt\}_2](PF_6)_2$ (72) where the

isocyanide ligands are trans to one another. An interesting observation is that the Pt-C(isocyanide) distances are significantly longer in the dicationic complexes than those in the neutral compounds.

A summary of available isocyanide geometries in square planar Pt(II) complexes is given in Table 6.10. Possible resonance forms contributing to the structure of the coordinated isocyanide ligand are as follows:

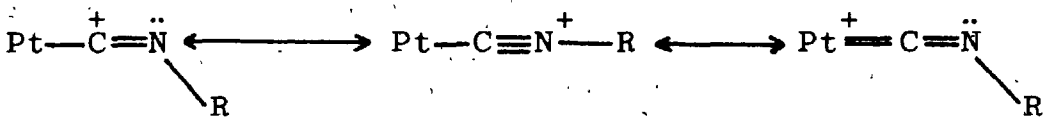

I II III

The Pt-C(5)-N(2) angle of 177(1)° at the isocyanide ligand shows only small deviation from linearity and slight bending is observed from the C(5)-N(2)-R3C(1) angle of 170(1)°. This together with the C(5)-N(2) bond length of 1.150(15) Å, which is in good agreement with 1.16(1) expected for a C-N bond order of three (88), indicate that the bonding in the isocyanide ligand is best described by II. These results are in good agreement with the infrared data where ν(C-N) occurs at 2218 cm^{-1} whereas that for the ν(C-N) of the formimidoyl ligand where the bond order is two, occurs at much lower energy (~ 1550 cm^{-1}) (Chapter 5).

The Pt-C(isocyanide) distance of 1.958(13) Å does not show significant multiple bond character in view of the Pt-C(sp) bond length of 1.98(2) Å in the complex trans-$Pt(C{\equiv}CPh)Cl(PEt_2Ph)_2$ (133) where no Pt-C(sp) multiple

TABLE 6.10

Geometries of Isocyanide Ligands in

Square Planar Platinum(II) Complexes

Complex	Pt-C (Å)	C≡N (Å)	N-C(sp^3)(Å)	Pt-C-N(deg)	C-N-C(deg)	Reference
cis-$Pt(C{\equiv}NEt)Cl_2PEt_2Ph$	1.83(4)	1.22(5)	1.45(5)	174(4)	172(3)	131
cis-$Pt(C{\equiv}NPh)_2Cl_2$	1.880(16)	1.19(2)	1.37(2)	170(2)	178(2)	132
	1.912(22)	1.14(3)	1.47(3)	178(2)	175(2)	
trans-$[Pt(C{\equiv}NMe)_2\{C(NHMe)(SEt)\}_2](PF_6)_2$	1.968(9)	1.120(10)	1.448(14)	175.6(7)	176.6(9)	72
trans-$[Pt(C{\equiv}N\text{-}p\text{-}tolyl)(MeC{=}NMe_2)(PMe_2Ph)_2](PF_6)_2$	1.958(13)	1.150(15)	1.414(16)	177(1)	170(1)	this work
trans-$[Pt(C{\equiv}NMe)_2\{MeHNC{=}NN(Me)CNHMe\}]BPh_4$	1.95(3)	1.14(2)	1.53(3)	172(2)	177(2)	34
	1.97(3)	1.16(2)	1.53(2)	175(2)	179(2)	

bonding can occur. The effects of the strong trans influence of the carbene ligand can compete with small π bonding effects on the Pt-C(sp) bond length. Thus accurate deductions as to the nature of the Pt-C(isocyanide) bond in this complex are not possible.

CHAPTER 7

THE CRYSTAL AND MOLECULAR STRUCTURE OF TRANS-METHYL-N,N-DIMETHYLAMINOCARBENE(DIMETHYLAMINO-p-TOLYLAMINO-CARBENE)BIS(DIMETHYLPHENYLPHOSPHINE)PLATINUM(II) HEXAFLUOROPHOSPHATE. Trans-$[Pt\{CH_3C{=}{=}N(CH_3)_2\}\{C(N(CH_3)_2)NH\text{-}p\text{-}C_6H_4CH_3\}\{P(CH_3)_2C_6H_5\}_2](PF_6)_2$

7.1 Introduction

The most common forms of tertiary carbene ligands are those belonging to groups 3a and 3b (Chapter 1).

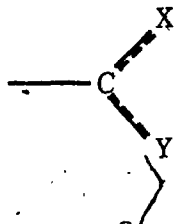

3a

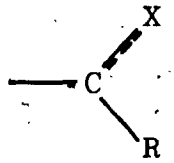

3b

X and/or Y = oxy, amino, thio

R = alkyl, aryl

For group 3a, two nucleophilic substituents are present to stabilize the C(sp^2) atom, whereas in group 3b only one such substituent is present. The four Pt(II) complexes that have been examined in this work have carbene ligands characteristic of 3b. Other structural determinations on square planar Pt(II) complexes have carbene ligands representative of 3a (34, 69-72).

In Chapter 5 is described the preparation of dicationic

bis-carbene complexes. In these compounds a 3a carbene ligand lies trans to a 3b carbene, while dimethylphenylphosphine ligands occupy the remaining two positions in the square planar coordination sphere. The X-ray crystallographic structure analysis of one such complex, trans-$[Pt(MeC{=}NMe_2)\{C(NMe_2)NH\text{-}p\text{-}C_6H_4Me\}(PMe_2Ph)_2](PF_6)_2$, was undertaken. This complex offers an ideal opportunity for a comparison of the bonding in two types of carbene ligands present in similar environments. A better understanding of the bonding trends and of any differences in bonding would allow a more detailed and knowledgeable comparison of all structural results available for Pt(II)-carbene complexes.

7.2 Experimental

A sample of the complex was prepared by the synthetic route detailed in Chapter 5. Colourless blocks suitable for X-ray examination were readily obtained from an acetone/ether mixture. Crystal data are summarized in Table 7.1. A photographic study revealed the systematic extinctions $h0\ell$, $h + \ell \neq 2n$; $0k0$, $k \neq 2n$. These absences are consistent only with the space group $P2_1/n$ (alternate setting of $P2_1/c$, C_{2h}^5, No. 14 (76). No symmetry constraints are imposed on entities crystallizing in space group $P2_1/n$ with four formula units in the unit cell.

The conditions for intensity data collection are shown in Table 7.2. 7448 reflections were recorded using Cu Kα radiation out to a 2θ value of 130°. The intensities of four strong reflections (200, $\bar{2}00$, 060, 002) were monitored after every 150 data recorded. No significant fluctuations were observed for the standard reflections. All data were processed. 5370 intensities had $I > 3\sigma(I)$, and only these were used in the solution and refinement of the structure. The crystal was measured and an absorption correction was performed on all data with $I > 0$. The maximum and minimum absorption coefficients differed by approximately 75% (Table 7.2). A diagram of the crystal is shown in Fig. 7.1.

TABLE 7.1

Crystal Data for Trans-$[Pt(MeC{=}NMe_2)\{C(NH\text{-}p\text{-}C_6H_4Me)(NMe_2)\}(PMe_2Ph)_2](PF_6)_2$

$C_{30}H_{45}F_{12}N_3P_4Pt$	f.w. = 994.7
Analysis found (calculated)	C, 36.04 (36.23); H, 4.51 (4.56); N, 3.82 (4.22)
Crystal description	colourless blocks elongated along [001]
Systematic absences	$h0\ell$, $h + \ell \neq 2n$; $0k0$, $k \neq 2n$
Laue symmetry	2/m
Crystal system	monoclinic
Space group.	$P2_1/n$
Equivalent positions (4)	$\pm(x, y, z)$, $\pm(\frac{1}{2} + x, \frac{1}{2} - y, \frac{1}{2} + z)$
Cell constants	a = 12.792(2)Å α = 90.0° b = 27.382(4)Å β = 99.47(1)° c = 11.839(2)Å γ = 90.0°
Cell volume	4090 Å^3
Wavelength used for cell determination	1.54056 Å
Temperature at which cell was determined	21°C
Method of density determination	flotation ($C_2H_4Br_2/CCl_4$)
Density (observed) (calculated)	1.69(1)g cm^{-3} 1.70g cm^{-3}
Z	4
Symmetry constraints	none

TABLE 7.2

Experimental Conditions for Data Collection

Radiation		Cu Kα
Wavelength		1.54056 Å
Filter		pre-filtered, Ni foil (0.018mm)
Mean ω scan width at half height (reflections)		0.093° (200, 020, 002)
Reflections centered; in 2θ range		25; 14° < 2θ < 65°
Scan range	a) low angle side of 2θ	0.60°
	b) high angle side of 2θ	0.75°
Scan rate		2.0° min^{-1}
Stationary background count time		10 sec
% available Bragg intensity obtained for a given reflection		80%
Take-off angle		1.5°
Tube KV; mA		14; 14
Collimator size		1mm
Crystal-counter distance		32cm
Crystal-aperture distance		30cm
Aperture dimensions		5mm x 5mm
2θ range		2.5° < 2θ ≤ 130°
Shells (No.; high angle limit)		6; 60°, 90°, 100°, 110°, 120°, 130°
Index limits		$-15 \leq h \leq 15$, $0 \leq k \leq 32$, $0 \leq \ell \leq 13$
No. of data collected		7448
p value		0.02
No. of reflections with $I > 3\sigma(I)$		5370
μ (Cu Kα)		86.23cm^{-1}
Crystal faces		$\{120\}, (021), (0\bar{2}1), (00\bar{1})$
Crystal dimensions		0.33mm x 0.19mm x 0.18mm
Absorption correction		analytical
Transmission coefficients	a) minimum	0.248
	b) maximum	0.440

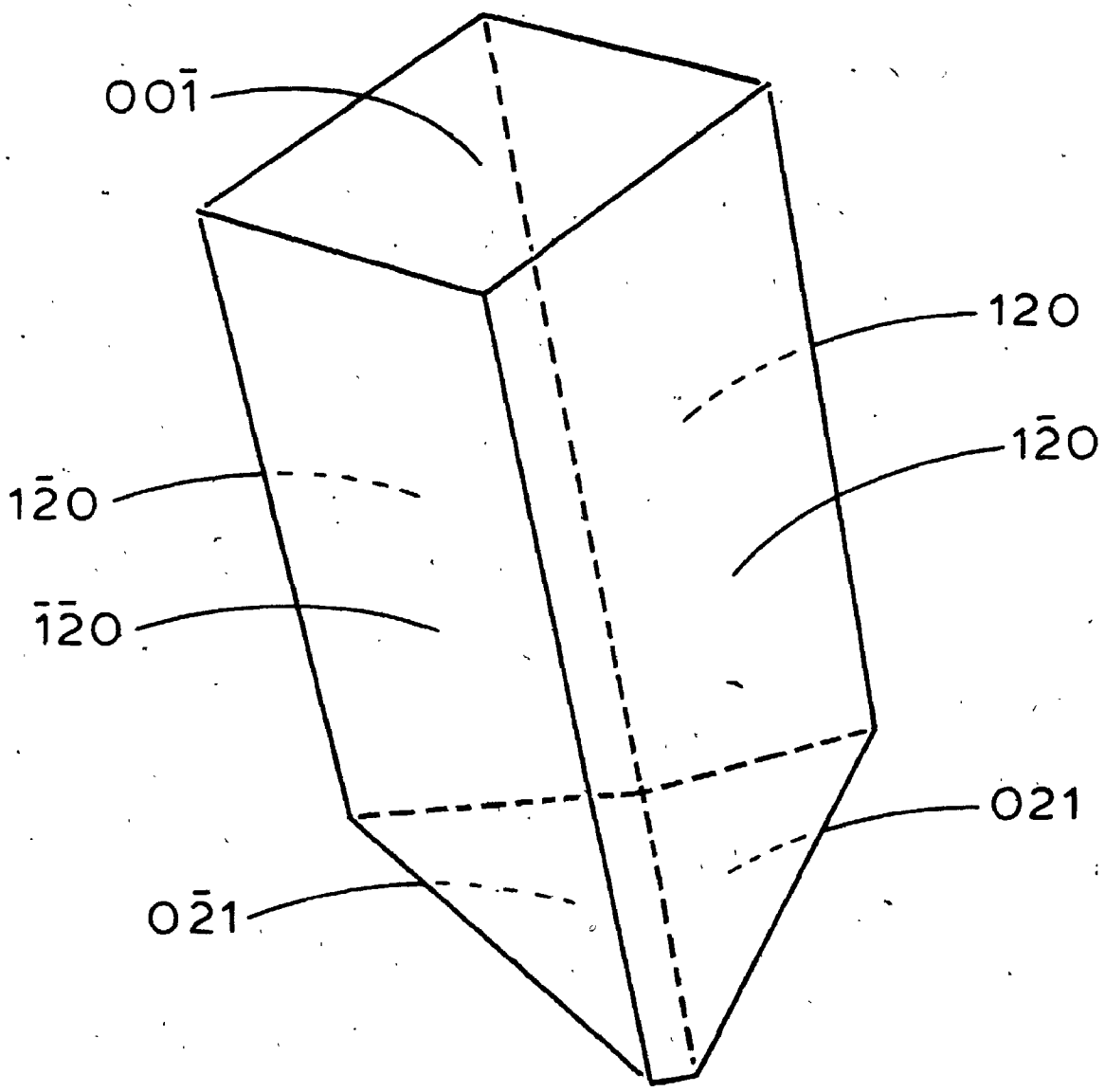

Fig. 7.1

A Drawing of the Data Crystal

Faces with dotted edges are hidden from view

7.3 Structure Solution and Refinement

The position of the Pt atom was obtained from a three dimensional Patterson function. Two least-squares cycles varying an overall scale factor and the positional parameters of the Pt atom gave $R_1 = 0.302$ and $R_2 = 0.397$. Positional parameters for the remaining non-hydrogen atoms were obtained from successive difference Fourier syntheses and least-squares refinements.

The F atoms of the two PF_6 anions, as well as the two phosphine phenyl rings and the p-tolyl phenyl ring, were described as rigid groups (Chapter 2). Two cycles of least-squares refinement with Pt and two phosphine P atoms vibrating anisotropically, and group isotropic thermal parameters being varied for the rigid groups, gave agreement factors $R_1 = 0.069$ and $R_2 = 0.090$. Large group thermal parameters were obtained for both F6 rigid groups (~15.0 $\AA^2$) and unusually large temperature factors (~6.0 $\AA^2$) were observed for the P atoms of the anions. Disorder of both anions is present. A difference Fourier synthesis showed the presence of a second set of six peaks around one of the P atoms. These had electron densities of approximately 2 $e\AA^{-3}$. Only two small residual peaks of electron density were observed about the second P atom. The residual peaks for both anions were close to F atom positions already included in least-squares calculations. A rigid group disorder model (Chapter 2) was calculated for the F atoms about P(4), whereas the disorder about P(3) was not

considered serious enough to be taken into account and normal refinement procedures were followed.

A thorough examination of the geometry, and least-squares parameters of the methyl-N,N-dimethylaminocarbene ligand provided results disturbingly similar to those obtained during the refinement of the isocyanide-carbene complex in Chapter 6. The isotropic thermal parameters for the C and N atoms were unusually large (~11.0 $Å^2$) and the $C(sp^2)$-N distance was found to be only 1.07 Å. By comparison, the $C(sp^2)$-N bond length observed for this ligand in Chapter 2 was 1.266(15) Å. Removal of the contributions of the carbene ligand atoms to the least-squares refinement, and calculation of an electron density map through the plane of this ligand, confirmed the presence of disorder. A reproduction of this map is presented in Fig. 7.2. A rigid group disorder model was formulated and refined as described in Chapter 6.

The contributions to F_c of fourteen phenyl H atoms (C-H distance of 0.95 Å) and of 30 methyl H atoms (C-H distance of 1.0 Å) were calculated as previously described (Chapter 2). A difference Fourier synthesis over the unique volume of the unit cell was examined for evidence of H atoms belonging to methyl groups of the disordered carbene ligand. Regions of positive electron density (0.3 - 0.6 $eÅ^{-3}$) were observed for all H atoms of Car-1, the rigid group of higher multiplicity. The contributions to F_c of these methyl H atoms were calculated and the

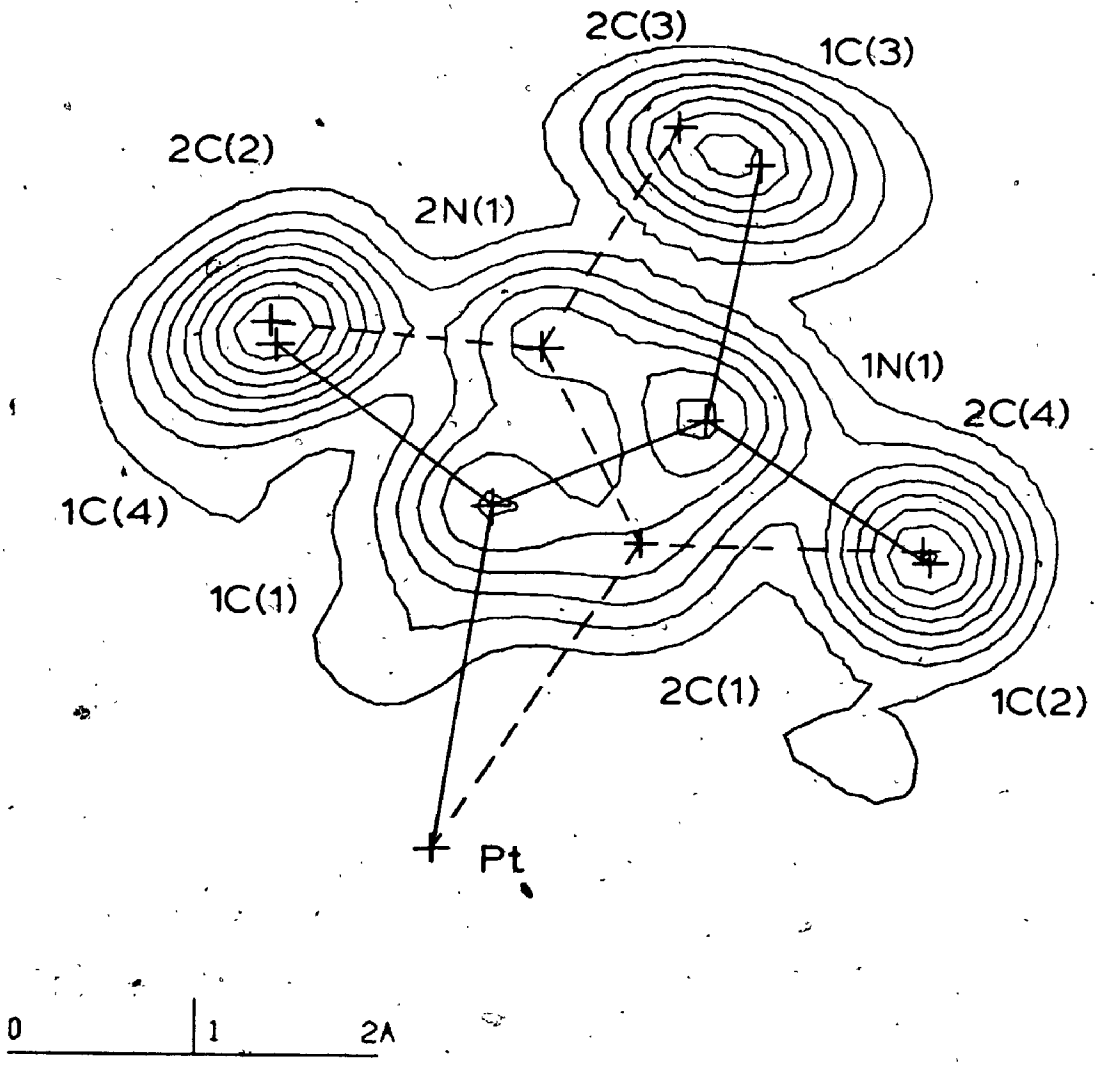

Fig. 7.2

An Electron Density Map Calculated Through the Plane of the Carbene Ligand
Contours are drawn at intervals of 0.5 $e\text{Å}^{-3}$.
Superimposed on the map are the final positions of the
atoms of the disordered ligand.

multiplicities were set equal to that of the parent carbene rigid group. Similar evidence for all H atoms of Car-2 was not present, so these were omitted from further calculations. A peak of about 0.5 $e\text{Å}^{-3}$ was observed for the amino H atom of the p-tolylamino substituent, so the contributions of this atom were included in the calculations of F_c (final N-H distance of 0.97 Å; $C(sp^2)$-N-H angle of 116.8°). All H atoms were assigned thermal parameters 1.0 Å^2 larger than those of the atoms to which they are bonded.

A summary of the conditions for, and the results of the final least-squares cycles is presented in Table 7.3. Individual group atom isotropic thermal parameters were refined only for those rigid groups not associated with disorder. The rigid group constraints for the p-tolyl phenyl ring were removed prior to the final least-squares cycles. These C atoms and the P atoms of the anions were allowed to vibrate isotropically. Anisotropic thermal parameters were varied for the remaining non-hydrogen atoms.

The final agreement factors are $R_1 = 0.054$ and $R_2 = 0.064$. The three largest peaks in a final difference Fourier synthesis have electron densities of 1.33(7), 1.06(7) and 1.05(7) $e\text{Å}^{-3}$. They are all associated with the F atoms about P(3) for which disorder was not taken into account. The next largest peak has an electron density of 1.04 (7) $e\text{Å}^{-3}$. It is related to the F atoms about P(4) for which a disorder model was calculated.

TABLE 7.3

Conditions and Results of Final Full Matrix Least-Squares Calculations

Observations	5356
Variables	216
Ratio (observations/variables)	24.8
Rigid groups	7
Disorder models (No; entities)	2; $MeC{\cdots}NMe_2$, PF_6
Non-group atoms	21
a) Anisotropic	13
b) Isotropic	8
H atoms included; No. (type)	45; 30(methyl), 14(phenyl), 1(amino)
Extinction coefficient	not refined
Maximum value of (parameter shift/ standard deviation)	0.13
Agreement factors: R_1	0.054
R_2	0.064
Final error on an observation of unit weight	2.91
Final difference Fourier synthesis:	
a) Position of largest peak	(-0.232, 0.177, 0.203)
b) Electron density	1.33(7) electrons
c) Associated with	PF_6 (undisordered)

A statistical examination of the structure factors (Chapter 2) showed no abnormal trends. In Table 7.4 are listed the individual atom positional and thermal parameters. The rigid group parameters are shown in Table 7.5, and derived group atom positional parameters are given in Table 7.6. Calculated H atom positional and thermal parameters are presented in Table 7.7. A list of $|F_o|$ and $|F_c| \times 10$ electrons is shown in Appendix III.

TABLE 7.4

Individual Atom Positional and Thermal Parameters

Atom	x	y	z	U_{11}[a]	U_{22}	U_{33}	U_{12}	U_{13}	U_{23}
Pt	0.30216(3)[b]	0.136617(14)	0.22729(4)	352(2)	398(2)	507(3)	-15(2)	47(2)	61(2)
P(1)	0.2419(2)	0.21681(9)	0.1993(2)	431(14)	426(14)	552(17)	23(11)	35(13)	39(13)
P(2)	0.3589(2)	0.05598(9)	0.2477(3)	427(14)	431(14)	600(18)	35(11)	15(13)	49(13)
P(3)	-0.1742(2)	0.22727(12)	0.1960(3)	0.0689(9)[c]					
P(4)	0.2384(3)	0.01839(14)	-0.2684(4)	0.0873(11)					
N(2)	0.5292(6)	0.1651(3)	0.2354(8)	431(46)	627(55)	648(62)	-120(40)	99(44)	102(47)
N(3)	0.4388(7)	0.1601(3)	0.0491(8)	587(55)	745(61)	503(60)	-89(46)	106(47)	12(49)
C(11)	0.1631(9)	0.2379(4)	0.3063(11)	695(74)	710(78)	874(95)	116(61)	358(70)	82(69)
C(12)	0.1557(9)	0.2250(4)	0.0592(11)	706(75)	693(76)	748(87)	151(60)	-176(66)	130(67)
C(21)	0.4296(9)	0.0398(4)	0.3921(11)	825(83)	501(66)	856(94)	93(59)	-269(72)	117(64)
C(22)	0.4498(9)	0.0389(4)	0.1490(12)	610(72)	678(77)	1106(110)	103(59)	298(73)	52(75)
C(5)	0.4379(8)	0.1555(3)	0.1634(9)	536(60)	429(53)	445(65)	-8(44)	21(52)	28(47)
C(6)	0.3499(9)	0.1440(4)	-0.0417(10)	853(82)	813(86)	495(70)	79(67)	70(63)	43(64)
C(7)	0.5315(10)	0.1753(6)	-0.0002(11)	807(90)	1572(141)	607(88)	-164(89)	391(74)	196(89)
C(8)	0.6317(11)	0.1153(5)	0.7286(12)	1233(111)	726(82)	685(90)	177(80)	37(83)	31(71)
R3C(1)[d]	0.5536(8)	0.1553(4)	0.3616(9)	0.050(2)					
R3C(2)	0.6480(8)	0.1314(4)	0.4025(10)	0.063(3)					
R3C(3)	0.6717(9)	0.1201(4)	0.5214(12)	0.075(3)					
R3C(4)	0.6011(8)	0.1303(4)	0.5991(10)	0.060(3)					
R3C(5)	0.5136(8)	0.1553(4)	0.5571(10)	0.058(3)					
R3C(6)	0.4870(7)	0.1680(3)	0.4403(9)	0.051(3)					

[a] The Uij's are the thermal parameters in terms of mean square amplitudes of vibration in $\AA^2$. Values are given as U x 10^4. The expression for the thermal ellipsoid is given in Appendix II.

[b] Numbers in parentheses given here and in other tables are estimated standard deviations in the least significant digits.

[c] Isotropic thermal parameters are given as U_{11} in $\AA^2$.

[d] Ring C atoms are numbered sequentially. R3C(1) is bonded to N(2).

TABLE 7.5

Rigid Group Parameters

Group	x_g[a]	y_g	z_g	δ	ε	η	Multiplicity
Ring-1	0.4251(4)	0.2964(2)	0.2026(5)	-0.793(5)	-2.732(5)	1.666(6)	
Ring-2	0.1622(4)	-0.0172(2)	0.1937(5)	2.244(5)	2.545(5)	-1.654(6)	
Car-1	0.1553(9)	0.1163(6)	0.2583(10)	1.90(4)	1.914(7)	1.60(4)	0.585(18)
Car-2	0.1796(11)	0.1229(7)	0.3289(15)	-1.14(3)	-2.280(10)	1.67(3)	0.415(18)
1-F6	-0.1738(4)	0.2265(2)	0.1973(4)	-2.333(5)	-2.430(4)	1.235(5)	
21-F6	0.2378(5)	0.0170(3)	-0.2703(6)	-1.325(10)	-2.267(6)	-1.693(12)	0.556(14)
22-F6	0.2373(7)	0.0242(3)	-0.2650(8)	0.613(10)	-2.353(9)	-0.510(10)	0.444(14)

[a] x_g, y_g, and z_g are the fractional coordinates of the group origin, and δ, ε, and η (radians) are the group orientation angles.

TABLE 7.6

Derived Group Atom Positional and Thermal Parameters

	Atom	x	y	z	B(Å²)
Ring-1					
	R1C(1)[a]	0.3133(5)	0.2627(2)	0.2008(7)	4.0(2)
	R1C(2)	0.3865(6)	0.2857(3)	0.3069(5)	5.9(3)
	R1C(3)	0.4683(6)	0.3191(3)	0.3086(7)	6.9(3)
	R1C(4)	0.5069(5)	0.3301(3)	0.2013(9)	7.9(4)
	R1C(5)	0.4636(7)	0.3070(3)	0.0982(7)	8.7(4)
	R1C(6)	0.3818(7)	0.2734(3)	0.0965(5)	6.5(3)
Ring-2					
	R2C(1)	0.2511(4)	0.0127(2)	0.2196(6)	3.8(2)
	R2C(2)	0.2162(6)	-0.0027(3)	0.1031(5)	5.4(3)
	R2C(3)	0.1273(6)	-0.0327(3)	0.0773(5)	7.2(3)
	R2C(4)	0.0733(5)	-0.0471(3)	0.1679(8)	6.8(3)
	R2C(5)	0.1082(6)	-0.0316(3)	0.2843(7)	6.5(3)
	R2C(6)	0.1970(6)	-0.0017(3)	0.3102(5)	5.0(2)
Car-1					
	1C(1)	0.1553(9)	0.1163(6)	0.2583(10)	
	1N(1)	0.1323(8)	0.1120(4)	0.3617(9)	
	1C(2)	0.2088(13)	0.1246(9)	0.4697(11)	B(group) = 5.2(3)
	1C(3)	0.0282(9)	0.0943(7)	0.3882(12)	
	1C(4)	0.0703(15)	0.1023(10)	0.1531(9)	
Car-2					
	2C(1)	0.1796(11)	0.1229(7)	0.3289(15)	
	2N(1)	0.0894(10)	0.1067(6)	0.2823(11)	
	2C(2)	0.061(2)	0.0984(13)	0.1526(12)	B(group) = 4.8(4)
	2C(3)	0.0021(12)	0.0943(10)	0.349(2)	
	2C(4)	0.200(2)	0.1302(13)	0.464(2)	
1-F6					
	1F(1)	-0.2582(5)	0.2373(3)	0.2806(6)	12.7(3)
	1F(2)	-0.0894(5)	0.2157(3)	0.1140(6)	14.0(3)
	1F(3)	-0.2424(6)	0.2566(3)	0.0937(6)	15.9(4)
	1F(4)	-0.1051(6)	0.1963(3)	0.3009(6)	15.4(4)
	1F(5)	-0.2359(6)	0.1785(2)	0.1510(7)	16.0(4)
	1F(6)	-0.1116(5)	0.2745(2)	0.2135(7)	13.3(3)
21-F6					
	21F(1)	0.3266(7)	0.0345(5)	-0.3419(10)	
	21F(2)	0.1490(8)	-0.0006(4)	-0.1987(10)	
	21F(3)	0.1598(8)	0.0080(4)	-0.3914(8)	B(group) = 10.4(3)
	21F(4)	0.3157(8)	0.0260(4)	-0.1492(8)	
	21F(5)	0.1961(8)	0.0712(3)	-0.2673(12)	
	21F(6)	0.2795(8)	-0.0372(3)	-0.2734(12)	
22-F6					
	22F(1)	0.3017(10)	0.0695(5)	-0.3006(13)	
	22F(2)	0.1728(12)	-0.0211(4)	-0.2291(13)	
	22F(3)	0.2880(10)	-0.0090(6)	-0.3539(12)	B(group) = 10.4(4)
	22F(4)	0.1865(11)	0.0575(5)	-0.1761(12)	
	22F(5)	0.1426(9)	0.0372(6)	-0.3681(11)	
	22F(6)	0.3320(10)	0.0112(5)	-0.1619(11)	

[a] Ring C atoms are numbered sequentially. R1C(1) is bonded to P(1).

TABLE 7.7

Derived Hydrogen Atom Positional and Thermal Parameters

Atom	x	y	z	B(Å²)[a]
H1C(11)	0.2018	0.2311	0.3887	6.81
H2C(11)	0.1512	0.2739	0.2964	6.81
H3C(11)	0.0936	0.2205	0.2935	6.81
H1C(12)	0.1315	0.2602	0.0501	6.94
H2C(12)	0.1939	0.2153	-0.0067	6.94
H3C(12)	0.0912	0.2043	0.0574	6.94
H1C(21)	0.3839	0.0469	0.4531	7.17
H2C(21)	0.4471	0.0042	0.3932	7.17
H3C(21)	0.4961	0.0594	0.4094	7.17
H1C(22)	0.4680	0.0036	0.1598	7.13
H2C(22)	0.4149	0.0148	0.0642	7.13
H3C(22)	0.5154	0.0592	0.1670	7.13
H1C(6)	0.3239	0.1722	-0.0942	6.74
H2C(6)	0.3752	0.1175	-0.0907	6.74
H3C(6)	0.2916	0.1314	-0.0019	6.74
H1C(7)	0.5744	0.1460	-0.0131	8.68
H2C(7)	0.5080	0.1925	-0.0773	8.68
H3C(7)	0.5753	0.1980	-0.0573	8.68
H1C(8)	0.5671	0.1031	0.7567	8.07
H2C(8)	0.6869	0.0890	0.7362	8.07
H3C(8)	0.6608	0.1443	0.7770	8.07
H1N(2)	0.5849	0.1802	0.1993	5.39
H11C(2)	0.2274	0.0944	0.5184	6.29
H21C(2)	0.2745	0.1385	0.4457	6.29
H31C(2)	0.1761	0.1492	0.5175	6.29
H11C(3)	-0.0214	0.1226	0.3866	6.29
H21C(3)	-0.0020	0.0697	0.3272	6.29
H31C(3)	0.0393	0.0790	0.4692	6.29
H11C(4)	0.0029	0.1196	0.1603	6.29
H21C(4)	0.0943	0.1119	0.0774	6.29
H31C(4)	0.0586	0.0661	0.1540	6.29
	Phenyl Hydrogen Atoms[b]			
R1H(2)	0.3600	0.2785	0.3781	6.95
R1H(3)	0.4978	0.3350	0.3811	7.97
R1H(4)	0.5628	0.3529	0.2056	8.84
R1H(5)	0.4901	0.3142	0.0271	9.71
R1H(6)	0.3524	0.2576	0.0241	7.50
R2H(2)	0.2532	0.0072	0.0413	6.44
R2H(3)	0.1037	-0.0432	-0.0022	8.23
R2H(4)	0.0129	-0.0676	0.1502	7.74
R2H(5)	0.0715	-0.0416	0.3461	7.51
R2H(6)	0.2209	0.0088	0.3896	6.02
R3H(2)	0.6952	0.1230	0.3496	5.97
R3H(3)	0.7376	0.1017	0.5503	6.88
R3H(5)	0.4673	0.1643	0.6105	5.51
R3H(6)	0.4236	0.1855	0.4133	5.06

[a] The isotropic thermal parameters for the H atoms are 1.0Å² greater than those of the atoms to which they are bonded.

[b] Ring H atoms are numbered sequentially. R1H(2) is bonded to R1C(2), R1H(3) is bonded to R1C(3), etc.

7.4 Description of the Structure

The anion to cation ratio of this compound in the unit cell is two to one, as expected for a dicationic complex with a singly charged anion. The shortest anion-cation separations are 3.12 Å between 1F(4) and 2C(3), and 3.08 Å between 22F(1) and 1C(2). Both anions lie near the disordered carbene ligand, but far enough away that discrete ionic units are maintained. One anion lies well above the plane of the methyl-N,N-dimethylaminocarbene ligand and one lies well below. The carbene ligand and the PF_6 anions are all disordered; furthermore, the refined disorder occupancy factor of the carbene ligand (0.585(18)), and that of the anion for which disorder was taken into account (0.556(14)), are not significantly different. One can therefore speculate that the disorder of the anions is related to that of the carbene ligand.

The disorder of the F atoms about P(4) was refined. Much of the F atom disorder about P(3) is taken up in the large thermal parameters of the F atoms (Table 7.6). A normal PF_6 geometry is observed about P(3) with the mean P-F distance being 1.58(1) Å. The mean F-P-F angle is 178.5(3)° for <u>trans</u> F atoms and 90.0(2)° for <u>cis</u> F atoms. The geometry about P(4) is slightly more distorted. This is indicative of a less than ideal disorder model. The mean P-F separation is 1.58(2) Å and the relevant mean F-P-F angles are 175(2)° and 89(1)°.

An ORTEP diagram of the cation giving the atom

labelling scheme is presented in Fig. 7.3. The inner coordination sphere of the Pt atom and the two orientations of the disordered carbene ligand are shown in Fig. 7.4. A stereoview of the cation is shown in Fig. 7.5. Selected bond distances and angles together with their estimated standard deviations are presented in Table 7.8.

The cation has approximately a square planar geometry. As observed previously (Chapter 7), distortion of this plane occurs at the disordered carbene ligand. A weighted least-squares plane calculated through the atoms Pt, P(1), P(2) and C(5) is shown in Table 7.9. P(2) is furthest from the plane, being 0.045(3) Å below it. Atoms 1C(1) and 2C(1) lie 0.366 Å below and 0.462 Å above this plane respectively. The P(1)-Pt-P(2) angle is 177.8(1)°, whereas the C(5)-Pt-1C(1) and C(5)-Pt-2C(1) angles are 169.4(5)° and 167.6(5)°. The mean C(5)-Pt-P angle is 90.0(3)°. The corresponding mean angle to the disordered C(carbene) atom is 90.0(5)°.

In this complex the dimethylphenylphosphine ligands have a staggered conformation in the solid state, as opposed to the seemingly more favoured eclipsed conformation observed in preceding chapters. A Newman projection down the P-Pt-P axis illustrates the different orientations of the phosphine ligands:

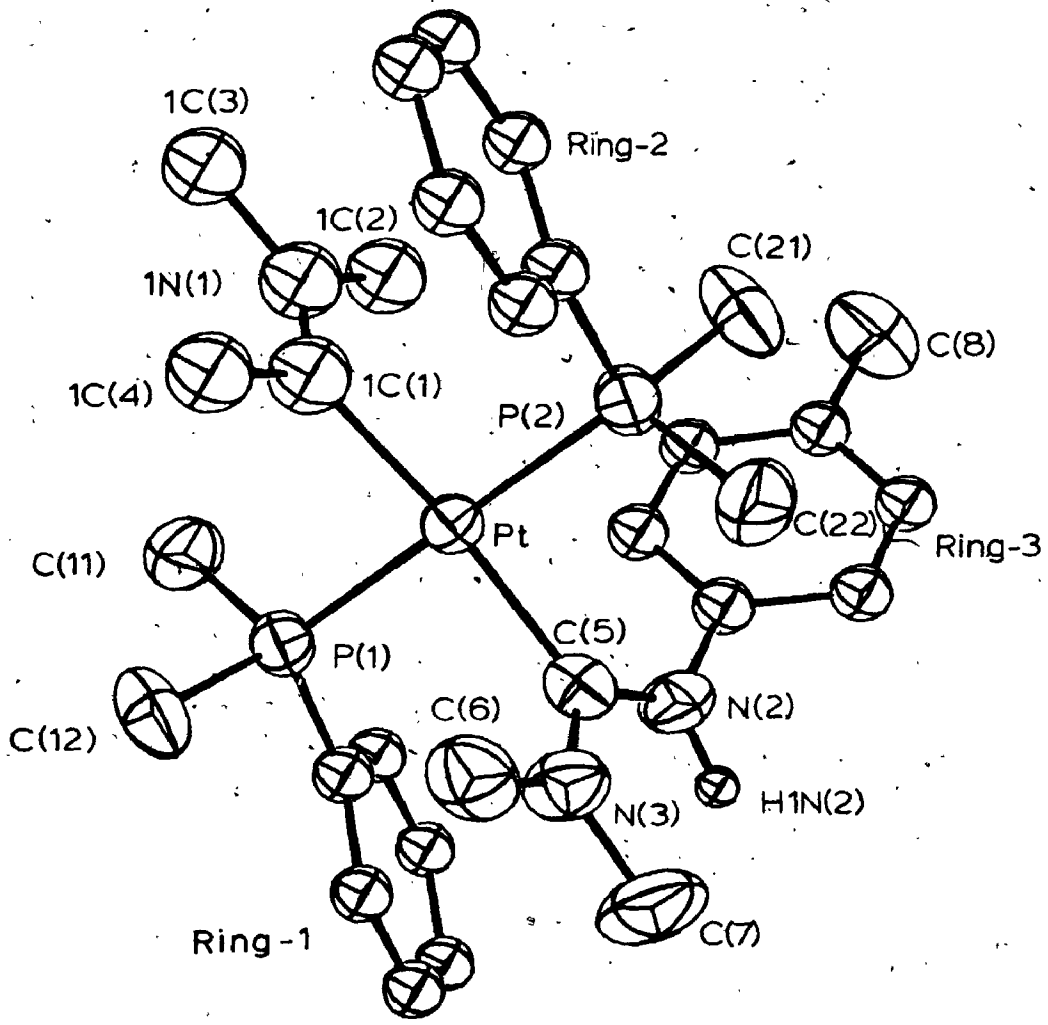

Fig. 7.3

An ORTEP View of the Cation Showing the Atom Numbering Scheme

All Ellipsoids are drawn at the 50% probability level.

In this and other drawings thermal parameters of the phenyl ring C atoms were set at 3.0 $Å^2$ and that of H1N(2) was set at 2.0 $Å^2$ for clarity.

Only one orientation of the disordered carbene ligand is shown.

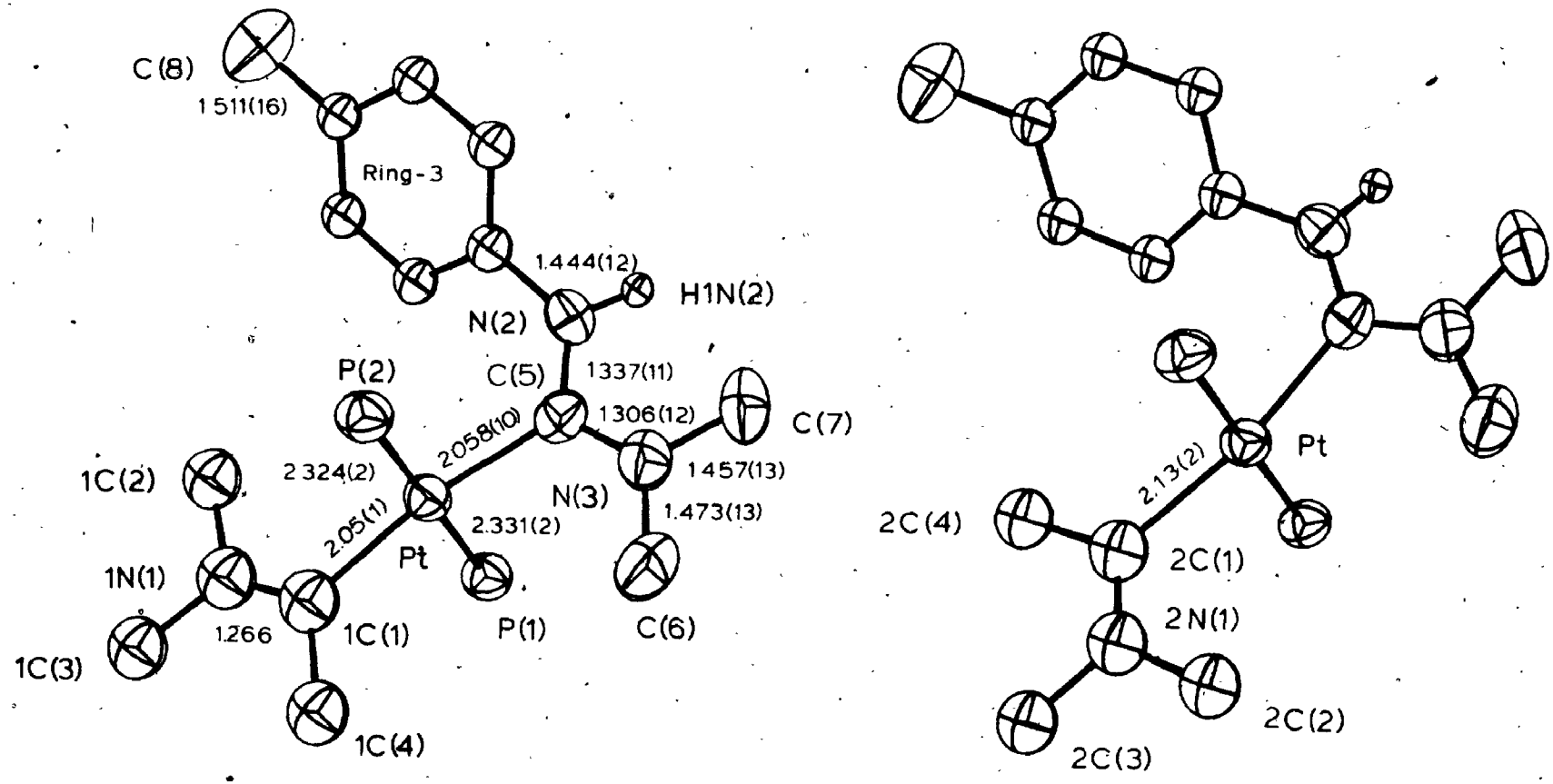

Fig. 7.4

The Carbene Ligands and the Inner Coordination Sphere of the Metal Atom.

The two final orientations of the disordered carbene ligand are shown.

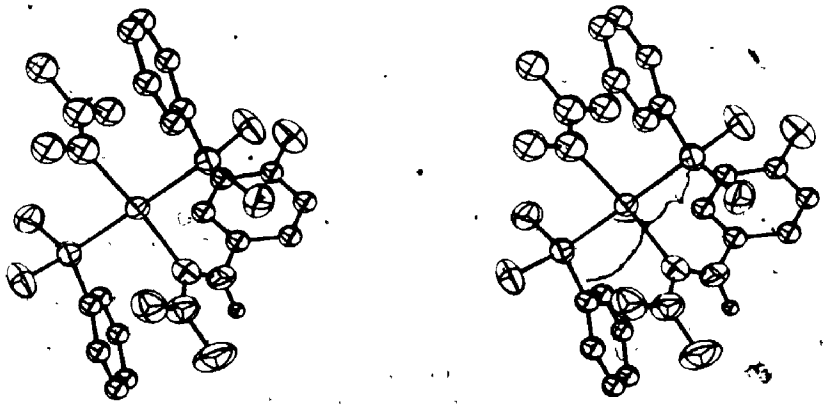

Fig. 7.5

A Stereoview of the Cation

TABLE 7.8

Selected Intramolecular Bond Distances and Angles

Distances(Å)		Angles(deg.)	
Metal Atom Inner Coordination Sphere			
Pt-P(1)	2.331(2)	P(1)-Pt-P(2)	177.8(1)
Pt-P(2)	2.324(2)	1C(1)-Pt-C(5)	169.4(5)
Pt-1C(1)	2.05(2)	2C(1)-Pt-C(5)	167.6(5)
Pt-2C(1)	2.13(2)	1C(1)-Pt-P(1)	89.3(4)
Pt-C(5)	2.058(10)	2C(1)-Pt-P(1)	89.0(4)
		1C(1)-Pt-P(2)	90.3(4)
		2C(1)-Pt-P(2)	91.4(4)
		C(5)-Pt-P(1)	89.7(3)
		C(5)-Pt-P(2)	90.3(3)
Phosphine Ligands			
P(1)-C(11)	1.803(12)	Pt-P(1)-C(11)	114.8(4)
P(1)-C(12)	1.795(11)	Pt-P(1)-C(12)	112.3(4)
P(1)-R1C(1)	1.804(7)	Pt-P(1)-R1C(1)	115.7(3)
P(2)-C(21)	1.794(11)	Pt-P(2)-C(21)	115.3(4)
P(2)-C(22)	1.809(12)	Pt-P(2)-C(22)	113.9(4)
P(2)-R2C(1)	1.806(7)	Pt-P(2)-R2C(1)	112.9(2)
		C(11)-P(1)-C(12)	103.4(5)
		C(11)-P(1)-R1C(1)	104.6(5)
		C(12)-P(1)-R1C(1)	104.8(4)
		C(21)-P(2)-C(22)	103.2(6)
		C(21)-P(2)-R2C(1)	104.7(4)
		C(22)-P(2)-R2C(1)	105.8(5)
Carbene Ligands			
		Pt-1C(1)-1N(1)	123(1)
		Pt-2C(1)-2N(1)	122(1)
		Pt-1C(1)-1C(4)	119(1)
		Pt-2C(1)-2C(4)	120(1)
C(5)-N(2)	1.337(11)	Pt-C(5)-N(2)	122.3(7)
C(5)-N(3)	1.306(12)	Pt-C(5)-N(3)	121.6(8)
N(2)-R3C(1)	1.444(12)	N(2)-C(5)-N(3)	116.0(9)
R3C(1)-R3C(2)	1.384(13)	C(5)-N(2)-R3C(1)	126.5(8)
R3C(2)-R3C(3)	1.373(15)	N(2)-R3C(1)-R3C(2)	117.0(9)
R3C(3)-R3C(4)	1.369(15)	N(2)-R3C(1)-R3C(6)	123.1(9)
R3C(4)-R3C(5)	1.362(13)	R3C(2)-R3C(1)-R3C(6)	120(1)
R3C(5)-R3C(6)	1.363(13)	R3C(3)-R3C(2)-R3C(1)	118(1)
R3C(6)-R3C(1)	1.380(13)	R3C(4)-R3C(3)-R3C(2)	122(1)
R3C(4)-C(8)	1.511(16)	R3C(5)-R3C(4)-R3C(3)	118(1)
N(3)-C(6)	1.473(13)	R3C(6)-R3C(5)-R3C(4)	122(1)
N(3)-C(7)	1.457(13)	R3C(1)-R3C(6)-R3C(5)	119.3(9)
		R3C(3)-R3C(4)-C(8)	120(1)
		R3C(5)-R3C(4)-C(8)	122(1)
		C(5)-N(3)-C(6)	122.5(9)
		C(5)-N(3)-C(7)	123.8(10)
		C(6)-N(3)-C(7)	113.2(9)

TABLE 7.9

Weighted Least-Squares Planes

Atom	Deviation from Plane(Å)
Atoms included: Pt, P(1), P(2), C(5)	
Equation of Plane: 3.80x + 5.77y + 9.89z = 4.18	
Pt	0.0022(4)
P(1)	-0.042(3)
P(2)	-0.045(3)
C(5)	-0.005(10)
1C(1)	-0.366
2C(1)	0.462
Atoms included: C(5), N(2), N(3), C(6), C(7), R3C(1)	
Equation of Plane: 4.42x - 25.60y - 1.56z = -2.20	
C(5)	-0.096(9)
N(2)	-0.052(8)
N(3)	-0.033(9)
C(6)	0.128(11)
C(7)	0.066(15)
R3C(1)	0.110(10)
Atoms included: R3C(1), R3C(2), R3C(3), R3C(4), R3C(5), R3C(6)	
Equation of Plane: 5.70x + 23.95y + 1.28z = 7.36	
R3C(1)	-0.016(10)
R3C(2)	0.003(10)
R3C(3)	0.020(12)
R3C(4)	-0.021(10)
R3C(5)	0.007(10)
R3C(6)	0.011(9)

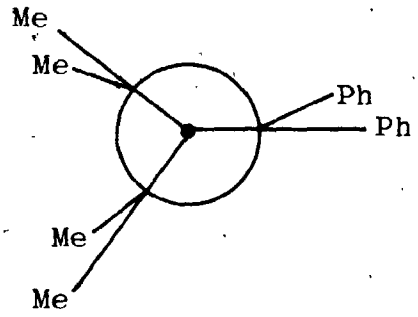

eclipsed

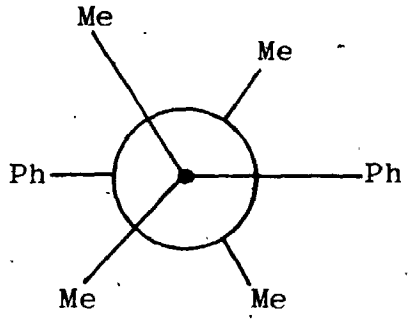

staggered

Although the phosphine ligands of this complex occupy a different orientation with respect to the square plane of the metal atom, the normals to the planes of the phosphine phenyl rings remain at similar angles to the normal to this plane. These angles are 77° and 81° for Ring-1 and Ring-2 respectively. Ring-2 is bent towards the disordered methyl-N,N-dimethylaminocarbene ligand and the P(2)-R2C(1)-R2C(4) angle is 177.3(4)°. This effect is similar to that observed in the previous structural determinations in this thesis. Ring-1 however is bent away from the dimethylamino(p-tolylamino)carbene ligand, and P(1)-R1C(1)-R1C(4) is 174.9(4)°. No further significant distortions occur at the phosphine phenyl rings. The mean P-C-C angle at Ring-1 and Ring-2 is 119.9(5)°. Characteristic distorted tetrahedral geometry is observed about the phosphine P atoms. The mean Pt-P-C angle is 114.2(6)° and the mean C-P-C angle is 104.4(4)°. The

average P-C distance is 1.802(2) Å.

The carbene rigid groups of the disorder model are constrained to be planar. The normal vectors of Car-1 and Car-2 are at angles of 87° and 91° respectively to the normal of the equatorial plane of the metal atom. The carbene disorder corresponds to a 180° rotation about the Pt-C(sp^2) bond, accompanied by a significant shift of C(sp^2) out of the equatorial plane (Table 7.9). The Pt-C(sp^2) distances to 1C(1) and 2C(1) are 2.05(1) Å and 2.13(2) Å respectively, with a mean value of 2.09(4) Å. These values are crystallographically equivalent to the value of 2.079(13) Å observed in trans-$[Pt(MeC{=}NMe_2)Me(PMe_2Ph)_2]PF_6$ (Chapter 2). The mean Pt-C(sp^2)-N(1) and Pt-C(sp^2)-C(4) angles are 122.7(6)° and 119.6(6)° respectively.

The dimethylamino(p-tolylamino)carbene ligand also lies approximately perpendicular to the equatorial plane of the complex. The angle of intersection of the normals to the two planes is 100°. A weighted least-squares plane calculated through the atoms N(2), N(3), C(5), C(6), C(7), and R3C(1) is shown in Table 7.9. Atom C(6) associated with the dimethylamino substituent is farthest from the plane, being 0.128(11) Å above it. A trans geometry of the p-tolyl group with respect to the dimethylamino entity is observed:

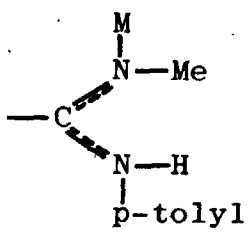

trans

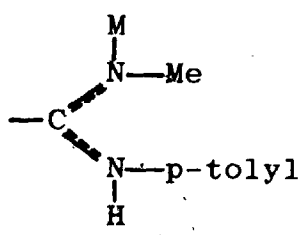

cis

The Pt-C(sp^2) distance is 2.058(10) Å. This is equivalent to the value of 2.06(1) Å obtained in the structure determination of the dicarbene complex trans-[Pt{C(NHMe)SEt}$_2$(C≡NMe)$_2$](PF$_6$)$_2$ (72). The angles about C(5) are indicative of sp^2 hybridization. The mean Pt-C(5)-N angle is 121.9(3)° and the N(2)-C(5)-N(3) angle is 116.0(9)°. N(2) and N(3) donate electron density to stabilize the C(sp^2) atom. The distances C(5)-N(2) of 1.337(11) Å and C(5)-N(3) of 1.306(12) exhibit a bond order considerably greater than one, since a C-N single bond is expected to be 1.47(1) Å long (88). The C(sp^2)-N distance in trans-[Pt{C(NHMe)SEt}$_2$(C≡NMe)$_2$]-(PF$_6$)$_2$ is 1.300(10) Å (72). The sp^2 character of the N atoms is indicated by the angles about N(2) and N(3). The mean C(5)-N(3)-C(sp^3) angle is 123.1(6)° and the C(5)-N(2)-R3C(1) angle is 126.5(8)°. The C(6)-N(3)-C(7) angle is 113.2(9)° compared to 113(1)° observed in the methyl-N,N-dimethylaminocarbene ligand of the complex examined in Chapter 2. The mean N(3)-C(methyl) separation is 1.465(8) Å, and the N(2)-R3C(1) distance is 1.444(12) Å.

No major distortion from ideal phenyl ring geometry is observed in Ring-3. The mean C-C distance is 1.372(4) Å and the mean C-C-C angle is 119.8(7)°. None of the C atoms deviate significantly from a least-squares plane calculated through the phenyl ring (Table 7.9). The plane of the phenyl ring intersects that of the carbene ligand at 47.2°. The p-tolyl C(methyl) lies 1.511(16) Å from R3C(4).

7.5 Discussion

As was observed in an earlier section (Chapter 2), large variations in phosphine ligand orientations can occur between related complexes in the systems under study. Addition of dimethylamine to the isocyanide complex examined in Chapter 6 to give the dicarbene species causes changes in the orientation of the dimethylphenylphosphine ligands in the solid state. The eclipsed conformation gives way to a staggered one. This may result from the steric effects of the bulky dimethylamino(p-tolylamino)-carbene ligand. In the structures examined in previous chapters, the phosphine phenyl rings are bent slightly inward (by approximately 3° with respect to the P-C(1)-C(4) angle), possibly as a result of packing forces.

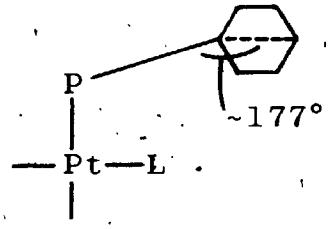

Ring-1, nearest the bulky carbene ligand, is bent slightly outward (~4°). The steric effects of the carbene ligand appear to be larger than those causing the phenyl rings to bend inward.

Disorder of the methyl-N,N-dimethylaminocarbene ligand limits the extent of comparison of the two different carbene ligands in this complex.

The mean Pt-1C(1) and Pt-2C(1) distance to the methyl-N,N-dimethylaminocarbene ligand is 2.09(4) Å. This distance

is equivalent to that of 2.079(13) Å observed in Chapter 2 where the same carbene ligand lies trans to methyl. But the carbene ligand is disordered, and as was described in Chapter 6, a consequence of this may be an unreliable Pt-C(sp^2) bond length. Indeed, the Pt-1C(1) and Pt-2C(1) distances differ by 3.6σ. This implies that the calculated standard deviations on bond lengths and angles to the disordered carbene ligand are underestimated.

The C(sp^2)-N distances of the dimethylamino(p-tolylamino)carbene ligand differ by 1.9σ and are not significantly different, though the trend is that which might be expected. Dimethylamine (pKa = 10.73) is a far stronger base than p-toluidine (pKa = 5.08) (134). In the Lewis sense dimethylamine is a much better electron donor than p-toluidine. A dimethylamino-substituent should stabilize the C(sp^2) atom to a greater extent and thus a shorter C(sp^2)-N distance should be observed. The dimethylamino-(p-tolylamino)carbene ligand can readily be compared to the methyl-N,N-dimethylaminocarbene ligand in the complex trans-[Pt(MeC$\equiv\equiv$NMe$_2$)Me(PMe$_2$Ph)$_2$]PF$_6$ (Chapter 2). The C(sp^2)-N separation observed in Chapter 2 is 1.266(15) Å. This bond length is significantly shorter than the C(sp^2)-N(p-tolylamino) bond distance (3.9σ); whereas it is shorter than the C(sp^2)-N(dimethylamino) bond by only 2.1σ. These differences indicate that although the p-tolylamino group does contribute considerable electron density to the C(carbene)-N bond, the contribution is significantly less

than that of the dimethylamino-group in the complex examined in Chapter 2. This is due partially to the lower nucleophilicity of the p-tolylamino substituent and also due to the presence of a second such group stabilizing the $C(sp^2)$ atom, especially when that second substituent is a such better electron donor. Similar conclusions have been made with respect to the $C(sp^2)$-O and $C(sp^2)$-N bond lengths of 1.346(5) Å and 1.328(5) Å respectively in $Cr\{C(NMe_2)OEt\}(CO)_5$ (53). The $C(sp^2)$-N distance observed in Chapter 2 is also significantly shorter (3.4σ) than that of 1.35(2) in the carbene ligand of the complex trans-$[Au\{C(NH\text{-}p\text{-}C_6H_4Me)_2\}_2I_2]ClO_4$ (135), where two p-tolylamino-groups stabilize the $C(sp^2)$ atom.

Although the use of valence bond theory to describe the bonding in the carbene ligands imposes constraints which may be avoided by use of MO theory, it is informative to study resonance structures from which overall impressions of the bonding trends can be readily interpreted when structural and spectral data are considered. Several resonance forms can be drawn for this type of tertiary carbene ligand:

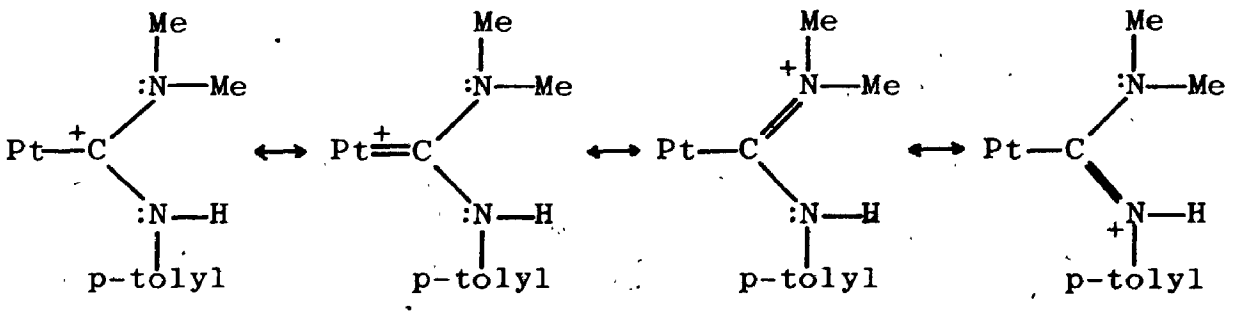

I II III IV

As observed in Chapter 2, and present results bear this out, metal π bonding is small in the presence of a carbene ligand containing a dimethylamino-substituent. The structural data indicate that the resonance forms III and IV contribute most to the observed structure. The contribution of III is probably greater than that of IV.

Thus the results indicate that the carbene ligands in groups 3a and 3b are similar with respect to their mode of bonding to the metal atom. In both types of ligands the bulk of the stabilization of C(carbene) comes from the amino-substituents with the extent of electron donation appearing to be dependent on both the nucleophilicity and the number of these groups present.

CHAPTER 8

GENERAL DISCUSSION AND CONCLUSIONS

Thus far, the discussions of the results have been limited in scope to individual structures. In this chapter an overview of the results is presented, and some trends and data, not yet brought to light, are examined.

In Fig. 8.1 is presented the reaction scheme for the preparation of bis-carbene complexes such as that discussed in Chapter 7. X-ray structural studies have been completed on examples of most of the complexes in this reaction sequence. The structure of a complex similar to II, trans-[Pt(MeC≡CMe)-Me(PMe_2Ph)$_2$]PF_6, has been determined (93). Although the acetylenic compounds are believed to be intermediates in carbene synthesis, carbene formation is inhibited when the acetylene is RC≡CR(R≠H), and complexes closely related to II can be isolated. The compounds III-VII all contain carbene ligands, and structure determinations of examples of all five types of complexes have been described in this thesis. The complexes are all cationic with square planar coordination geometry and have mutually trans dimethylphenylphosphine ligands.

Although some disorder problems were encountered, the structural data provide valuable bonding information.

Fig. 8.1

Synthesis of Bis-carbene Complexes of Pt(II)

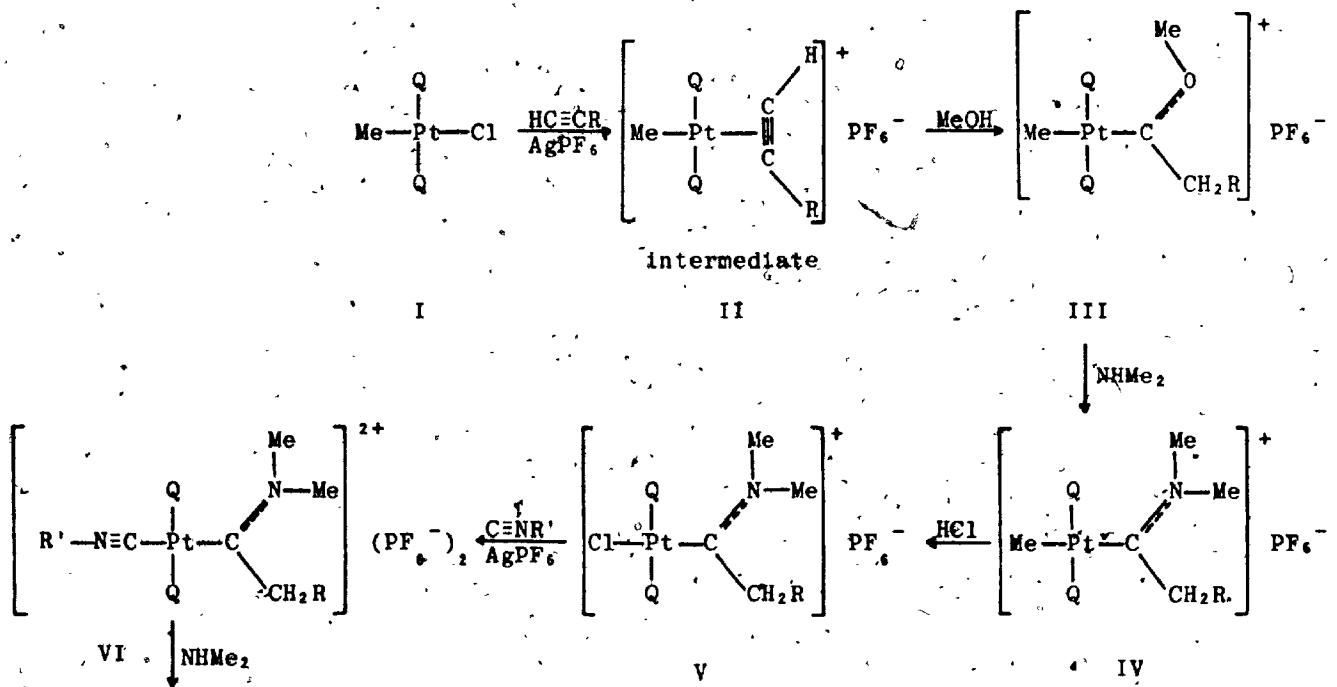

I II III IV V VI VII

Q = PMe_2Ph; R = alkyl, aryl; R' = p-tolyl

8.1 The Carbene Ligands

The most interesting and widely discussed aspects of bonding in carbene ligands are those related to π bonding about C(carbene).

Both pπ-pπ bonding with the nucleophilic substituents, and dπ-pπ backbonding from the metal atom are possible. To what extent do each of these interactions occur?

i. The C(carbene)-Heteroatom Bond

Virtually all crystallographic data on carbene ligands belonging to groups 3a, 3b and 2a (Fig. 1.1) show that a large portion of the stabilization of C(carbene) comes from the heteroatoms (O, N, S etc.) as pπ-pπ bonding. A summary of $C(sp^2)$-heteroatom bond lengths for Pt(II) and Cr(0) carbene complexes is presented in Table 8.1, together with data recently accumulated for secondary (2a) carbene ligands.

The accepted value for a C-N single bond is 1.47(1) Å and that for a triple bond is 1.16(1) Å. A C-O single bond is 1.43(1) Å long while a double bond is 1.23(1) Å in length (88). The C-X (X=O, N) bond lengths in Table 8.1 range from 1.26(2) to 1.37(2) Å. Thus it is readily apparent that these bonds have a bond order greater than 1.

Closer examination of the data reveals another interesting trend related to the different types of carbene ligands. Those belonging to group 3a have two nucleophilic substituents bonded to C(carbene) whereas those of groups 3b and 2a (Fig. 1.1) have only one such electron rich substituent.

TABLE 8.1

$C(sp^2)$ - Heteroatom Bond Lengths in Carbene Ligands

Complex	C=X(Å)	Metal Atom	Heteroatomic Substituent(X)	Carbene Type (Fig. 1.1)	Reference
trans-$[Pt(MeC{=}NMe_2)Me(PMe_2Ph)_2]PF_6$	1.266(15)	Pt(II)	NMe_2	3b	Chapter 2
trans-$[Pt(CH_2C{=}OCH_2CH_2)Me(PMe_2Ph)_2]PF_6$	1.26(2)	Pt(II)	OCH_2CH_2-	3b	Chapter 3
trans-$[Pt\{HO(CH_2)_3C{=}NMe_2\}Cl(PMe_2Ph)_2]PF_6$	1.293(16)	Pt(II)	NMe_2	3b	Chapter 4
trans-$[Pt\{C(NMe_2)NH\text{-}p\text{-}C_6H_4Me\}(MeC{=}NMe_2)(PMe_2Ph)_2](PF_6)_2$	1.306(12)	Pt(II)	NMe_2	3a	Chapter 7
	1.337(11)		NH-p-C_6H_4Me		
cis-$Pt\{C(NPhCH_2)_2\}Cl_2PEt_3$	1.327(11)	Pt(II)	$NPhCH_2$	3a	71
	1.327(11)		$NPhCH_2$		
trans-$Pt\{C(NPhCH_2)_2\}Cl_2PEt_3$	1.37(2)	Pt(II)	$NPhCH_2$	3a	71
	1.33(2)		$NPhCH_2$		
cis-$Pt\{C(OEt)NHPh\}Cl_2PEt_3$	1.33(2)	Pt(II)	OEt	3a	69
	1.33(3)		NHPh		
trans-$[Pt\{C(NHMe)SEt\}_2(C{\equiv}NMe)_2](PF_6)_2$	1.300(10)	Pt(II)	NHMe	3a	72
	1.681(8)		SEt		
$[Pt\{MeNHCNN(Me)CNHMe\}(C{\equiv}NMe)_2](BPh_4)$	1.43(2)	Pt(II)	NHMe	3a	34
	1.36(3)		N(Me)NCNHMe		
$RuI_2\{HC{=}N(Me)\text{-}p\text{-}C_6H_4Me\}CO(C{\equiv}N\text{-}p\text{-}C_6H_4Me)(PPh_3)$	1.28	Ru(II)	N(Me)-p-C_6H_4Me	2a	21
$RhCl_3(HC{=}NMe_2)(PEt_3)_2$	1.289(14)	Rh(III)	NMe_2	2a	20
$Cr(PhC{=}OMe)(CO)_5$	1.33(2)	Cr(0)	OMe	3b	47
$Cr(MeC{=}OMe)(CO)_5$	1.32(2)	Cr(0)	OMe	3b	48
$Cr(MeC{=}NHMe)(CO)_5$	1.33	Cr(0)	NHMe	3b	49
$Cr(MeC{=}NEt_2)(CO)_5$	1.31(1)	Cr(0)	NEt_2	3b	50
$Cr\{(MeOC\text{-}CH_2)C{=}NHC_6H_{11}\}(CO)_5$	1.32(2)	Cr(0)	NHC_6H_{11}	3b	51
$Cr\{(PhC{\equiv}C)C{=}OEt\}(CO)_5$	1.32(2)	Cr(0)	OEt	3b	54
$Cr\{C(OEt)NMe_2\}(CO)_5$	1.346(5)	Cr(0)	OEt	3a	53
	1.328(5)		NMe_2		

Assuming that the net stabilization of the C(carbene) atom in all three types of carbene ligands is similar, the nucleophilic substituent in a carbene ligand of group 3b or 2a must contribute more electron density to C(carbene) than either substituent in a carbene ligand belonging to group 3a. The structural data for carbene complexes of Pt(II) are in agreement with this supposition (Table 8.1). Thus the C-X bond lengths for ligands of group 2a or 3b are consistently shorter than 1.30 Å, whereas those for carbene ligands of group 3a are consistently longer than 1.30 Å. Large estimated standard deviations on some of the bond lengths are present, resulting in C-X bond lengths that are not always significantly different from 1.30 Å, but the aforementioned trend is clearly present for the carbene complexes of Pt(II).

Many of the Cr(0) complexes in Table 8.1 contain carbene ligands belonging to group 3b, and these have C-X bond distances unexpectedly greater than 1.30 Å. This suggests that the nucleophilic substituents stabilize C(carbene) to a smaller extent in Cr(0) complexes than in those of Pt(II), and that the role of the metal atom in π bonding to C(carbene) is more important in complexes where the metal atom has a lower formal oxidation state.

ii. The Platinum-C(carbene) Bond

Metal-ligand bond length data for square planar complexes of Pt(II) containing carbonyl, isocyanide and carbene ligands

are presented in Table 8.2. These ligands are all capable of π bonding with the metal atom. Some values for Pt-C(sp^2) bonds expected to be purely σ in character are also given. The bond lengths can be examined for the extent of Pt-C π bonding in complexes containing the different types of ligands. Since the hybridization of the C atom is essentially sp in carbonyl and isocyanide ligands, and sp^2 in carbene ligands, comparison of the bond lengths is difficult. An effective covalent radius of Pt(II) can be calculated by subtracting the covalent radii of C(sp^2) (0.73 Å) and C(sp) (0.71 Å) (94) from the bond lengths. These 'effective radii' should all be approximately equal if the Pt-C bonds are unaffected by π bonding or other effects such as <u>trans</u> influence. Moreover, the values should approach that of the covalent radius of Pt(II) (1.31 Å) (94). The calculated radii of Pt(II) are presented in Table 8.2. For the carbonyl complexes these values vary from 1.07 to 1.15 Å, and those for the isocyanide compounds range from 1.12 to 1.26 Å. Where carbene ligands are present the values are 1.22 Å to 1.36 Å. The mean values for the three types of ligands are in the order carbonyl < isocyanide < carbene. The average radii where carbonyl and isocyanide ligands are present are 1.12(2) Å and 1.21(2) Å respectively. These are considerably smaller than the accepted covalent radius of Pt(II). The average effective radius for the carbene complexes is 1.30(2) Å. This is equivalent to the accepted covalent radius and to the value of 1.293(7) Å calculated for complexes containing purely σ Pt-C(sp^2) bonds.

TABLE 8.2

Metal-Carbon Bond Length Data for Carbonyl, Isocyanide and Carbene Complexes of Pt(II)

Complex	Pt-C(Å)	Effective Radius of Pt(Å)[a]	Trans Ligand	Reference
Carbonyl				
trans-$Pt(CO)Cl(PEt_3)_2$	1.78	1.07	Cl^-	136
$[(n\text{-}Bu)_4N][Cl_3(CO)Pt]$	1.82(1)	1.11	Cl^-	137
cis-$Pt(CO)Cl_2(PPh_3)$	1.858(7)	1.15	PPh_3	104
Mean Values[b]	1.82(2)	1.11(2)		
Sum of Covalent Radii	2.02			
Isocyanide				
cis-$Pt(C{\equiv}NEt)Cl_2(PEt_2Ph)$	1.83(4)	1.12	Cl^-	131
cis-$Pt(C{\equiv}NPh)_2Cl_2$	1.880(18) 1.91(2)	1.17 1.20	Cl^-	132
$[Pt(C{\equiv}NMe)_2\{MeNHCNN(Me)CNHMe\}](BPh_4)$	1.95(3) 1.97(3)	1.24 1.26	MeNHCNN(Me)CNHMe	34
trans-$[Pt(C{\equiv}N\text{-}p\text{-}C_6H_4Me)(MeC{=}NMe_2)(PMe_2Ph)_2](PF_6)_2$	1.958(13)	1.25	$MeC{=}NMe_2$	Chapter 6
trans-$[Pt(C{\equiv}NMe)_2\{C(NHMe)SEt\}_2](PF_6)_2$	1.968(9)	1.26	$C{\equiv}NMe$	72
Mean Values	1.92(2)	1.21(2)		
Sum of Covalent Radii	2.02			
Carbene				
$[Pt\{MeNHCNN(Me)CNHMe\}(C{\equiv}NMe)_2](BPh_4)$	1.95(2)	1.22	$C{\equiv}NMe$	34
cis-$Pt\{C(OEt)NHPh\}Cl_2PEt_3$	1.962(18)	1.23	Cl^-	69
trans-$[Pt\{HO(CH_2)_3C{=}NMe_2\}Cl(PMe_2Ph)_2]PF_6$	1.978(12)	1.25	Cl^-	Chapter 4
trans-$[Pt(CH_2C{=}OCH_2CH_2)Me(PMe_2Ph)_2]PF_6$	2.00(2)	1.27	Me	Chapter 3
cis-$Pt\{C(NPhCH_2)_2\}Cl_2PEt_3$	2.009(13)	1.28	Cl^-	71
trans-$Pt\{C(NPhCH_2)_2\}Cl_2PEt_3$	2.020(16)	1.29	PEt_3	71
trans-$[Pt\{C(NMe)SEt\}_2(C{\equiv}NMe)_2](PF_6)_2$	2.058(7)	1.33	C(NHMe)SEt	72
trans-$[Pt\{C(NMe_2)NH\text{-}p\text{-}C_6H_4Me\}(MeC{=}NMe_2)(PMe_2Ph)_2](PF_6)_2$	2.058(10)	1.33	$MeC{=}NMe_2$	Chapter 7
trans-$[Pt(MeC{=}NMe_2)Me(PMe_2Ph)_2]PF_6$	2.079(13)	1.35	Me	Chapter 2
trans-$[Pt(MeC{=}NMe_2)(C{\equiv}N\text{-}p\text{-}C_6H_4Me)(PMe_2Ph)_2](PF_6)_2$	2.085(5)[c]	1.36	$C{\equiv}N\text{-}p\text{-}C_6H_4Me$	Chapter 6
trans-$[Pt(MeC{=}NMe_2)\{C(NMe_2)NH\text{-}p\text{-}C_6H_4Me\}(PMe_2Ph)_2](PF_6)_2$	2.09(4)[c]	1.36	$C(NMe_2)NH\text{-}p\text{-}C_6H_4Me$	Chapter 7
Mean Values	2.03(2)	1.30(2)		
Sum of Covalent Radii	2.04			
Complexes with purely σ Pt-C(sp^2) bonds				
$Pt(o\text{-}Ph_2PC_6H_4C{=}CHC_6H_4PPh_2\text{-}o)Cl_2$	2.01(1)	1.28	Cl^-	101
trans-$Pt(MeC{=}N\text{-}p\text{-}C_6H_4Cl)I(PEt_3)_2$	2.09(11)	1.30	I^-	96
trans-$Pt(CH{=}CH_2)Cl(PEt_3)_2$	2.03(2)[c]	1.30	Cl^-	133
Mean Values	2.023(7)	1.293(7)		

a. Effective radius is calculated by subtracting covalent radius of C from the metal-ligand bond length. Radius of C(sp^2) used is 0.73Å and that for C(sp) is 0.71Å.

b. Estimated standard deviations on mean values here and in other tables are calculated from the expression given in Appendix II.

c. Mean bond length for disordered carbene ligand.

Although the radii may be affected by structural *trans* influence effects, the same trends are observed if only the complexes with Cl^- lying opposite the ligands in question are considered. We therefore conclude that little $d\pi$-$p\pi$ back-bonding from Pt(II) to the carbene ligands occurs in these complexes. These crystallographic results are in agreement with those obtained from ESCA experiments on Pt(II) carbene and isocyanide complexes (105).

In contrast, structural and ESCA data for Cr(0) carbene complexes indicate a greater role for the metal atom in π bonding to C(carbene) (7, 44).

As noted above, a structural *trans* influence can significantly affect metal-ligand bond lengths in square planar complexes of Pt(II). The effects of *trans* influence on Pt-C(sp^2) bond lengths are now examined.

8.2 Structural Trans Influence and the Pt-C(sp^2) Bond

The trans influence of ligands has been discussed in previous chapters. Relatively little has been said about the effect on the Pt-C(sp^2) bond of having ligands of varying trans influence occupying the opposite coordination site. From Table 8.2 it is apparent that Pt-C(sp^2) bond lengths range from 1.95(2) Å to 2.09(4) Å. In general when C(sp^2) is trans to a halide ligand, the shortest bond distances are observed (2.03 Å or less). These values are less than the sum of the covalent radii (2.04 Å). Bond lengths greater than 2.04 Å are generally observed when strong trans influence ligands such as methyl or carbene are trans to C(sp^2).

Three striking anomalies to these trends are observed in Table 8.2. Two of these arise from structural data obtained in this study. The complex trans-[Pt($\overline{CH_2C{=}{=}OCH_2CH_2}$)Me-$(PMe_2Ph)_2$]$PF_6$ (Chapter 3) has a Pt-C(sp^2) bond of only 2.00(2) Å when the carbene ligand lies trans to methyl. The short distance is thought to be a result of a slight increase in π back donation from the metal atom in the presence of an alkoxycarbene ligand (Chapter 3). Secondly, in the complex trans-[Pt($MeC{=}{=}NMe_2$)(C≡N-p-tolyl)$(PMe_2Ph)_2$]$(PF_6)_2$ (Chapter 6), the Pt-C(sp^2) bond is 2.085(5) Å in length, a value much larger than might be expected with isocyanide in the trans coordination site. The carbene ligand in this complex is disordered. A less than perfect disorder model could result in a longer Pt-C(sp^2) bond than expected. Also, as described in Chapter 6, the disordered carbene ligand may be influenced

by packing forces, resulting in a large deviation in $C(sp^2)$ from the square plane of the metal atom. Such effects could also cause a longer $Pt-C(sp^2)$ bond than would normally be observed. A similar disorder occurs in Chapter 7, where a very long $Pt-C(sp^2)$ bond length is also observed, but here the carbene ligand lies trans to a second carbene ligand. Since carbene exerts strong trans influence, a longer $Pt-C(sp^2)$ bond is expected.

The third complex which does not conform to the observed trend is trans-$Pt\{C(NPhCH_2)_2\}Cl_2PEt_3$ (71) where the $Pt-C(sp^2)$ bond is 2.020(16) Å. The phosphine ligand opposite is expected to have a strong trans influence. No explanation is given by the authors for the short $Pt-C(sp^2)$ separation observed, nor is any apparent to us.

Crystallographic results do not permit formulation of a detailed trans influence series because bond length differences are often too small to be significant with respect to the estimated standard deviations obtained. This problem occurs even when heavier atoms such as Cl are involved, and becomes more serious for smaller atoms such as C. Thus from Table 8.2 one can only predict that Cl^-, I^-, and possibly C≡NMe are ligands of very weak structural trans influence, while methyl and carbene are much stronger trans influence ligands.

8.3 The Dimethylphenylphosphine Ligands

Discussion of the dimethylphenylphosphine ligands common to all five structural studies of this work has till now been limited to the relative configuration of the ligands in the different complexes. The geometry and coordination of these ligands will now be examined more closely.

Three other structural determinations have been performed on square planar Pt(II) complexes where dimethylphenylphosphine ligands occupy mutually trans coordination sites. A summary of the mean bond length and bond angle data for this phosphine ligand in the various complexes is presented in Table 8.3. The internal geometry of the ligands is similar for all complexes. The overall mean P-C bond length is 1.810(5) Å, and the average bond angles are 114.2(2)° and 104.6(3)° for the Pt-P-C and C-P-C angles respectively. As has been observed with other complexes containing phosphine ligands, as well as in triphenylphosphine itself (138), the geometry is distorted tetrahedral. The three organic groups tend to bend towards each other by 4.9(3)°. This has been previously interpreted to mean that the P-C bonds have a p character greater than sp^3 (139).

The mean Pt-P bond lengths range from 2.293(3) Å to 2.336(1) Å. These distances are considerably shorter than the value of 2.41 Å predicted from the sum of the covalent radii (94). This may be a result of π backbonding from the metal atom into the vacant 3d orbitals of the P atom. The Pt-P distance in the neutral complex is 2.293(3) Å, and the

TABLE 8.3[a]

Mean Dimethylphenylphosphine Geometries in Square Planar Complexes of Pt(II)

Complex	Pt-P distance(Å)	P-C distance(Å)	Pt-P-C angle(deg)	C-P-C angle(deg)	Reference
trans-$PtCl(CH_2SiMe_3)(PMe_2Ph)_2$	2.293(3)	1.84(1)	115(2)	103.3(9)	95
trans-$[PtMe(MeC{\equiv}CMe)(PMe_2Ph)_2]PF_6$	2.303(3)	1.80(1)	114(1)	105(1)	93
trans-$[PtMe(MeO{-}CMe)(PMe_2Ph)_2]PF_6$	2.283(3)	1.796(3)	114.4(9)	104(2)	92
trans-$[PtMe(MeO{-}NMe_2)(PMe_2Ph)_2]PF_6$	2.294(3)	1.812(6)	114.4(7)	104.1(5)	Chapter 2
trans-$[PtMe(\overline{CH_2C{-}O{-}CH_2CH_2})(PMe_2Ph)_2]PF_6$	2.305(5)	1.820(6)	114(2)	104.2(6)	Chapter 3
trans-$[PtCl\{HO(CH_2)_3C{=}NMe_2\}(PMe_2Ph)_2]PF_6$	2.312(4)	1.813(8)	112.8(8)	106.5(7)	Chapter 4
trans-$[Pt(MeO{-}NMe_2)(C{\equiv}N\text{-}p\text{-}C_6H_4Me)(PMe_2Ph)_2](PF_6)_2$	2.336(1)	1.800(6)	113.4(9)	105.2(3)	Chapter 6
trans-$[Pt(MeO{-}NMe_2)\{C(NMe_2)NH\text{-}p\text{-}C_6H_4Me\}(PMe_2Ph)_2](PF_6)_2$	2.328(3)	1.802(2)	114.2(6)	104.4(4)	Chapter 7
Mean Values		1.810(5)	114.2(2)	104.6(3)	

[a]All values given are averaged over the two phosphine ligands in each complex.

mean value for the mono-cationic complexes is not significantly longer 2.299(5) Å. The average bond length for the dicationic compounds is 2.332(4) Å, longer by 5.5σ and 7.8σ than those for the mono-cationic and neutral complexes respectively. This could mean that significantly less electron density is available for π backbonding from the metal atoms in the dicationic complexes.

Phosphine ligands are described as being capable of exerting a strong trans influence (67). The shortest Pt-P bond length for trans dimethylphenylphosphine ligands is 2.283(3) Å. This can be compared with a value of 2.244(8) Å obtained for the similar diethylphenylphosphine in cis-$Pt(PEt_2Ph)Cl_2(C{\equiv}NEt)$ (131) where the phosphine ligand lies opposite Cl^-. The bond distance from Table 8.3 is longer by 4.3σ. The difference may be due to the strong trans influence of the phosphine ligands in the complexes of Table 8.3.

The steric properties of phosphine ligands have become the foci of a large amount of research. There has been great interest in how the steric bulk of a ligand can affect the rate and final outcome of a chemical reaction. Since a large number of phosphine, and other phosphorus ligands of varying size are readily available, much of the research has been centered on these ligands.

i. Phosphine Ligand Cone Angles

Tolman first used molecular models to measure cone angles

for phosphorus ligands, and these have been correlated with equilibrium data for Ni complexes (140, 141). The cone angle of a phosphorus ligand has been defined as the angle at the apex of a cone just large enough to enclose the Van der Waals radii of the outermost atoms of the ligand. Marzilli and Trogler recently utilized NMR chemical shift data from cobaloxime complexes containing phosphorus ligands to calculate similar cone angles (142).

Present models assume that phosphorus ligands are conically symmetric and encompass the total volume of the cone. The values obtained give a good approximation of the relative bulk of one phosphorus ligand compared to another. Unfortunately the cone angles are a poor representation of the actual shape and size of the individual ligands. Many phosphine complexes have been prepared and found to be stable where an examination of the cone angles would lead one to predict that the compound should be very unstable or even impossible to synthesize. The most outstanding examples of this are observed with tricyclohexylphosphine complexes of Pt(II). Complex cations of the form trans-$[PtHL(PCy_3)_2]^+$ where L = PEt_3, PPh_3 and even PCy_3 have been prepared (143, 144). These complexes are expected to be square planar. Certainly the Tolman Cone Angles (TCA) of 132°, 145° and 179° for PEt_3, PPh_3 and PCy_3 respectively do not predict the existence of these compounds. For two PCy_3 ligands should occupy 358° in the square plane of the Pt atom, leaving little space for the coordination of any other ligands.

The main reason for the breakdown of the TCA concept is that phosphine ligands do not behave as solid cones. In fact various ligands can mesh with the phosphine ligands to give a 'cogwheel' effect. This is best observed from the X-ray crystal structure of the trigonal complex $Pt(CF_3C{\equiv}CCF_3)(PCy_3)_2$ (145). The two phosphine ligands in this complex are so oriented that the acetylene ligand which lies approximately in the Pt, P, P plane, is wedged between two cyclohexyl groups on each phosphine ligand.

Observations such as this prompted us to consider the concept of variable cone angles, where the cone angle is a function of rotation of the phosphine ligand about the M-P bond. X-ray studies provide an excellent source of data for such calculations, especially since modern intensity data collection techniques are good enough that H atom positions can be determined with reasonable precision. Also, idealized H atom positions can be calculated for some phosphine ligands such as PPh_3 and PCy_3. A method was devised for calculating cone angles from X-ray structural data and shall now be briefly described (121).

The phosphine ligand was rotated in increments of 10° about the metal-phosphorus bond, such that the internal geometry remained constant (Fig. 8.2 i). At each increment of rotation a cone angle was calculated with respect to atoms XI and X2 lying cis to the phosphine ligands. Obviously square planar, or octahedral structures are ideally suited for these calculations. Where trigonal or trigonal bypyramidal

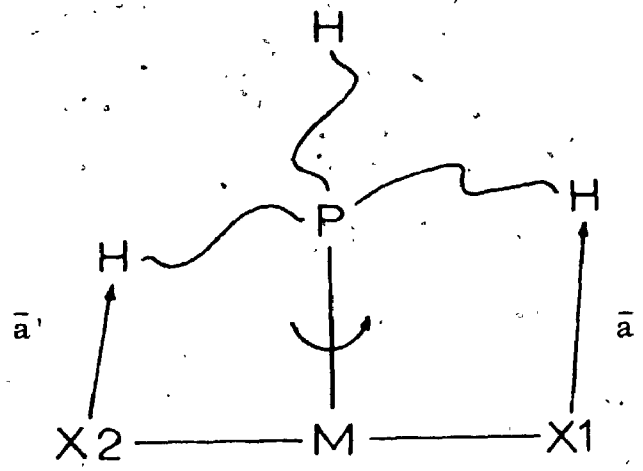

i

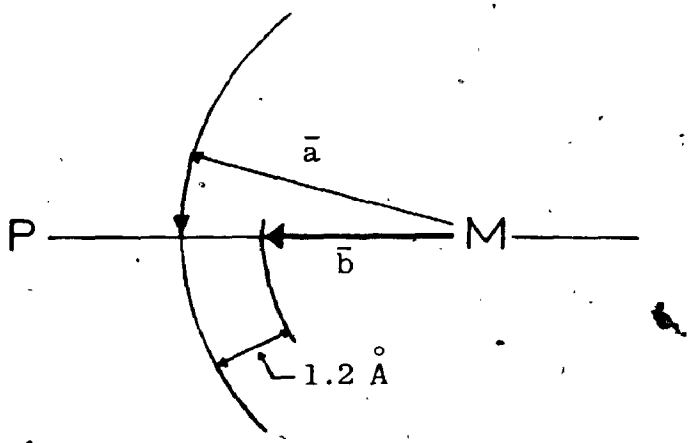

ii

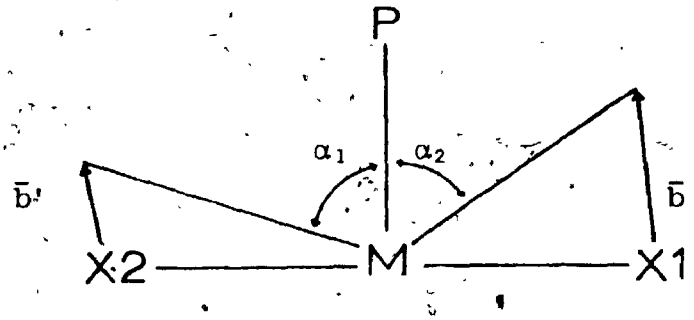

iii

Fig. 8.2

Calculation of Cone Angles

structures were encountered, idealized cis atom positions were first calculated in the equatorial plane. Tetrahedral structures were not considered. The lengths of the vectors from XI and X2 to all non phosphorus atoms of the phosphine ligands were calculated (Fig. 8.2 i). All but the shortest vectors $\bar{a}$ and $\bar{a}'$ were rejected. These vectors were then rotated into the M, P, XI, X2 plane and the Van der Waals radius of the atom to which $\bar{a}$ and $\bar{a}'$ were subtended were taken into account, giving new vectors $\bar{b}$ and $\bar{b}'$ (Fig. 8.2 ii). The Van der Waals radius for H was taken as 1.2 Å. Half cone angles α_1 and α_2 were then calculated and summed to give the total cone angle at that orientation of the phosphine ligand (Fig. 8.2 iii). This calculation was repeated at each 10° increment of rotation about the M-P bond until the ligand had been rotated 360°.

The calculations were performed on all ten dimethylphenylphosphine ligands studied in this thesis, and on several other types of common phosphine ligands. The cone angle values can be plotted as a function of increment of rotation of the phosphine ligand. A sample plot for dimethylphenylphosphine is presented in Fig. 8.3. The plot has an approximate periodicity of 180°, as expected. The minimum values occur at approximately 0° of rotation, the orientation of the phosphine ligand observed in the solid state. This was the case for all phosphine ligands in the trigonal and square planar complexes examined.

In Table 8.4 are presented the minimum, maximum and mean

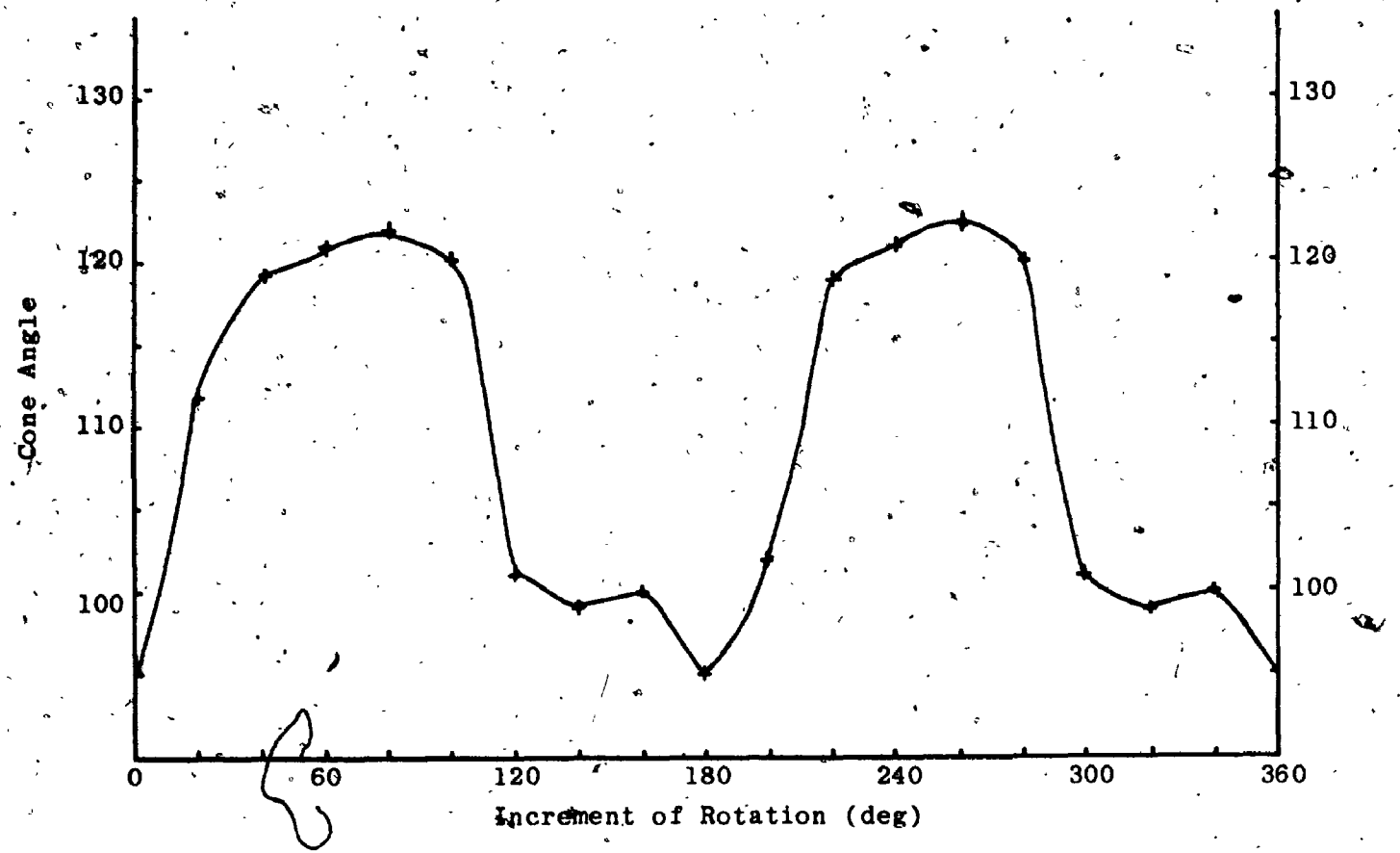

Fig. 8.3

Plot of Cone Angle v's Increment of Rotation for a Dimethylphenylphosphine Ligand

TABLE 8.4

Cone Angles for Dimethylphenylphosphine Ligands

Complex	Phosphorus Atom	Cone Angles(deg) Minimum	Maximum	Mean	Reference
trans-[Pt(MeC=NMe$_2$)Me(PMe$_2$Ph)$_2$]PF$_6$	P(1)	97.6	117.9	109.6	Chapter 2
	P(2)	97.2	124.6	109.8	
trans-[Pt(CH$_2$O=CCH$_2$CH$_2$)Me(PMe$_2$Ph)$_2$]PF$_6$	P(1)	91.0	125.6	109.8	Chapter 3
	P(2)	95.0	123.3	110.1	
trans-[Pt{HO(CH$_2$)$_3$C=NMe$_2$}Cl(PMe$_2$Ph)$_2$]PF$_6$	P(1)	91.2	122.4	108.5	Chapter 4
	P(2)	98.7	123.0	109.6	
trans-[Pt(MeC=NMe$_2$)(C≡N-p-C$_6$H$_4$Me)(PMe$_2$Ph)$_2$](PF$_6$)$_2$	P(1)	96.8	117.0	106.6	Chapter 6
	P(2)	93.9	121.5	107.9	
trans-[Pt(MeC=NMe$_2$){C(NMe$_2$)NH-p-C$_6$H$_4$Me}(PMe$_2$Ph)$_2$](PF$_6$)$_2$	P(1)	96.1	118.6	106.6	Chapter 7
	P(2)	97.1	116.8	108.8	
Mean Values		95.5(8)	121(1)	108.7(4)	

cone angles (averaged over 360° of rotation) for the 10 dimethylphenylphosphine ligands determined in this study. It is encouraging to note that all values show only small deviations from their means. A summary of the cone angles for several common phosphine ligands is presented in Table 8.5 and these are compared to the TCA values. The calculations were based upon data obtained in our laboratories and from published results in the current literature. No corrections were made in the present calculations for any small differences in M-P bond lengths.

In Table 8.5 the more bulky phosphine ligands tend to have the larger minimum and maximum values. The mean cone angles represent the overall relative sizes of the ligands, and follow a trend similar to that of the TCA values. Only PEt_3 and PPh_3 are anomalous in that PEt_3 has a slightly larger mean value than PPh_3. The TCA values suggest that PPh_3 is the more bulky ligand.

The minimum cone angles give a more realistic representation of the spatial requirements of these ligands than do the TCA values. For example, the existence of the complex cation $[PtH(PCy_3)_3]^+$ can be predicted using the minimum angle for PCy_3. The phosphine ligands require 345° of a possible 360 degrees of arc about the Pt atom. This leaves some space for the coordination of the hydride ligand.

These preliminary calculations indicate that very good descriptions of the steric bulk of various ligands can be obtained from structural data. It is clear that the effective

TABLE 8.5

Phosphine Ligand Cone Angles

Phosphine	Cone Angles(deg) Minimum	Maximum	Mean	Tolman	Number of Ligands Examined
$P(t\text{-butyl})_3$	141	159	150	182	1
$P(C_6H_{11})_3$	115(4)	168(3)	145(2)	179	3
$P(C_2H_5)_3$	105(3)	166(3)	129(1)	132	3
$P(C_6H_5)_3$	99(2)	150(2)	125(1)	145	12
$PCH_3(C_6H_5)_2$	88(2)	144(2)	116(1)	136	3
$P(CH_3)_2C_6H_5$	96(1)	121(1)	109(1)	127	10

cone angle of a phosphine ligand is dependent on the orientation of that ligand; moreover, the phosphine ligand orientation in the solid state is such as to present a minimum cone angle at the coordination plane of the metal atom, presumably to accommodate the neighboring ligands which lie in the plane.

8.4 Summary

The bonding of the carbene ligand in the cationic square planar complexes of Pt(II) is dominated by electron donation from the nucleophilic oxy- or amino-substituents. The results indicate that carbene ligands are at best poor acceptors of π electron density from the metal atom.

The mode of bonding to the Pt atom for the tertiary carbene ligands 3a and 3b is similar.

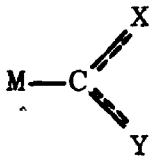

3a

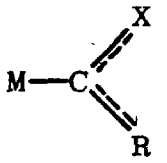

3b

X = alkylamino or alkoxy

Y = alkylamino

R = alkyl

The trends in the C-X and C-Y bond lengths indicate that the extent of multiple bonding is greater for 3b than 3a carbene ligands. The amount of M-C metal π bonding appears to be the same for aminocarbene ligands of type 3a and 3b. The presence of an alkoxy substituent in a 3b carbene results in a slight increase in metal-carbene π bonding.

The carbene ligands exert a strong <u>trans</u> influence, and the Pt-C(carbene) bond length is affected to a small extent by the <u>trans</u> influence of the ligand lying opposite.

APPENDIX I

DESCRIPTION OF COMPUTING PROGRAMS

All computing was performed employing the facilities at the University of Western Ontario Academic Computing Center, where a DEC PDP-10 and a CDC Cyber 73/14 are available.

The programs were modified (by N.C. Payne) versions of programs from the program library of J.A. Ibers at Northwestern University. Other local programs written by N.C. Payne, R.G. Ball and the author were also used. Details of specific programs follow:

1. PICKTT was used for least-squares refinement of the diffractometer setting angles to obtain unit cell parameters, their estimated standard deviations and the orientation matrix. It is a modified version of J.A. Ibers PICK, which utilized the logic of W.C. Hamilton's MODE1.

2. WOFACA, used for reduction of the raw diffractometer data was written at the University of Western Ontario.

3. FORDAP is a combined Fourier summation, peak search and interpolation program, written by A.A. Zalkin. Patterson and Fourier syntheses were calculated using this program.

4. WOCLS was used for structure factor calculations and least-squares refinements. The program is a rewrite and revision of NUGLS by R.J. Doedens and J.A. Ibers, which in turn is a highly modified version of ORFLS by W.R. Busing and H.A. Levy.

5. ANGLE was used to calculate interfacial angles from

goniometric measurements on the crystals. This permitted indexing of the crystal faces. The program was written by J.A. Ibers.

6. AGNOST is the absorption correction program. Modified by C. Cahen and J.A. Ibers, it has both analytical and Gaussian options.

7. RBANG was used to calculate rigid group orientation parameters for use in WOCLS when rigid group refinement was performed. The program is a modified version of that written by S.F. Watkins.

8. SADIAN was used to calculate bond distances and angles. This is a rewrite of Baur's program. In the later stages of this work, NUDAP, based on the routines from C.K. Johnson's ORFFE was used for these calculations.

9. FAME by R.B. Dewar was used to calculate Wilson statistics, and to determine whether the data were best described by centric or acentric space groups.

10. BIJVOET, written by R.G. Ball, was used to tabulate relative magnitudes of the observed and calculated structure factors of Friedel pairs when polar space groups were encountered.

11. METHROT by D. Bright was used to obtain idealized H atom positions for methyl groups. K. Raymond's FINDH was used to calculate idealized positions for methylene H atoms. In the later stages of this work all idealized H atom positions were calculated using HYDRA, a rewrite of PHLA by E.V. Fleischer.

12. PLANE by J. Marsh and modified by N.C. Payne was used to calculate angles between planes.

13. RANGER by P.W.R. Corfield and modified by N.C. Payne was used for statistical examination of observed and calculated structure factors.

14. ORFFEC, a modification of the Busing-Martin-Levy function and error program was employed in bond angle and distance calculations. Estimated standard deviations for these values were also calculated. Estimated standard deviations in bond lengths and angles involving rigid group atoms were calculated using N.C. Payne's ERROR.

15. ORTEP2 by C.K. Johnson, the non-overlap version of ORTEP was used for illustrations of the molecules and for crystal drawings.

16. LIST by D. Bright and modified by N.C. Payne was used to sort data according to indices and to print the data in a suitable form for deposition and publication.

17. PUBLISH by N.C. Payne was used to obtain final positional and thermal parameters in tabular form suitable for publication. In the later stages TABLE, a rewrite of PUBLISH was used.

APPENDIX II

KEY FORMULAE

The general expression for the calculated structure factor is:

$$|F_{hk\ell}| = (A^2_{hk\ell} + B^2_{hk\ell})^{\frac{1}{2}}$$

where

$$A_{hk\ell} \equiv \sum_j f_j \cos 2\pi(hx_j + ky_j + \ell z_j)$$

$$B_{hk\ell} \equiv \sum_j f_j \sin 2\pi(hx_j + ky_j + \ell z_j)$$

f_j is the scattering factor for the jth atom.

The expression for the phase angle is:

$$\alpha_{hk\ell} = \tan^{-1}\left(\frac{B_{hk\ell}}{A_{hk\ell}}\right)$$

The function minimized in least-squares refinement is:

$$\Sigma w(|F_o| - |F_c|)^2$$

where w is the weight given by

$$w = 4F_o^2/\sigma^2(F_o^2)$$

The agreement factors are:

$$R_1 = \frac{\Sigma||F_o| - |F_c||}{\Sigma|F_o|}$$

$$R_2 = \left[\frac{\Sigma w(|F_o| - |F_c|)^2}{\Sigma F_o^2}\right]^{\frac{1}{2}}$$

The thermal parameters of the atoms are given by:

$$\text{isotropic} \qquad \exp\left[\frac{-B \sin^2\theta_{hk\ell}}{\lambda^2}\right] = \exp\left[\frac{-8\pi^2 U \sin^2\theta_{hk\ell}}{\lambda^2}\right]$$

where B is the isotropic temperature factor in $\mathring{A}^2$ and U is the mean-square amplitude of vibration in $\mathring{A}^2$

$$\text{anisotropic} \qquad \exp[-2\pi^2(U_{11}h^2a^{*2} + U_{22}k^2b^{*2} + U_{33}\ell^2c^{*2} +$$

$$2U_{12}hka^*b^* + 2U_{13}h\ell a^*c^* + 2U_{23}k\ell b^*c^*)]$$

where the U_{ij} are the thermal parameters expressed in terms of mean-square amplitudes of vibration in $\mathring{A}^2$.

The expression utilized to account for secondary extinction is that of W.H. Zachariasen:

$$F_{corr} = F_o[cBI_o + \{1.0 + (cBI_o)^2\}^{\frac{1}{2}}]^{\frac{1}{2}}$$

where F_{corr} is the corrected structure factor, c is the extinction coefficient, B is a function taking into account the angular dependence of the extinction correction and I_o is the observed integrated intensity.

The error on an observation of unit weight is calculated from:

$$\left[\frac{\Sigma\{w(|F_o|-|F_c|)^2\}}{(NO-NV)}\right]^{\frac{1}{2}}$$

Calculation of Errors

Errors on differences are calculated from:

$$\sigma = (\sigma_1^2 + \sigma_2^2)^{\frac{1}{2}}$$

where σ_1 and σ_2 are the estimated standard deviations on two quantities. Errors on mean values are obtained from the expression:

$$\sigma = \left[\frac{\sum_{i=1}^{n} (x_i - \bar{x})^2}{n(n-1)} \right]^{\frac{1}{2}}$$

where $\bar{x}$ is the mean value of x in n observations.

APPENDIX III

OBSERVED AND CALCULATED STRUCTURE FACTORS

($10|F_o|$ vs. $10|F_c|$ in electrons)

Trans-[Pt(MeC—NMe$_2$)Me(PMe$_2$Ph)$_2$] PF_6

k	l	F_o	F_c	k	l	F_o	F_c	k	l	F_o	F_c	k	l	F_o	F_c	k	l	F_o	F_c	k	l	F_o	F_c	k	l	F_o	F_c	k	l	F_o	F_c	k	l	F_o	F_c
[illegible]	[illegible]	[illegible]	[illegible]	[illegible]	[illegible]	[illegible]	[illegible]	[illegible]	[illegible]	[illegible]	[illegible]	[illegible]	[illegible]	[illegible]	[illegible]	[illegible]	[illegible]	[illegible]	[illegible]	[illegible]	[illegible]	[illegible]	[illegible]	[illegible]	[illegible]	[illegible]	[illegible]	[illegible]	[illegible]	[illegible]	[illegible]	[illegible]	[illegible]	[illegible]	[illegible]

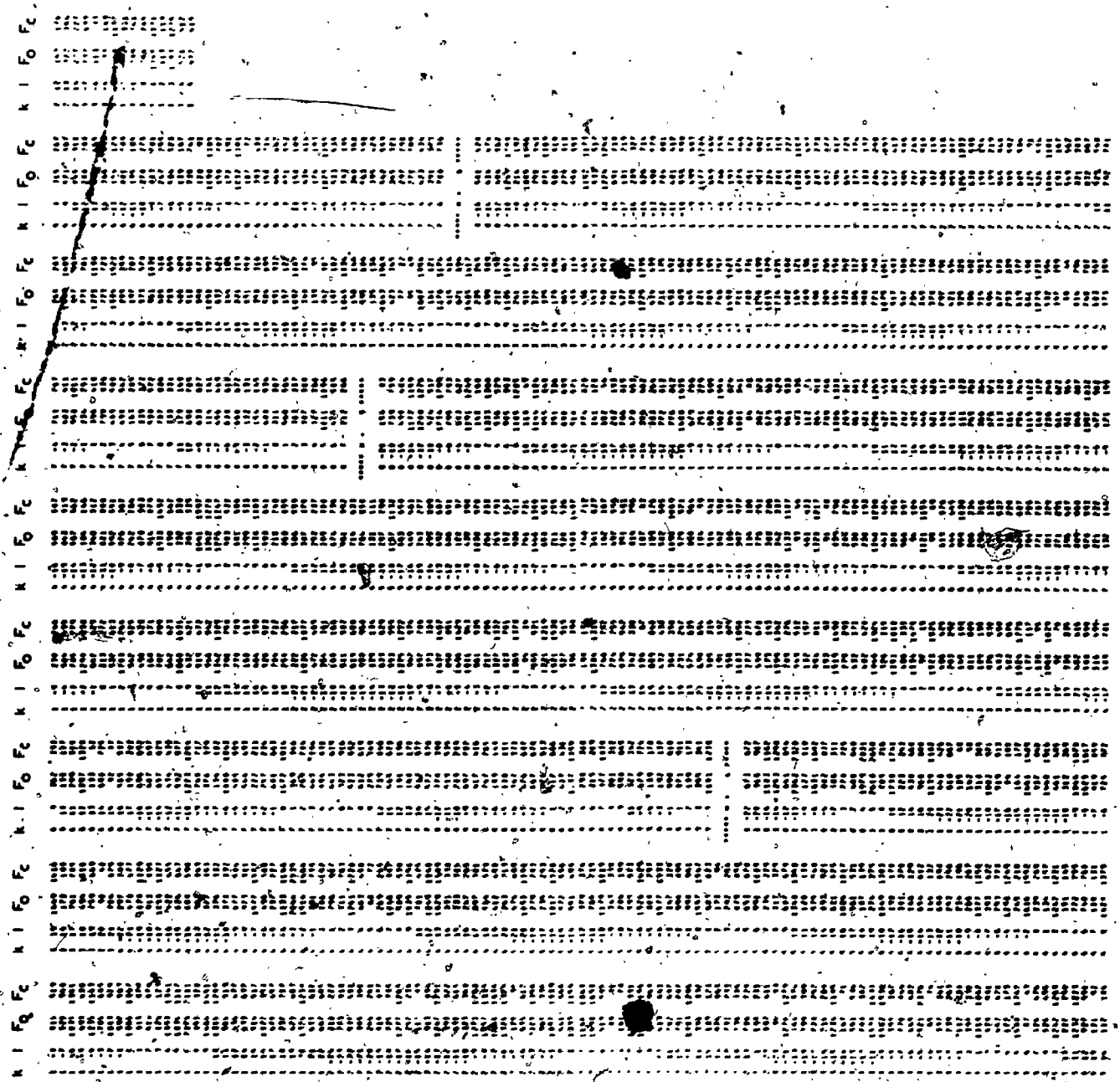
K
Fo
Fc


Fc
Fo
x
1
Trans-[PtCH2C=OCH2CH2Me(PMe2Ph)2]PF6

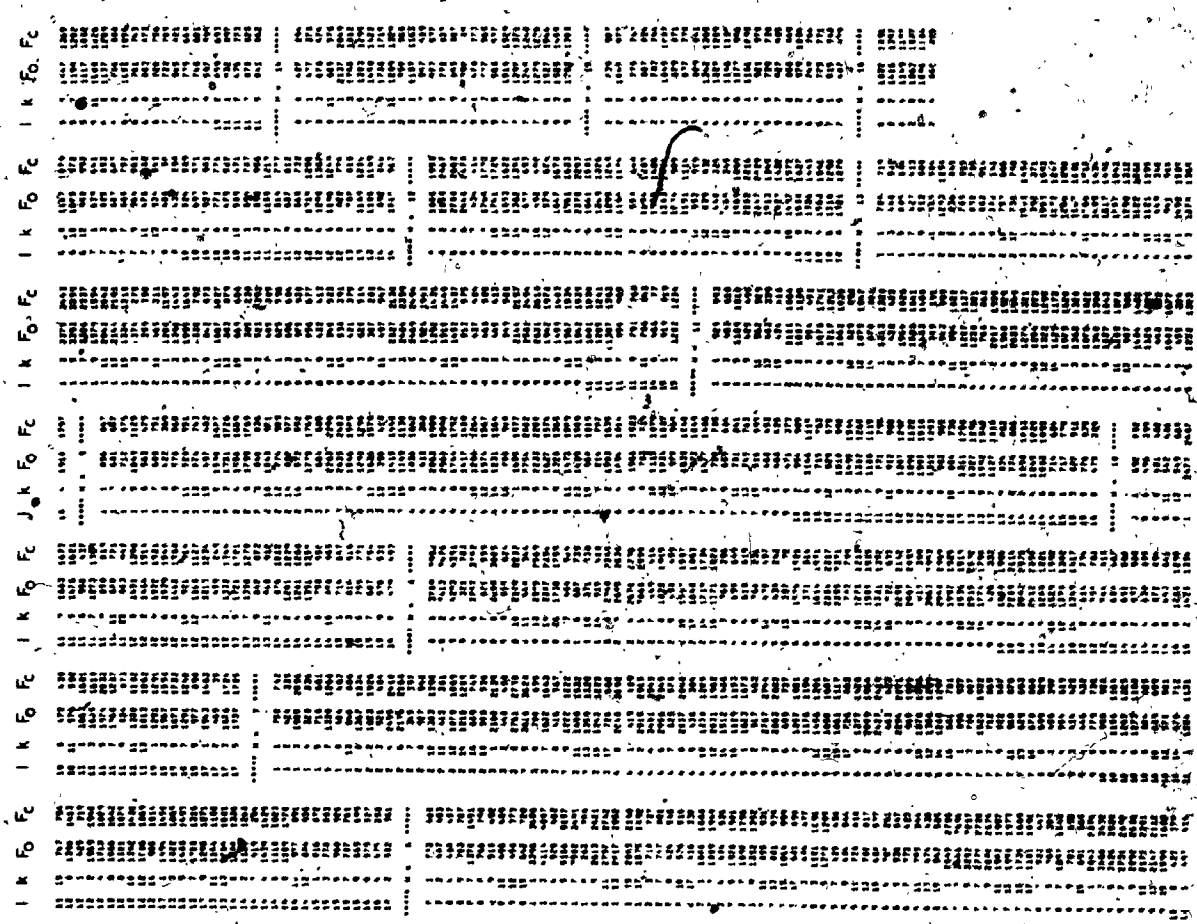

Trans-[Pt(HO(CH$_2$)$_3$C=NMe$_2$)Cl(PMe$_2$Ph)$_2$]PF$_6$

h	l	F_o	F_c

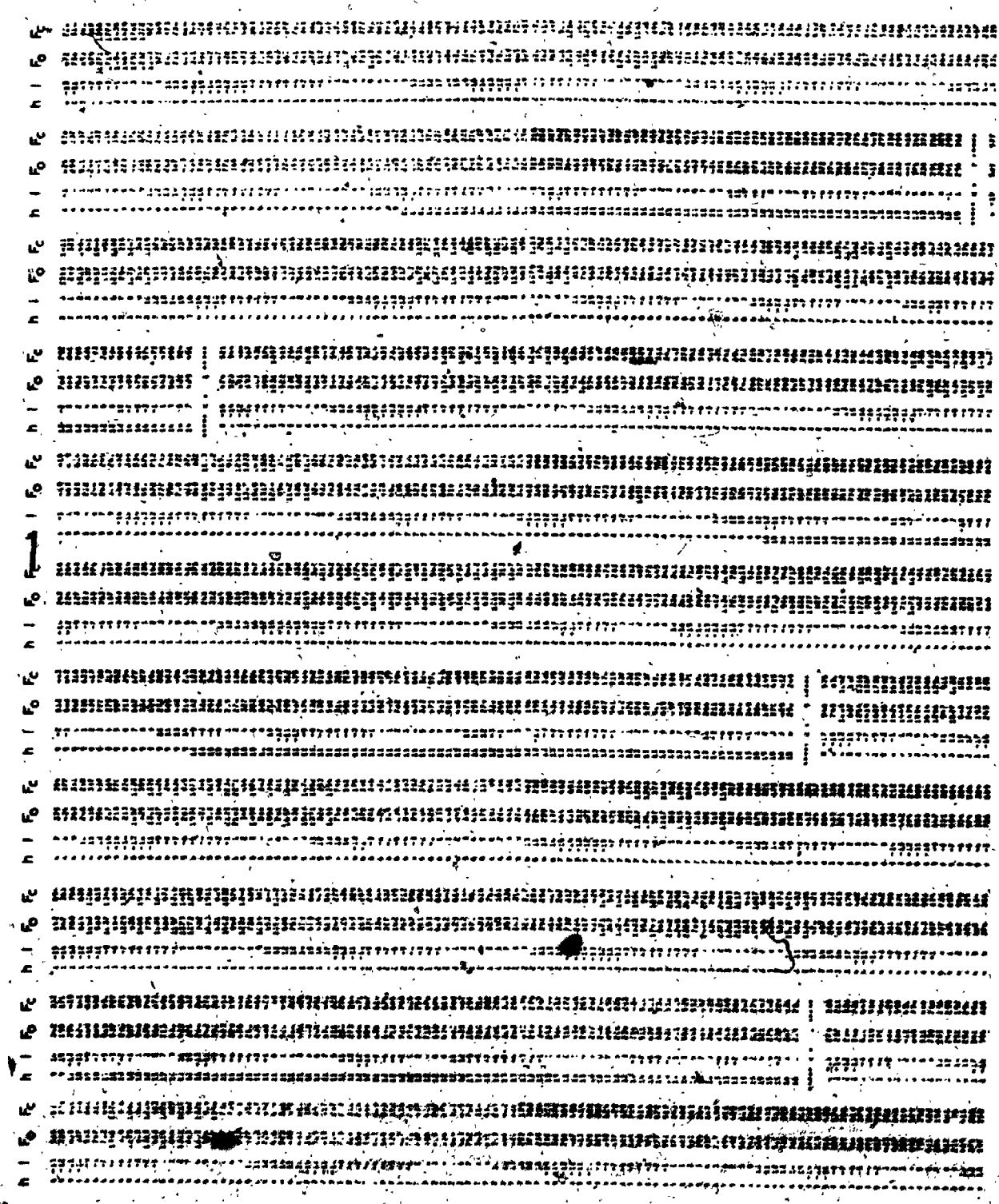

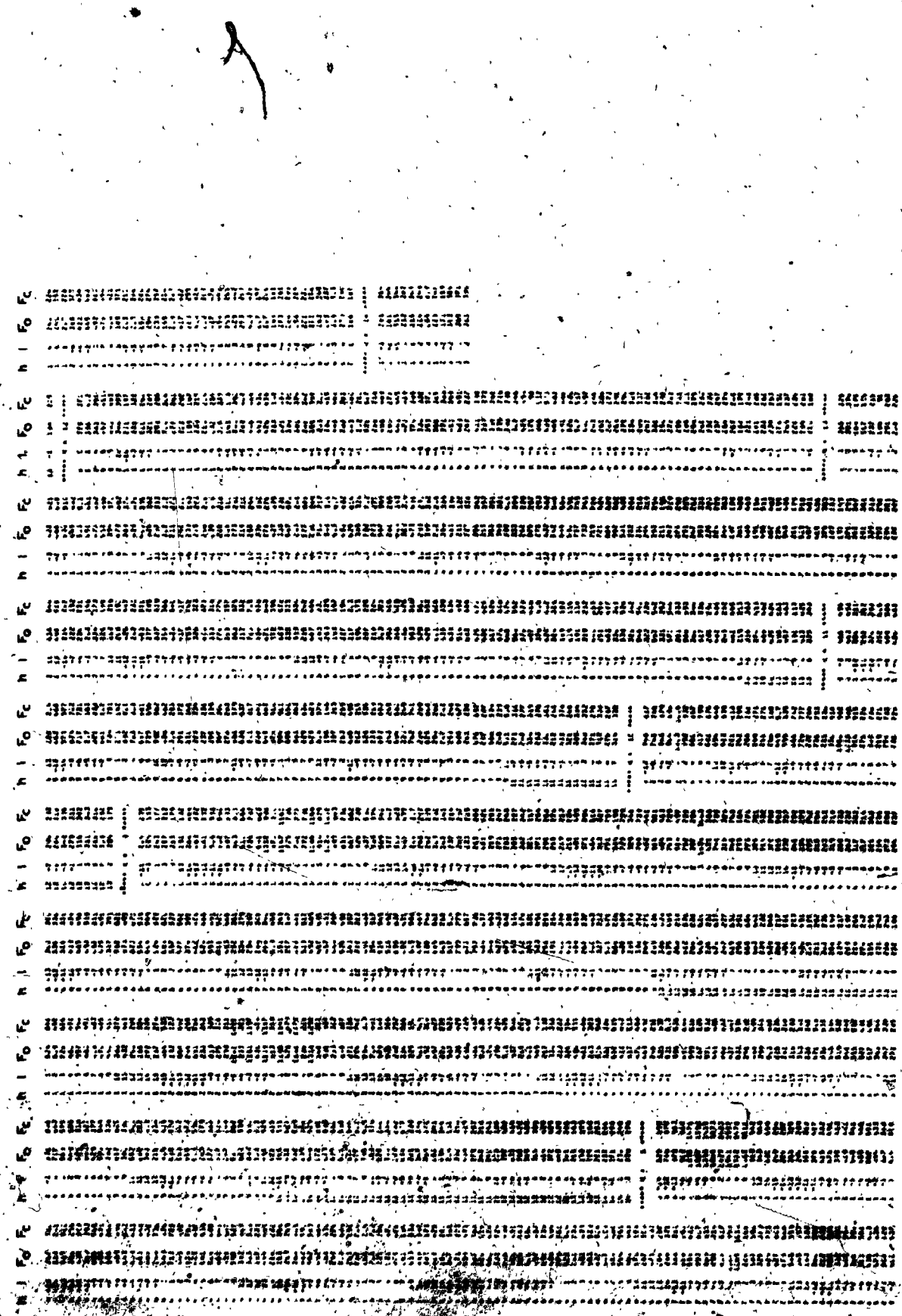

Trans-[Pt(C≡N-p-C_6H_4Me)(MeC=NMe$_2$X(PMe$_2$Ph)$_2$](PF$_6$)$_2$

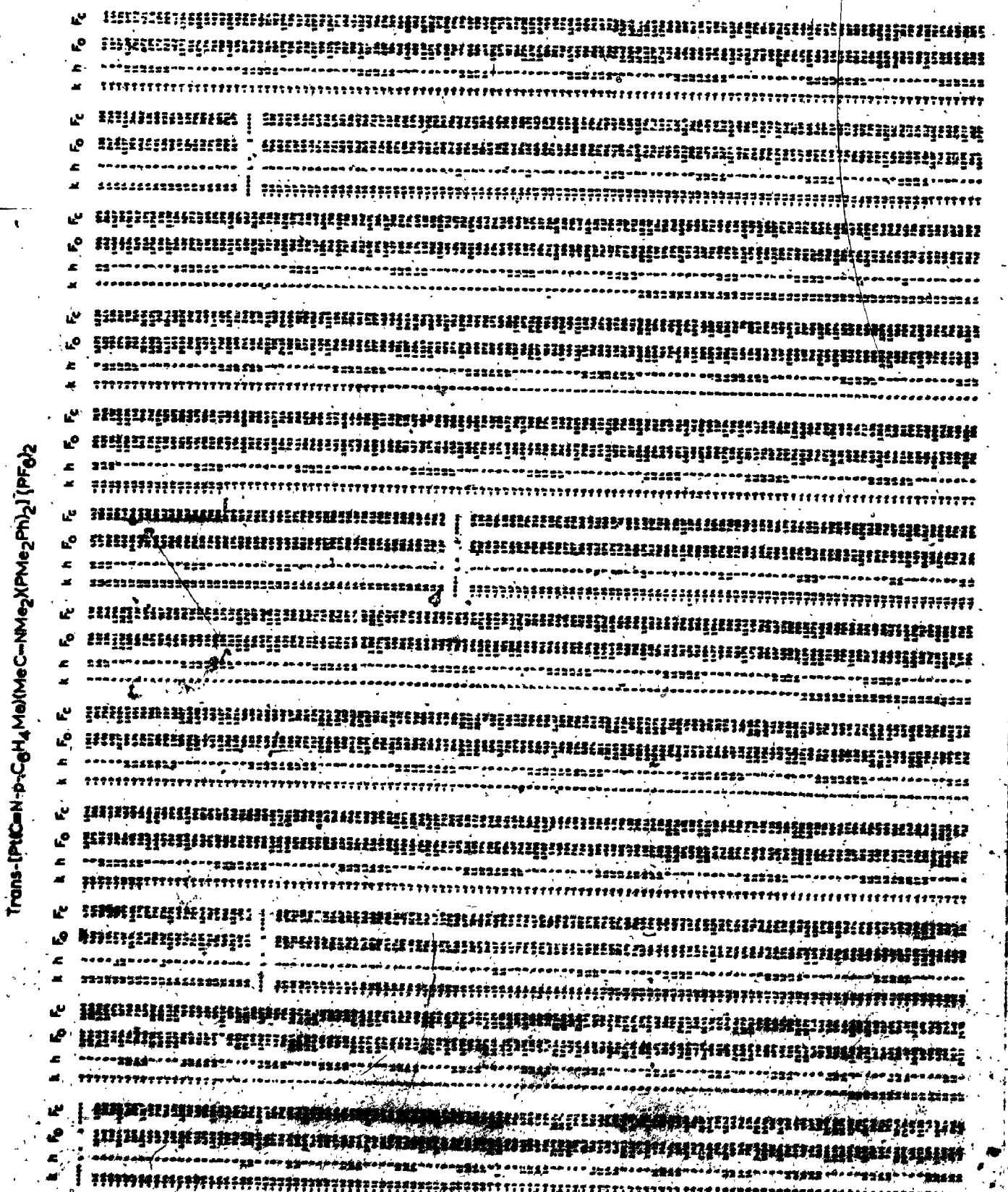

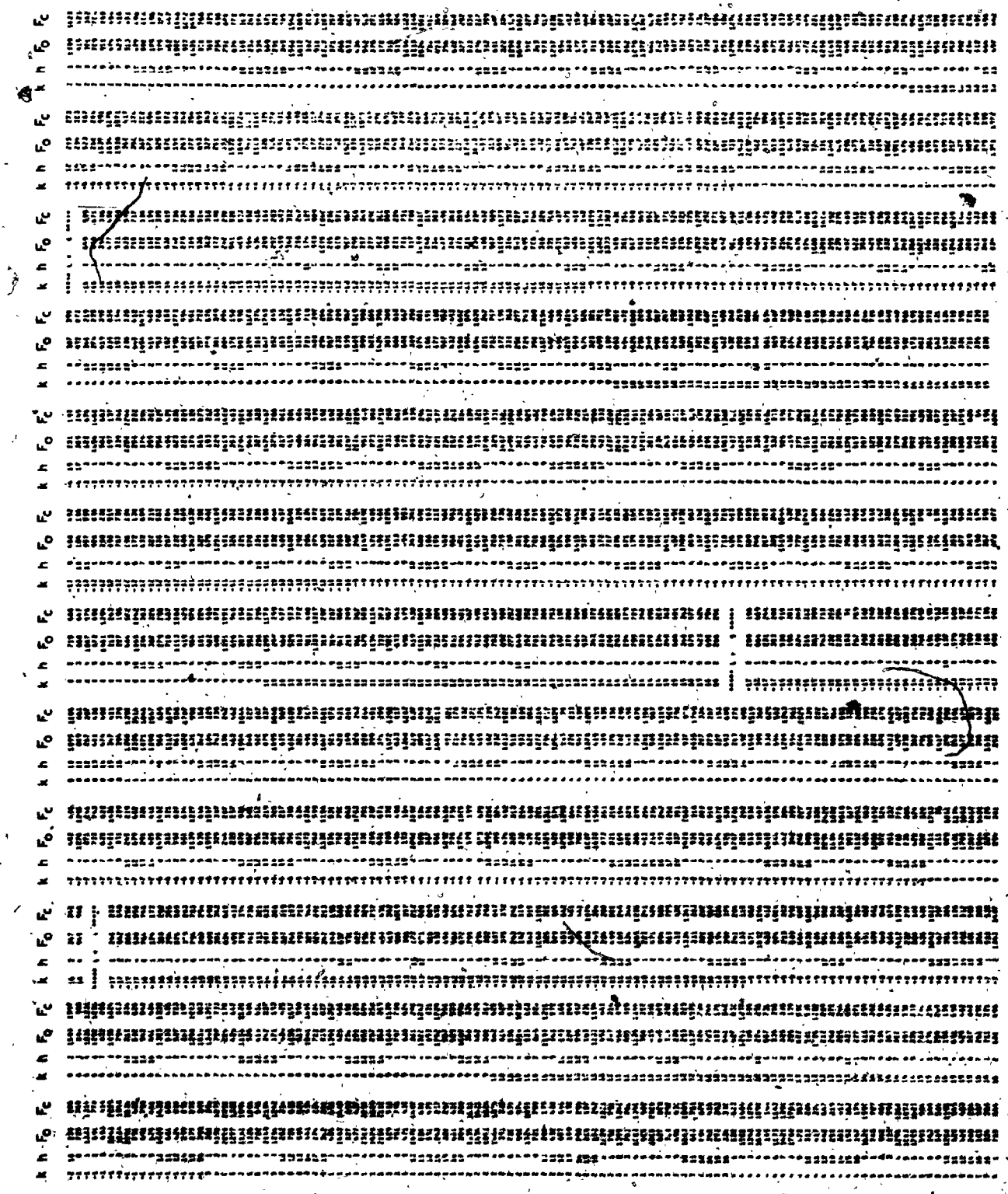

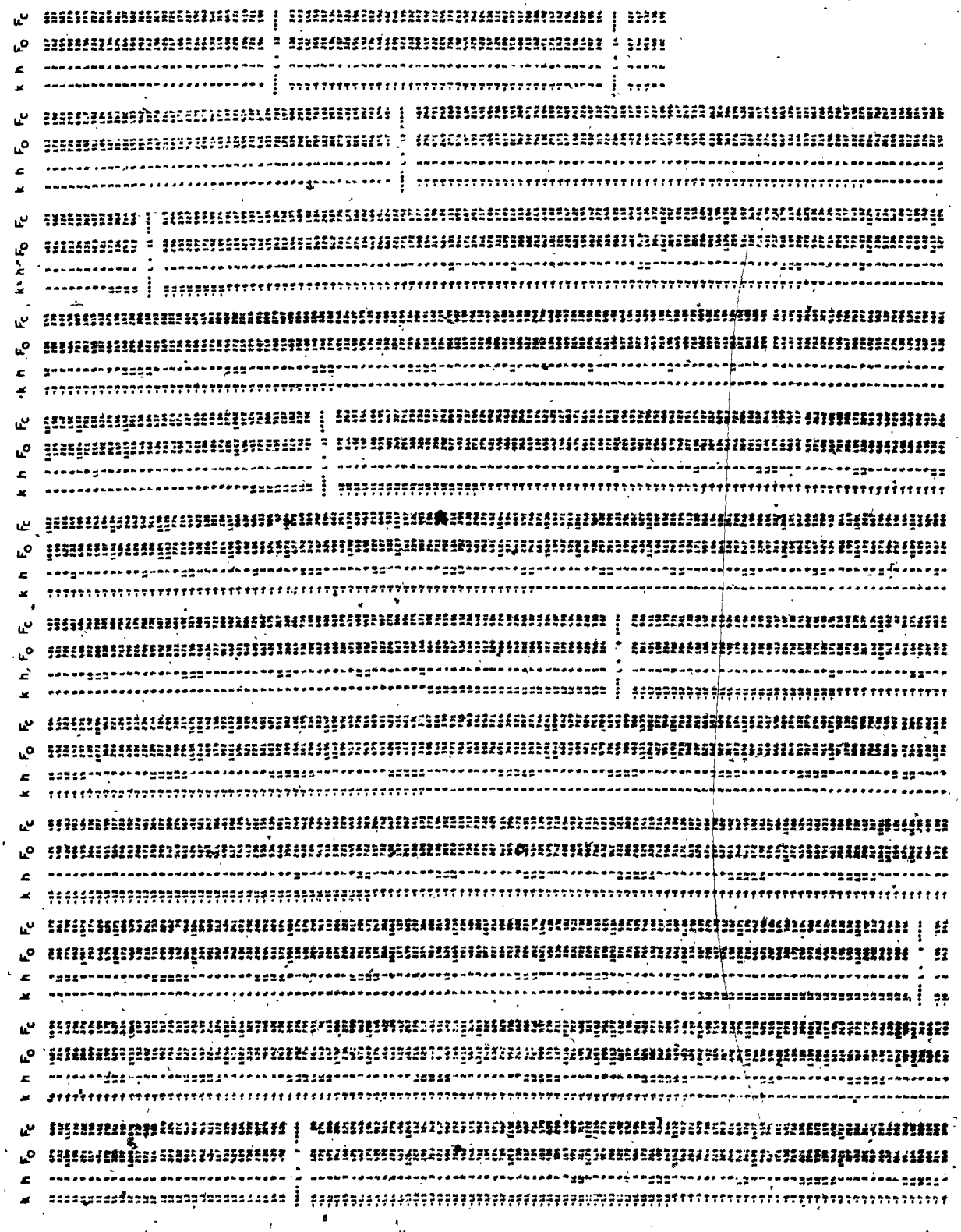

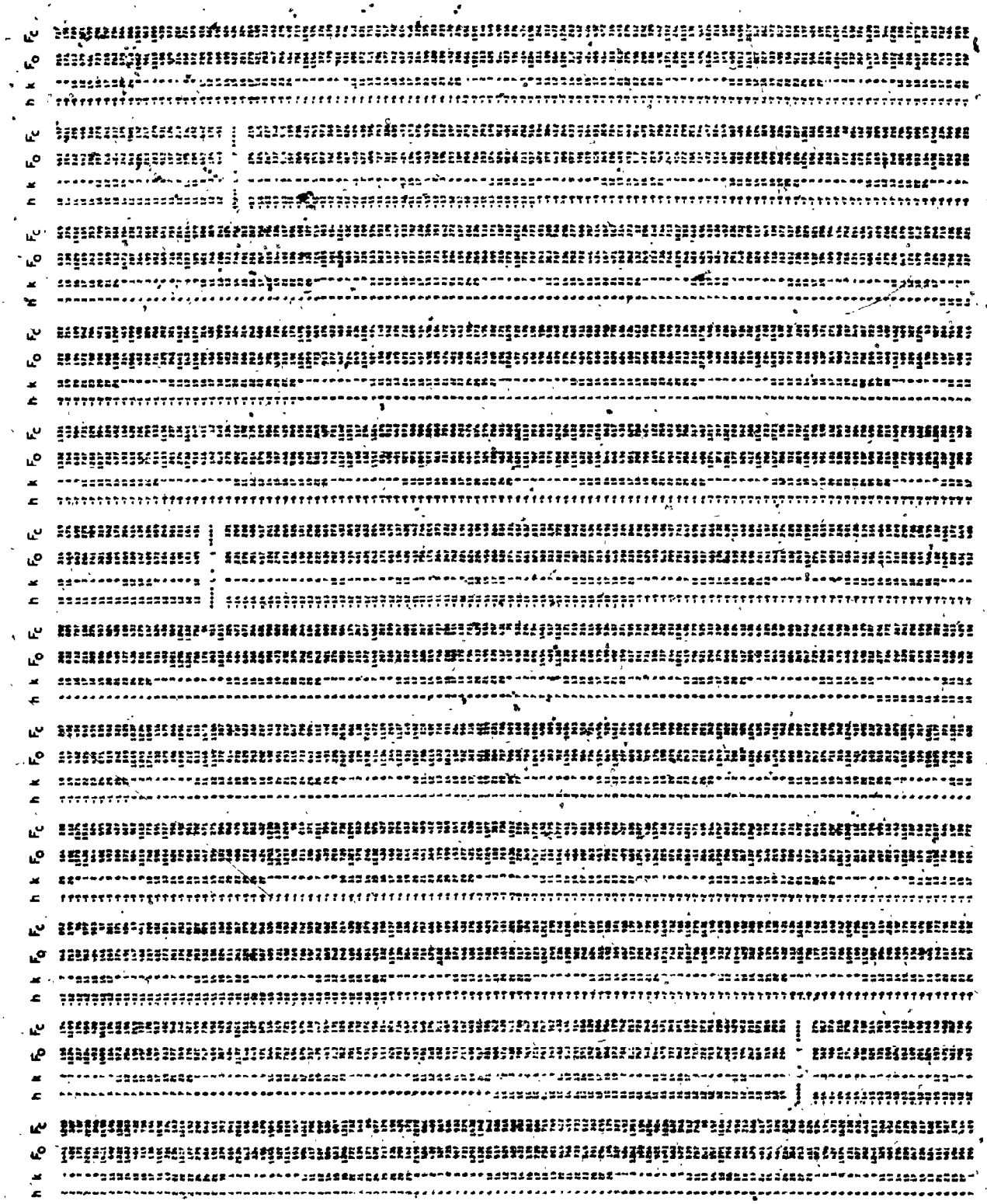

trans-[Pt(Me$_2$N=C-NH-p-C$_6$H$_4$Me)(MeC=NMe$_2$)(PMe$_2$Ph)$_2$] (PF$_6$)$_2$

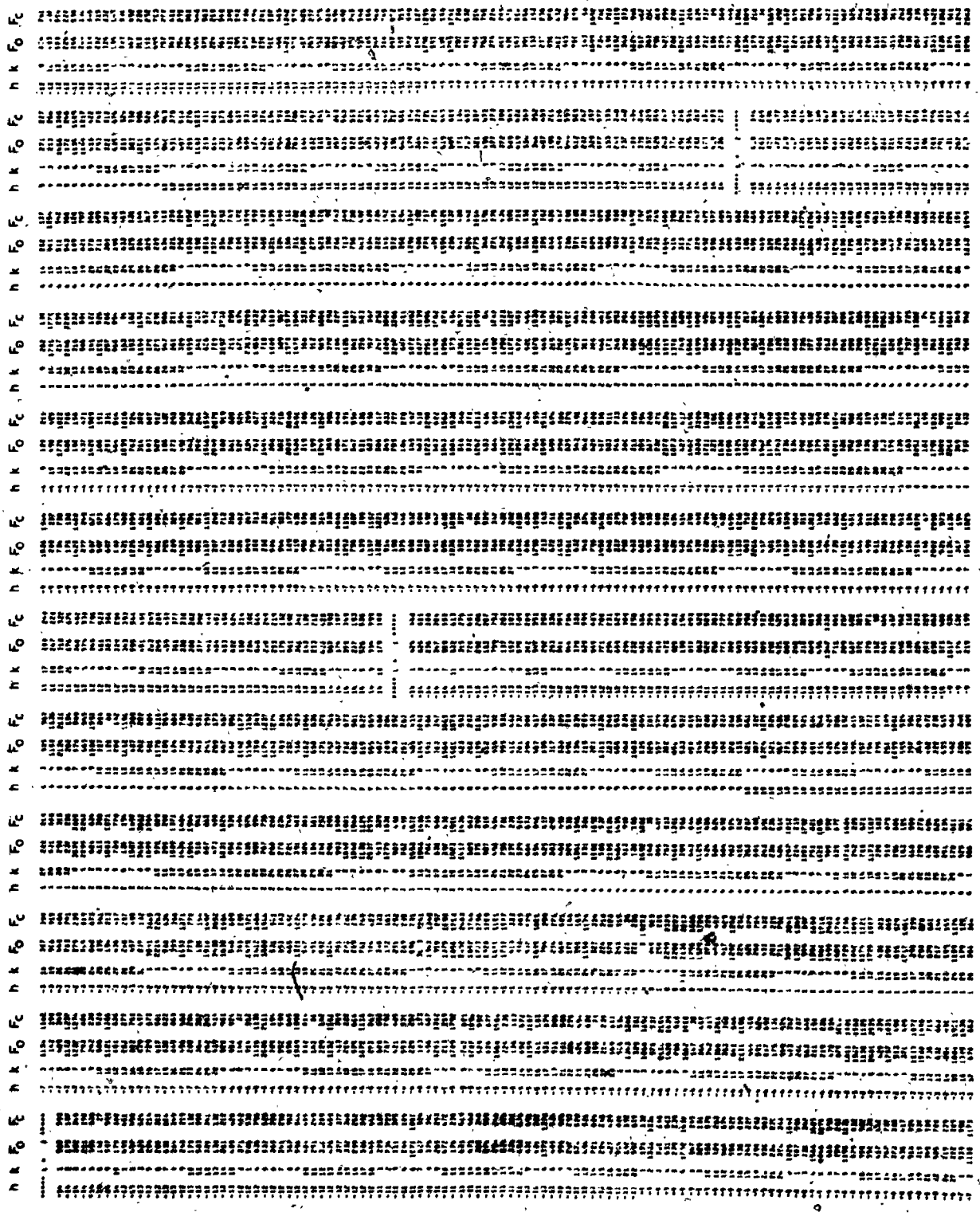

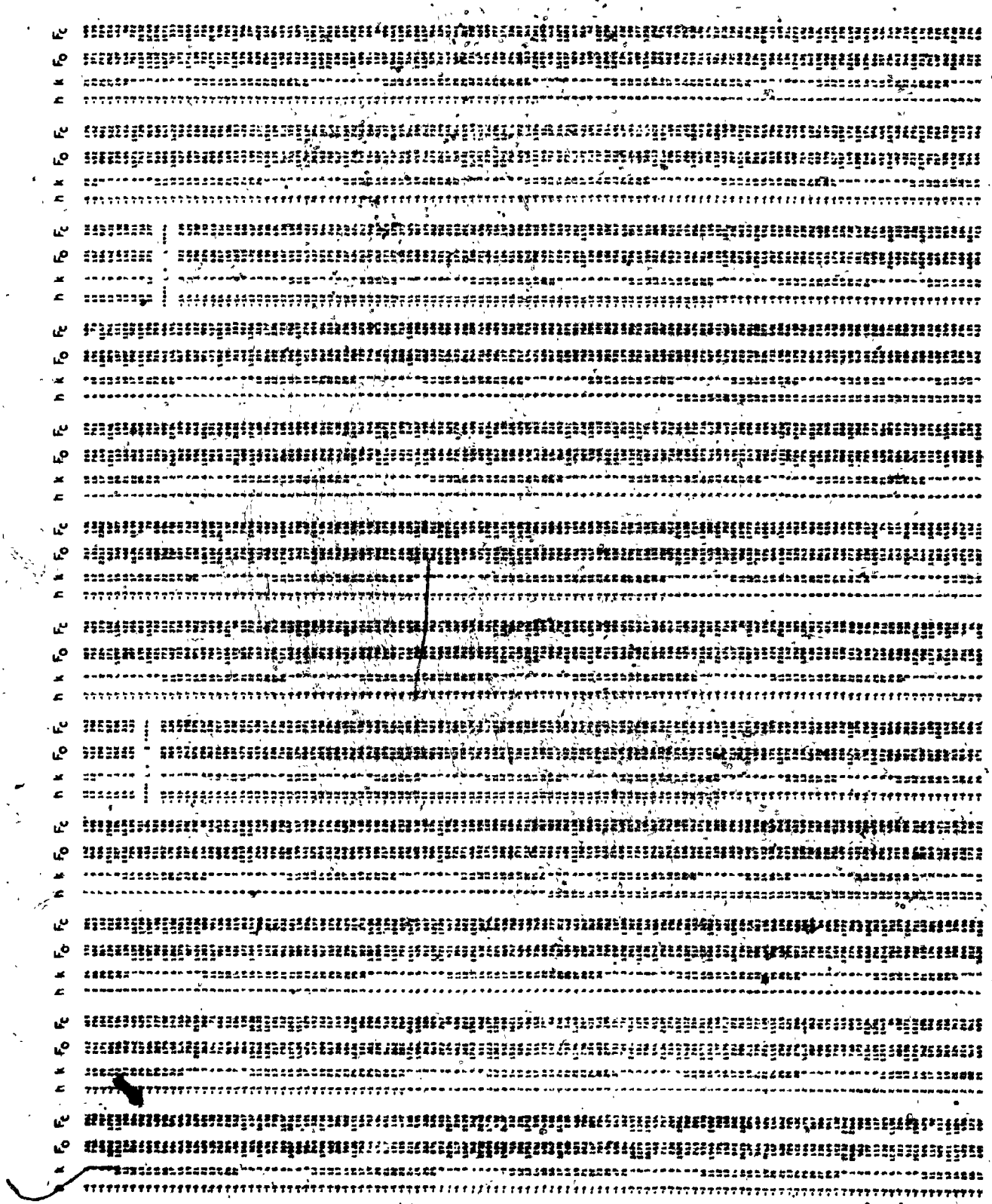
h k Fo Fc

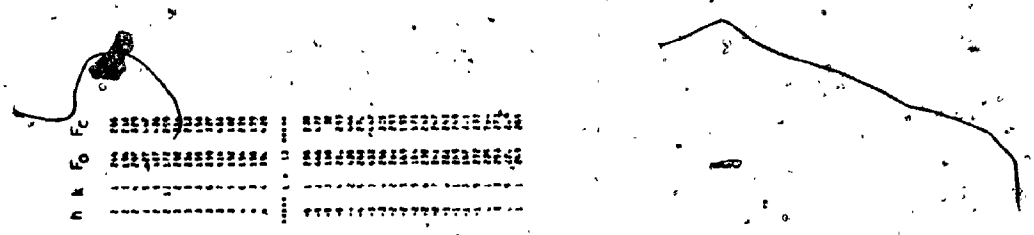

REFERENCES

1. J. Halpern, Discuss. Faraday Soc., 46, 7 (1968).
2. J.P. Collman, Accounts Chem. Res., 1, 386 (1970).
3. G.E. Coates, M.L.H. Green, and K. Wade; 'Organometallic Compounds,' Vol. II, Methuen and Co., London (1968).
4. E.O. Fischer and A. Maasböl, Angew. Chem. Internat. Ed., 3, 580 (1964).
5. E.O. Fischer, Pure Appl. Chem., 24, 407 (1970).
6. E.O. Fischer, ibid, 30, 353 (1972).
7. E.O. Fischer, Adv. Organometal. Chem., 13, 1 (1976).
8. D.J. Cardin, B. Cetinkaya, and M.F. Lappert, Chem. Rev., 72, 545 (1972).
9. D.J. Cardin, B. Cetinkaya, M.J. Doyle and M.F. Lappert, Chem. Soc. Rev., 2, 99 (1973).
10. F.A. Cotton and C.M. Lukehart, Progr. Inorg. Chem., 16, 487 (1972).
11. J.A. Connor, 'Organometallic Chemistry,' Specialist Periodical Reports, The Chemical Society, London, Vol. 2, p. 302 (1972).
12. J.A. Connor, ibid, Vol. 3, p. 243 (1973).
13. J.A. Connor, ibid, Vol. 4, p. 235 (1974).
14. W. Kirmse, 'Carbene Chemistry,' Academic Press Inc., New York (1964).
15. R.R. Schrock, J. Amer. Chem. Soc., 97, 6577 (1975).
16. L.J. Guggenberger and R.R. Schrock, ibid, 97, 6578 (1975).
17. W.R. Roper and D.F. Christian, J. Organometal. Chem., 80, C35 (1974).

18. B. Cetinkaya, M.F. Lappert and K. Turner, Chem. Commun., 851 (1972).

19. D.F. Christian and H.C. Clark, J. Organometal. Chem., 85, C9 (1975).

20. B. Cetinkaya, M.F. Lappert, G.M. McLaughlin and K. Turner, J. Chem. Soc., Dalton, 1591 (1974).

21. D.F. Christian, G.R. Clark and W.R. Roper, J. Organometal. Chem., 81 C7 (1974).

22. R.R. Schrock, J. Amer. Chem. Soc., 96, 6796 (1974).

23. K. Öfele, Angew. Chem. Internat. Ed., 7, 950 (1968).

24. P. Hong, N. Nishii, K. Sonogashiru and N. Hagihara, ibid, 993 (1972).

25. R.B. King and M.S. Saran, J. Amer. Chem. Soc., 94, 1784 (1972).

26. R.B. King and M.S. Saran, ibid, 95, 1811 (1973).

27. R.B. King and M.S. Saran, ibid, 95, 1817 (1973).

28. R.B. King and M.S. Saran, Chem. Commun., 1053 (1972).

29. Y.T. Struchkov et al., J. Organometal. Chem., 110, C36 (1976).

30. L.J. Todd et al., Chem. Commun., 354 (1974).

31. G. Huttner, S. Schelle and O.S. Mills, Angew. Chem. Internat. Ed., 8, 515 (1969).

32. R.M. Kirchner and J.A. Ibers, Inorg. Chem., 13, 1667 (1974).

33. Y. Yamamoto, K. Aoki and H. Yamazaki, J. Amer. Chem. Soc., 96, 2647 (1974).

34. J.H. Enemark, J.E. Parks, W.M. Butler and A.L. Balch, Inorg. Chem., 12, 451 (1973).

35. A.L. Balch, J. Miller and J.H. Enemark, J. Amer. Chem. Soc., 93, 4613 (1971).

36. P. Domiano, A. Musatti, M. Nordelli and G. Predieri, J. Chem. Soc., Dalton, 2165 (1975).

37. K.W. Muir and R. Walker, ibid, 272 (1975).

38. J.A. Ibers et al., J. Amer. Chem. Soc., 97, 4748 (1975).

39. O.S. Mills and P.F. Lindley, J. Chem. Soc., A, 1279 (1969).

40. M.J. Bennett and W.A.G. Graham, J. Amer. Chem. Soc., 96, 5931 (1974).

41. J.S. Miller and A.L. Balch, Inorg. Chem., 11 2069 (1972).

42. P.B. Hitchcock, M.F. Lappert and P.L. Pye, Chem. Commun., 644 (1976).

43. M.Y. Darensbourg and D.T. Darensbourg, Inorg. Chem., 9, 32 (1970).

44. W.B. Perry, T.F. Schoof, W.L. Jolly, L.J. Todd and D.L. Cronin, Inorg. Chem., 13, 2038 (1974).

45. C.G. Kreiter and V. Formacek, Angew. Chem. Internat. Ed., 11, 141 (1972).

46. T.F. Block, R.F. Fenske and C.P. Cassey, J. Amer. Chem. Soc., 98, 441 (1976).

47. O.S. Mills and A.D. Redhouse, Angew. Chem. Internat. Ed., 4, 1082 (1965); J. Chem. Soc., A, 642 (1972).

48. O.S. Mills and A.D. Redhouse, Chem. Commun., 814 (1966); J. Chem. Soc., A, 1274 (1969).

49. P.E. Baikie, E.O. Fischer and O.S. Mills, Chem. Commun., 1199 (1967).

50. J.A. Connor and O.S. Mills, J. Chem. Soc., A, 334 (1969).

51. G. Huttner and S. Lange, Chem. Ber., 103, 3149 (1970).

52. O.S. Mills and R.J. Hoare, J. Chem. Soc., Dalton, 653 (1972).

53. G. Huttner and B. Kreig, Chem. Ber., 105, 67 (1972).

54. G. Huttner and H. Lorenz, ibid, 108, 186 (1975).

55. L. Chugaev and M. Skanavy-Grigorizeva, J. Russ. Chem. Soc., 47, 776 (1915).

56. G. Rouchias and B.L. Shaw, J. Chem. Soc., A, 2097 (1971).

57. W.M. Butler and J.H. Enemark, Inorg. Chem., 10, 2416 (1971).

58. P.M. Treichel, J.J. Benedict, R.W. Hess and J.P. Stenson, Chem. Commun., 1627 (1970).

59. P.J. Fraser, W.R. Roper and F.G.A. Stone, J. Organometal. Chem., 50, C54 (1973).

60. H.C. Clark and D.F. Christian, ibid, 85, C9 (1975).

61. D.F. Christian, H.C. Clark and R.F. Stepaniak, ibid, 112, 227 (1976).

62. M.H. Chisholm and H.C. Clark, Chem. Commun., 763 (1970).

63. M.H. Chisholm and H.C. Clark, Inorg. Chem., 10, 1711 (1971).

64. M.H. Chisholm, H.C. Clark, W.S. Johns, J.E.H. Ward and K. Yasufuku, ibid, 14, 900 (1975).

65. M.H. Chisholm and H.C. Clark, ibid, 10, 2557 (1971).

66. A. Pidcock, R.E. Richards and L.M. Venanzi, J. Chem. Soc., A, 1707 (1966).

67. H.C. Clark, T.G. Appleton and L.E. Manzer, Coord. Chem. Rev., 10, 335 (1973).

68. Lj. Manojlovicic-Muir and K.W. Muir, Inorg. Chim. Acta., 10, 47 (1974).

69. E.M. Badley, J. Chatt, R.L. Richards and G.A. Sim; Chem. Commun., 1322 (1969); J. Chem. Soc., Dalton, 1930 (1976).

70. D.J. Cardin et al., J. Organometal. Chem., 44, C59 (1972).

71. K.W. Muir and Lj. Manojlovicic-Muir, J. Chem. Soc., Dalton, 2427 (1974).

72. W.M. Butler and J.H. Enemark, Inorg. Chem., 12, 540 (1973).

73. G.H. Stout and L.H. Jensen, 'X-ray Structure Determination,' MacMillan, London (1968).

74. C.W. Bunn, 'Chemical Crystallography' 2nd Ed., Oxford University Press, New York (1961).

75. M.J. Buerger, 'X-ray Crystallography,' Wiley, New York (1942).

76. International Tables for X-ray Crystallography, 3rd Ed., Kynoch Press, Birmingham, England, Vol. I (1969).

77. W.A. Zachariasen, Acta. Crystallogr., 18, 705 (1965).

78. Software for the PDP8-L computer is supplied as part of the FACS-1 system by Picker Corporation. The programs were adapted from those written by W.R. Busing and H.A. Levy. Alterations to the programs have been made locally by R.G. Ball.

79. W.R. Busing and H.A. Levy, Acta. Crystallogr., 22, 457 (1967).

80. T.C. Furnas, 'Single Crystal Orienter Instruction Manual,' General Electric Company, Milwaukee, Wisconsin (1957).

81. P.W.R. Corfield, R.J. Doedens and J.A. Ibers, Inorg. Chem., 6, 197 (1967).

82. D. Cahen and J.A. Ibers, J. Appl. Crystallogr., 5, 298 (1972).

83. D.T. Cromer and D. Liberman, J. Chem. Phys., 53, 1891 (1970).

84. D.T. Cromer and J.H. Waber, Acta. Crystallogr., 18, 104 (1965).

85. R.F. Stewart, E.R. Davidson and W.T. Simpson, J. Chem. Phys., 42, 3175 (1965).

86. J.A. Ibers and W.C. Hamilton, Acta. Crystallogr., 17, 781 (1964).

87. R. Eisenberg and J.A. Ibers, Inorg. Chem., 4, 773 (1965).

88. 'Interatomic Distances,' Special Publication No. 11, The Chemical Society, London, p. M196 (1958).

89. W.H. Zachariasen, 'Theory of X-ray Diffraction in Crystals,' Dover Publications, New York (1967).

90. H. Bode and H. Clausen, Z. Anorg. Chem., 265, 229 (1951).

91. H. Bode and G. Teufer, Acta. Crystallogr., 9, 825 (1956).

92. R.F. Stepaniak and N.C. Payne, J. Organometal. Chem., 31, 213 (1973).

93. B.W. Davies and N.C. Payne, Canad. J. Chem., 51, 3477 (1973).

94. L. Pauling, 'The Nature of the Chemical Bond,' 3rd Ed., Cornell University Press, Ithaca, New York (1960).

95. B. Jovanovic, Lj. Manojlovicic-Muir and K.W. Muir, J. Chem. Soc., Dalton, 195 (1974).

96. K.P. Wagner, P.M. Treichel and J.C. Calabresse, J. Organometal. Chem., C33 (1973).

97. R.F. Stepaniak and N.C. Payne, Inorg. Chem., 13, 797 (1974).

98. M.H. Chisholm, H.C. Clark, L.E. Manzer, J.B. Stothers and J.E.H. Ward, J. Amer. Chem. Soc., 95, 8574 (1973).

99. M. Green, J.R. Moss, I.W. Nowell and F.G.A. Stone, Chem. Commun., 1339 (1972).

100. J.A. Connor. E.M. Jones, E.W. Randall and E. Rosenberg, J. Chem. Soc., Dalton, 2419 (1972).

101. M.A. Bennett, P.W. Clark, G.B. Robertson and P.O. Whimp, J. Organometal. Chem., 63, C15 (1973); and references therein.

102. R.F. Stepaniak and N.C. Payne, ibid, 72, 453 (1974).

103. W.C. Hamilton, Acta. Crystallogr., 18, 502 (1965).

104. R. Walker, Lj. Manojlovicic-Muir and K.W. Muir, J. Organometal. Chem., 66, C21 (1974); J. Chem. Soc., Dalton, 1279 (1976).

105. P. Brant, J.H. Enemark and A.L. Balch, J. Organometal. Chem., 114, 99 (1976).

106. P.M. Treichel and R.W. Hess, J. Amer. Chem. Soc., 92, 4731 (1970).

107. P.M. Treichel, K.P. Wagner and R.W. Hess, Inorg. Chem., 12, 1471 (1973).

108. Y. Yamamoto and H. Yamazaki, Bull. Chem. Soc., Japan, 44, 1873 (1971).

109. D.F. Christian, H.C. Clark and R.F. Stepaniak, J. Organometal. Chem., 112, 209 (1976).

110. P.M. Treichel, Adv. Organometal. Chem., 11, 21 (1973).

111. J.P. Collman and S.R. Winter, J. Amer. Chem. Soc., 95, 4089 (1973).

112. J.F. Van Baar, K. Vrieze and D.J. Stufkens, J. Organometal. Chem., 81, 247 (1974).

113. B.E. Mann, B.L. Shaw and N.I. Tucker, J. Chem. Soc., A, 2667 (1971).

114. J.M. Jenkins and B.L. Shaw, Proc. Chem. Soc., London, 279 (1963).

115. R.K. Harris, Canad. J. Chem., 42, 2275 (1964).

116. H.C. Clark and L.E. Manzer, Inorg. Chem., 11, 503 (1972).

117. E.M. Badley, J. Chatt and R.L. Richards, J. Chem. Soc., A, 21 (1971).

118. M.H. Chisholm, H.C. Clark, J.E.H. Ward and K. Yasufuku, Inorg. Chem., 14, 893 (1975).

119. R.L. Richards et al., J. Chem. Soc., Dalton, 1800 (1972).

120. E. Moser and E.O. Fischer, J. Organometal. Chem., 13, 387 (1968).

121. R.F. Stepaniak and N.C. Payne, unpublished results.

122. K.C. Ingold, F.R. Shaw and I.S. Wilson, J. Chem. Soc., 1283 (1928).

123. R.A.R. Kleinstück and D.K. Z[illegible]hr, Angew. Chem. Internat. Ed., 10, 132 (1971).

124. J.J. Howard, M. Sc. Thesis, University of Western Ontario (1971).

125. J.D. Ruddick and B.L. Shaw, J. Chem. Soc., A, 2801 (1969).

126. J.D. Ruddick and B.L. Shaw, ibid, 2964 (1969).

127. L.E. Manzer, Ph.D. Thesis, University of Western Ontario (1973).

128. L. Malatesta and F. Bonati, 'Isocyanide Complexes of Metals,' Wiley-Interscience, New York (1969).

129. F.A. Cotton and F. Zingales, J. Amer. Chem. Soc., 83, 351 (1961).

130. J.A. Connor et al., J. Chem. Soc., Dalton, 1246 (1972).

131. B. Jovanovic and Lj. Manojlovicic-Muir, ibid, 1176 (1972).

132. B. Jovanovic, Lj. Manojlovicic-Muir and K.W. Muir, ibid, 1176 (1972).

133. C.J. Cardin, D.J. Cardin, M.F. Lappert and K.W. Muir, J. Organometal. Chem., 60, C70 (1973).

134. 'Handbook of Chemistry and Physics,' 49th Ed., The Chemical Rubber Company, Cleveland, Ohio (1968),

135. Lj. Manojlovicic-Muir, J. Organometal. Chem., 73, C45 (1974).

136. H.C. Clark, P.W.R. Corfield, K.R. Dixon and J.A. Ibers, J. Amer. Chem. Soc., 89, 3360 (1967).

137. D.R. Russell, P.A. Tucker and S. Wilson, J. Organometal. Chem., 104, 387 (1976).

138. J.J. Daly, J. Chem. Soc., 3799 (1964).

139. V.G. Albano, G.M. Basso Ricci and P.L. Bellon, Inorg. Chem., 8, 2109 (1969).

140. C.A. Tolman, J. Amer. Chem. Soc., 92, 2956 (1970).

141. C.A. Tolman, W.C. Seidel and L.W. Gosser, ibid, 96, 53 (1974).

142. W.C. Trogler and L.G. Marzilli, Inorg. Chem., 14, 2942 (1975).

143. T.G. Attig and H.C. Clark, personal communication.

144. M.J. Dymarski and H.C. Clark, personal communication.

145. J.F. Richardson and N.C. Payne, personal communication.